

ON THE MONTHLY MEAN LOWER TROPOSPHERIC CIRCULATION
AND THE ANOMALOUS CIRCULATION DURING THE 1961/62
FLOODS IN EAST AFRICA

BY

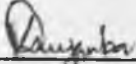
EBBY KAMILA ANYAMBA

A thesis submitted in part fulfilment for the degree of
Master of Science in the University of Nairobi

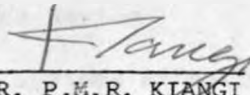
November 1983

DECLARATION

This thesis is my original work and has not been presented for a degree in any other University.


EBBY KAMILA ANYAMBA

This thesis has been submitted for examination with my approval as University supervisor.


DR. P.M.R. KIANGI

30/11/83

Department of Meteorology

University of Nairobi

P.O. Box 30197

NAIROBI, Kenya

TABLE OF CONTENTS

	Page
Title	i
Declaration	ii
Table of Contents	iii
List of Figures	vi
List of Plates	xiii
List of Tables	xiv
Abstract	xv
CHAPTER 1	
1.0 INTRODUCTION AND LITERATURE REVIEW	1
1.1.0 Introduction	1
1.1.1 The Climate of East Africa	3
1.1.2 The Floods of 1961-1962	7
1.1.3 Objective of Study	12
1.2.0 Literature Review	13
1.2.1.0 Synoptic Systems affecting East Africa	13
1.2.1.1 The Monsoons	13
1.2.1.2 The Inter-tropical Convergence Zone (ITCZ)	16
1.2.1.3 Equatorial Westerlies	20
1.2.1.4 Easterly Waves	23
1.2.1.5 Influences from the middle latitude instabilities	26
1.2.1.6 Tropical Cyclones	28
1.2.2 Local Circulations	29

	Page
CHAPTER 2	
2.0	DATA SOURCES AND ANALYSES 33
2.1.0	Data sources 33
2.1.1	The Magnetic tape pibal data file - Problems and Errors 36
2.2.0	Analyses 39
2.2.1	Determination of mean flow patterns 39
2.2.2	Determination of the 1961/62 wind anomaly fields 40
2.2.3	Determination of Divergence and Relative Vorticity fields 42
2.2.4	Vertical motion field 43
CHAPTER 3	
3.0	RESULTS AND DISCUSSIONS 48
3.1.0	Mean wind flow characteristics 48
3.1.1.0	The Northeast Monsoon Season 49
3.1.1.1	Mean horizontal motion 49
3.1.1.2	Mean divergence and vertical motion fields 52
3.1.2.0	The Long Rains Season 78
3.1.2.1	Mean horizontal motion 78
3.1.2.2	Mean Divergence and Vertical motion fields 80
3.1.3.0	The Southeast-southwest Monsoon Season 110
3.1.3.1	Mean horizontal motion 110
3.1.3.2	Mean Divergence and Vertical motion fields 115

	Page	
3.1.4.0	The Short Rains Season	140
3.1.4.1	Mean horizontal motion	140
3.1.4.2	Mean Divergence and Vertical motion fields	141
3.2.0	The Floods : September 1961-January 1962	167
3.2.1	Weather disturbances during September-October 1961	167
3.2.2	Weather disturbances during November 1961	171
3.2.3	Weather disturbances during December 1961- January 1962	173
CHAPTER 4		
4.0	SUMMARY AND CONCLUDING REMARKS	220
4.1.0	The monthly mean wind flow patterns	220
4.1.1	The Northeast Monsoon Season	221
4.1.2	The Long Rains Season	222
4.1.3	The Southeast-southwest Monsoon Season	224
4.1.4	The Short Rains Season	227
4.2	The Floods of 1961-1962	228
Acknowledgements		231
References		232

LIST OF FIGURES

Figure	Page
1 Map of East Africa showing the location of pilot balloon stations used in the study.	2
2 Levels of lake Victoria (metres above datum) at the Jinja gauge ($\frac{1}{2}^{\circ}\text{N}$, 33°E).	10
3 Mean wind field (a) at the surface in January, (b) at 1525 m above mean sea level (AMSL) in December, (c) at 1525 m AMSL in January and (d) at 1525 m AMSL in February. Figure plotted at each station the wind speed in knots.	55
4 Mean wind field at 3050 m AMSL in (a) December, (b) January and (c) February.	59
5 Mean wind field at 4270 m AMSL in (a) December, (b) January and (c) February.	62
6 Mean wind field at 5490 m AMSL in (a) December, (b) January and (c) February.	65
7 Mean wind field at 7320 m AMSL in (a) December (b) January and (c) February.	68
8 Mean divergence field ($\times 10^{-6} \text{ s}^{-1}$) at 1525 m AMSL in (a) December, (b) January and (c) February.	71
9 Mean divergence field ($\times 10^{-6} \text{ s}^{-1}$) at (a) 3050 m AMSL in December, (b) 3050 m AMSL in January, (c) 3050 m AMSL in February and (d) 4270 m AMSL in January.	71

Figure	Page
10 Mean divergence field ($\times 10^{-6} \text{ s}^{-1}$) at 5490 m AMSL in (a) December, (b) January and (c) February.	72
11 Mean divergence field ($\times 10^{-6} \text{ s}^{-1}$) at 7320 m AMSL in (a) December, (b) January and (c) February.	73
12 Mean January vertical motion field ($\times 10^{-2} \text{ ms}^{-1}$) at (a) 1525 m AMSL, (b) 3050 m AMSL and (c) 5490 m AMSL.	74
13 Mean monthly rainfall maps for (a) December, (b) January and (c) February.	75
14 Mean wind field at (a) 1525 m AMSL in March, (b) the surface in April, (c) 1525 m AMSL in April and (d) 1525 m AMSL in May.	85
15 Mean wind field at 3050 m AMSL in (a) March, (b) April and (c) May.	89
16 Mean wind field at 4270 m AMSL in (a) March, (b) April and (c) May.	92
17 Mean wind field at 5490 m AMSL in (a) March, (b) April and (c) May.	95
18 Mean wind field at 7320 m AMSL in (a) March, (b) April and (c) May.	98
19 Mean divergence field ($\times 10^{-6} \text{ s}^{-1}$) in March at (a) 1525 m AMSL, (b) 3050 m AMSL, (c) 5490 m AMS L and (d) at 7320 m AMSL.	101

Figure	Page	
20	Mean divergence field ($\times 10^{-6} \text{ s}^{-1}$) in April : (a) at 1525 m AMSL; (b) at 3050 m AMSL; (c) at 4270 m AMSL; (d) at 5490 m AMSL; (e) at 7320 m AMSL; (f) vertical cross-section along latitude 1°S ; (g) vertical cross-section along longitude 36°E .	102
21	Mean April vertical motion field ($\times 10^{-2} \text{ ms}^{-1}$) at (a) 1525 m AMSL, (b) 3050 m AMSL and (c) 5490 m AMSL.	105
22	Mean divergence field ($\times 10^{-6} \text{ s}^{-1}$) in May at (a) 1525 m AMSL, (b) 3050 m AMSL, (c) 5490 m AMSL and (d) 7320 m AMSL.	106
23	Mean monthly rainfall maps for (a) March, (b) April and (c) May.	107
24	Mean wind field at (a) 1525 m AMSL in June, (b) surface in July, (c) 1525 m AMSL in July and (d) at 1525 m AMSL in August.	117
25	Mean wind field at 3050 m AMSL in (a) June, (b) July and (c) August.	121
26	Mean wind field at 4270 m AMSL in (a) June, (b) July and (c) August.	124
27	Mean wind field at 5490 m AMSL in (a) June, (b) July and (c) August.	127
28	Mean wind field at 7320 m AMSL in (a) June, (b) July and (c) August.	130

Figure	Page
29 Mean divergence field ($\times 10^{-6} \text{ s}^{-1}$) at 1525 m AMSL in (a) June, (b) July and (c) August.	133
30 Mean divergence field ($\times 10^{-6} \text{ s}^{-1}$) at (a) 3050 m AMSL in June, (b) 3050 m AMSL in July, (c) 3050 m AMSL in August and (d) at 4270 m AMSL in July.	133
31 Mean divergence field ($\times 10^{-6} \text{ s}^{-1}$) at 5490 m AMSL in (a) June, (b) July and (c) August.	134
32 Mean divergence field ($\times 10^{-6} \text{ s}^{-1}$) at 7320 m AMSL in (a) June, (b) July and (c) August.	135
33 Mean July vertical motion field ($\times 10^{-2} \text{ ms}^{-1}$) at (a) 1525 m AMSL, (b) 3050 m AMSL and (c) 5490 m AMSL.	136
34 Mean monthly rainfall maps for (a) June, (b) July and (c) August.	137
35 Mean wind field in September at (a) 1525 m AMSL, (b) 3050 m AMSL, (c) 4270 m AMSL, (d) 5490 m AMSL and (e) at 7320 m AMSL.	144
36 Mean wind field at (a) surface in October, (b) 1525 m AMSL in October, (c) 1525 m AMSL in November, (d) 3050 m AMSL in October, (e) 3050 m AMSL in November, (f) 4270 m AMSL in October, (g) 4270 m AMSL in November, (h) 5490 m AMSL in October, (i) 5490 m AMSL in November, (j) 7320 m AMSL in October and (k) 7320 m AMSL in November.	149

Figure	Page	
37	Mean divergence field ($\times 10^{-6} \text{ s}^{-1}$) in September at (a) 1525 m AMSL, (b) 3050 m AMSL, (c) 5490 m AMSL and (d) 7320 m AMSL.	160
38	Mean divergence field ($\times 10^{-6} \text{ s}^{-1}$) in October at (a) 1525 m AMSL, (b) 3050 m AMSL (c) 4270 m AMSL (d) 5490 m AMSL and (e) 7320 m AMSL.	161
39	Mean October vertical motion field (ms^{-1}) at (a) 1525 m AMSL, (b) 3050 m AMSL and (c) 5490 m AMSL.	162
40	Mean divergence field ($\times 10^{-6} \text{ s}^{-1}$) in November at (a) 1525 m AMSL, (b) 3050 m AMSL (c) 5490 m AMSL and (d) 7320 m AMSL.	163
41	Mean monthly rainfall maps for (a) September, (b) October and (c) November.	164
42	September 1961 : Streamlines and isotachs of wind anomalies at (1525 m AMSL, (b) 2440 m AMSL, (c) 3050 m AMSL, (d) 4270 m AMSL, (e) 5490 m AMSL and (f) 7320 m AMSL; (g) rainfall anomalies.	177
43	October 1961 : (a) Streamlines and isotachs of wind anomalies at (a) 1525 m AMSL, (b) 2440 m AMSL, (c) 3050 m AMSL, (d) 4270 m AMSL, (e) 5490 m AMSL, and (f) 7320 m AMSL; (g) rainfall anomalies.	184

Figure	Page
<p>44 November 1961 : (a) rainfall anomalies; streamlines and isotachs of wind anomalies at (b) 1525 m AMSL, (c) 2440 m AMSL, (d) 3050 m AMSL, (e) 4270 m AMSL, (f) 5490 m AMSL and (g) 7320 m AMSL.</p>	191
<p>45 Divergence fields associated with weather disturbances in November 1961 : (a) 1525 m AMSL, (b) 2440 m AMSL, (c) 3050 m AMSL, (d) 4270 m AMSL, (e) 5490 m AMSL, (f) 7320 m AMSL, (g) vertical cross-section along longitude 36°E; (h) vertical cross-section along the equator.</p>	198
<p>46 Vertical motion fields ($\times 10^{-2} \text{ms}^{-1}$) associated with weather disturbances in November 1961 : (a) 1525 m AMSL, (b) 3050 m AMSL, (c) 5490 m AMSL, (d) vertical cross-section along the equator; (e) vertical cross-section along longitude 36°E.</p>	200-
<p>47 December 1961 : Streamlines and isotachs of wind anomalies at (a) 1525 m AMSL, (b) 2440 m AMSL, (c) 3050 m AMSL (d) 4270 m AMSL, (e) 5490 m AMSL and (f) 7320 m AMSL.</p>	201
<p>48 January 1962 : Streamlines and isotachs of wind anomalies at (a) 1525 m AMSL, (b) 2440 m AMSL, (c) 3050 m AMSL, (d) 4270 m AMSL, (e) 5490 m AMSL and (f) 7320 m AMSL.</p>	207

Figure		Page
49	Observed mean wind vectors at 3050 m AMSL in (a) December 1961 and (b) January 1962.	213
50	Divergence fields associated with weather disturbances in January 1962 : (a) 1525 m AMSL, (b) 2440 m AMSL, (c) 3050 m AMSL, (d) 4270 m AMSL, (e) 5490 m AMSL and (f) 7320 m AMSL.	215
51	Vertical motion fields ($\times 10^{-2} \text{ms}^{-1}$) associated with weather disturbances in January 1962 : (a) 1525 m AMSL, (b) 3050 m AMSL and (c) 5490 m AMSL.	216
52	Rainfall anomalies in (a) December 1961 and (b) January 1962.	218

LIST OF PLATES

Plate		Page
1	Inundation in Bunyala location, Central Nyanza during the 1961/62 Flood episode.	10
2	Flood waters from the Nyando River flowing over the Kisumu-Ahero Road during the 1961/62 Flood episode.	10

LIST OF TABLES

Table		Page
1	Monthly mean low cloud cover and rainfall for some stations on the east-facing slopes of the Kenya/Tanzania eastern highlands.	6
2	Rainfall anomalies for some stations in East Africa during the period January 1961 through January 1962.	8
3	Number of years with pilot balloon data for each of the stations used in the study.	35
4	Rainfall stations used in the study.	37

ABSTRACT

The period between September 1961 and January 1962 saw the most severe floods experienced in East Africa (Kenya, Uganda, Tanzania) this century. Flooded rivers damaged both road and rail communications, agricultural activities were disrupted and inhabitants of the worst-hit areas were rendered homeless. Lake levels rose drastically, lake Victoria having a record rise of about 1.8 metres by June 1962. An estimate of the total loss and damage in Kenya alone was quoted at about 40 million Kenya shillings.

This study attempts to establish the characteristic features of the weather systems that gave rise to the extremely heavy rains which culminated into the widespread floods of 1961/62 in East Africa. To achieve this objective we first establish the monthly mean wind flow patterns in the lowest 7 km AMSL over East Africa. The main weather disturbances during the 1961/62 flood episode are then identified.

Daily wind vectors for 31 pilot balloon stations in East Africa have been used to establish the mean wind flow patterns. Data for 24 stations has been utilised in determining the 1961/62 wind field for the weather disturbances.

The monthly mean wind fields are presented and discussed under the four well-known seasons in East Africa : the northeast monsoon season (December-February), the long rains season

(March-May), the southeast-southwest monsoon season (June-August) and the short rains season (September-November).

The northeast monsoon air current is evident in the lowest 3 km AMSL in December. It reaches maximum development in January-February. During this period, it extends to the 4 km level. The current bifurcates over northeastern Kenya as part of it flows westwards into the interior of Africa while the other branch flows southwards almost parallel to the East African coast. The easterly current across northern Kenya is generally the stronger of the two branches. The northeast monsoon current begins to decay in March, beginning first in the lowest levels and working upwards.

The long rains season is characterised by the retreat of the northeast monsoon current and the establishment of the southeast-southwest monsoon current. The flow between 700 mb and 500 mb in April and May depicts a well-defined convergence zone (ITCZ) between northerly and southerly currents.

The southeast-southwest monsoon current is evident at the lowest levels as early as April and May. The current intensifies progressively and reaches maximum intensity in July/August. One major feature of the low level flow during this season is the well-known East African low level jet which has mean peak speeds of about 13.5 ms^{-1} in July/August at the 850 mb level. The southeast-southwest monsoon current is, like the northeast monsoon current, highly diffluent between 35°E and 40°E , and confluent in the lake Victoria

region. Over coastal Tanzania, one branch of the monsoon air flows westwards to form a speed maximum of about 8 ms^{-1} over central Tanzania. Similar branching is observed over northern Kenya. The SE-SW monsoon current influences East Africa for a longer period (April-October) and is more intense than the northeast monsoon current (December-March). However, the former is shallower (surface-3 km AMSL) than the latter which extends to the 4 km level during its period of maximum intensity.

There are two weather phenomena which are persistently evident in the lower tropospheric flow over East Africa during the SE-SW monsoon season. These are the cyclonic disturbance over the lake Victoria region and western Kenya/eastern Uganda and the 600-500 mb level anticyclone in the vicinity of Nairobi. The observed active weather conditions in the lake Victoria/western Kenya region during July/August, an otherwise dry period for the rest of East Africa, is due to interactions between land-lake breezes and this cyclonic disturbance. The dry westerly winds which have been referred to in previous studies are found to be part of the outflow from the mid-tropospheric anticyclone that is centred near Nairobi.

The short rains season is characterised by the retreat of the SE-SW monsoon current in September-October and the establishment of the ITCZ.

The divergence patterns associated with the mean flow show that the monsoon currents are not only diffluent but also highly divergent in the eastern low-lying parts of Kenya and Tanzania. Maximum divergence is about $3 \times 10^{-6} \text{ s}^{-1}$ and is observed at the 850 mb level over eastern Tanzania and eastern Kenya. This area of maximum divergence at the 850 mb level, roughly coincides with the well-known zone of rainfall deficiency in Kenya and Tanzania. During the two wet seasons, the ITCZ, is depicted as a zone of maximum convergence ($\sim 1.5 \times 10^{-6} \text{ s}^{-1}$) with ascending motion of upto $4 \times 10^{-2} \text{ ms}^{-1}$ at the 500 mb level. The ITCZ has a slight equatorward tilt with height.

The onset of the 1961/62 flood episode was marked by dramatic 2-3 day intense falls at the Kenyan coast towards the end of September 1961.

The major weather disturbances in September and October 1961 included anticyclones over southern Tanzania and off the northeastern part of East Africa. Outflow from the anticyclone over southern Tanzania was well-organised and converged into the central parts of East Africa. The low level air flow in this region was characterised by well-marked air inflows in the entire lower troposphere. This was capped aloft by a well-organised air outflow. This configuration gave rise to the heavy rainfalls during October 1961.

The wettest month during the flood period was November 1961. During this month, the whole of East Africa was engulfed by an anomalous westerly air current which converged into the vortices that are found in the ITCZ over the Kenya highlands

and off the Kenyan coast. The air current was convergent in a deep layer extending to the 500-400 mb levels. The magnitude of convergence associated with the westerly perturbation was about $1.5 \times 10^{-6} \text{ s}^{-1}$ while the maximum upward motions were about $5 \times 10^{-2} \text{ ms}^{-1}$.

In the next two months, that is, December 1961 and January 1962, the westerly disturbance intensified and the air current converged into the ITCZ vortices now centred over southeast Tanzania/northern Mozambique. The westerly disturbance that prevailed during this period gave rise to a westerly flow which completely replaced the normally diffluent northeast monsoon current in December and January. The origin of the westerly air flow, which was dominant in December 1961 and January 1962, seems to have consisted of two sources : the Congo/SE Atlantic westerlies and a recurved northeast monsoon air current from the southwest Indian Ocean.

and off the Kenyan coast. The air current was convergent in a deep layer extending to the 500-400 mb levels. The magnitude of convergence associated with the westerly perturbation was about $1.5 \times 10^{-6} \text{ s}^{-1}$ while the maximum upward motions were about $5 \times 10^{-2} \text{ ms}^{-1}$.

In the next two months, that is, December 1961 and January 1962, the westerly disturbance intensified and the air current converged into the ITCZ vortices now centred over southeast Tanzania/northern Mozambique. The westerly disturbance that prevailed during this period gave rise to a westerly flow which completely replaced the normally diffluent northeast monsoon current in December and January. The origin of the westerly air flow, which was dominant in December 1961 and January 1962, seems to have consisted of two sources : the Congo/SE Atlantic westerlies and a recurved northeast monsoon air current from the southwest Indian Ocean.

CHAPTER 1

1.0 INTRODUCTION AND LITERATURE REVIEW

1.1.0 Introduction

East Africa, comprising Kenya, Uganda and Tanzania (Fig. 1), lies between latitudes 4°N and 11°S and longitudes 30°E and 42°E . It covers an area of about 1.8 million square kilometres which is characterised by great variation of topography. The region is bounded to the east by the Indian ocean, with a coastline of about 1200 km long. In the interior, the land rises from the coastal plains to over 5000 metres in the East African eastern highlands which include, the Aberdares, Mount Kenya in Kenya, and, Mount Kilimanjaro and the Pare-Usambara mountain ranges in northeastern Tanzania.

The eastern highlands are separated from the western highlands by the eastern branch of the Great Rift Valley which runs through Kenya and Tanzania in a north-south direction. Within this branch are lakes Turkana, Baringo, Nakuru, Naivasha and Elementaita in Kenya, and, Natron and Eyasi in Tanzania. To the west of the eastern Rift Valley branch is another meridionally-oriented chain of mountains comprising of Elgon on the Kenya/Uganda border, Iringa and Rungwe highlands and the Fipa plateaux in Tanzania. East Africa is bordered to the west by the western branch of the Rift Valley. Within this branch are

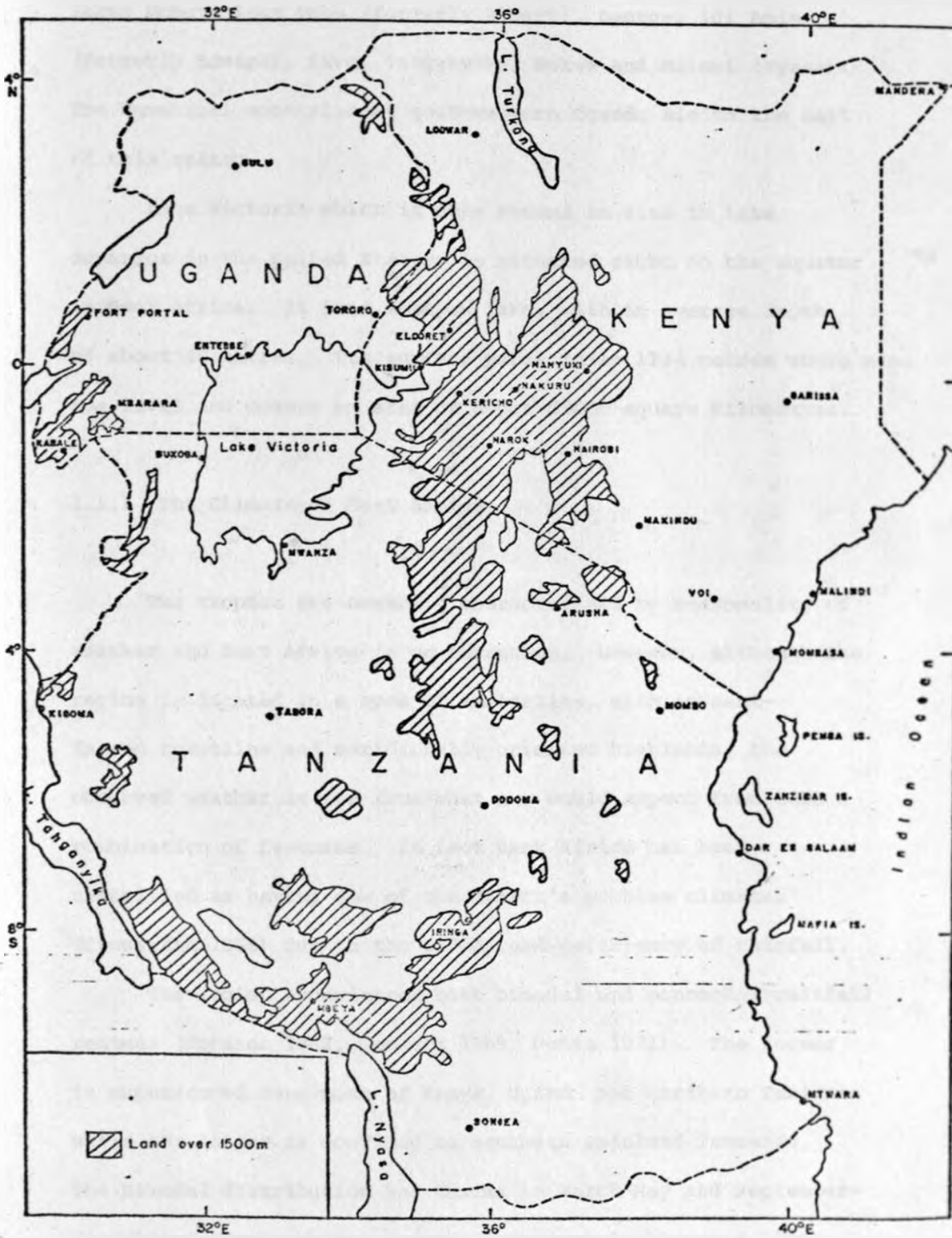


Fig. 1 : Region of study and location of pilot balloon stations used in the study.

lakes Mobutu Sese Seko (formerly Albert), George, Idi Amin (formerly Edward), Kivu, Tanganyika, Rukwa and Malawi (Nyasa). The Ruwenzori mountains of southwestern Uganda lie to the east of this branch.

Lake Victoria which is only second in size to lake Superior in the United States, is situated right on the equator in East Africa. It is a shallow lake, with an average depth of about 40 metres. Its surface water is at 1134 metres above mean sea level and covers an area of about 69000 square kilometres.

1.1.1 The Climate of East Africa

The tropics are normally characterised by seasonality of weather and East Africa is no exception. However, although the region is located in a zone of easterlies, with an east-facing coastline and meridionally oriented highlands, the observed weather is far from what one would expect from such a combination of features. In fact East Africa has been classified as having one of the "earth's problem climates" (Trewartha 1966) due to the widespread deficiency of rainfall.

The region experiences both bimodal and monomodal rainfall regimes (Johnson 1962, Tomsett 1969, Potts 1971). The former is experienced over most of Kenya, Uganda and northern Tanzania while the latter is confined to southern mainland Tanzania. The bimodal distribution has maxima in March-May and September-November. These two wet seasons are commonly known as "long rains" and "short rains" respectively, and occur when the Inter-tropical Convergence Zone (ITCZ) has maximum influence

over most of East Africa. The single maximum in southern Tanzania occurs in November-May when the ITCZ reaches its southmost extent over the continent of Africa.

Between the two wet seasons, there are two dry seasons when East Africa comes under the influence of the monsoon air currents of the West Indian ocean. The northeast monsoon occurs during the southern hemisphere summer season while the southeast-southwest monsoon occurs during the northern hemisphere summer season.

The northeast monsoon air current is hot and dry in most parts of East Africa and is part of the equatorward outflow from the Arabian high pressure. The southeast-southwest monsoon air, on the other hand, flows from the Mascarene high in the south and is cool and moist. These monsoon currents are shallow, being confined to the lowest 3 kilometres above mean sea level (Findlater 1968). They are over-ridden aloft by an easterly current. The diminished precipitational activities over most parts of East Africa during the monsoon seasons have been attributed to the pronounced diffluence/divergence of the monsoon currents along the East African coastal plains (Forsdyke 1949, Glover et al 1954, Trewartha 1966, Findlater 1968). They also tend to flow parallel to the coast and the north-south running East Africa highlands. Thus, apart from being unable to advect moisture from the Indian ocean into the interior, these winds do not experience appreciable orographic lifting which would enhance vertical motion and hence precipitation. However, there are occasions, especially

during the month of January, when the northeast monsoon current has a long track along the ocean. Such occasions are accompanied by rainy periods.

The southeast-southwest monsoon, although dry over most parts of East Africa, is accompanied by extreme cloudiness especially over the eastern highlands (Atkinson and Sadler 1970). Table 1 shows the monthly mean cloud cover and rainfall totals for a few stations in this region. The inconsistency between cloudiness and precipitation in this area during the SE/SW monsoon season has been attributed to the existence of an inversion layer whose base is near 700 mb and top near the 650 mb levels (Taljaard 1955). This inversion damps further cloud development, rendering them shallow and therefore unable to precipitate.

Apart from the seasonal rains, East Africa also benefits from out of season rains. Among the systems which bring such rains are, moist unstable westerlies from the Congo region, subtropical upper troughs which have penetrated deep into the low latitudes, northward penetration of residual instability associated with middle latitude cold fronts, and easterly waves. We consider each of these influences in section 1.2.

The seasonal features discussed above undergo year to year variations so that we have years of heavy rainfalls leading to severe flooding, and years of deficient rainfall that lead to drought; years of strong monsoon currents and years when systems are weaker than normal. Such are the variations that one would wish to be in a position to predict.

	Nairobi/Embakasi (01°19'S 36°55'E)		Voi (03°24'S 38°34'E)		Same (04°05'S 37°43'E)		Makindu (02°17'S 37°50'E)	
	Cloud cover (oktas)	Rainfall (mm)	Cloud cover (oktas)	Rainfall (mm)	Cloud cover (oktas)	Rainfall (mm)	Cloud cover (oktas)	Rainfall (mm)
January	3.2	56	4.3	32	3.0	43	4.7	40
February	3.5	48	4.3	30	3.2	61	4.7	31
March	4.2	78	5.1	82	4.0	87	5.5	81
April	5.0	144	5.2	93	4.6	122	5.7	113
May	5.2	124	5.7	29	4.5	68	6.1	29
June	4.9	22	5.6	7	4.1	8	5.8	2
July	5.7	6	6.0	3	4.1	6	5.3	1
August	5.8	15	6.1	8	4.3	11	6.2	1
September	5.1	13	5.7	15	3.8	13	5.3	2
October	5.1	45	5.1	28	4.4	30	5.2	28
November	4.9	152	5.3	100	4.1	53	5.9	178
December	3.9	81	4.7	122	3.1	67	5.6	119

Table 1 : Monthly mean low cloud cover (at 1200 GMT) and mean rainfall for some stations on the east-facing slopes of the Kenya/Tanzania eastern highlands.

East Africa experienced such a weather anomaly from September 1961 to January 1962, when there was widespread and continuous rain which resulted in severe floods.

1.1.2 The Floods of 1961-1962

During the first 7-8 months of 1961, Kenya and Tanzania suffered severe drought. The drought was succeeded by very wet conditions which culminated in very severe flooding in most parts of East Africa. Table 2 shows rainfall anomalies for some stations in East Africa during 1961/62. The East African countries were plunged into a long famine resulting from an interplay between two extremes of drought and floods. "This year is unique. Until October 1 it was the driest for 40 years. Since that time it has been the wettest for 100 years". This was said by the then Kenya's Agriculture Minister while announcing the setting of a committee to make urgent assessment of the total damage caused to the country's agriculture (DAILY NATION, OCTOBER 1961).

In Kenya, the first heavy falls occurred near the coast between 25 and 27 September, destroying the bridge over Sabaki river north of Malindi (Grundy 1963). By October, rainfall was widespread with heavy falls occurring at frequent intervals. Peak values of river stages were reached towards the end of November. In some parts of Western Kenya, these unusual weather conditions were to recur with even greater intensity during the long rains of 1962. An estimate of the total loss and damage

	1961												1962
	Jan.	Feb.	Mar.	Apr.	May	Jun.	Jul.	Aug.	Sept.	Oct.	Nov.	Dec.	Jan.
Lodwar (03°07'N 35°37'E)	-1.1	-6.5	-16.0	-13.2	-22.2	9.2	1.3	2.0	-3.0	80.7	94.4	184.7	-1.1
Lamu (02°16'S 40°54'E)	-5.0	27.8	-9.6	-12.6	-239.0	-7.8	184.5	12.7	446.3	12.9	177.9	0.7	-2.7
Entebbe (0°03'N 32°27'E)	44.5	-10.3	11.9	-20.8	-89.1	-27.8	9.9	20.4	60.3	154.2	222.5	90.8	-7.0
Mtwara (10°21'S 40°11'E)	-106.1	-8.8	62.1	61.6	78.0	-6.6	33.7	-6.2	-37.1	6.0	66.3	61.9	327.6
Tororo (00°41'N 34°10'E)	-37.0	-0.8	-18.0	55.2	-1.7	7.0	31.1	109.8	38.7	12.1	155.1	161.4	20.6
Dodoma (06°10'S 35°46'E)	-97.5	43.2	-43.6	9.7	-5.0	-1.0	0.3	0.0	-1.0	-0.2	21.0	157.6	112.2
Dar es Salaam (06°53'S 39°12'E)	-67.3	108.5	-107.1	-109.6	83.2	34.6	123.4	-10.7	-4.2	224.8	293.3	196.0	9.0
Mandera (03°56'N 41°52'E)	1.0	-8.0	-11.3	10.0	3.0	-0.5	-1.0	1.5	1.0	-12.8	145.2	7.0	-1.0
Mwanza (02°28'S 32°55'E)	-87.5	48.0	-18.0	28.5	-34.7	-11.0	-13.0	66.3	-9.8	170.6	261.3	60.4	95.1
Mbeya (08°56'S 33°28'E)	-39.7	-7.9	-2.8	7.6	13.2	-1.0	-1.0	-1.0	5.0	27.9	62.6	230.4	131.2
Nairobi (Embakasi) (01°19'S 36°55'E)	-55.2	-36.1	19.8	-70.8	-15.8	8.8	-0.8	-4.5	20.1	178.9	332.0	195.0	56.2

Table 2 : Rainfall anomalies (mm) for some stations in East Africa from January 1961 through January 1962. Negative values are below average while positive values are above average monthly rainfalls.

in Kenya alone was quoted at about 40 million Kenya shillings (East African Meteorological Department Annual Report, 1961/62).

In Tanzania, the heaviest falls occurred during November, with coastal, northern and lake regions having record falls. February and May 1962 were relatively dry. April had a most irregular distribution, with lake region and south coast having above normal rainfalls, while north coast had very little rain, if any. Zanzibar was very wet in April. In Uganda, there was gradual increase in rainfall from July 1961. Between October and December, most stations recorded their heaviest ever falls.

The widespread flooding in the region caused lake levels to rise dramatically. Lake Victoria level at the Jinja gauge was recorded to have had a rise of 1.57 metres from September 1961 to June 1962 (Fig. 2). Rivers burst through their banks flooding low-lying areas (Plates 1-2). Many bridges were destroyed or submerged for periods of days (Grundy 1963) and many roads and rail embankments washed away. River gauging stations were destroyed, equipment washed away and some channels suffered so much erosion that the stations had to be abandoned. The East African Meteorological Department attributed the unusual heavy rains to "massive horizontal convergence in the low level wind field" (Grundy 1963), coupled with advection of large amounts of water vapour into the East African lower troposphere.

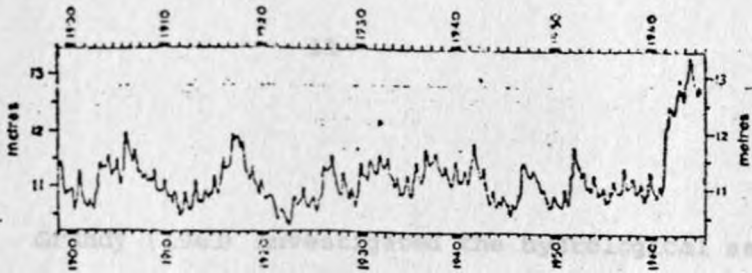


Fig. 2: Levels of Lake Victoria (metres above datum) at the Jinja gauge ($1^{\circ} N 33^{\circ} E$): (after Morth 1967).

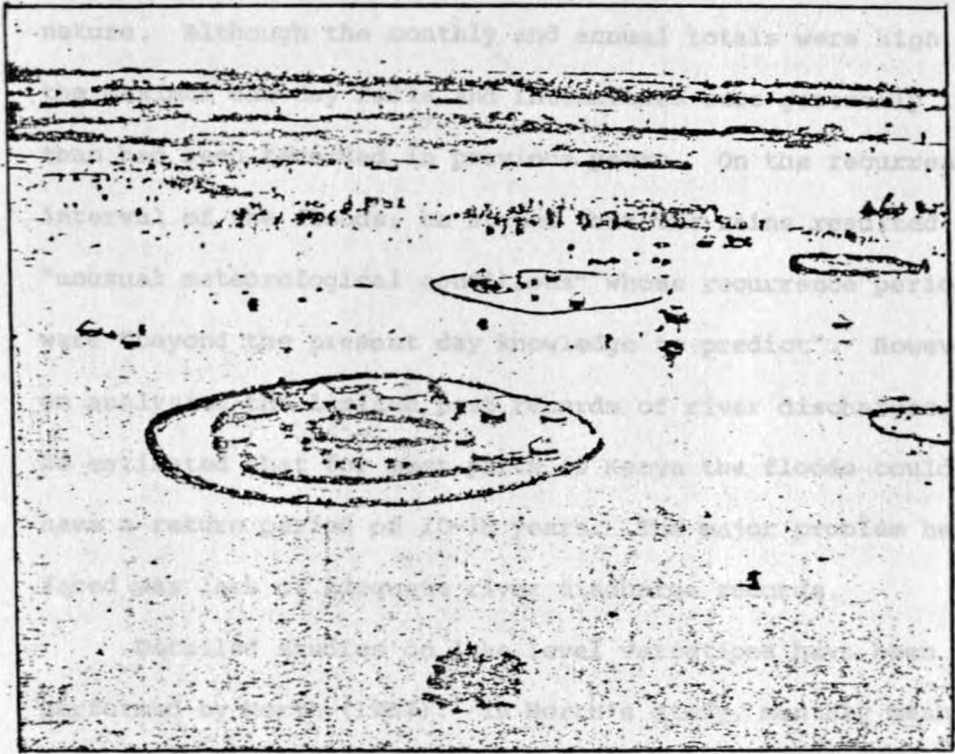


Plate 1.—Inundation in Bunyala Location, Central Nyarza (after Grundy 1963)

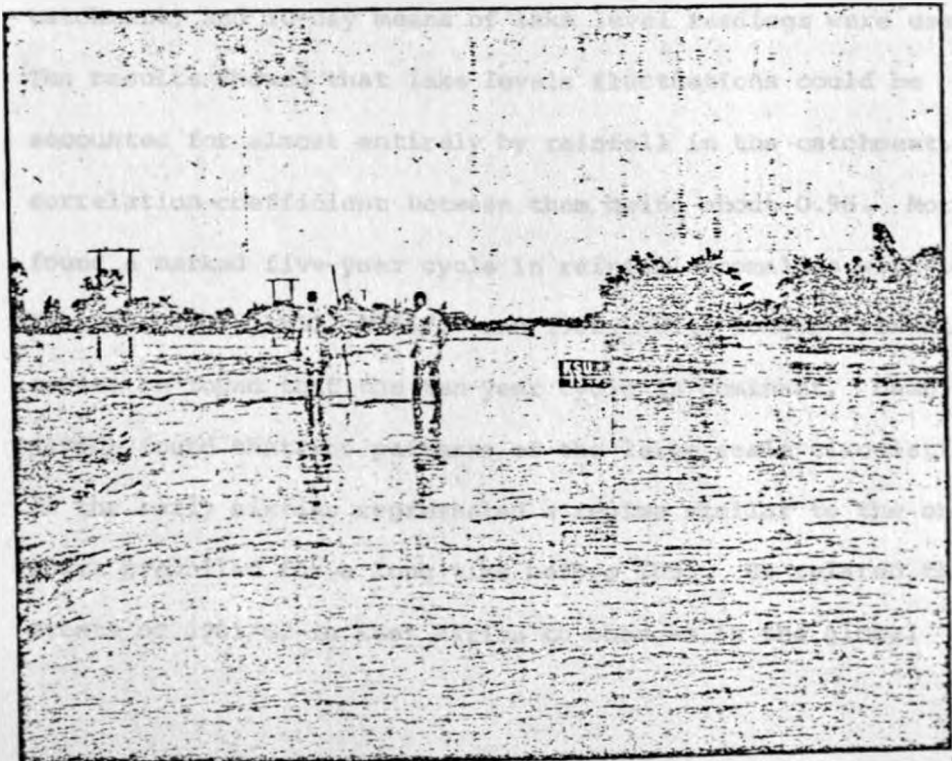


Plate 2.—Flood waters from the Nyando River flowing over the Kisumu-Ahero Road (after Grundy 1963)

Grundy (1963) investigated the hydrological aspects of the floods. He noted that the most peculiar feature of the rainfall during the episode was its continuous and widespread nature. Although the monthly and annual totals were high, the maximum one-day falls and intensities were generally lower than had been recorded in previous years. On the recurrence interval of the floods, he stated that the rains resulted from "unusual meteorological conditions" whose recurrence periods were "beyond the present day knowledge to predict". However, on analysing the limited past records of river discharges, he estimated that for most parts of Kenya the floods could have a return period of 10-18 years. The major problem he faced was lack of adequate river discharge records.

Detailed studies on lake level variations have been performed by Morth (1967). In Morth's study, monthly mean rainfall amounts for 150-300 raingauges in the lake Victoria catchment, and 10-day means of lake level readings were used. The results showed that lake levels fluctuations could be accounted for almost entirely by rainfall in the catchment, correlation coefficient between them being about 0.96. Morth found a marked five-year cycle in rainfall anomalies with peaks in 1942, 1947, 1952, 1956/57 and 1962. With longer rainfall series he found that the ten-year cycle is dominant. Lamb (1966) found that the patterns of the large scale circulation in the early sixties represented a regime similar to the one which prevailed for a long time before 1895. He related the events of 1961/62 in East Africa to changes in the global

circulation of the atmosphere.

Although the effects of the 1961/62 floods were far reaching, no detailed studies have been carried out regarding the meteorological factors responsible for the very heavy rainfalls that led to the floods. It is the purpose of this study to investigate the weather systems which gave rise to the abnormally wet conditions of 1961/62.

1.1.3 Objective of Study

The aim of the study is to establish the characteristic features of the weather systems that gave rise to the unusually rainy conditions of 1961/62 in East Africa. To achieve the object of this study we propose to do the following:-

- (a) First we determine the mean characteristics of the horizontal motion fields in the atmosphere over East Africa. This is done on monthly basis using available optical pilot balloon data.
- (b) Secondly, we attempt to establish the characteristic features of the transient rain-bringing weather systems that gave rise to the abnormally wet conditions in East Africa during the period September 1961-January 1962.

1.2.0 LITERATURE REVIEW

1.2.1.0 Synoptic Systems affecting East Africa

The major synoptic systems affecting East Africa include the monsoon currents, the ITCZ, westerly winds from the Congo region, Easterly waves, tropical cyclones, and indirect effects from remnants of middle latitude frontal instability and upper level troughs in the westerlies. In addition to the synoptic scale systems, East Africa has strong meso-scale systems in the form of land-sea and land-lake breezes and mountain winds.

1.2.1.1 The Monsoons

East Africa experiences two different monsoon systems in a year. These are the northeast monsoon and the southeast-southwest monsoon of northern winter and summer season respectively. The monsoon currents and in particular the SE/SW monsoon of the west Indian ocean, have been studied widely since the pioneering work of Findlater (1969a,b, 1971, 1974) and the monthly mean wind analyses of Ramage and Raman (1972).

The northeast monsoon, whose roots are in the high pressure centre over Arabia and India during northern winter, is known to be shallow and highly diffluent (Findlater 1968, 1971). It is well-developed over the northeastern coast of Africa. Over East Africa, it bifurcates into two streams. One flows southwards along the coast while the other flows westwards into the interior. High speed flows occurs in both branches and on occasions, speeds of $30-40 \text{ ms}^{-1}$ have been

recorded (Findlater 1971). Unlike the SE/SW monsoon over the region, the northeast monsoon has not attracted much scientific interest, probably due to its dryness over most parts of East Africa. However, the northeast monsoon season is the major rainy period for southern and southwestern Tanzania (Johnson 1962, Tomsett 1969, Potts 1971, Alusa and Mushi 1974). During this period, the ITCZ is in the southern hemisphere and has maximum influence on weather activities in southern Tanzania.

The southeast-southwest monsoon current is characterised by the presence of the East African low level jet (EALLJ) (Findlater 1969a, 1971, 1972, 1974), whose observational aspects have been summarised by Findlater (1977). The northern summer cross-equatorial air current over the west Indian ocean has important contributions towards the inter-hemispheric exchanges of mass and energy (Findlater 1969b, Cadet and Reverdin 1980). The EALLJ flows from the vicinity of Mauritius and Madagascar (Findlater 1969a, Desai et al 1976), across the East African coast and through the Somali coast towards India. The jet core is located between 1-1.5 km AMSL and has mean speeds of about 12.5 ms^{-1} . The dimensions of the jet have been estimated to be 200-400 km wide, 500-1000 km long and about 1 km deep. The jet exhibits marked diurnal oscillation in the intensity and altitude of peak wind speeds (Ngara 1977, Ardanuy 1979, Rao and Van de Boogaard 1981). Afternoon speeds are about two thirds of the morning speeds. Spectral analysis of the jet's intensity has demonstrated the existence of 4-5 day (Ngara and Asnani 1978) and quasi-biweekly (~15 days)

oscillations (Krishnamurti and Bhalme 1976).

On the theoretical aspects of the jet, several studies (Anderson 1976, Krishnamurti et al 1976, Bannon 1979a,b) have indicated that the low level jet can be viewed as a western boundary current. Hart (1977) describes some of the theoretical models used for studying this jet.

Although the flow off the East African coastal plains has had a fair amount of scientific investigation, very little is known about the behaviour of the monsoon current immediately to the west of the coastal plains. Findlater's analyses cover a good portion of the interior of Kenya, but not Uganda and Tanzania. The analyses of Ramage and Raman (1972) do not adequately resolve the flow over East Africa as they used sparse data network in the region. Recently Kiangi et al (1981) presented a detailed analysis of the wind flow over East Africa for the months of April and May.

The SE/SW monsoon season is generally dry over most parts of East Africa. However, some parts of western Kenya/eastern Uganda experience their wettest conditions during this season (Tomsett 1969). The extreme wetness of this region during the northern summer monsoon season when the rest of East Africa is dry, has not been explained satisfactorily. Kiangi et al (1981) have suggested that the rains are due to interactions between the southeast monsoon current and the lake Victoria thermally induced meso-scale circulation. It is believed that the quasi-permanent orographic-induced trough over central Africa (Semazzi 1979) intensifies and subsequently

merges with the lake Victoria trough during this season.

We shall discuss possible causes of these rains in section 3.1.3.1.

1.2.1.2 The Inter-tropical Convergence Zone (ITCZ)

In the past there has been much controversy as to the nomenclature to be applied to the zone of confluence (or convergence zone) between southerly and northerly flows in the tropics (Palmer 1951, Thompson 1957a, Johnson 1963, Sanson 1963, Dean and LaSeur 1974). Palmer (1951) divided tropical meteorologists into three "Schools of thought". The "Climatological School" is that group who emphasised large scale features on mean charts and diurnal features associated with geographical influences. According to this group, the confluence zone between southerly and northerly flows in any one season, was referred to as either the Equatorial Trough or the Inter-tropical Convergence Zone. The "air mass-frontal school" referred to the confluence zone as the Inter-tropical Front (ITF) and attempted to interpret weather activities in this front in a similar fashion to its counterpart in the middle latitudes. This approach met with some success in West Africa where there are distinct discontinuities in air mass characteristics between the warm dry continental northeasterlies and the cool-moist maritime southwesterlies. However observations showed that there were dissimilarities between the weather associated with the ITF and that associated with middle latitude

fronts. This approach was then abandoned. In West Africa, (Okulaja 1970, Adefolalu 1974) the term "Inter-tropical Discontinuity" (ITD) has been adopted. The third school of thought is the "Perturbation school" who recognised the formation in the confluence zone, of easterly waves which play a major role in weather activities of West Africa during northern summer season (Hamilton and Archbold 1945, Carlson 1969, Burpee 1972, Adefolalu 1974).

In East Africa, the position of the ITCZ on daily synoptic charts and monthly mean charts is difficult to locate (Thompson 1957a). During the equinoctical periods when East Africa receives most of its rain, we have one monsoon retreating, the other advancing. Winds from both hemispheres have a more easterly component and are weak (Thompson 1957a, Trewartha 1966). The confluence between them is diffuse and is hardly detectable on daily charts. The diffuse nature of the ITCZ can be attributed to orographic influences. The seasonal rains do not fall in any organised zonal belt. Rain just falls in scattered areas simultaneously then fades away (Johnson 1963). One cannot therefore locate the ITCZ by studying the spatial distribution of rain areas. However, since East Africa rains are seasonal, lagging behind the sun's declination by a month or two (Trewartha 1966), it is generally accepted that they are associated with the ITCZ (Johnson 1962, Alusa and Mushi 1974).

The earliest major research aimed at relating the observed behaviour of rainfall in East Africa to the upper air wind and pressure fields is that of Johnson and Morth (1960).

Their study used data from about fifty synoptic stations in East Africa. Johnson and Morth carried out the first ever contour analyses in the region. They were able to identify certain models useful for forecasting in East Africa. The most frequently observed models were:-

- (i) The "equatorial duct" which is observed when two high pressure centres lie on either side of the equator causing the flow between them to be quasi-geostrophic.
- (ii) "cross-equatorial drift" which is the cross-contour flow observed when a high pressure or ridge lies on one side and a low pressure or trough lies on the other side of the equator. A mathematical description, partly based on empirical results pertaining to the cross-equatorial flow during the SE/SW monsoon season, has been given by Obasi (1972).
- (iii) The "equatorial bridge" is observed when there are low pressure centres on either side of the equator. The flow between them is quasi-geostrophic.

On daily charts, the observed situations are variations of these primary models. The Duct situation describes the flow over East Africa when the ITCZ is over the region. In this case we have the Arabian high and the Mascarene high forming a duct with entrance over East Africa. This results

in deep convergence over most of the area excluding southern Tanzania. The intensity of weather activities over East Africa during the two wet seasons is therefore determined by the intensity and orientation of the two high pressure cells. The short rains over East Africa are believed to be almost entirely from ducts created by these two highs (Johnson and Morth 1960).

The wind analyses of Kiangi et al (1981) for the months of April and May depict the ITCZ as a line of confluence between north-easterlies and south-easterlies. At the 700 mb level, the ITCZ is found over northern Tanzania and southern Kenya in April and over central Kenya and Uganda in May. The zone is found to slant equatorward with height, having a slope of 1:100 to 1:350 in May and 1:100 to 1:200 in April.

The ITCZ migrates north-south following the seasonal march of the overhead sun and also exhibits fluctuations with a time scale extending beyond a few days (Sansom 1963, Sawyer 1970, Adefolalu 1974). Sawyer (1970) suggested that the occurrence of wet and dry spells within the seasonal rains in East Africa could be due to these intermediate oscillations of the ITCZ. Sansom and Sawyer attributed these fluctuations to changes on synoptic scale pressure fields. Adefolalu (1974) has found a 4-5 day meridional synoptic scale oscillation in the monsoon trough over West Africa during northern summer season. The ITCZ over East Africa exhibits diurnal oscillations due to changes in surface pressure distribution. Sansom (1963)

pointed out that these diurnal oscillations are more pronounced in areas of strong meso-scale circulations such as the lake Victoria region.

1.2.1.3 Equatorial Westerlies

Westerly winds in equatorial regions are believed to be rain bringers. A theoretical explanation (Flohn 1960, Johnson and Morth 1960) is to be found in the expression for vertical acceleration:

$$\frac{dw}{dt} = -\alpha \frac{\partial p}{\partial z} + 2u\Omega \cos\phi - g$$

where $-\alpha \frac{\partial p}{\partial z}$ and $2\Omega \cos\phi u$ are the vertical components of the pressure gradient force and Coriolis force respectively, while g is acceleration due to gravity. The Coriolis term contributes to vertical acceleration positively when the flow is westerly, and negatively when the flow is easterly. In large scale motions this term is normally neglected on the basis that it is very small compared to the other two forces. However, it has been argued (Johnson and Morth 1960) that the term is appreciable in the tropics, being maximum at the equator, and cannot therefore be ignored in low latitudes.

East African equatorial westerlies have attracted considerable scientific interests (Thompson 1957a, Flohn 1960, Johnson and Morth 1960, Nakamura 1968). Flohn (1960) found a belt of westerlies spanning equatorial Africa. The altitude

of these westerlies was 2-3 km AMSL. Flohn referred to the 700 mb level westerlies observed at Kisumu, Nairobi and Mombasa in East Africa during northern summer, as being a bridge between the Congo westerlies and the west Indian ocean southwesterlies. He noted that, unlike the trades, these westerlies were more variable in time and space. Their persistency over oceans was 60% and lower over land. Nakamura (1968) concluded that these westerlies were more like the extra-tropical westerlies with their frequent perturbations. In East Africa, it is generally accepted that occasions of deep westerlies are more productive of rain than those when easterlies prevail (Johnson and Morth 1960). Of westerly incursions in the region, Thompson (1957a) writes, "They provide the forecaster with his happiest and most confident predictions, except he is never sure when the inevitable recession will occur". Although the causes of their occurrence are obscure, a definite westerly flow occurs in southern Tanzania when a tropical cyclone is located north of Madagascar (Thompson 1957a). According to Henderson (1949), westerlies affecting Uganda may occur at any time of the year. Those affecting southern Tanzania occur from December to April (Thompson 1957a) and chiefly in January-February. Nakamura (1968) distinguished two regimes of westerlies in East Africa, those occurring in January-March in southern Tanzania and the May-October westerlies. The latter were observed to affect a wider area, chiefly the eastern parts of East Africa, extending from 10°S , across the equator into the northern hemisphere. They were found between 700-500 mb, embedded in

easterly currents.

In addition to the diversity of opinion concerning the times of occurrence of East African westerlies, there are disagreements as to their origin. Most workers (Henderson 1949, Glover et al 1954, Tomsett 1969, Griffiths 1959) have attributed the relative wetness of the western parts of East Africa to incursions of westerlies which are believed to be unstable and originating from the Congo area. The lower rainfall variability in western East Africa has, in fact, been attributed to the more frequent occurrence of Congo westerly air current in this region (Glover et al 1954, Griffiths 1959). Nakamura (1968), on the other hand, noted that the westerlies, especially those observed in the vicinity of Nairobi during May-October, could not be from the Congo (Zaire) since they were least frequent in the western parts of East Africa. Furthermore, although regarded as rain bringers, the statistical analyses of Johnson and Morth (1960) between mean wind directions in the layer 750-550 mb, and raininess in the vicinity of Nairobi, revealed many occasions of rainless westerlies during June-October. Nakamura found similar results and observed further that these westerlies, although moist, were neither cooler nor more unstable than the easterlies.

1.2.1.4 Easterly Waves

These are westward propagating wavelike perturbations within the easterly current on the equatorward sides of the subtropical high pressure belts. They have, especially those occurring in the north Atlantic ocean, been described in detail by Riehl (1954). Equatorial waves in the Pacific ocean have been studied by Palmer (1952). The main difference between the equatorial waves and Riehl's easterly waves is that the former are close enough to the equator for troughs and crests on either side of the equator to both represent cyclonic circulations. In west Africa, they are observed in the neighbourhood of the ITCZ during northern summer (Carlson 1969, Burpee 1972, Adefolalu 1974).

Although it is now accepted that easterly waves exist in the entire tropical belt, they have received very little attention in the southern hemisphere. There are a number of difficulties encountered. For one, these waves are relatively feeble features that are not easily noticed on tropical synoptic charts where quasi-permanent synoptic systems are dominant. Secondly, these waves do not have uniform structure and their properties vary from place to place. Thirdly, there is general paucity of data in the southern hemisphere.

The occurrence of easterly waves in the southwest Indian ocean was first mentioned during the second World War (Forsdyke 1960). In later years it was reported that easterly waves

moved across the west Indian ocean during northern summer season (Zangvil 1975). Cadet and Olory-Togbe (1977) studied time-longitude sections of cloud cover in the Indian ocean between June and August 1975. They found the existence of tropical disturbances which were eastward moving north of the equator and westward moving south of the equator. The easterly disturbances south of the equator were hardly discernible at the East African coast (Mombasa and Dar es Salaam).

Thompson (1957a) observed organised belts of rainfall oriented in SSW-NNE direction (approximately normal to the air flow) during northern summer season. These rainfall belts moved towards the East African coast but never penetrated more than 80 km inland. Gichuiya (1970) investigated 18 episodes of heavy rainfall at coastal stations during the cool-dry season of July-September 1967. In each case he followed the disturbance from the ocean using surface chart analysis, satellite pictures and aircraft reports. Gichuiya found that the rain-bringing disturbances exhibited similar properties to the Caribbean easterly waves, over the ocean areas where the prevailing flow was easterly. However, on approaching the East African coast where the flow was southerly, differences were observed.

The waves studied by Gichuiya exhibited the following properties:-

- (i) The direction of propagation was northwest.
- (ii) The cyclonic curvature was manifested most clearly between 700-500 mb where closed circulations could occur.
- (iii) There were no significant temperature changes.
- (iv) The disturbances were preceded by clear weather
- (v) The area of maximum precipitation lay along a well-defined line.

Fremming (1970) has given an account of an easterly disturbance which affected the East African coast between 5-7 September 1967. The disturbance had similar properties to those of easterly waves. The passage of the wave was marked by backing of wind from SSW to SE, and heavy rainfall. On reaching the coast, the wave did not penetrate inland. Instead, it moved slowly northward towards Lamu (2°S , 41°E) where the highest 24-hour rainfall (214 mm) was recorded during the whole season. Failure of easterly waves to penetrate inland was attributed to pronounced diffluence in the low level monsoon current over the East African coast (Thompson 1957a). Even during the wet seasons, when the ITCZ lies over the area, no waves of the type described by Palmer (1952) had been detected in the interior.

However, the recent work by Njau (1982), in which time series of upper wind data at Nairobi, Entebbe and Dar es Salaam

were subjected to spectral analysis, revealed wave disturbances with periods ranging from 2-3.5, 3.7-5, 5.7-8, 9, 10, 12-15 and 17-22 days. These disturbances were propagating westwards. The 2-3.5 day oscillation had a zonal wavelength of 20° longitude, phase speed of 7° longitude/day and was observed during all seasons. The 3.7-5 day disturbance had a wavelength of 25° longitude and a phase speed of 6° longitude/day. The disturbances had maximum intensity in the lower and middle troposphere, and were either nearly vertical or had a slight westward tilt with height. Rainfall series exhibited fluctuations with similar periods to those observed in the wind field.

1.2.1.5 Influences from the Middle Latitude Instabilities

It is recognised that some of the out of season rains in East Africa are due to influences from southern subtropics (Henderson 1949, Thompson 1957a, Forsdyke 1960, Johnson 1963, Lumb 1966). Forsdyke (1960) has described northward movement of a cold front from off the southeast African coast. According to Forsdyke, these fronts do not bring much rain to East Africa except for a few cool cloudy days. Johnson (1963) and Lumb (1966) associated some of the coastal rains with residual instabilities associated with cold fronts which had intruded into the equatorial regions. These fronts, occurring during southern winter season, are accompanied by pressure rises (or surges). These surges, which are recorded at all coastal stations upto Mogadishu in Somali, are associated with

build up or decay of southern winter systems.

Another middle latitude influence is what Forsdyke (1960) refers to as "Tropical waves". These are sub-tropical upper troposphere westerly disturbances which bring rain to East Africa when they penetrate deep into the low latitudes. When an upper level trough in the southern hemisphere extra-tropical westerlies extends into equatorial regions, cool air is introduced aloft, resulting in instability (Thompson 1965). Johnson and Morth (1960) describe a case when the axis of the surface or 850 mb ridge in South Africa comes directly under an upper trough. This intensifies the sub-tropical anticyclone. Pressure gradient into the East African region is intensified and simultaneously there is instability due to introduction of cool air aloft. The system moves eastwards from the Congo and only fades when the upper and lower systems go out of phase. Such a situation is however rare since many factors have to coincide for it to be effective.

The recent work of Okoola (1982), who applied spectral analysis to surface pressure and wind data collected during MONEX-79, has revealed 5-day and quasi-biweekly oscillations in these elements in the region between the equator and 30°S . The 5-day oscillation had a zonal wavelength of 60° longitude, phase speed of 15 ms^{-1} and moved from west to east. The troughs and ridges were oriented in a north-south direction. This oscillation was associated with trough/ridge movements in the southern extra-tropical westerlies during southern winter season. He associated the quasi-biweekly oscillation

with the Hardley Cell circulation.

1.2.1.6 Tropical Cyclones

Tropical cyclones (storms) form in the west Indian ocean equatorward of 20° latitude (Gray 1968). North of the equator they form between 5° - 10° N in northern spring and late fall and move northwestwards into the Arabian sea. South of the equator, they form mainly during December-April with over 70% of the storms occurring during January-March (Atkinson 1971). They move west-southwestwards into the Mozambique channel or recurve off the east coast of Madagascar and move south-southeastwards to fade in the cool waters of the southwest Indian ocean (Thompson 1965). Those that move into the Mozambique channel affect the weather of East African coast considerably. The late occurrence of tropical storms delay the onset of long rains in April.

On very rare occasions do these storms cross into the East African mainland. In 1872 a cyclone hit Zanzibar and caused considerable damage on the Tanzania coast (Sansom 1953) and some 80 years later, on 15 April 1952, a small but intense cyclone (named Lindi Cyclone), formed off the coast of Tanzania and crossed to the mainland. The life history of the Lindi Cyclone is given in detail in Sansom (1953). It developed suddenly and dissipated completely in 48 hours. Within this time, it had caused 34 deaths and damage amounting to about 50 million Tanzania shillings.

Neave (1967) has given an account of another tropical storm named Lily. Lily was first reported by Mauritius at $7\frac{1}{2}^{\circ}\text{S}$, $65\frac{1}{2}^{\circ}\text{E}$ on 22 April 1966. It moved westwards and came very close to the East African coast before filling on 3 May at about $4\frac{1}{2}^{\circ}\text{S}$, 40°E . Little damage was caused over land by this cyclone. However, heavy rainfalls were received over eastern Tanzania and southeastern Kenya between 30 April and 4 May. Neave attributed Lily's abnormal track to the presence of high pressure all the way upto 300 mb. This high pressure was located to the immediate south as far west as 45°E then to the southwest thereafter.

North of the equator, cyclones occur only rarely in the Arabian sea and none has been recorded to have crossed the coast (Thompson 1965). However, in October 1972, a cyclone formed in the Arabian sea and was first identified at the meteorological analysis centre in Nairobi on the 1200 GMT charts on 23 October at $12-13^{\circ}\text{N}$, 57°E . It moved westwards and filled at 10°N , 50°E between 26-27 October, at the coast of the Horn of Africa. Heavy rain falls were experienced as far south as Somalia and northern Kenya.

1.2.2 Local Circulations

The varied topography, proximity of the Indian ocean and location of the vast lake Victoria in the central part of East Africa give rise to meso-scale circulations which have

significant contributions towards the complex weather patterns observed over East Africa (Lumb 1970, Sansom and Gichuiya 1971, Nieuwolt 1973, Tomsett 1975, Alusa 1976, Hills 1978, Asnani and Kinuthia 1979).

Lumb (1970) found that the contrast between diurnal variations in thunderstorm activity at Entebbe on the western shore and Kisumu on the eastern shore of lake Victoria, was due to the local topography of the area. While Entebbe has an early morning maximum, Kisumu has an afternoon maximum in thunderstorm activity. This is because of the difference in the interactions of the land/lake breezes and the large scale easterly wind flow. In Kisumu the lake breeze interacts with the prevailing easterlies to yield active weather. For Entebbe, the lake breeze is parallel to large scale easterlies, and the land breeze interacts with the prevailing easterlies to yield the observed night-time active weather.

The Kericho-Nandi Hills area experiences severe thunderstorms/hail storms. The occurrence of hail storms in this area has one of the highest frequencies of occurrence in the world (Sansom and Gichuiya 1971, Alusa 1976). Kericho is situated on high ground to the east of lake Victoria. To its east, the land slants gradually from the Kenya highlands down to the coastal plains. During the day, we have lake breeze and upslope winds from the west and sea breeze, upslope winds and the general easterly current from the east. These moist air currents converge just east of Kericho-Nandi Hills. The

convergence of these currents leads to severe thunderstorms/hailstorms that move westward with the general flow to hail over the Kericho area (Alusa 1976).

Asnani and Kinuthia (1979) looked at the mesoscale systems that are responsible for the observed diurnal patterns of rainfall over East Africa. They concluded that diurnal patterns of rainfall in the region are determined largely by interactions between mesoscale flows and the synoptic scale low level flow. Tomsett (1975) observed that the times of occurrence of maximum rainfall exhibited seasonal variations. This manifests the interaction between meso-scale flows and the seasonally varying synoptic scale flow in East Africa. Chaggar (1977) in his study of the temporal and spatial distribution of frequency of thunderstorm days over East Africa, found that the movement and distribution of thunderstorms from one month to another depended more on the local topography than the simple north-south movement of ITCZ.

Of particular interest is the extremely high frequency of thunderstorm activity in western Kenya/eastern Uganda during the southeast-southwest monsoon season (Alusa 1976, Chaggar 1977). Chaggar observed that it was difficult to relate the observed distribution of thunderstorms to the known synoptic and climatological situations. We discuss this feature further in a later section when dealing with northern summer rains in western Kenya/eastern Uganda.

Over coastal Tanzania, where monsoon currents are relatively strong, Nieuwolt (1973) found that during the northeast monsoon season, the sea breeze is dominant, while during the SE/SW monsoon season, the dominant flow at low levels is from land. It is only during the intermediate periods between the monsoons that there develops a distinct reversal between land and sea breezes, another example of the interaction between land/sea breezes and the seasonally varying synoptic flow.

Theoretical studies on meso-scale circulations in the area are few (Fraedrich 1972, Okeyo 1982). Fraedrich used a simple analytic model to simulate the climatological features of the nocturnal meso-scale circulation over lake Victoria. His results agreed well with the observed features. Okeyo (1982), on the other hand, used a two-dimensional hydrostatic model in an attempt to simulate lake/land and sea/land breezes over Kenya. The results from his experiments show a well-defined convergence zone over the Kericho-Nandi Hills areas during the afternoon hours, in good agreement with the observed organisation of cumulus convection over the Kenya highlands during the day. It was further shown by Okeyo that the combined land/lake and land/sea breezes and upslope and downslope winds produced more intense circulation than land/lake and land/sea breezes over flat terrain.

CHAPTER 2

2.0 DATA SOURCES AND ANALYSES

2.1.0 DATA SOURCES

In East Africa, optical pilot balloon observations are normally taken at 0600 GMT and 1200 GMT (local time is three hours ahead of GMT). Although most stations had at least two observations in a day, one in the morning and one in the afternoon hours, a few stations, like Kericho, had only morning observations. Stations located at airports had more than two observations per day. For this study, all available wind vectors, irrespective of their times of observation, have been utilized.

The data used is that which has been transferred from the original manuscripts to magnetic tapes via punched cards. Unfortunately, sometime back, it was decided that, as an economy measure, punching of data for stations which already had 10 years' data on cards, be suspended. This decision has to some extent had negative effects on this study. For our study, we required those stations with long enough records for determination of the mean wind fields. At the same time, these records were required to include the 1961-1962 data for the determination of the 1961/62 wind flow anomalies. Stations

like Mandera and Malindi had part of their records missing on the tapes. Despite these drawbacks we ended up with 31 pilot balloon stations (Fig. 1) with record lengths that lay within the range of 6-12 years (Table 3) in the period 1952-1973. Wind data from these stations were used in the computation of long term mean wind vectors.

For determination of the 1961/62 anomalies only 24 of the 31 stations were used. This is because some of the stations (e.g. Tororo, Kericho) started operating after 1962. Also some stations like Malindi, Garissa and Mandera did not have observations during the floods. It is well known that one major shortcoming of optical pilot balloon observations is that they are inadequate and least reliable when most needed, i.e. during disturbed weather conditions. The region most affected by absence of adequate observations is northeastern Kenya. The analyses for wind flow anomalies (perturbations) in northern Kenya during September through December 1961 were largely based on careful extrapolations of wind information and should therefore be regarded cautiously.

Pilot balloon observations in East Africa are available at every 1000 feet for the first 8000 feet above mean sea level, then at every 2000 feet upto 20 000 feet, then at 24 000 feet, and after every 3000 feet, and so on (Nyoni 1981). Surface winds are also given in the form of direction and speed. In this study, levels upto 24 000 feet above mean sea level were considered. The choice of the top most level was mainly due to the fact that observations generally decreased with height so that above

Station	Jan.	Feb.	Mar.	Apr.	May	Jun.	Jul.	Aug.	Sept.	Oct.	Nov.	Dec.	Period
Mandera	5	5	5	5	5	4	5	5	5	5	5	5	53-62
Lodwar	10	10	10	11	11	11	10	11	11	11	11	11	52-62
Gulu	9	10	11	11	10	11	11	11	9	10	11	9	52-62
Fort Portal	12	12	12	10	12	12	11	11	10	11	12	12	52-63
Tororo	10	10	10	10	10	10	10	11	11	11	11	10	63-73
Nanyuki	11	11	9	11	11	11	11	11	11	12	12	12	52-63
Garissa	9	10	9	8	9	9	9	9	9	8	10	10	64-73
Nakuru	4	2	4	4	4	4	5	5	5	5	4	5	59-63
Kericho	5	6	6	6	6	6	6	5	6	6	6	6	68-73
Kisumu	9	9	9	9	9	9	9	9	9	9	9	9	55-63
Entebbe	11	11	11	11	11	11	11	11	11	11	11	11	52-62
Mbarara	8	8	9	8	8	8	9	7	9	10	9	9	59-69
Kabale	12	10	10	10	10	10	11	11	11	10	11	11	52-63
Bukoba	9	10	10	11	12	11	9	11	10	10	10	9	62-73
Narok	11	7	10	11	11	11	12	12	12	10	10	10	52-63
Nairobi	9	5	9	7	7	8	7	8	9	7	7	7	53-63
Makindu	12	12	11	12	12	12	12	12	12	12	12	12	52-63
Voi	9	9	9	9	9	9	9	9	9	9	9	9	55-63
Malindi	5	6	5	5	5	5	5	6	6	5	5	7	62-73
Mombasa	11	11	11	11	11	11	20	11	11	10	10	11	53-72
Mombo	9	8	9	7	10	10	10	9	9	9	10	10	58-67
Arusha	7	7	7	7	7	7	7	7	7	7	8	8	60-67
Mwanza	10	10	10	10	11	10	10	10	10	10	10	10	59-69
Kigoma	9	9	9	10	10	10	9	10	11	9	9	9	52-63
Tabora	11	11	11	11	11	11	11	12	11	10	10	10	52-63
Dodoma	12	12	12	12	12	12	12	12	12	12	12	12	52-63
Dar es Salaam	6	6	6	6	6	6	6	6	6	6	6	6	52-63
Iringa	8	8	8	7	7	8	8	7	8	9	9	8	66-73
Mbeya	12	11	11	12	12	12	12	12	12	11	12	11	52-63
Songea	11	11	11	11	11	11	11	11	11	11	11	11	52-63
Mtwara	7	7	8	7	7	7	7	8	8	7	8	8	56-64

Table 3 : Number of years used in the study for each pilot balloon station.

24 000 feet, they were very few at many stations. Six pilot balloon levels were considered and these are 5000 feet (1525 m), 6000 feet (1830 m), 10 000 feet (3050 m), 14 000 feet (4270 m), 18 000 feet (5490 m) and 24 000 feet (7320 m) above mean sea level.

The mean monthly rainfall used in this study was obtained from the East African Meteorological Department's publications "Climatological Statistics for East Africa" (1975). The daily rainfall totals were obtained from magnetic tapes. Data for 53 stations (Table 4) was used.

2.1.1 The Magnetic Tape Pibal Data File - Problems and Errors

There were a number of problems encountered when extracting data from the magnetic tapes. The initial problem was that there was very poor documentation of the data file so that it was not known which stations' records were contained in which tapes. Furthermore, the records were not entered in any organised manner. The first exercise was therefore to list and sort and merge the tapes so that we had continuous records for every station. This process took quite some time because of the amount of data involved and the relatively limited internal memory of the University computer.

There were certain common errors in the data which we would like to mention here for the benefit of future users of these tapes. The most common error was when a non-numeral (e.g. "f") was punched instead of a numeral. The convenient thing to

Station	Latitude	Longitude	Station	Latitude	Longitude
Lodwar	03°07'N	37°37'E	Tanga	05°05'S	39°04'E
Mandera	03°56'N	41°52'E	Dodoma	06°10'S	35°46'E
Masindi	01°41'N	31°43'E	Morogoro	06°51'S	37°40'E
Soroti	01°43'N	33°37'E	Iringa	07°40'S	35°45'E
Fort Portal	00°40'N	30°17'E	Mbeya	08°56'S	33°28'E
Tororo	00°41'N	34°10'E	Moyale	03°32'N	39°03'E
Wajir	01°45'N	40°04'E	Songea	10°41'S	35°35'E
Mbarara	00°37'S	30°39'E	Mtwara	10°21'S	40°11'E
Kisumu	00°06'S	34°45'E	Dar es Salaam	06°53'S	39°12'E
Entebbe	00°03'N	32°27'E	Nanyuki	00°01'N	37°04'E
Garissa	00°28'S	39°38'E	Mwanza	02°28'S	32°55'E
Kabale	01°15'S	29°59'E	Embu	00°41'S	37°20'E
Bukoba	01°20'S	31°49'E	Equator	00°01'S	35°33'E
Narok	01°08'S	35°50'E	Isiolo	00°21'N	37°35'E
Nairobi/Embakasi	01°19'S	36°55'E	Kisii	00°41'S	34°47'E
Musoma	01°30'S	33°48'E	Magadi	01°53'S	36°17'E
Arusha	03°20'S	36°37'E	Machakos	01°35'S	37°14'E
Moroto	02°33'N	34°46'E	Naivasha	00°43'S	36°26'E
Voi	03°24'S	38°34'E	Arua	03°01'N	30°55'E
Malindi	03°16'S	40°03'E	Lira	02°17'N	32°56'E
Makindu	02°17'S	37°50'E	Ilonga	06°46'S	37°02'E
Lamu	02°16'S	40°54'E	Mafia	07°55'S	39°40'E
Kigoma	04°53'S	29°38'E	Moshi	03°21'S	37°20'E
Mombo	04°55'S	38°14'E	Same	04°05'S	37°43'E
Mombasa	04°02'S	39°37'E	Zanzibar	06°15'S	39°13'E
Tabora	05°05'S	32°50'E	Mbale	01°06'N	34°11'E
Mubende	00°35'N	31°22'E			

Table 4 : Rainfall stations used in the study.

do is to use a subroutine which skips all records with such errors. However we found that one loses a lot of records this way. So it was decided that the following procedure be followed:

A record on the tape may look like this:

Level	Station Number	Day	Month	Year	Ascent Number	-v+100	-u+100	DD	FF
1	820	04	07	56	1001	080	101	180	20

If the error was in the level or station number, then the record was discarded since it was not known to which station or what level the information belonged. If the error was in the day, month, year or time, then the ascent number would be referred to in order to identify the time when the ascent was made. If the error was found in the values of u or v then the direction (DD) and speed (FF) values would be used to determine the meridional and zonal components. With this procedure we managed to save many more records from being discarded.

Another error encountered and which proved to be most disastrous was one where one or more of the numbers in the record had been missed out while punching. It may be appreciated from the example above that if the '1' for level is missed out and instead the '8' for station takes its position, then values of (-v+100) and (-u+100) will be 801 and 11 respectively, giving $v = -701$ and $u = 89$ knots which are unrealistic. The problem with this error is that it is difficult to detect with

a fortran compiler which simply interprets blanks as zeros. However in most such cases, the errors were easily noticeable in the results obtained since this led to unrealistically high values of wind speeds. Such results were abandoned and new ones re-computed after tracing and eliminating the erroneous records. This type of error was found in records of at least half the stations.

Finally the cleaned up pilot balloon data was used in this study.

2.2.0 ANALYSES

2.2.1 Determination of Mean Flow Patterns

Mean resultant wind vectors (\vec{V}_{mean}) at each station were computed by first obtaining the time averages of zonal (\bar{u}) and meridional (\bar{v}) components then compounding them. The resultant wind vectors were plotted at each station. Streamline and isotach analyses were then carried out subjectively at six levels for all the twelve calendar months. The flow at the 1830 m level is very similar to that at 1525 m level and is therefore not presented in this study. Results for 1525 m, 3050 m, 4270 m, 5490 m and 7320 m are presented and discussed in the next chapter. These levels approximately translate to the pressure levels 850 mb, 700, 600, 500 and 400 mb respectively. We observe that streamlines and isotachs at 850 mb, although given, have no physical meaning in areas where this level is

below the ground.

2.2.2 Determination of the 1961/62 Wind Anomaly Field

For rainfall to occur, there must be adequate supply of moisture in the atmosphere. Cooling must take place so that rain processes may be initiated by condensation. Upward motion of air enables cooling to take place and is therefore the prime cause of rainfall. Downward motion and lack of moisture are responsible for deficiency of rainfall. The major process leading to upward motion in the tropical atmosphere is horizontal convergence in the low levels (Thompson 1965). Orographic lifting and random thermal convection take a secondary role.

As regards the year 1961, although drought conditions prevailed during the earlier months, large amounts of moisture were present in the atmosphere during the southeast-southwest monsoon season. It is apparent that it was not until the end of September 1961 that the low level wind field became favourable for upward motion to take place over a large area and in a deep enough layer for precipitation to be initiated. We therefore study the wind anomaly patterns in the period September 1961 through January 1962 when the rains receded. The wind anomaly field was determined as follows:

First the mean monthly wind components (\bar{u}, \bar{v}) at each station were computed from all the available wind observations. Thus at each station, we obtained \bar{u} and \bar{v} for September,

October, November and December 1961 and January 1962.

The monthly wind departures from the long term mean flow for the five months were then determined by subtracting the long term monthly mean components (\bar{u}, \bar{v}) from the monthly mean components (\bar{u}, \bar{v}) during the flood episode. If \vec{V} is the mean resultant vector for any of the five months considered, and \vec{V}_m is the long term mean resultant wind vector for the month in question, then the departure \vec{V}' is given by:

$$\vec{V}' = \vec{V} - \vec{V}_m \quad \dots(1)$$

This process filters out the mean flow which (as discussed in chapter 1) is dominant in East Africa and would tend to mask the disturbances we are interested in. The departures (\vec{V}') were then plotted at six pilot balloon levels: 1525 m, 2440 m, 3050 m, 4270 m, 5490 m and 7320 m above mean sea level. The inclusion of the 2440 m level (~800 mb) gives an improved vertical resolution of the disturbances in the lower levels. Streamline and isotach analyses were carried out subjectively. Results are presented in figures 42-44 and 47-48, and discussed in detail in section 3.2

2.2.3 Determination of Divergence and Relative Vorticity Fields

From the streamline and isotach analyses, values of wind direction and speed were tabulated at 1° longitude by 1° latitude grid points. There were altogether 252 grid points. The tabulated wind vectors were then resolved into the zonal (u) and meridional (v) components. The resolution process used expressions of the following form:

$$u = -|\vec{V}| \sin (\text{DIR}) \quad \dots (2)$$

$$v = -|\vec{V}| \cos (\text{DIR}) \quad \dots (3)$$

where $|\vec{V}|$ and DIR are the wind speed and direction respectively. The ensuing u and v components at each grid point were used to determine numerical values of Divergence (D) and the curl of the horizontal wind vector (ζ). The equations for horizontal divergence and vertical component of relative vorticity for spherical flow are given as follows:

$$D = \frac{\partial u}{\partial x} + \frac{\partial v}{\partial y} - v/a \tan \phi \quad \dots (4)$$

$$\zeta = \frac{\partial v}{\partial x} - \frac{\partial u}{\partial y} + u/a \tan \phi \quad \dots (5)$$

where a is the mean radius of the earth and ϕ is the latitude angle. In determining the numerical values of D and ζ in equations (4) and (5), use is made of the centred differencing scheme. The grid distance DY in the y-direction is a constant

1.111×10^5 metres while that in the x-direction varies with the cosine of the latitude angle due to the convergence of meridians.

Divergence (\bar{D}) and relative vorticity ($\bar{\zeta}$) of the mean wind field (\vec{V}_m) were determined for the twelve calendar months at 5 levels in the lower troposphere. The computed divergence fields are presented in figures 8-11, 19-20, 22, 29-32 and 37-40, and their salient features discussed in section 3.1. Unless otherwise stated, the shaded areas in these figures represent those areas under the influence of convergent air currents while the unshaded areas have divergent air flow.

The divergence (D') and vorticity (ζ') fields associated with the 1961/62 disturbances were determined in a similar way. However, only two months during the flood episode were considered. The two months are the short rains' month of November and the northeast monsoon month of January. For these two months we present (figures 45 and 50) divergence fields at six levels in the lower troposphere.

2.2.4 Vertical Motion Field

The statement of mass conservation (continuity equation) in x, y, z, t system is given by

$$\frac{\partial \rho}{\partial t} = - \nabla \cdot \rho \vec{V} = - \vec{V} \cdot \nabla \rho - \rho \nabla \cdot \vec{V} \quad \dots (6)$$

where \vec{V} is the three-dimensional wind vector.

In equatorial regions, variation of ρ with time is very small. Horizontal gradients of ρ are also very small. Even in the vertical, ρ varies very slightly in the lower troposphere. Hence in this study we take ρ to be constant in time and space.

Equation (6) reduces to $\nabla \cdot \vec{V} = 0$

$$\frac{\partial u}{\partial x} + \frac{\partial v}{\partial y} + \frac{\partial w}{\partial z} = 0$$

$$\text{or} \quad \frac{\partial w}{\partial z} = -\left(\frac{\partial u}{\partial x} + \frac{\partial v}{\partial y}\right) = -D \quad \dots(7)$$

Equation (7) may be integrated in the vertical to get the vertical motion w :

$$\int_{z_1}^{z_2} \frac{\partial w}{\partial z} dz = - \int_{z_1}^{z_2} D dz$$

where z_1 and z_2 are heights above mean sea level of two consecutive levels where analyses have been done.

$$(w)_{z_2} - (w)_{z_1} = - \int_{z_1}^{z_2} D dz \quad \dots(8)$$

If z_1 is taken as the height of the ground above mean sea level, then equation (8) may be solved for vertical motion at z_2 and subsequent levels, given the vertical motion at the ground.

Vertical motion at the earth's surface:

If we consider a rigid surface at rest, such as the earth's surface, motion due to sloping terrain will be tangential to the surface. Thus if the equation of the surface is

$$f(x,y,z) = 0 \quad \text{WMO (1973)}$$

and \vec{V}_s is the three-dimensional wind vector at the surface, we have

$$\vec{V}_s \cdot \nabla f = 0 \quad \dots(9)$$

since ∇f is normal to the surface.

Now let the height of the surface above mean sea level be given by

$$z = h(x,y)$$

The equation of the surface may then be expressed as

$$f(x,y,z) = z-h(x,y) = 0$$

and condition (9) becomes

$$\vec{V}_s \cdot \nabla(z-h(x,y)) = 0$$

$$\text{or } w_s - u_s \frac{\partial h}{\partial x} - v_s \frac{\partial h}{\partial y} = 0$$

The vertical motion (w_s) at the surface, induced by sloping terrain is then given by

$$w_s = u_s \frac{\partial h}{\partial x} + v_s \frac{\partial h}{\partial y} \quad \dots(10)$$

The components of the surface wind vector, $\vec{V}_s = (u_s, v_s)$, were obtained by first tabulating surface wind direction and speed values at $1^\circ \times 1^\circ$ grid points from streamline and isotach analyses of surface wind (\vec{V}_s). These surface wind vectors were then resolved into their meridional (v_s) and zonal (u_s) components. The height of the surface above mean sea level (h) was obtained at $1^\circ \times 1^\circ$ grid points, from the Department of Meteorology at the University of Nairobi. The orography data was originally extracted from maps kept by the Survey of Kenya.

The right hand side of equation (8) may be approximated to $-\bar{D}(z_2 - z_1)$ where \bar{D} is the mean divergence in the layer (z_1, z_2) and is given by

$$\bar{D} = \frac{(D)_{z_1} + (D)_{z_2}}{2}$$

Hence equation (8) becomes

$$(w)_{z_2} = (w)_{z_1} - \bar{D}(z_2 - z_1) \quad \dots(11)$$

In the lowest levels, the integration interval $\Delta z = z_2 - z_1$ varies in the horizontal due to varied orography. It is only above the 3 km level that Δz is constant throughout our region of study.

After computing the mean vertical motion at the surface from equation (10), the mean vertical motion at 1525, 1830, 3050, 4270, 5490 and 7320 metres above mean sea level was computed from equation (11) as follows:

$$(w)_{1525 \text{ m}} = (w)_s - \frac{(D_{1525} + D_s)(1525-h)}{2}$$

$$(w)_{1830 \text{ m}} = (w)_{1525 \text{ m}} - \frac{(D_{1525} + D_{1830})(1830 - 1525)}{2}$$

and likewise for subsequent levels. For highland areas above the 1830 metre level, the vertical motion was computed at surface, 3050, 4270, 5490 and 7320 metres above mean sea level. The results for the four mid-season months of January, April, July and October are presented and discussed in the next chapter.

Similar procedure was followed when computing the vertical motion field (w') for the wind anomaly fields associated with the flood episode of 1961/62. The results for November 1961 and January 1962 are presented and discussed in the next chapter. Unless otherwise stated, the shaded areas in the vertical motion fields represent those areas with ascending motion while the unshaded areas have descending motion.

CHAPTER 3

3.0 RESULTS AND DISCUSSIONS

3.1.0 MEAN WIND FLOW CHARACTERISTICS

The monthly mean wind flow patterns over East Africa and their respective divergence and vertical motion fields are presented in figures 3-12, 14-22, 24-33, 35-40. The discussions on these fields are divided into four sections that cover the four seasons in East Africa. The four seasons are:

- (i) The Northeast monsoon season (December-February),
- (ii) The long rains season (March-May),
- (iii) The southeast-southwest monsoon season (June-August),
- (iv) The short rains season (September-November).

The mean vertical motion fields are given for the four mid-season months of January, April, July and October. The vertical motion fields for the other months of the year may be inferred from the vertical profiles of the respective divergence fields.

3.1.1.0 The Northeast Monsoon Season

3.1.1.1 Mean Horizontal Motion

The mean wind flow patterns for the months of December, January and February are presented in figures 3-7. The most persistent feature in the low levels throughout the season is the northeast monsoon current. Figure 3a shows the surface air flow during January. The monsoon current becomes highly diffluent over Tanzania as part of it flows southwards into the ITCZ (Thompson 1965, Ramage and Raman 1972) while the other stream turns northwards into the lake Victoria trough. Winds are very light ($1-2 \text{ ms}^{-1}$) over most areas excluding northern Kenya and coastal regions.

The air flow at 1525 m (~850 mb) for December, January and February is shown in figures 3b-d. The monsoon system has apparently shifted north-westwards of its surface position. At this level, the monsoon current has its maximum intensity with speeds of upto 10 ms^{-1} in northern Kenya. The air current enters the East African region in northeastern Kenya, as a northeasterly flow. In the neighbourhood of the equator, between 38°E and 41°E , it bifurcates into two main streams. One flows westward north of the equator, while the other flows almost parallel to the East African coast as a northerly. The easterly branch, which flows into the quasi-permanent trough in Central Africa (Semazzi 1979), is generally stronger than the northerly branch along the coast. The two branches have been

known to co-exist on any one day and occasional high speeds of upto 45 ms^{-1} (Findlater 1968) have been recorded at Lodwar and Voi below 2100 metres AMSL.

In December, the northeast monsoon current at the 1.5 km level (Fig. 3b) is generally less diffluent than in the succeeding two months. In January and February (Figs. 3c-d), the current turns to a northwesterly as it flows into the ITCZ trough in the Indian ocean. There is confluence into western Kenya and Uganda. The cyclonic vortices associated with the lake Victoria circulation at the surface are no longer evident at this level.

The northeast monsoon current at 3050 m (~700 mb) is shown in figures 4a-c. The flow has intensified inland, having speeds of upto 7.5 ms^{-1} , while coastal winds in the main monsoon current have weakened. The extreme diffluence in the current is still evident with the highly diffluent area having shifted northward of its location at lower levels. In December (Fig. 4a) the flow is everywhere northeasterly, flowing towards the low pressure centre in Central Africa. In January (Fig. 4b), and especially February (4c), central and southern Tanzania experience extreme diffluence in the monsoon current. Here, part of the air turns to a northwesterly and flows into the ITCZ over the Indian ocean. The northwesterlies observed in southern Tanzania at the 3050 m level during January-March form part of the western branch of a cyclonic circulation around vortices in the ITCZ over the Indian ocean. The change in the air flow over southern Tanzania from December through February is a clear indication of the gradual response

of the monsoon air current to the intensification of the southern summer ITCZ over southern Africa as the summer season matures.

Figures 5a-c show the flow over East Africa at the 4270 m (~600 mb) level. In December (Fig. 5a), the northeast monsoon current is in the build-up phase and is absent at the 4 km level. Instead, the flow at this level is mainly easterly with a small northerly component. In January and February (Figs. 5b-c), the months of maximum development of the northeast monsoon, the NE monsoon current is evident even at the 600 mb level. However, the air current at this level is less diffluent than at lower levels.

At 5490 m (~500 mb), the air flow is more or less easterly everywhere in all the three months (Figs 6a-c). The depth of the northeast monsoon current reaches its maximum in January-February, but even then, it does not extend to the 5.5 km level. Wind speeds at this level are relatively high in the neighbourhood of the equator and to the north of it. The strength of the air current at this level is about 7.5 ms^{-1} . The wind flow patterns at the 7 km level (Figs. 7a-c) are very similar to those at the 5.5 km level (Figs. 6a-c).

3.1.1.2 Mean Divergence and Vertical Motion Fields

The divergence patterns associated with the wind flow during the northeast monsoon season are presented in figures 8-11. The vertical motion field for January, the month when the northeast monsoon has reached maximum intensity, is presented in figures 12a-c. A striking feature of the divergence/convergence patterns in this season is the divergent zone running from north to south along the East African coastal plains (Figs. 8a-c). This north-south oriented divergence zone coincides with the axis of the northeast monsoon current. Maximum divergence is observed in northeast Tanzania and is of the order of $3 \times 10^{-5} \text{ s}^{-1}$ at the 850 mb level (Figs. 8a-c). The monsoon air current over the coastal plains of Kenya and Tanzania is divergent upto 700-600 mb (Figs. 9a-d).

Over northern Kenya, one notes that inspite of the rather diffluent streamlines observed in the previous section (Figs. 3b-d), the area is actually convergent at the 850 mb level. An explanation to this may be sought in the expression for Divergence in Natural coordinates:

$$D = V K_{OS} + \frac{\partial V}{\partial s}$$

where K_{OS} is the horizontal curvature of curves which are locally normal to the streamlines.

The curvature term $V K_{OS}$ is > 0 when streamlines diverge, and < 0 when streamlines converge. The shear term $\partial V / \partial s$ is > 0

when the speed increases downwind along the streamlines and < 0 when speed decreases downwind.

In northern Kenya, one observes that although the curvature term $V K_{OS} > 0$, the shear term is negative ($\frac{\partial V}{\partial S} < 0$). It is evident that the shear term contributes more towards the net divergence field in this area. We can use the same argument for those areas in Tanzania which are convergent whereas the monsoon air current is diffluent. Along the coast, we observe that while the streamlines remain diffluent, the shear term is insignificant as the strength of the monsoon current is the same everywhere ($\sim 5 \text{ ms}^{-1}$). Hence the curvature term plays a major role in determining whether the flow is divergent or convergent. The lake Victoria region and parts of Uganda are convergent in the lower troposphere throughout the season.

The vertical motion field (Figs. 12a-c) is consistent with the divergence fields. The monsoon current along the eastern plains is associated with descending motion while the lake Victoria region and a small part of northern Kenya have a deep layer of ascending motion extending above the 500 mb level (Fig. 12c). However, lack of moisture in the northeast monsoon air is, in part, responsible for the very low rainfall received in these areas in this season.

The northeast monsoon period is the rainy season for most of Tanzania south of 4°S . It is observed (Figs. 8a-9d) that convergence exists in parts of coastal Tanzania, central region and northwestern Tanzania. The spatial distribution of

divergence and vertical motion fields agree well with Tomsett's wet zone during this season (Figs. 13a-c). The vertical motion in these areas is however not very high, the maximum being about $7 \times 10^{-3} \text{ ms}^{-1}$ at the 700 mb level (Fig. 12b).

The highlands of southern Tanzania are the wettest parts of Tanzania during this season (Figs. 13a-c). However, the monsoon air current appears to be divergent (Figs. 8a-9d) in a deep layer extending to the mid-troposphere. The resulting vertical motion (Figs. 12a-c) is downward in this area. Therefore our mean divergence/convergence and the ensuing vertical velocity patterns seem to contradict the observed rainfall patterns in the area. Why this is so is not quite clear, but we know that orography plays a very important role in initiating rainfall activities through orographic lifting (Nieuwolt 1974, Asnani and Kinuthia 1979). Another reason for this discrepancy may be poor resolution of the wind field at low levels over southern Tanzania. From figures 3b-d, we note that the flow over this area is very weak and observations scarce. One would therefore expect the error in the interpolation of wind speeds at grid points to be quite appreciable.

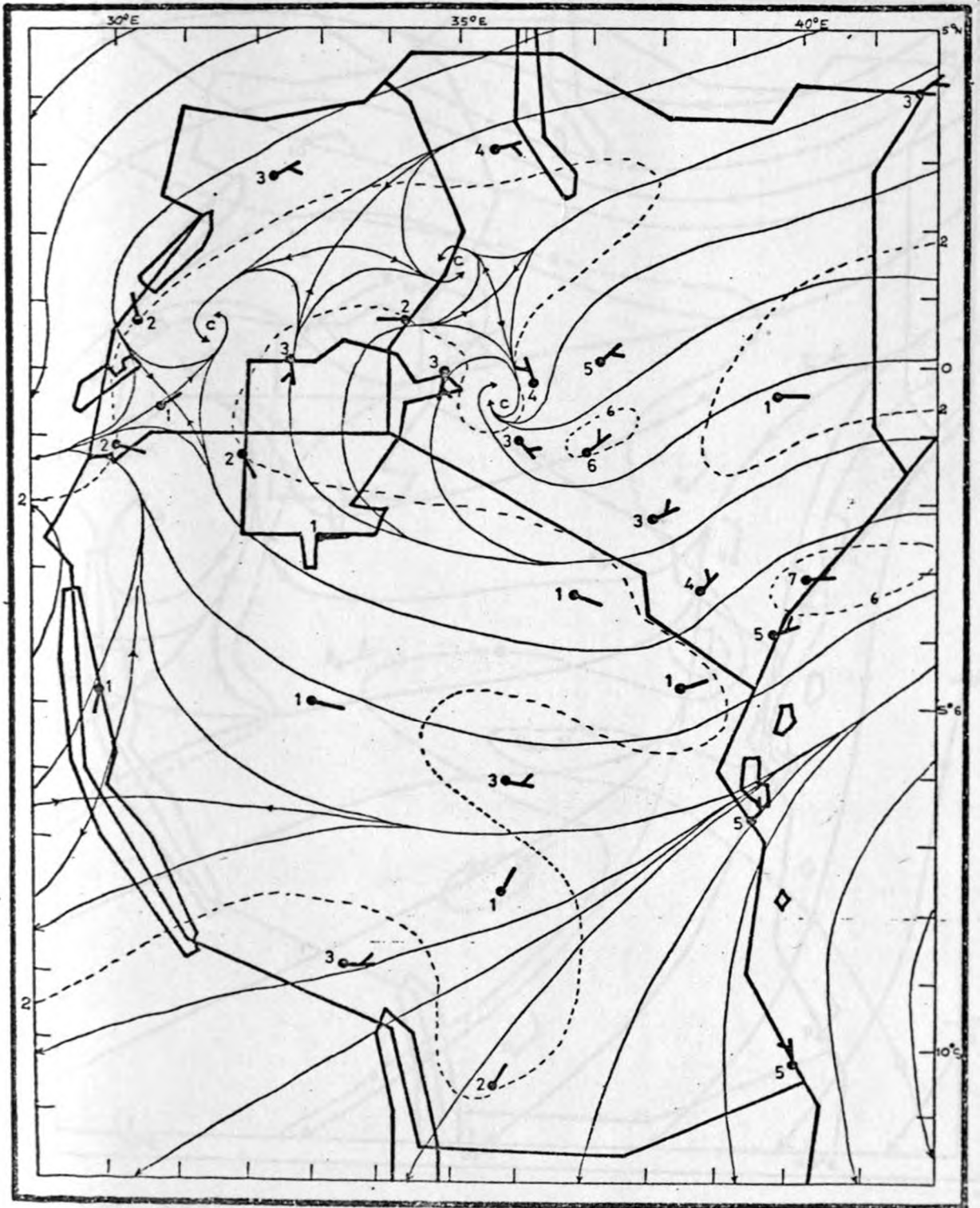


Fig. 3(a) : Mean wind field at the surface in January
(speed in knots).

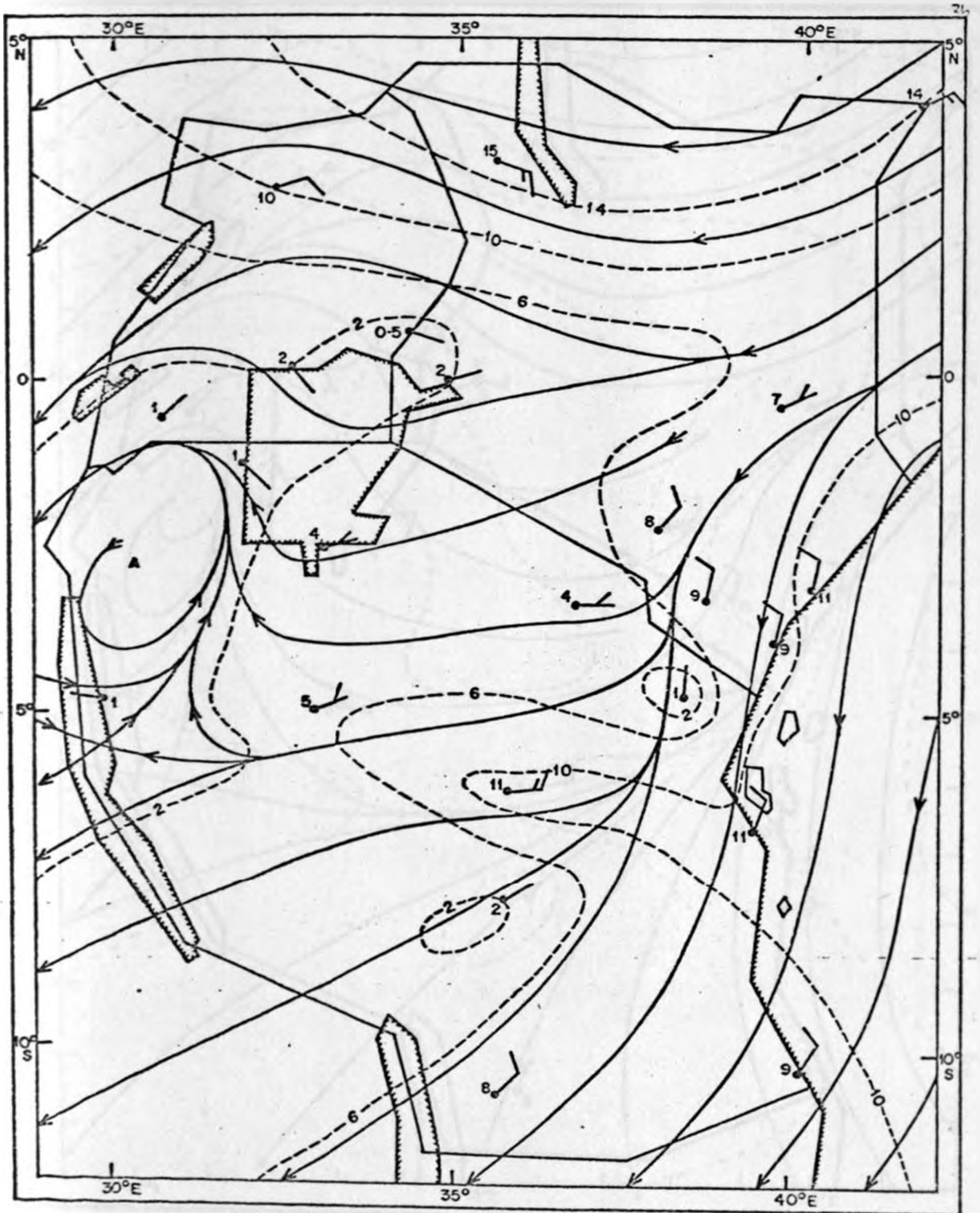


Fig. 3(b) : Mean wind field at 1525 m AMSL in December.

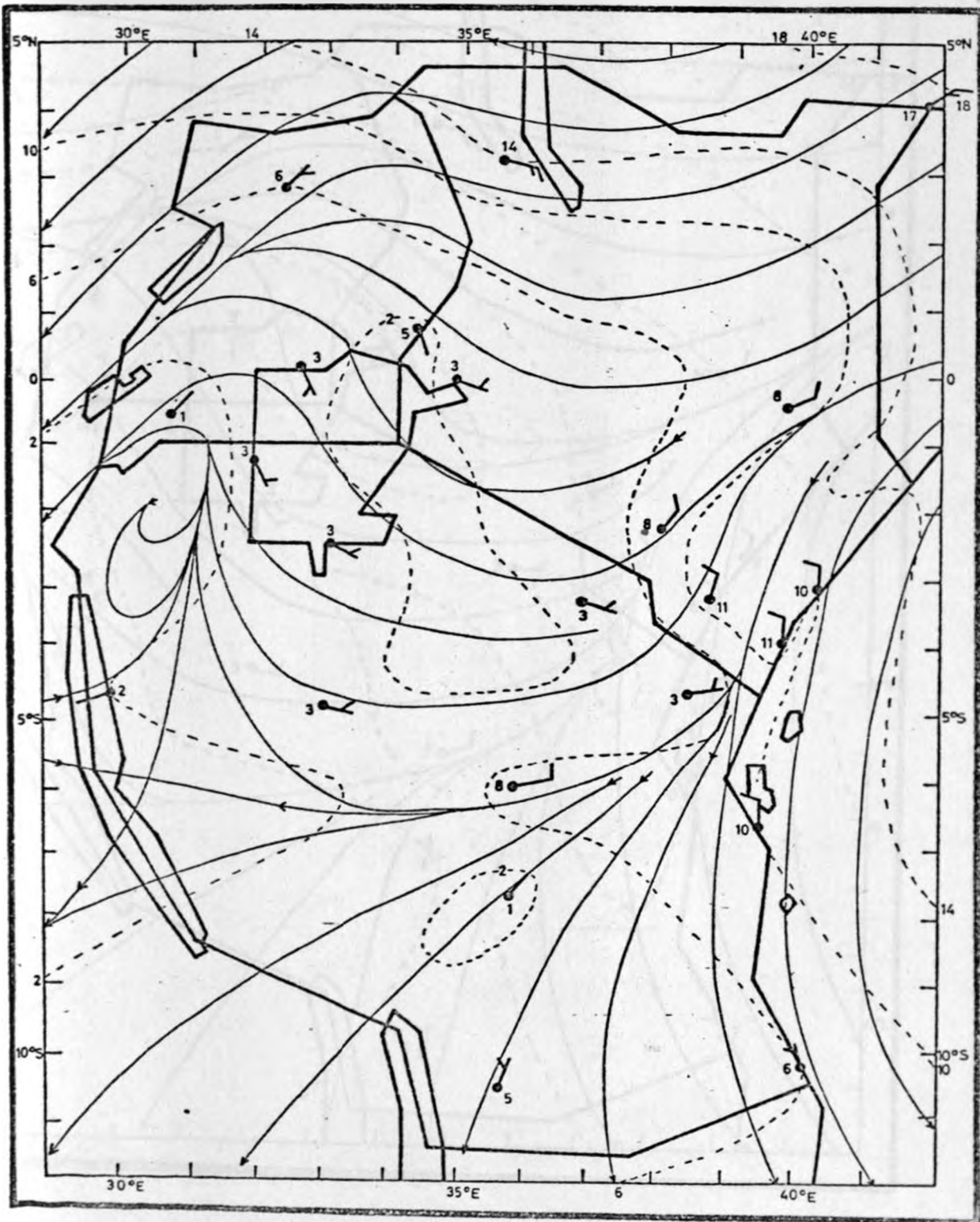


Fig. 3(c) : Mean wind field at 1525 m AMSL in January.

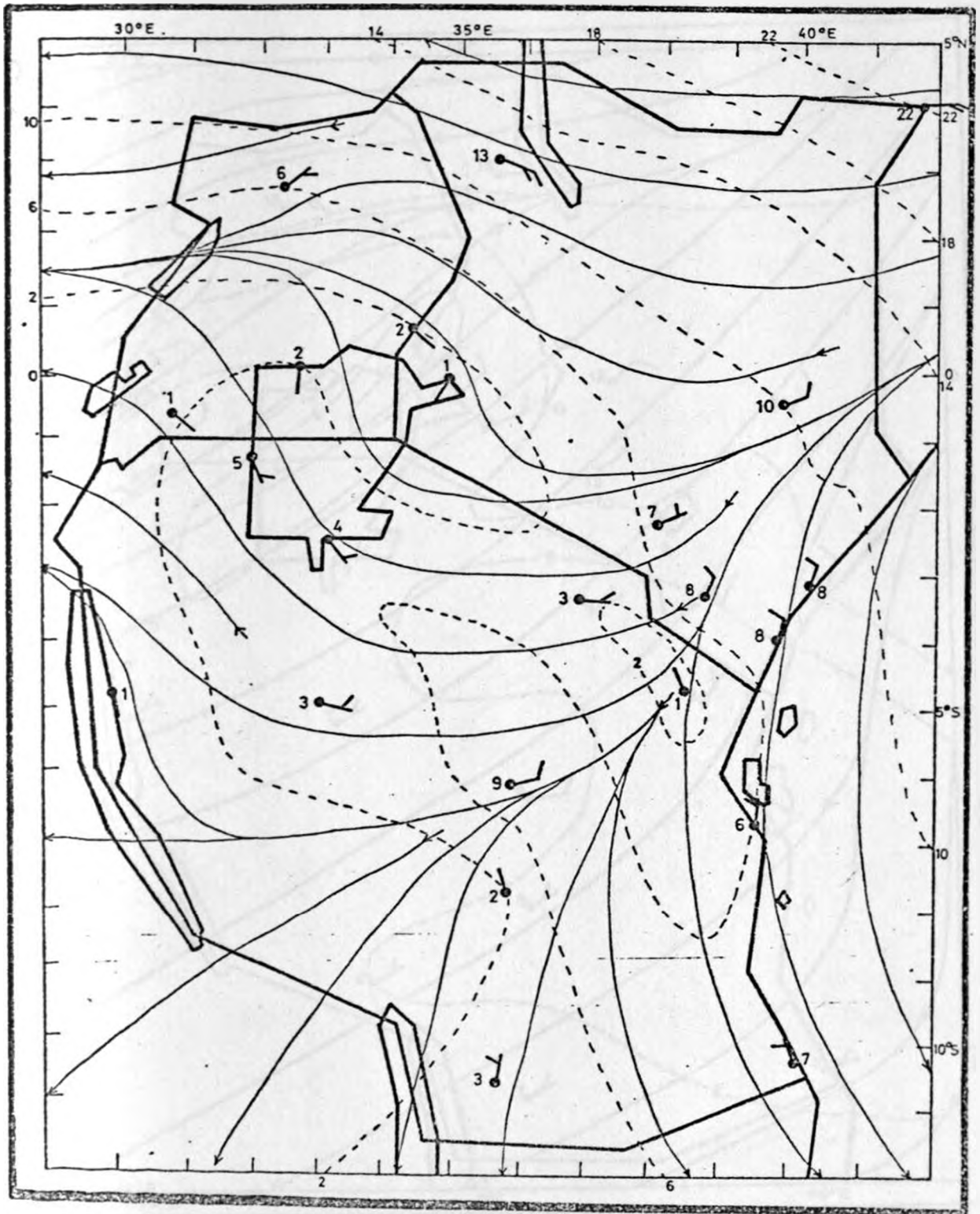


Fig. 3(d) : Mean wind field at 1525 m AMSL in February.

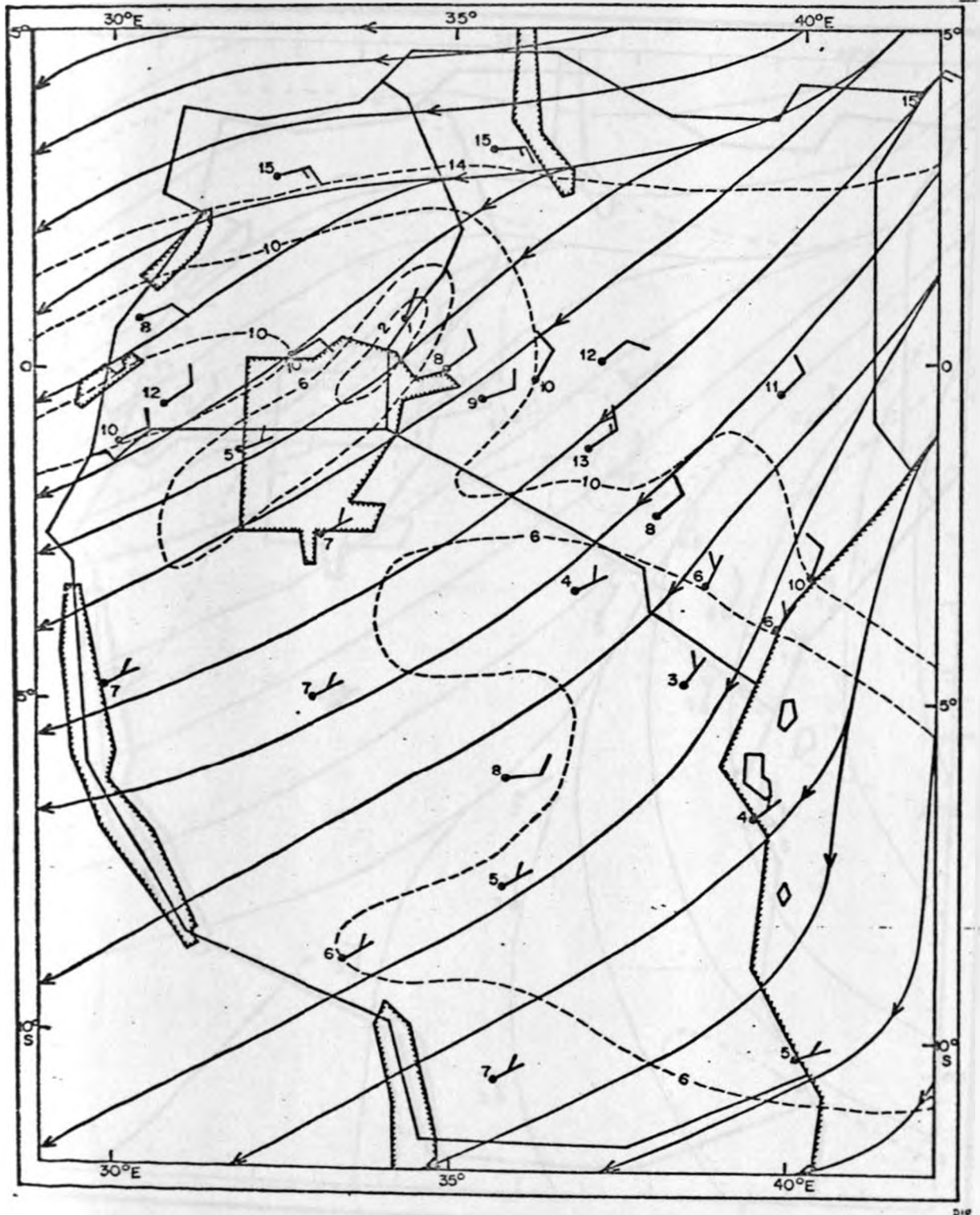


Fig. 4(a) : Mean wind field at 3050 m AMSL in December.

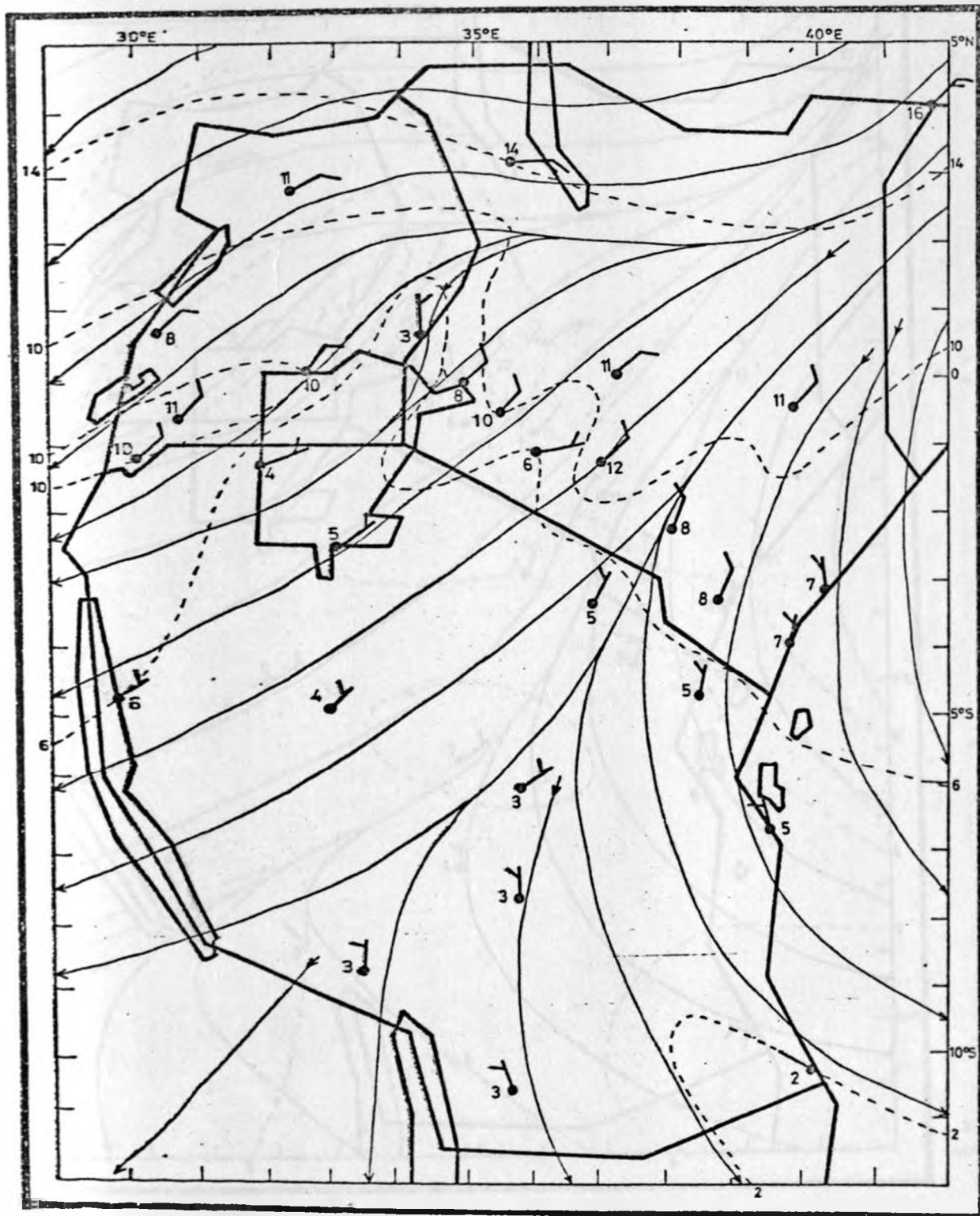


Fig. 4(b) : Mean wind field at 3050 m AMSL in January.

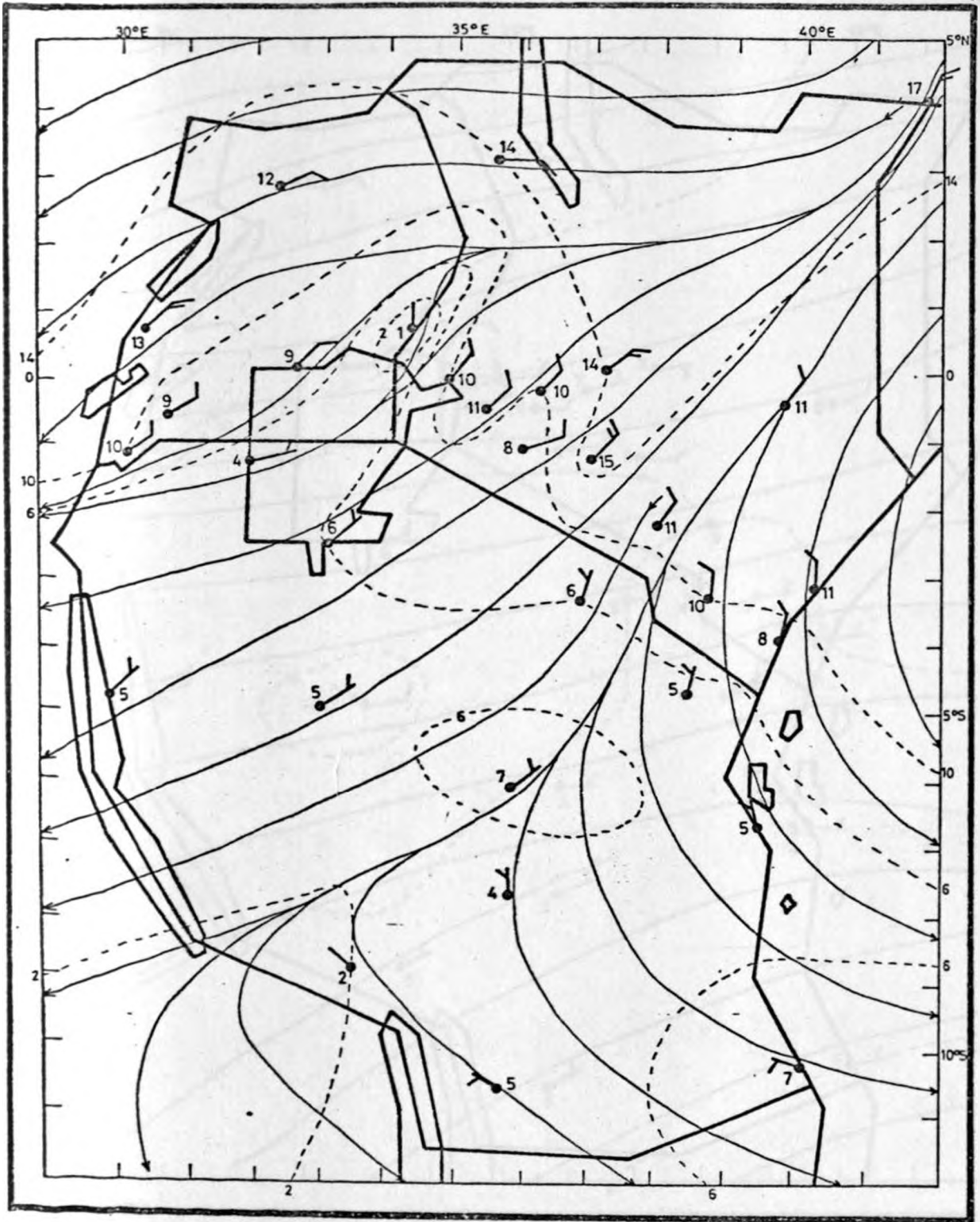


Fig. 4(c) : Mean wind field at 3050 m AMSL in February.

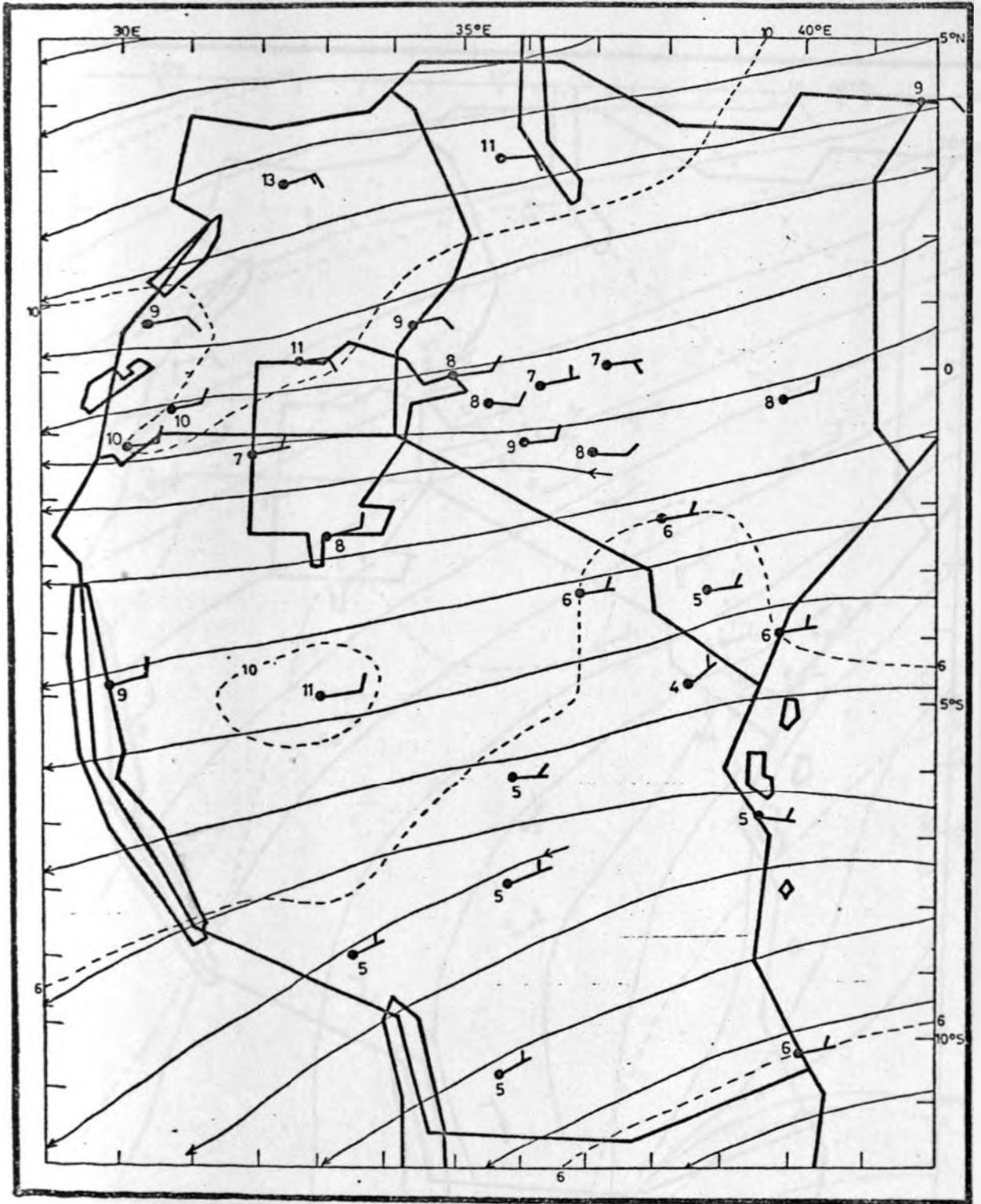


Fig. 5(a) : Mean wind field at 4270 m AMSL in December.

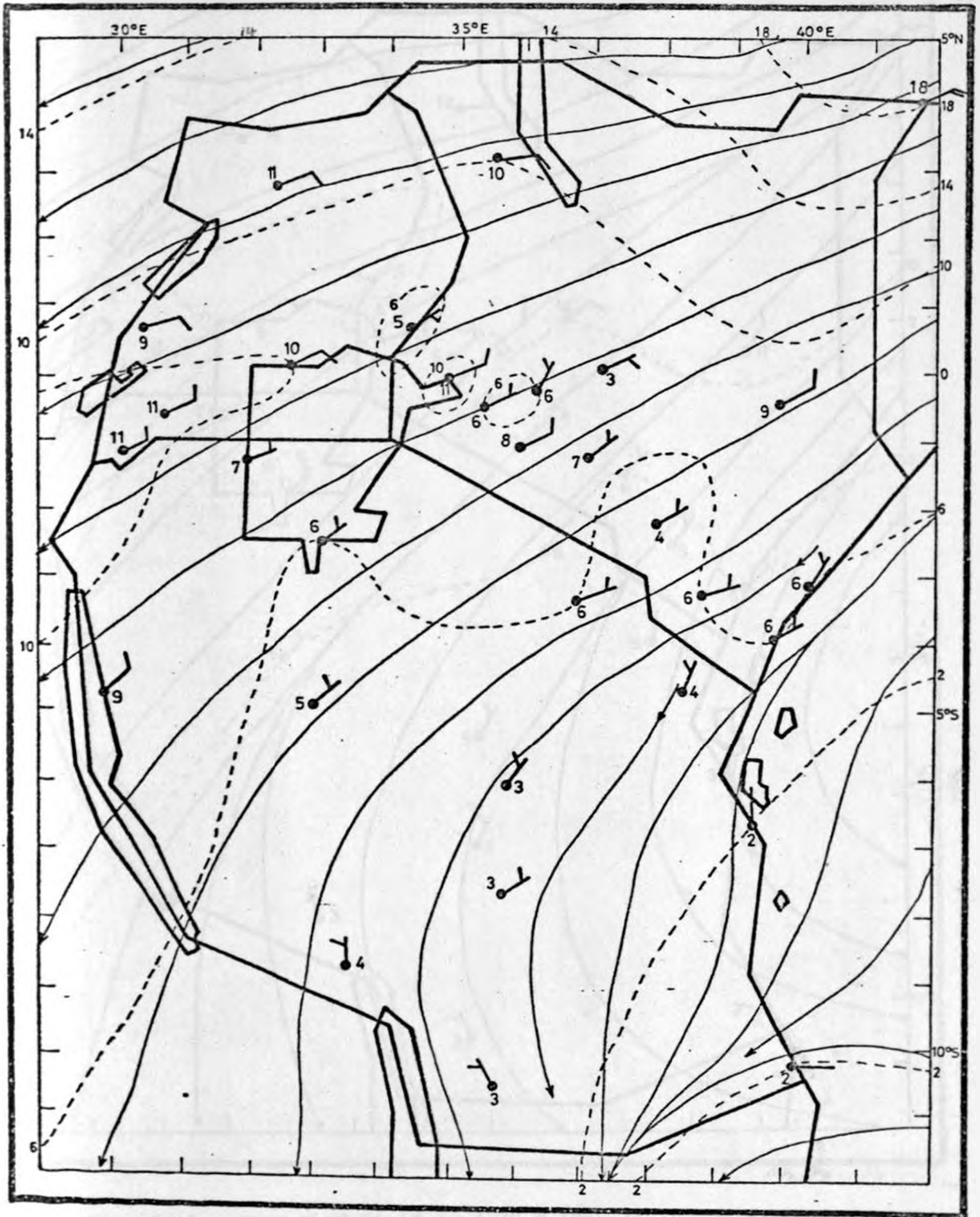


Fig. 5(b) : Mean wind field at 4270 m AMSL in January.

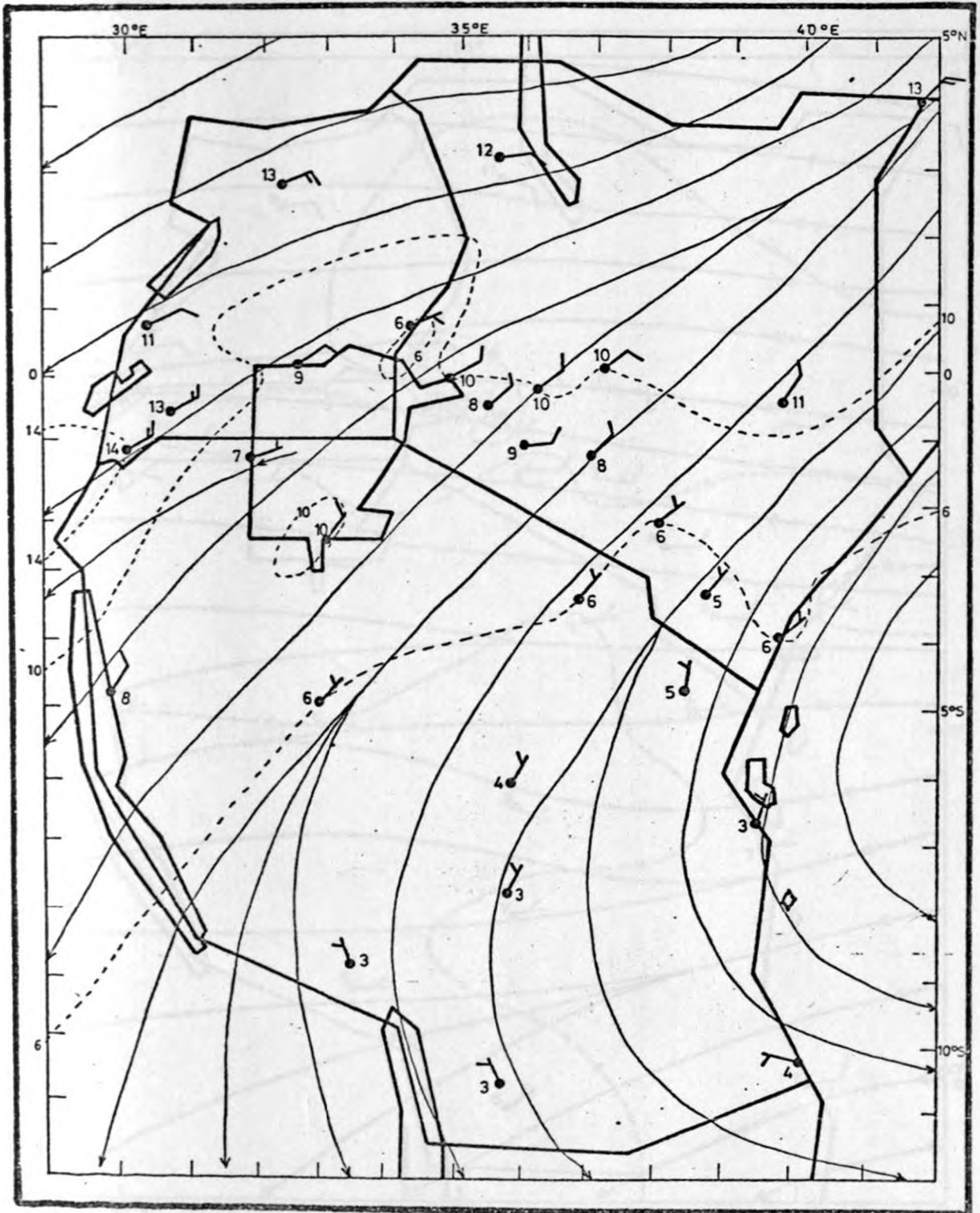


Fig. 5(c) : Mean wind field at 4270 m AMSL in February.

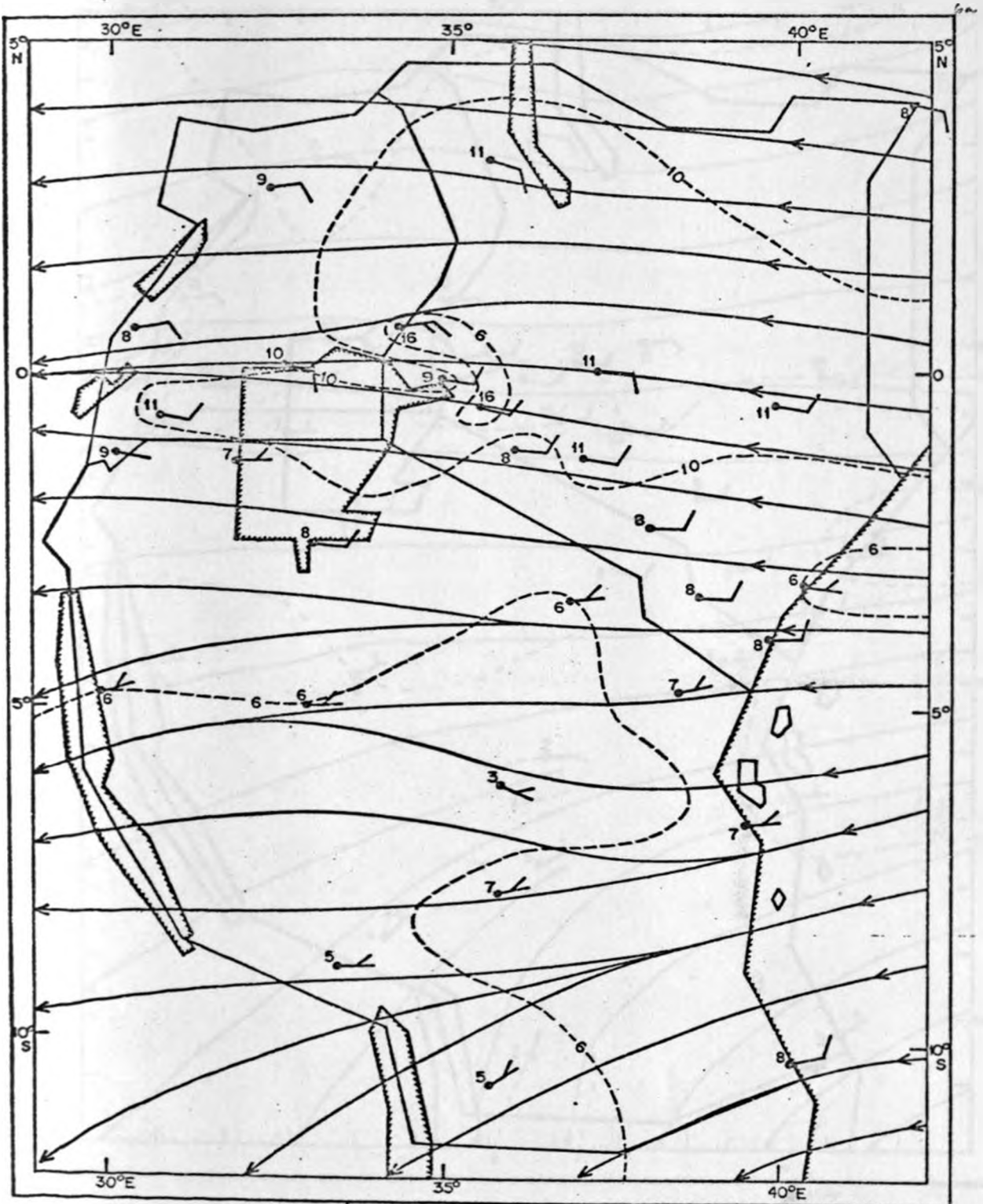


Fig. 6(a) : Mean wind field at 5490 m AMSL in December.

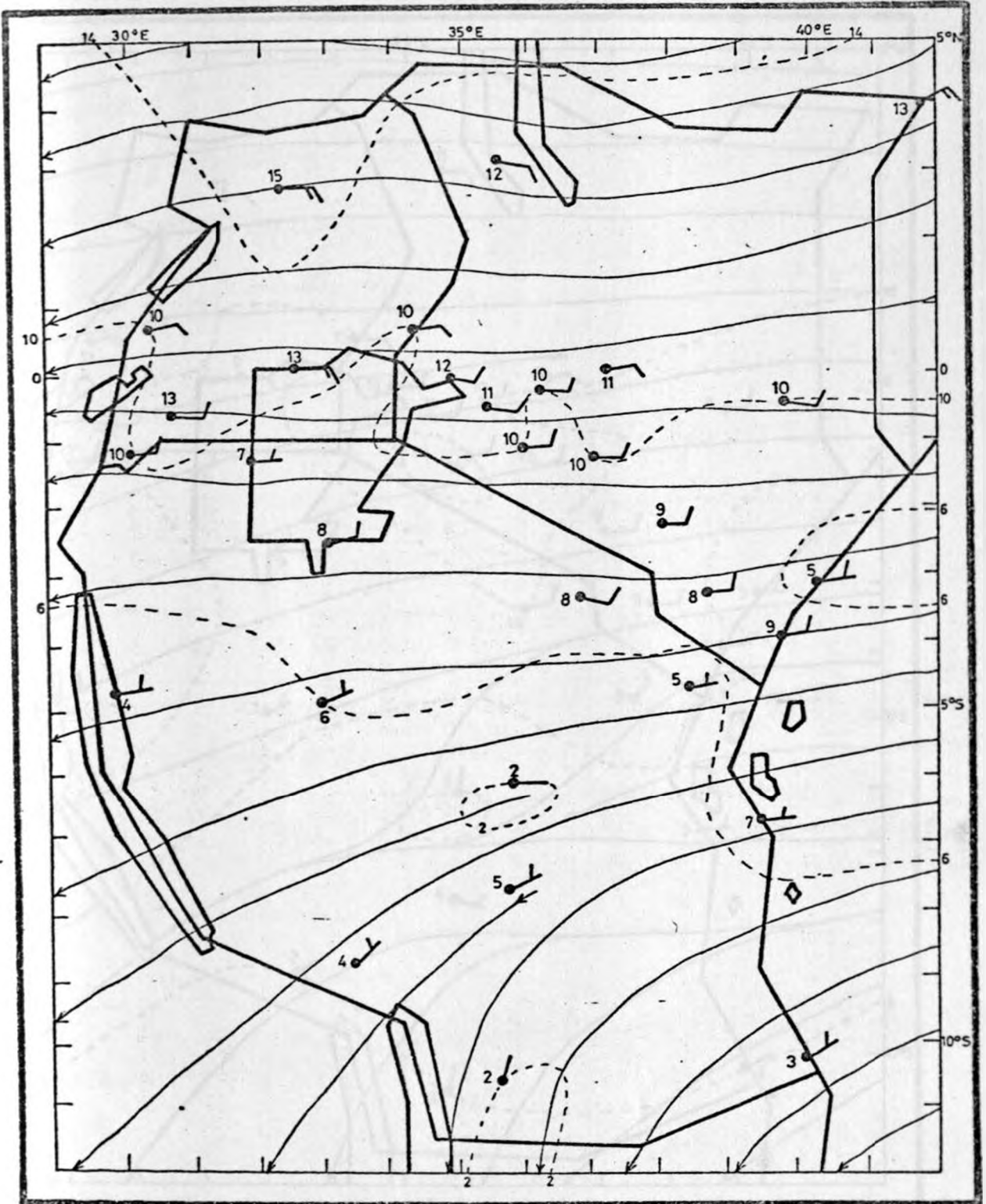


Fig. 6(b) : Mean wind field at 5490 m AMSL in January..

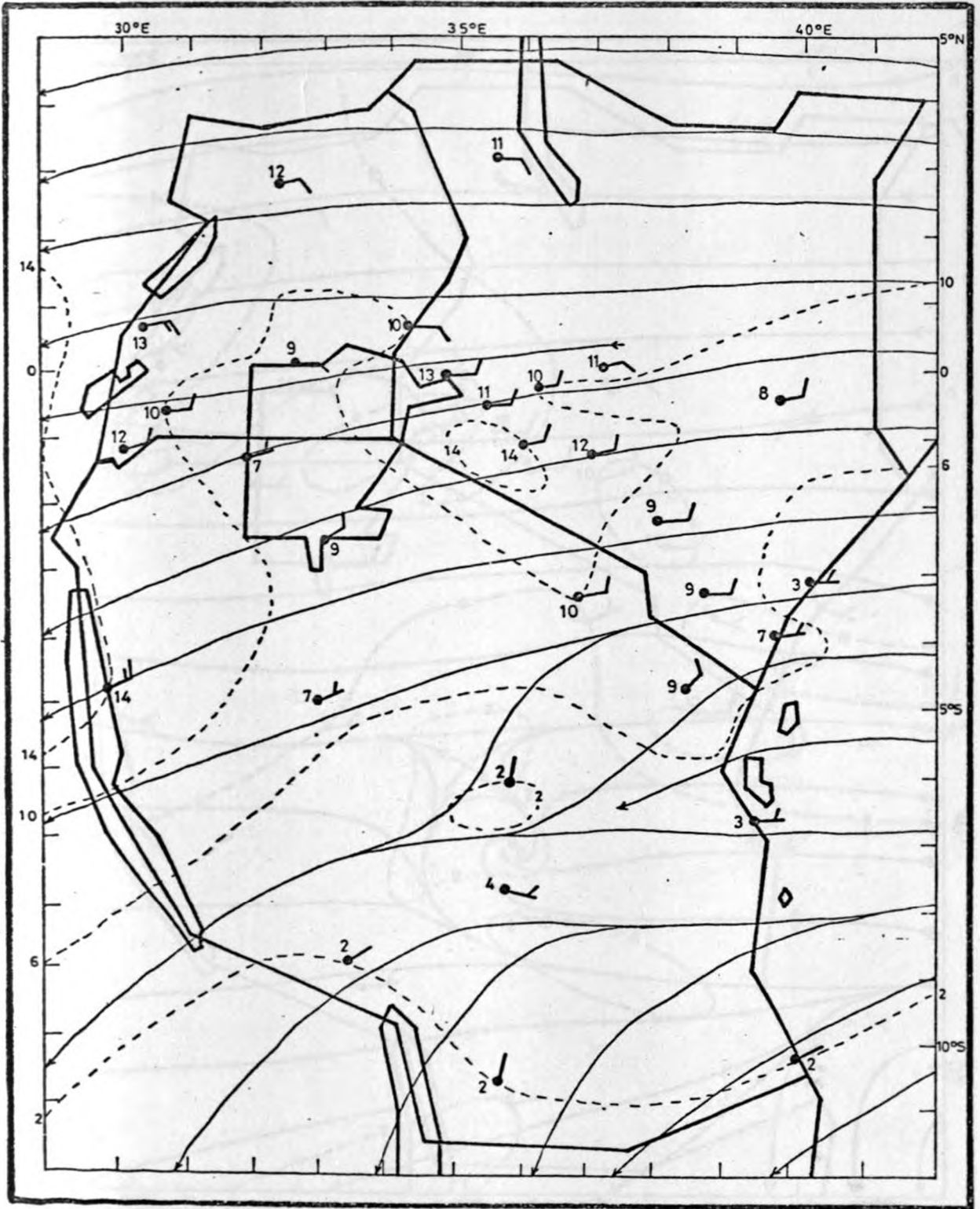


Fig. 6(c) : Mean wind field at 5490 AMSL in February.

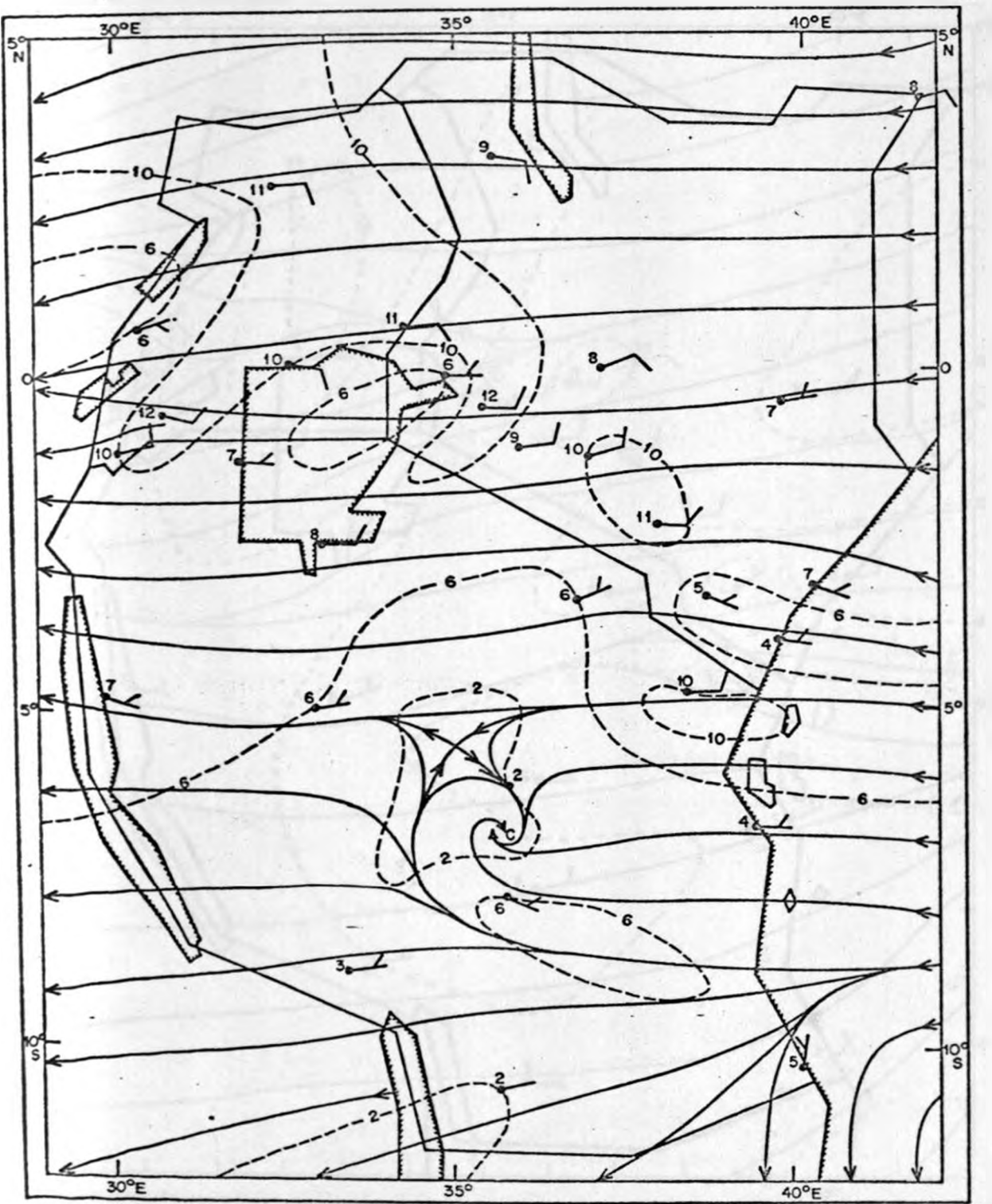


Fig. 7(a) : Mean wind field at 7320 m AMSL in December.

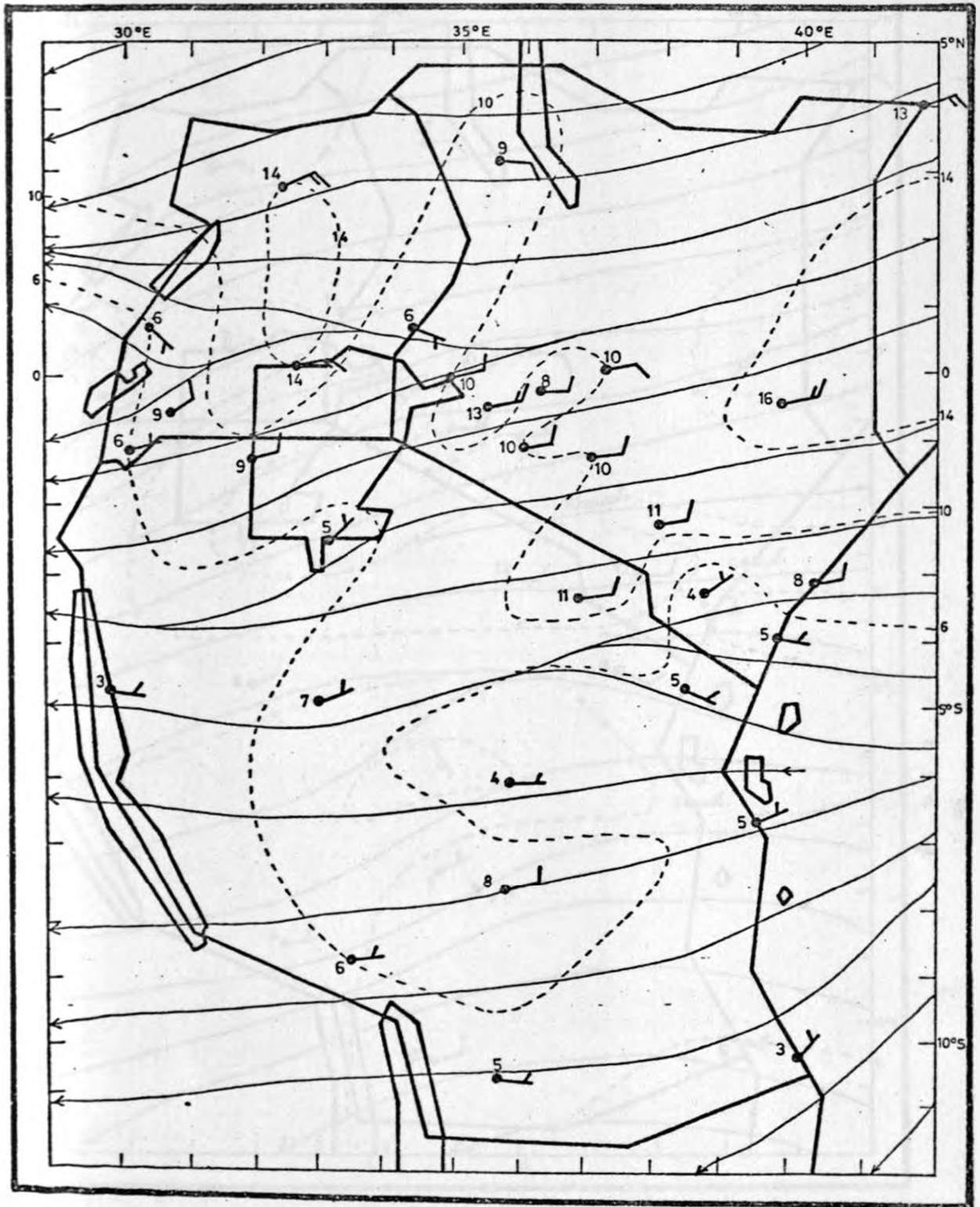


Fig. 7(b) : Mean wind field at 7320 m AMSL in January.

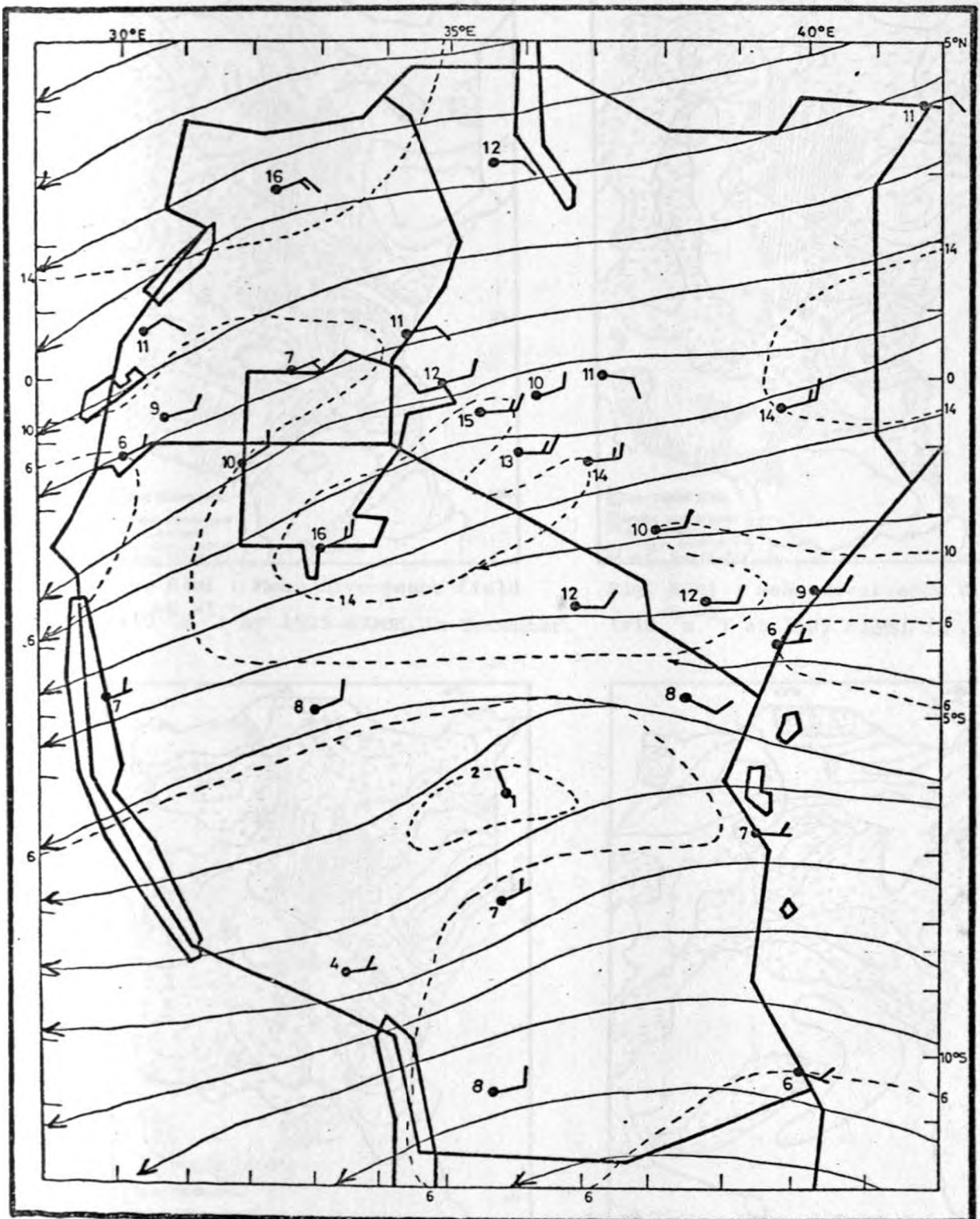


Fig. 7(c) : Mean wind field at 7320 m AMSL in February.



Fig. 8(a) : Mean divergence field ($\times 10^{-6} \text{ s}^{-1}$) at 1525 m AMSL in December.



Fig. 8(b) : Mean divergence field ($\times 10^{-6} \text{ s}^{-1}$) at 1525 m AMSL in January.



Fig. 8(c) : Mean divergence field ($\times 10^{-6} \text{ s}^{-1}$) at 1525 m AMSL in February.

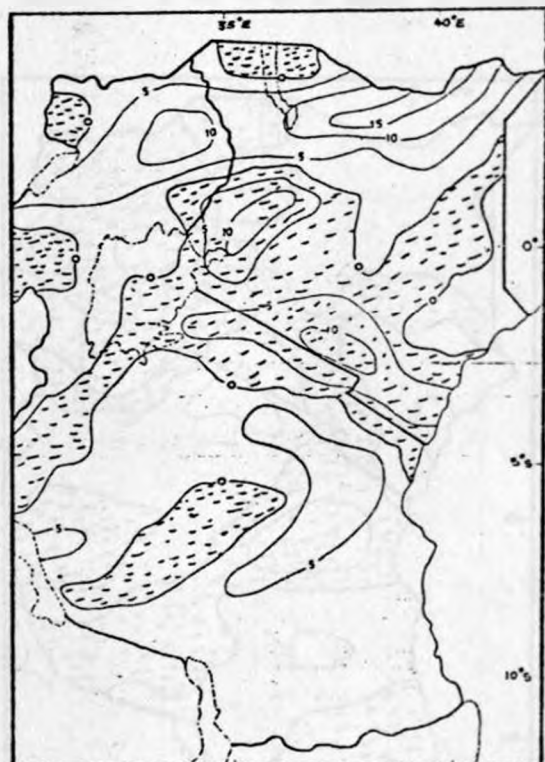


Fig. 9(a) : Mean divergence field ($\times 10^{-6} \text{ s}^{-1}$) at 3050 m AMSL in December.



Fig. 9(b) : Mean divergence field
($\times 10^{-6} \text{ s}^{-1}$) at 3050 m AMSL in January.

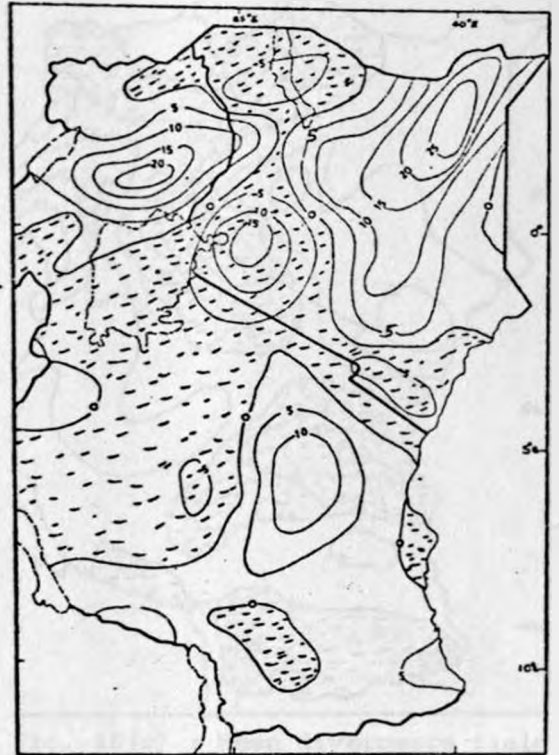


Fig. (c) : Mean divergence field
($\times 10^{-6} \text{ s}^{-1}$) at 3050 m AMSL in February.



Fig. 9(d) : Mean divergence field
($\times 10^{-6} \text{ s}^{-1}$) at 4270 m AMSL in January.

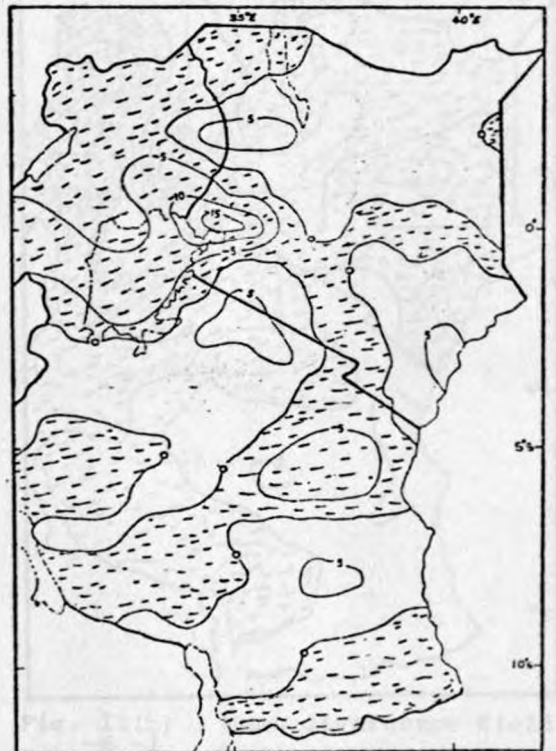


Fig. 10(a) : Mean divergence field
($\times 10^{-6} \text{ s}^{-1}$) at 5490 m AMSL in December.

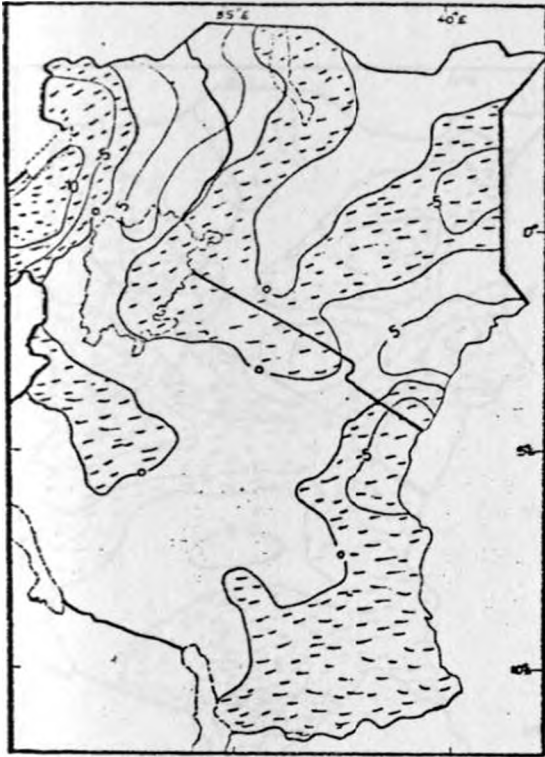


Fig. 10(b) : Mean divergence field ($\times 10^{-6} \text{ s}^{-1}$) at 5490 on AMSL in January.



Fig. 10(c) : Mean divergence field ($\times 10^{-6} \text{ s}^{-1}$) at 5490 on AMSL in February



Fig. 11(a) : Mean divergence field ($\times 10^{-6} \text{ s}^{-1}$) at 7320 m AMSL in December.



Fig. 11(b) : Mean divergence field ($\times 10^{-6} \text{ s}^{-1}$) on 7320 m AMSL in January.



Fig. 11(c) : Mean divergence field ($\times 10^{-6} \text{ s}^{-1}$) at 7320 m AMSL in February.



Fig. 12(a) : Mean January vertical motion field ($\times 10^{-2} \text{ ms}^{-1}$) at 1525 m AMSL.



Fig. 12(b) : Mean January vertical motion field ($\times 10^{-2} \text{ ms}^{-1}$) at 3050 m AMSL.

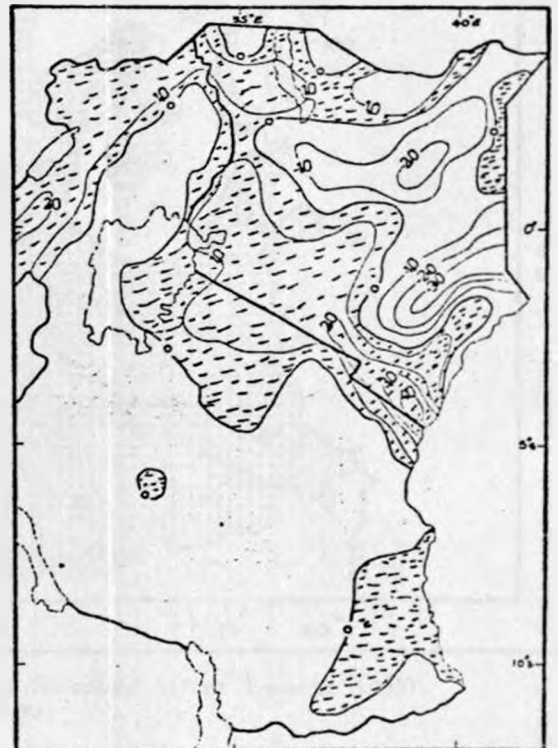


Fig. 12(c) : Mean January vertical motion field ($\times 10^{-2} \text{ ms}^{-1}$) at 5490 m AMSL.

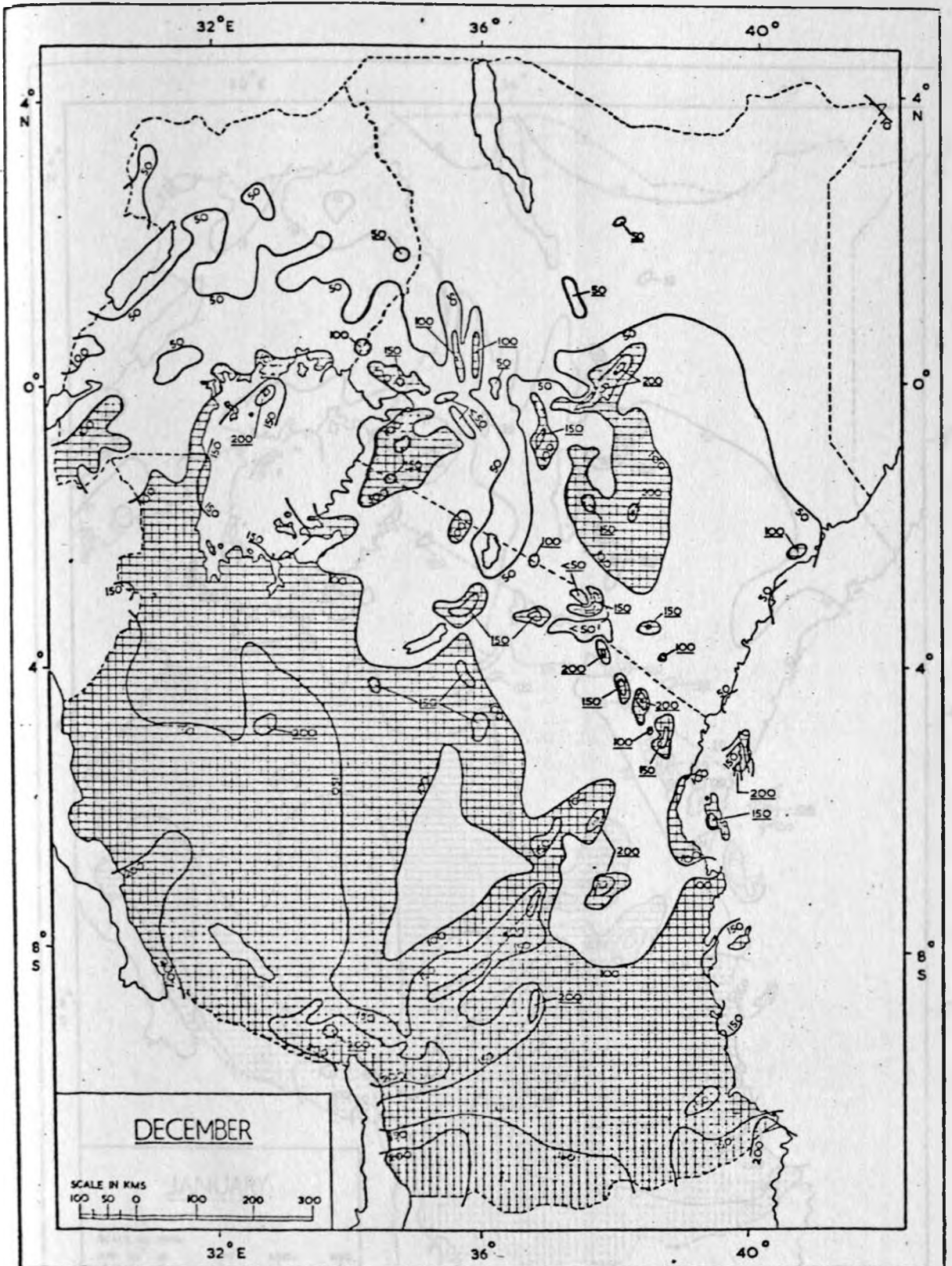


Fig. 13(a) : Mean monthly rainfall (mm) for December (after Tomsett 1969).
Shaded area receives over 100 mm.

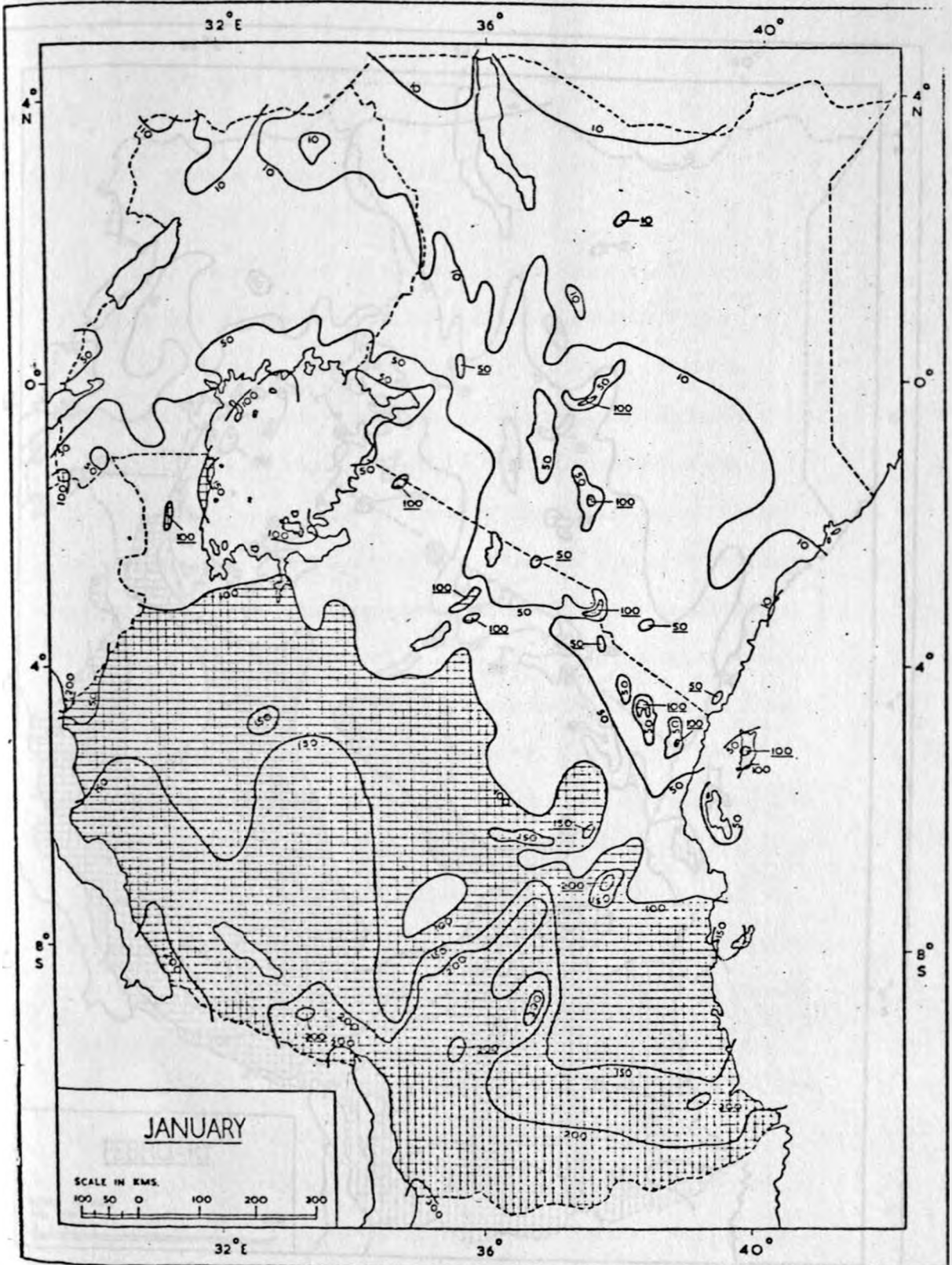


Fig. 13(b) : Mean monthly rainfall (mm) for January (after Tomsett 1969).
Shaded area receives over 100 mm.

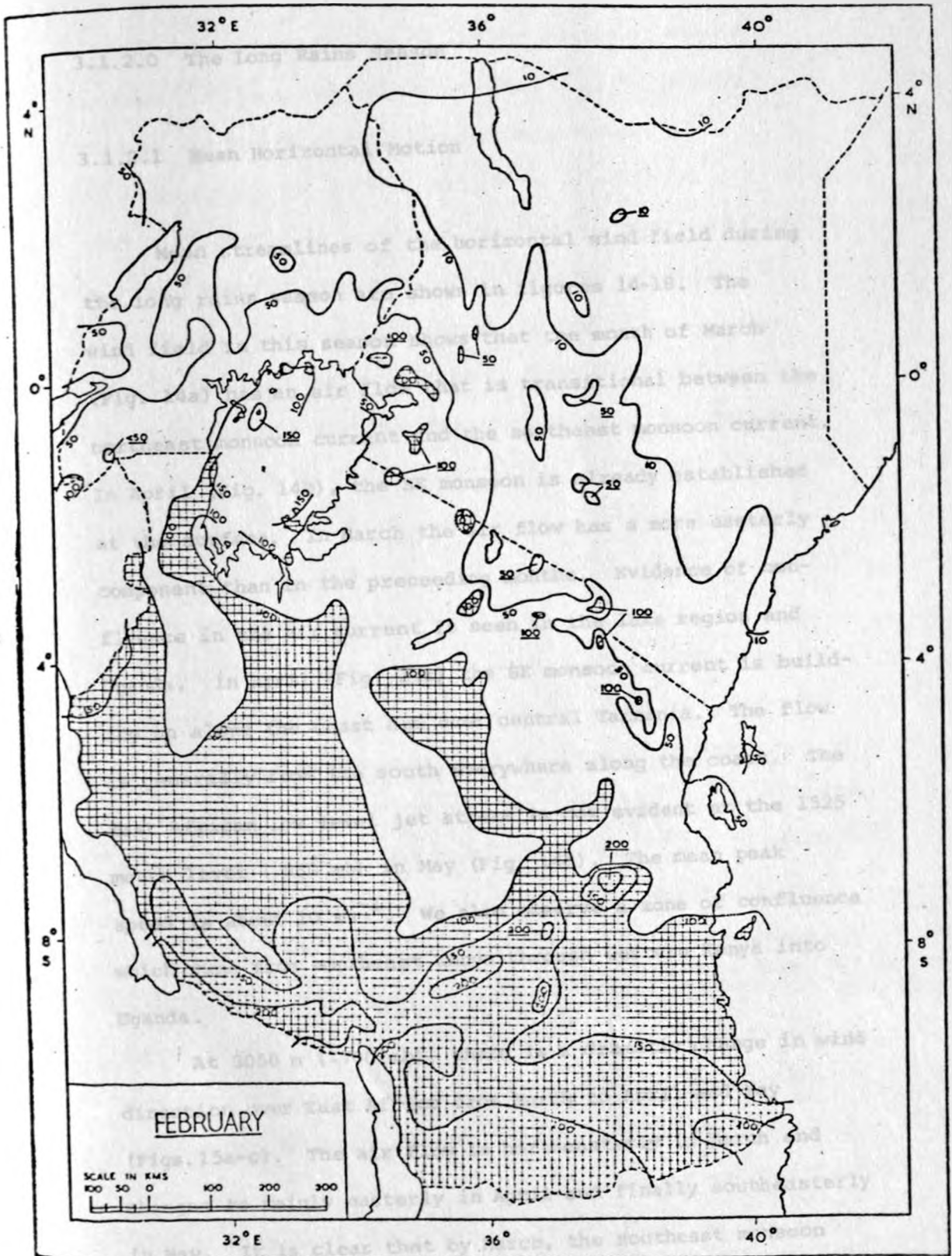


Fig. 13(c) : Mean monthly rainfall (mm) for February (after Tomsett 1969).
Shaded area receives over 100 mm.

3.1.2.0 The Long Rains Season

3.1.2.1 Mean Horizontal Motion

Mean streamlines of the horizontal wind field during the long rains season are shown in figures 14-18. The wind field in this season shows that the month of March (Fig. 14a) has an air flow that is transitional between the northeast monsoon current and the southeast monsoon current. In April (Fig. 14b), the SE monsoon is already established at the surface. In March the air flow has a more easterly component than in the preceding months. Evidence of confluence in the air current is seen in the lake region and Uganda. In April (Fig. 14c) the SE monsoon current is building up along the coast and over central Tanzania. The flow is generally from the south everywhere along the coast. The East African low level jet stream is now evident at the 1525 metre level (~850 mb) in May (Fig. 14d). The mean peak speed is about 10 ms^{-1} . We also observe a zone of confluence which runs from southeast Kenya through western Kenya into Uganda.

At 3050 m (~700 mb), there is a dramatic change in wind direction over East Africa from March to April and May (Figs. 15a-c). The air flow is northeasterly in March and changes to mainly easterly in April and finally southeasterly in May. It is clear that by March, the southeast monsoon has already set in near the surface where as medium levels

remain under the influence of the dry northeast monsoon current. In fact the 700 mb air flow in March is very similar to that observed during January-February.

In April, the ITCZ at the 700 mb level (Fig. 15b) is easily identified as a zone of confluence between northeasterly and southeasterly currents. The ITCZ lies generally over southern Kenya and western Kenya. In May (Fig. 15c) the ITCZ is observed over northeastern Kenya, Kenya highlands, the lake Victoria region and western Uganda. The southeast monsoon current is still discernible at this level along the coastal belt. The 700 mb level is the transitional level between the young southeast monsoon current in the low levels and the easterly current aloft.

At 4270 m (~600 mb), the flow in March (Fig. 16a) is similar to that in February. In April (Fig. 16b), the air flow is east-northeasterly north of the equator and east-southeasterly south of the equator. There is weak confluence between these two streams near latitudes 1° - 2° S. In southern Tanzania we observe some form of anticyclonic circulation, an indication of the equatorward ridging of the Mascarene high. In May (Fig. 16c), the flow is wholly northeasterly in Kenya, Uganda and northern Tanzania. Elsewhere in Tanzania, it is either easterly or southeasterly. The confluence between the different streams lies between 1° N and 4° S.

The flow at 5490 m (~500 mb) in March is east-northeasterly almost everywhere in East Africa (Fig. 17a). The diffluence that is present in southern Tanzania at lower levels is weakly

evident at this level. In April (Fig. 17b), the air flow is more or less easterly everywhere, with very weak confluence that is located over the Kenya highlands. The wind flow at this level is relatively strong in the neighbourhood of the equator, with speeds of upto 7 ms^{-1} . In May (Fig. 17c), there are two zones of confluence, one is located over northeastern Tanzania and the other in the neighbourhood of the equator in Kenya.

At 7320 m (~400 mb), the wind flow in March and April (Figs. 18a-b) is easterly almost everywhere. High wind speeds in this air flow are found in the vicinity of the equator. In May (Fig. 18c), southeasterly flow is dominant over most of Tanzania. The northern parts of East Africa are under the influence of northeasterly flow. The confluence between these two air currents is located over southern Kenya/northeastern Tanzania. An anticyclonic circulation is now evident over southwestern parts of Tanzania.

3.1.2.2 Mean Divergence and Vertical Motion Fields

The Divergence/convergence patterns associated with the wind flow fields during the long rains season are presented in figures 19-20 and 22. The vertical motion fields for April, the mid-season month, are shown in figures 21a-c. From figure 19a we note that inspite of the rather dramatic change of wind direction at 850 mb from northeasterly in February to mainly easterly-to-southeasterly in March, the

divergence/convergence pattern for March remains very similar to that established during the preceding northeast monsoon months. However, the magnitude of divergence over eastern Kenya and northeastern Tanzania has decreased considerably. The only major change from February to March seems to be in the low level wind direction in which there is a pronounced onshore easterly component in March. When the flow is easterly in the low levels one expects advection of moisture into the East African region. The moisture advection into existing convergent zones leads to active weather conditions. It is further seen from figure 19a that the convergent area in western Tanzania has extended to cover most of western, northwestern and southwestern parts of Tanzania. The level of transition between low level convergence/divergence and upper level divergence/convergence lies between 500-400 mb (Figs. 19c-d).

The convergent area that was established in preceding months in western Tanzania has moved northeastwards in April (Fig. 20a) and now lies in a southeast-to-northwest direction spanning from southeast to northwestern Tanzania. Another convergence zone lies across the northern part of East Africa. This zone runs from Kenya coast into northwestern Uganda. At 700 mb (Fig. 20b) the convergence zone across Kenya and Uganda is distinct. The maximum convergence values in this zone are of the order of $1.7 \times 10^{-5} \text{ s}^{-1}$ near the lake Victoria region in Kenya. The convergence zone present in Tanzania is still evident at this level. Hills (1978), in

his study of organisation of rainfall in East Africa, observed rainfall patterns during the long rains that resemble these spatial patterns of divergence-convergence values. He found that the two wet belts, one in southern Tanzania, the other across Kenya and Uganda, were quite independent of each other. We would like to suggest here that, while the Kenya/Uganda/northern Tanzania rains in April are in association with the ITCZ, the rains in southern Tanzania are associated with convergence within the southeast monsoon current over the area. The movement of the convergent zones from February through May is in close agreement with Hills' observation of the movement of wet zones during the long rains season. The southern summer ITCZ over Africa is located near 5°N in West Africa. It then runs meridionally through central Africa into southern Africa where it is located between 15° - 20°S (Thompson 1965). During the onset of the long rains season in East Africa, the meridional branch over central Africa approaches the East African region from western Tanzania while the zonal branch across southern Africa enters East Africa from southern Tanzania. This movement of the ITCZ into East Africa is well demonstrated in the divergence/convergence patterns at low levels from February through May.

The convergent zones are evident even at the 600 mb level (Fig. 20c). At 500 mb (Fig. 20d), the two zones link up across southeastern Kenya. The discussion hitherto shows that the lake Victoria region of Kenya and parts of Uganda have a

deep layer of convergence extending to near 400 mb (Fig. 20e). These areas receive high rainfall amounts during this month (Fig. 23b).

A vertical cross-section (Fig. 20f) along latitude 1°S , the latitude of maximum convergence (ITCZ), has a slight westward tilt (towards the lake region) with height. Figure 20g shows a cross-section along longitude 36°E . We note that below 600 mb, the ITCZ has a slight equatorward tilt with height. Above this level, there is no appreciable tilt. The convergent zone in southern Tanzania has an equatorward tilt with height. The gradient of the vertical tilt of the ITCZ is about 1:100 between 850 mb and 600 mb. Aspliden (1974) found a value of 1:100 in the eastern parts of Africa while Kiangi et al (1981) found the slope of the ITCZ to be between 1:100 and 1:200 in April.

The vertical motion fields for April are given in figures 21a-c. We note from these figures that at 850 mb there is, as one would expect, ascending motion on the southeast facing slopes of the eastern East African highlands. We also observe that at 700 mb (Fig. 21b) and 500 mb (Fig. 21c), the vertical motion field takes on a pattern that is in agreement with the divergence/convergence patterns. The vertical motion in the ITCZ increases from $1 \times 10^{-2} \text{ ms}^{-1}$ near the surface to reach a maximum of about $4 \times 10^{-2} \text{ ms}^{-1}$ near the 500 mb level. Newell et al (1974) have computed vertical velocity for large scale motions in the tropics. Their maximum value at 500 mb over tropical Africa is of the order of $5 \times 10^{-3} \text{ ms}^{-1}$. Hence the maximum vertical

velocity computed in this study is somewhat higher than that obtained by Newell et al.

In May (Figs. 22a-d), when the southeast monsoon current is establishing itself, the eastern plains of East Africa become once more markedly divergent at the 850 mb level (Fig. 22a). Maximum divergence at this level is observed between longitudes 38° - 39° E just to the west of the EALLJ axis. On either side of the jet axis, we observe very steep zonal gradients of divergence. Convergence is prevalent in southwestern Tanzania. This convergent zone in southwestern Tanzania is overlain by divergence at the 700 mb level. This configuration leads to diminished precipitational activities as indicated by the abrupt disappearance of the rainy zone that was present in April (Figs. 23b-c).

At the 700 mb level (Fig. 22b) the air current is convergent across eastern Kenya, lake region and northwestern Uganda. The lake region and northwestern Uganda are, in fact, convergent in a deep layer (Fig. 22c-d). This is in good agreement with the observed rainfall distribution in May (Fig. 23c). Generally the southeast-southwest monsoon current is over-ridden by a convergent air current.

On the whole, we have noted from the temporal and spatial variation of the divergence field that the progression of areas of low level convergence during the long rains season is in close agreement with the temporal march of rainfall patterns in East Africa (Tomsett 1969, Hills 1978). The convergence/divergence patterns presented in this study conform with the

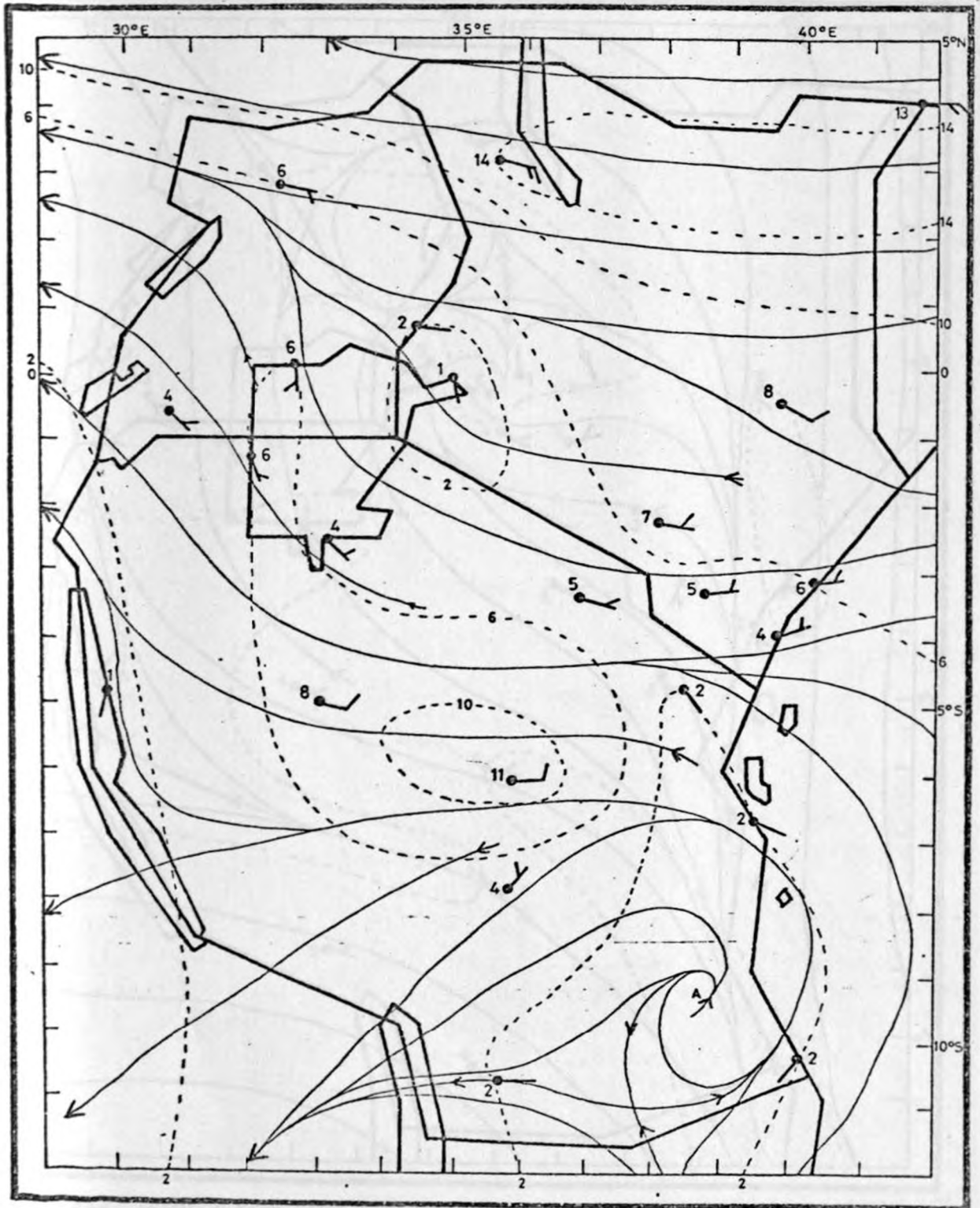


Fig. 14(a) : Mean wind field at 1525 m AMSL in March.

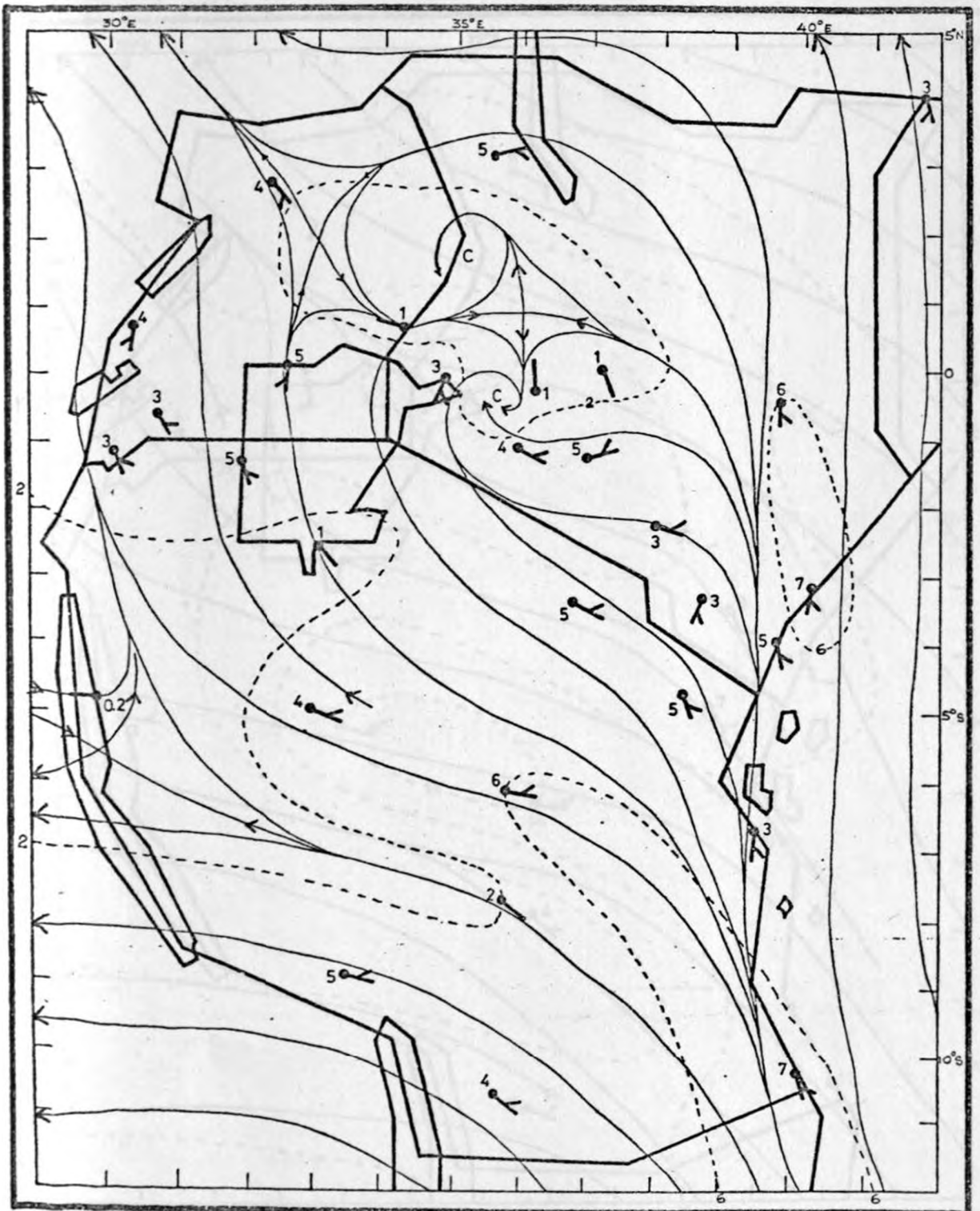


Fig. 14(b) : Mean wind field at the surface in April.

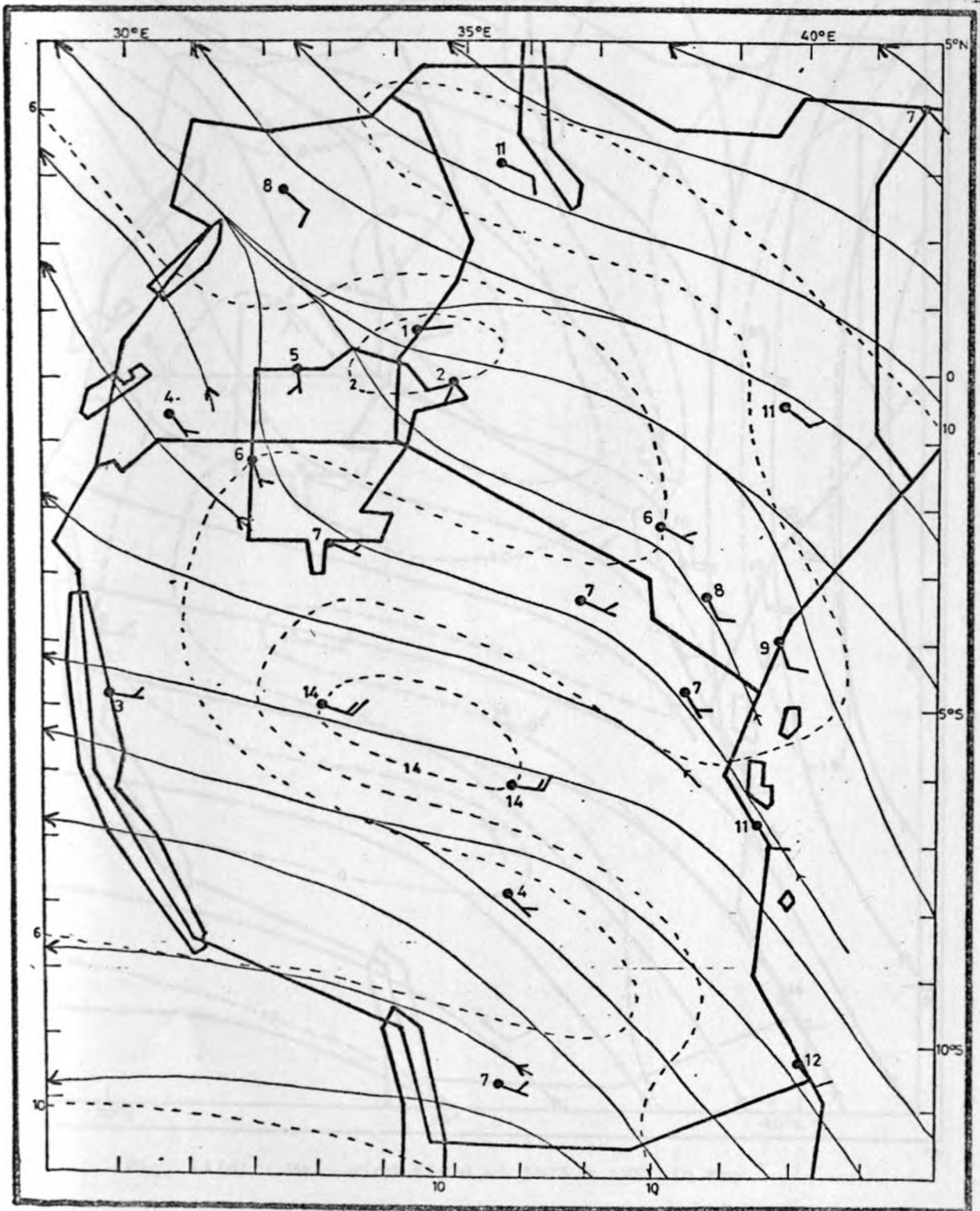


Fig. 14(c) : Mean wind field at 1525 m AMSL in April.

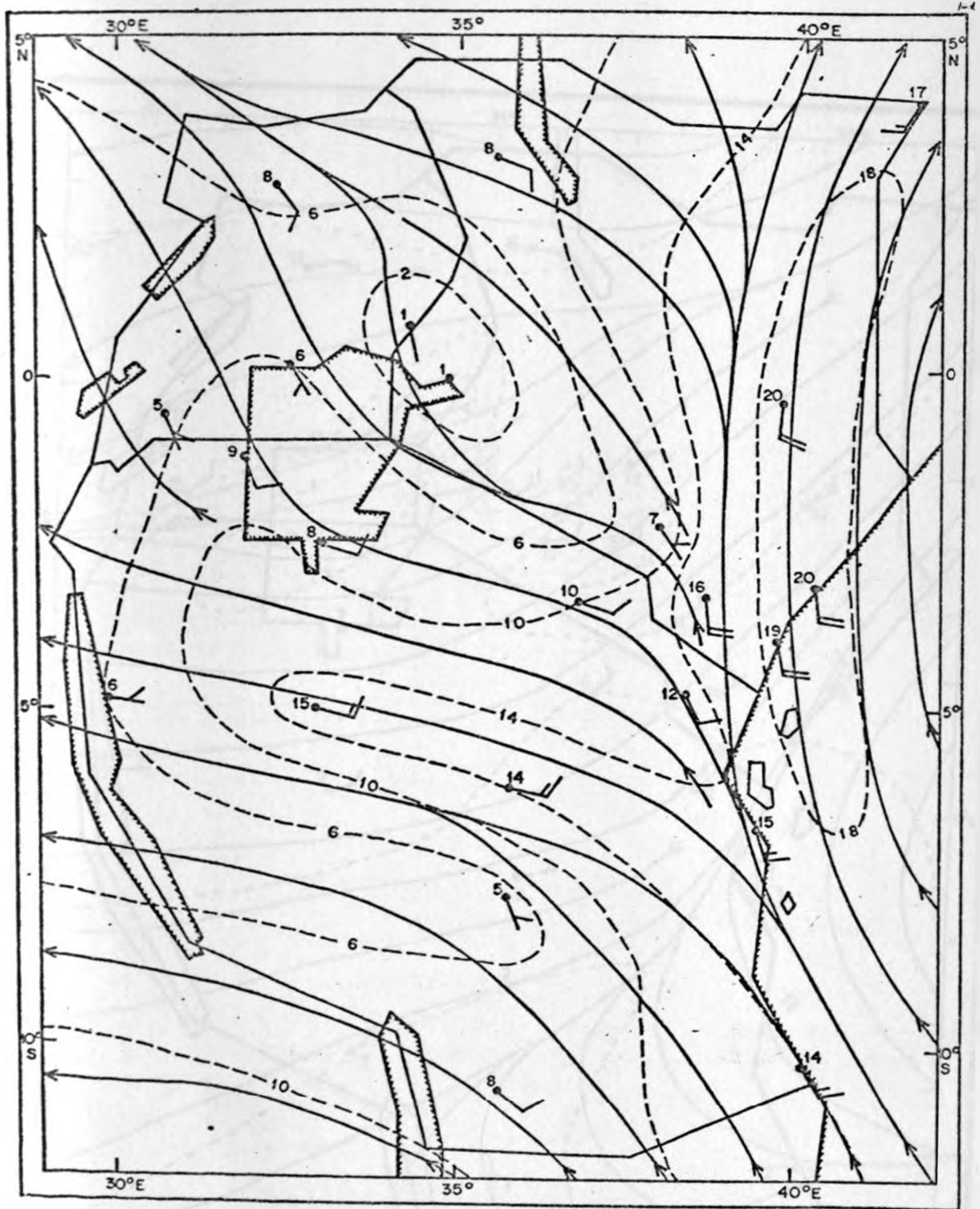


Fig. 14(d) : Mean wind field at 1525 m AMSL in May.

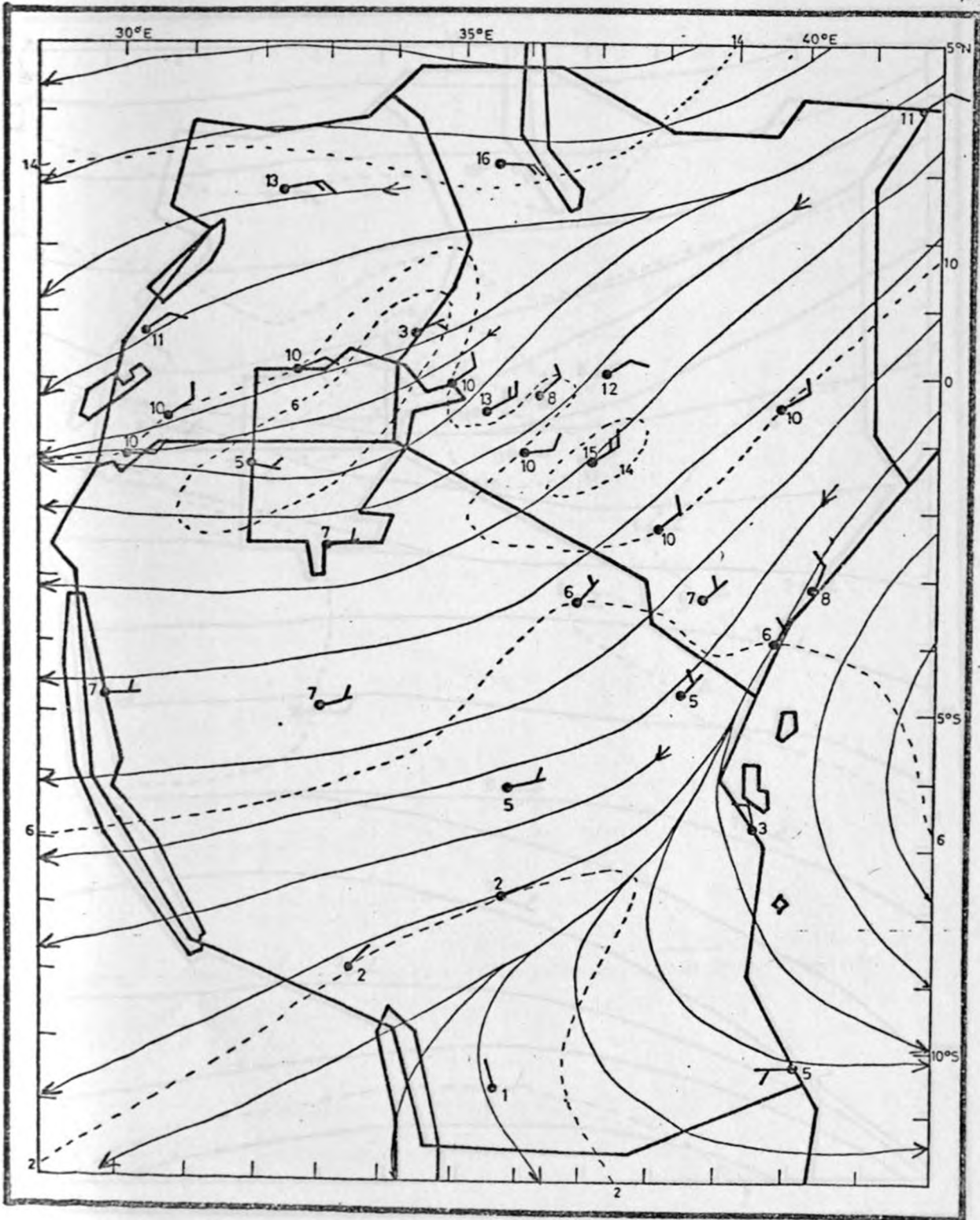


Fig. 15(a) : Mean wind field at 3050 m AMSL in March.

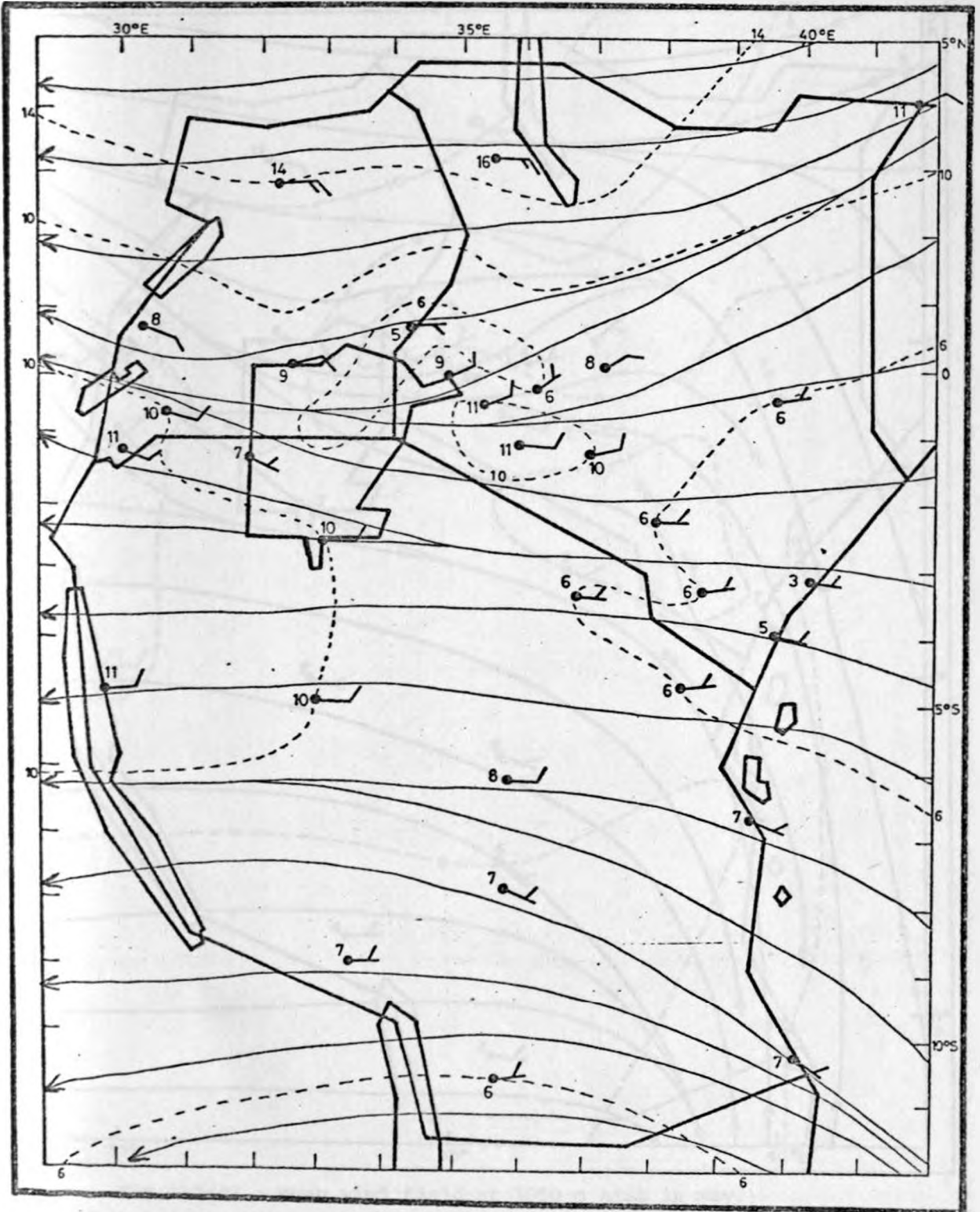


Fig. 15(b) : Mean wind field at 3050 m AMSL in April.

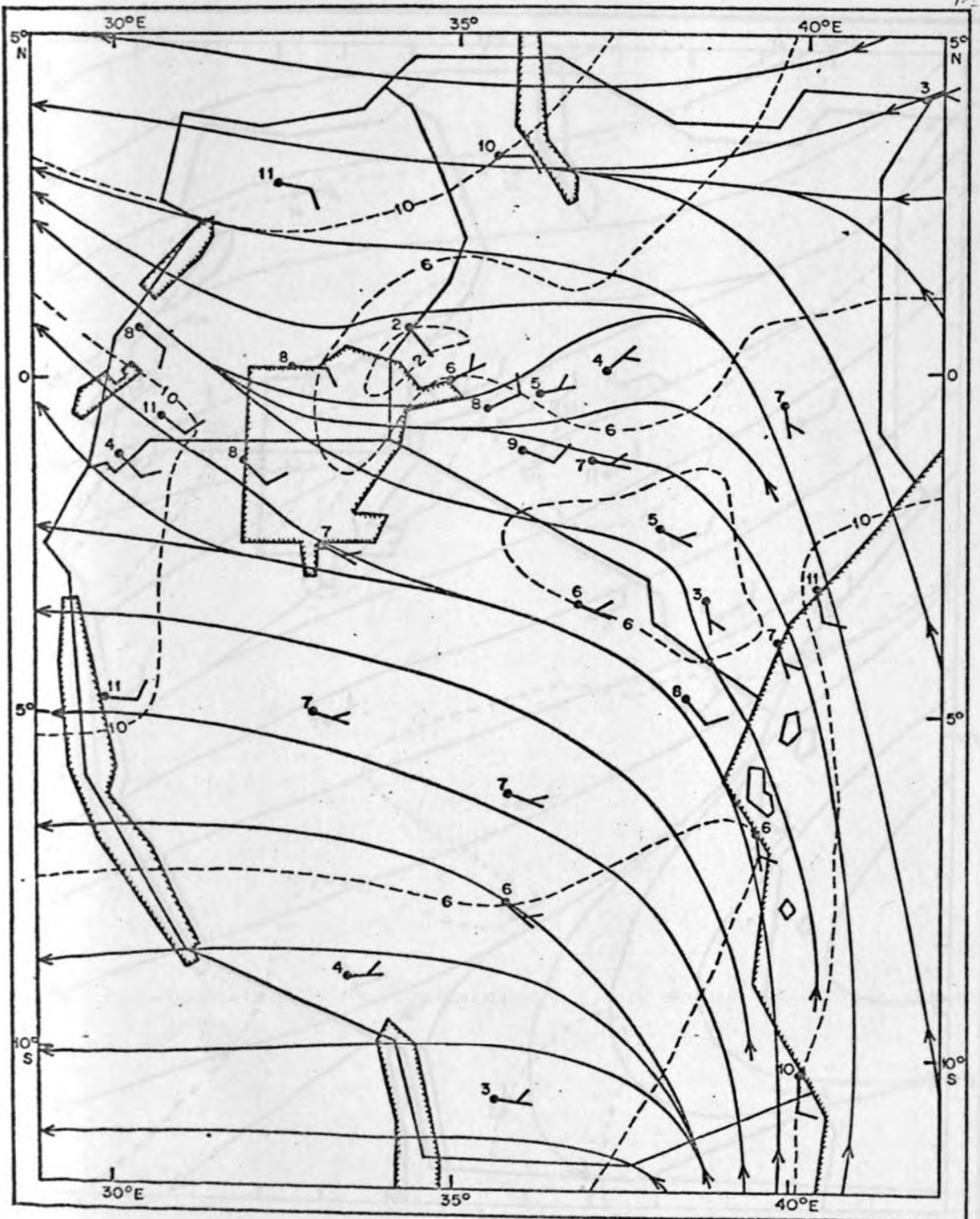


Fig. 15(c) : Mean wind field at 3050 m AMSL in May.

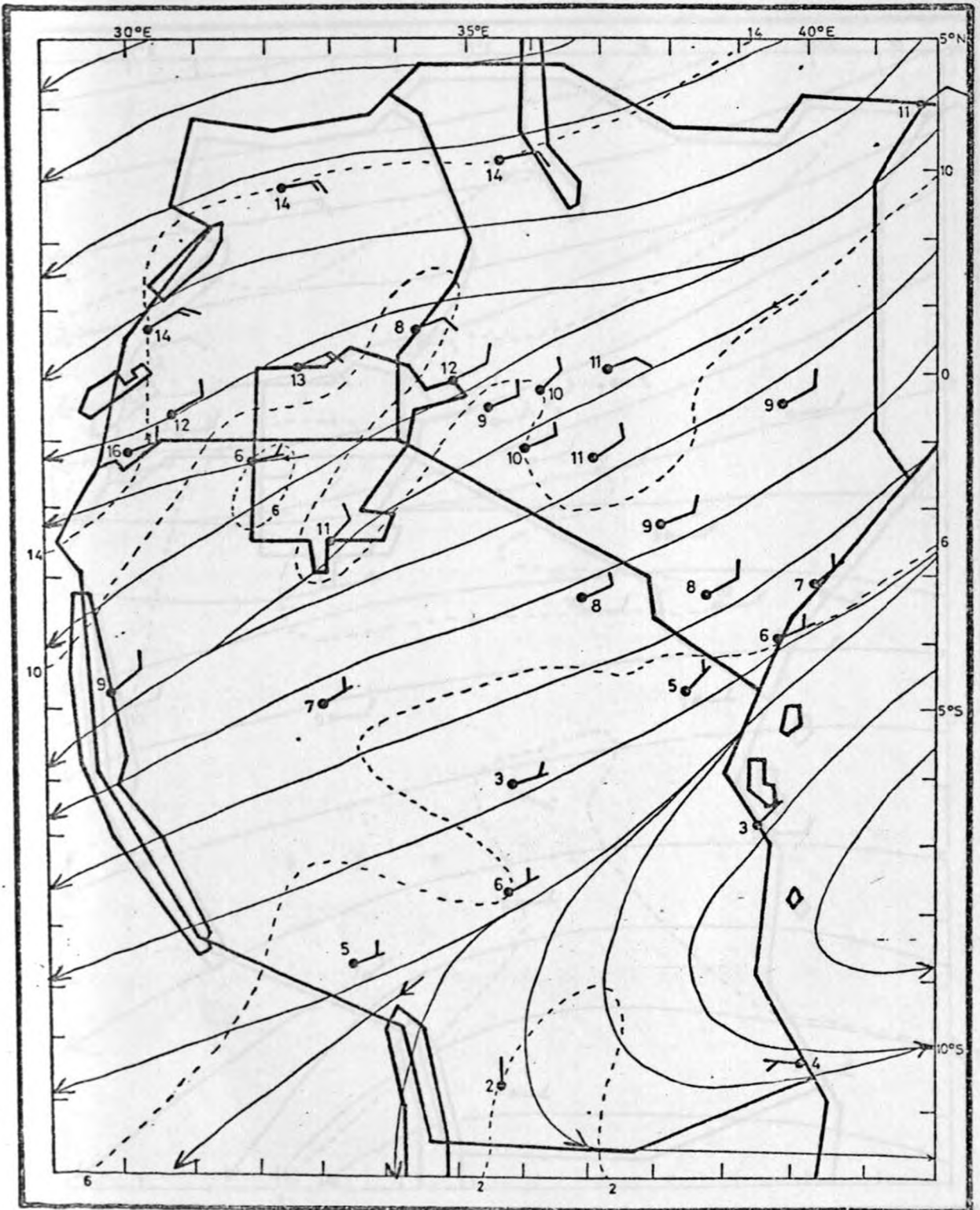


Fig. 16(a) : Mean wind field at 4270 m AMSL in March.

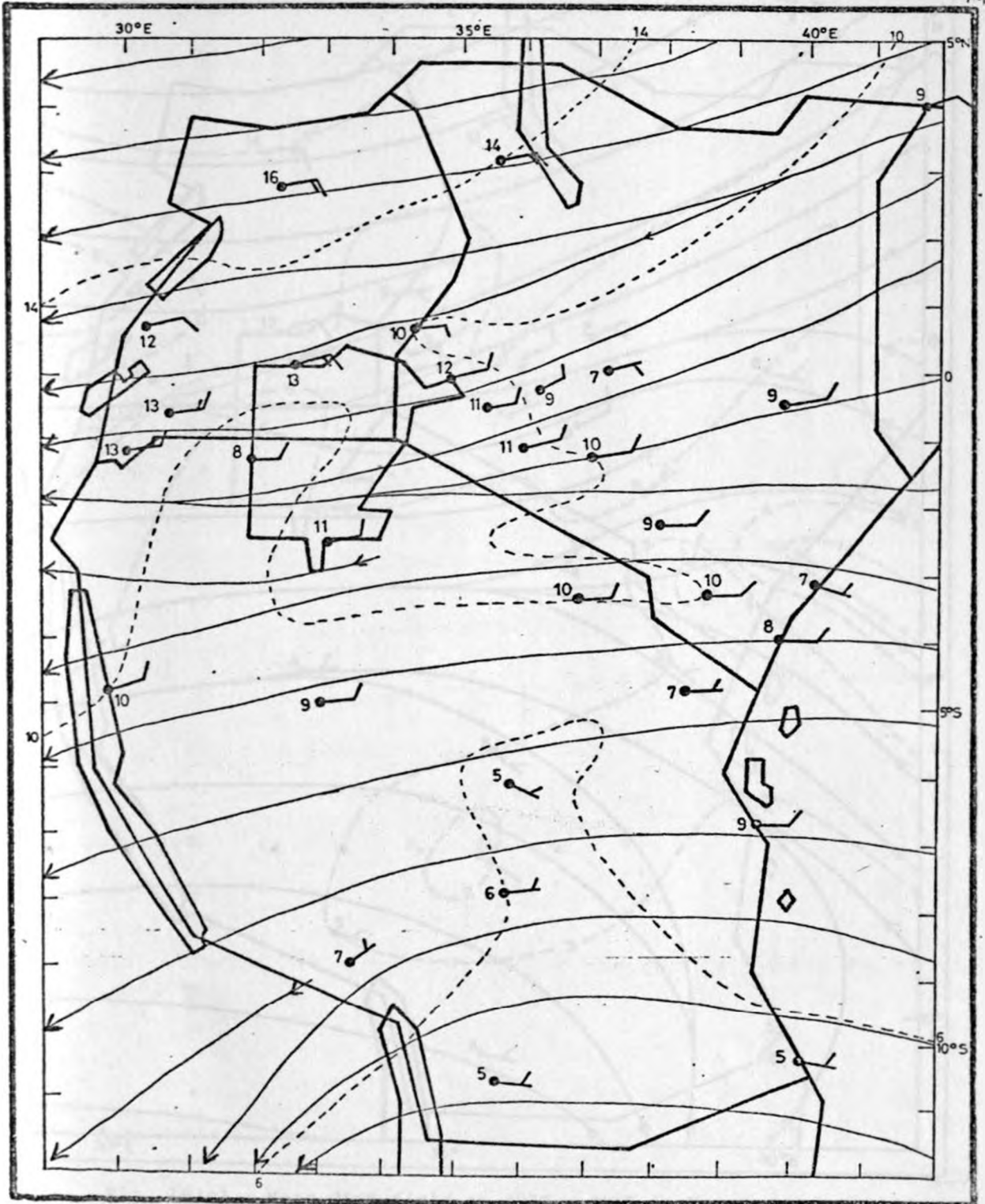


Fig. 16(b) : Mean wind field at 4270 m AMSL in April.

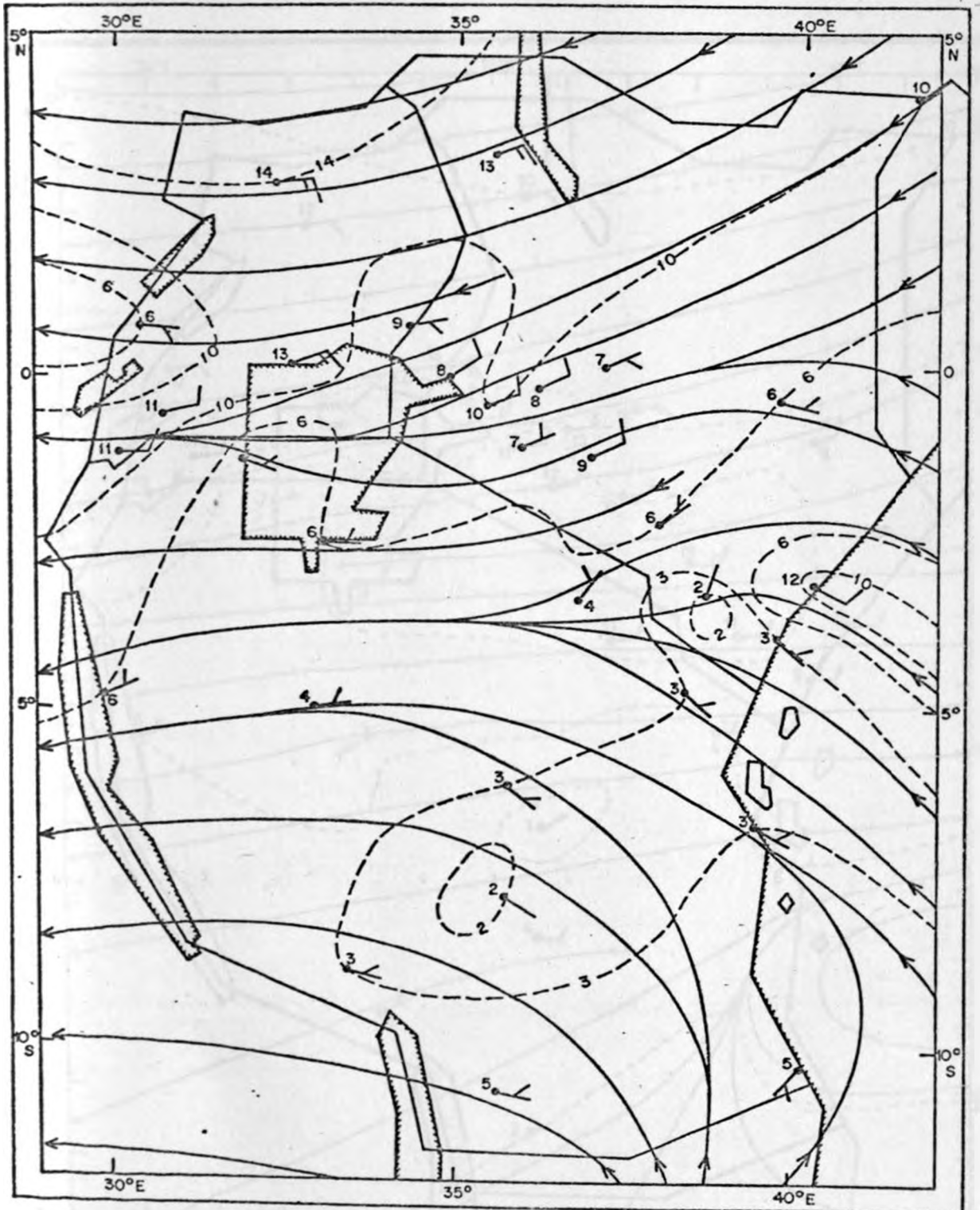


Fig. 16(c) : Mean wind field at 4270 m AMSL in May.

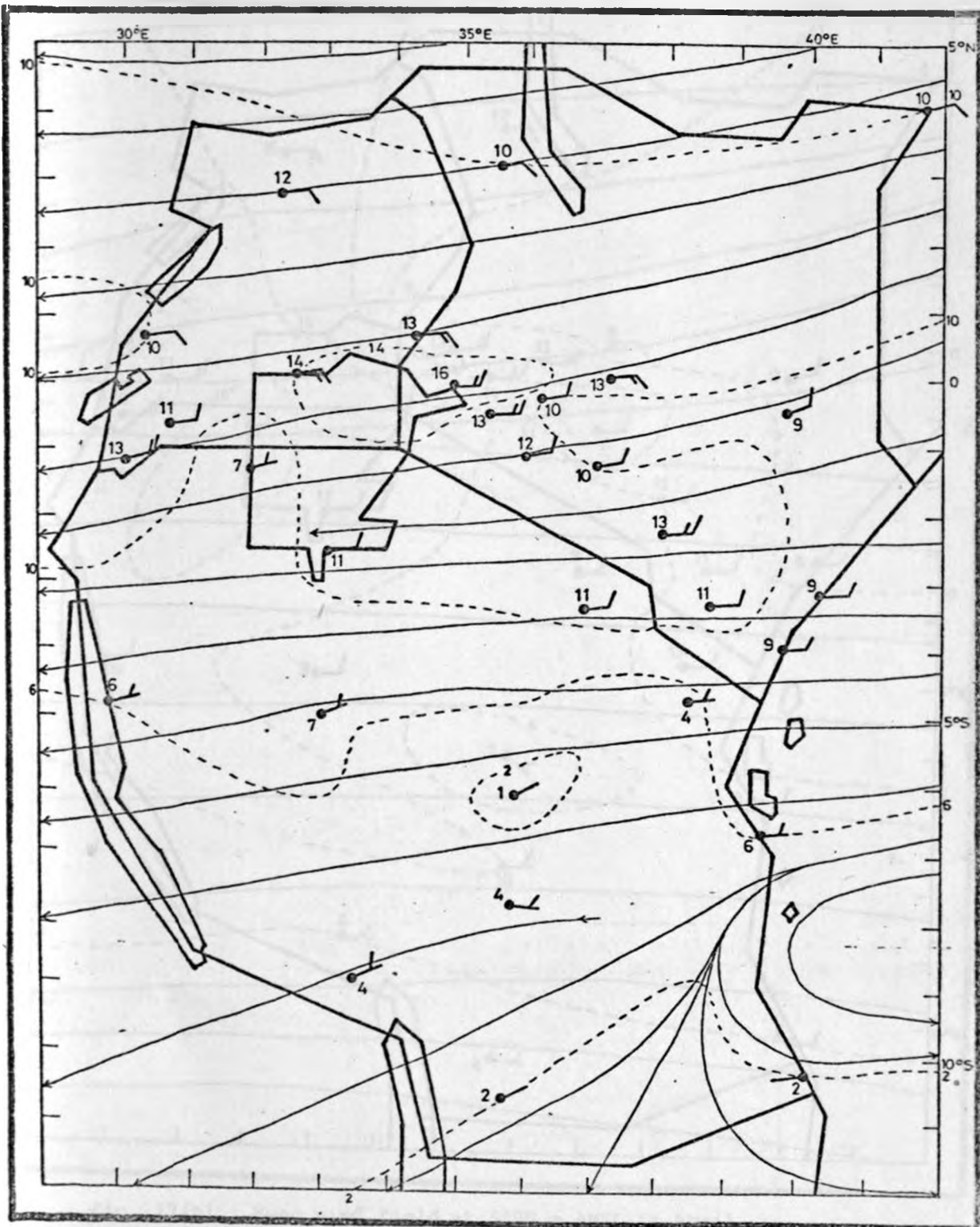


Fig. 17(a) : Mean wind field at 5490 m AMSL in March.

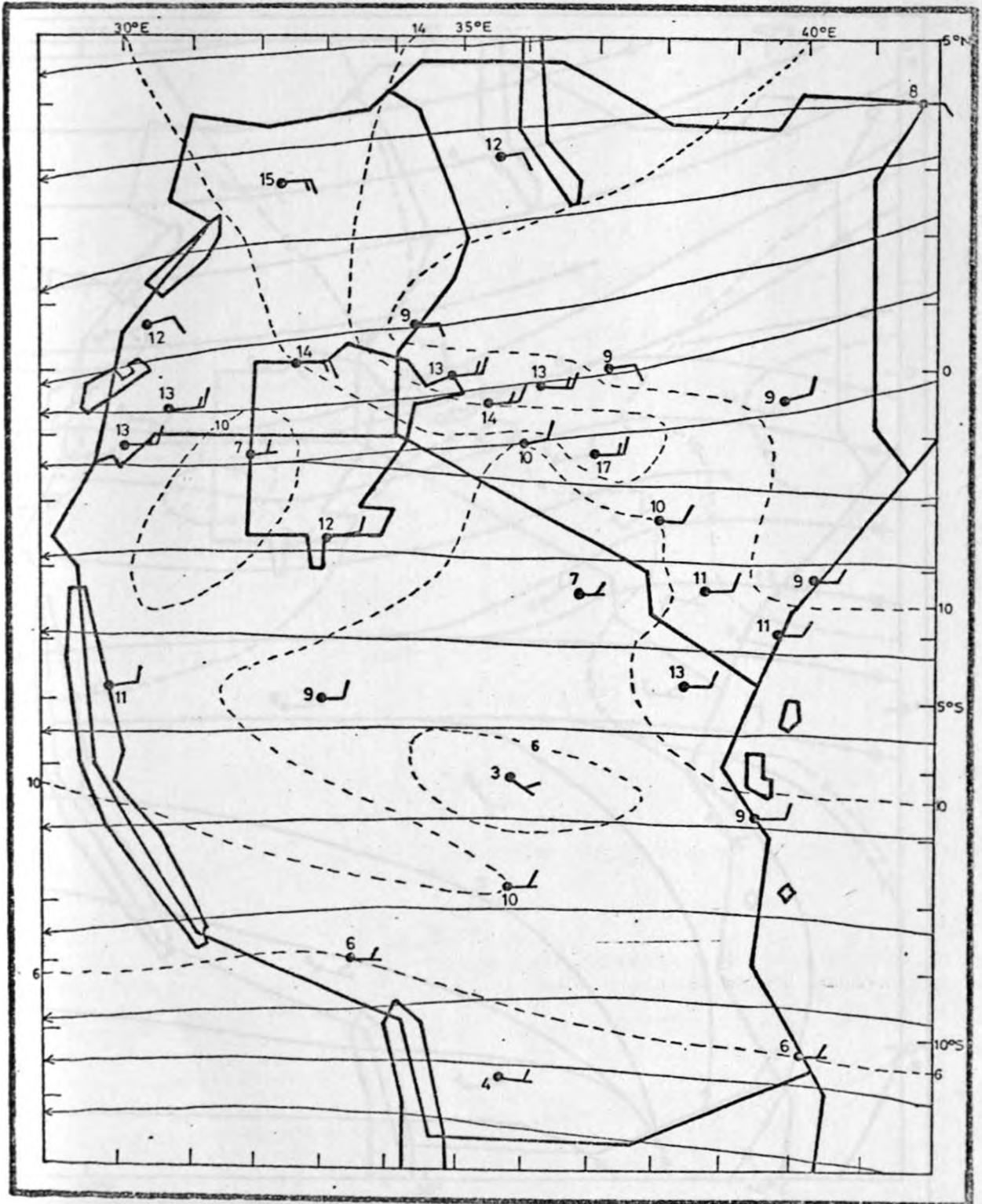


Fig. 17(b) : Mean wind field at 5490 m AMSL in April.

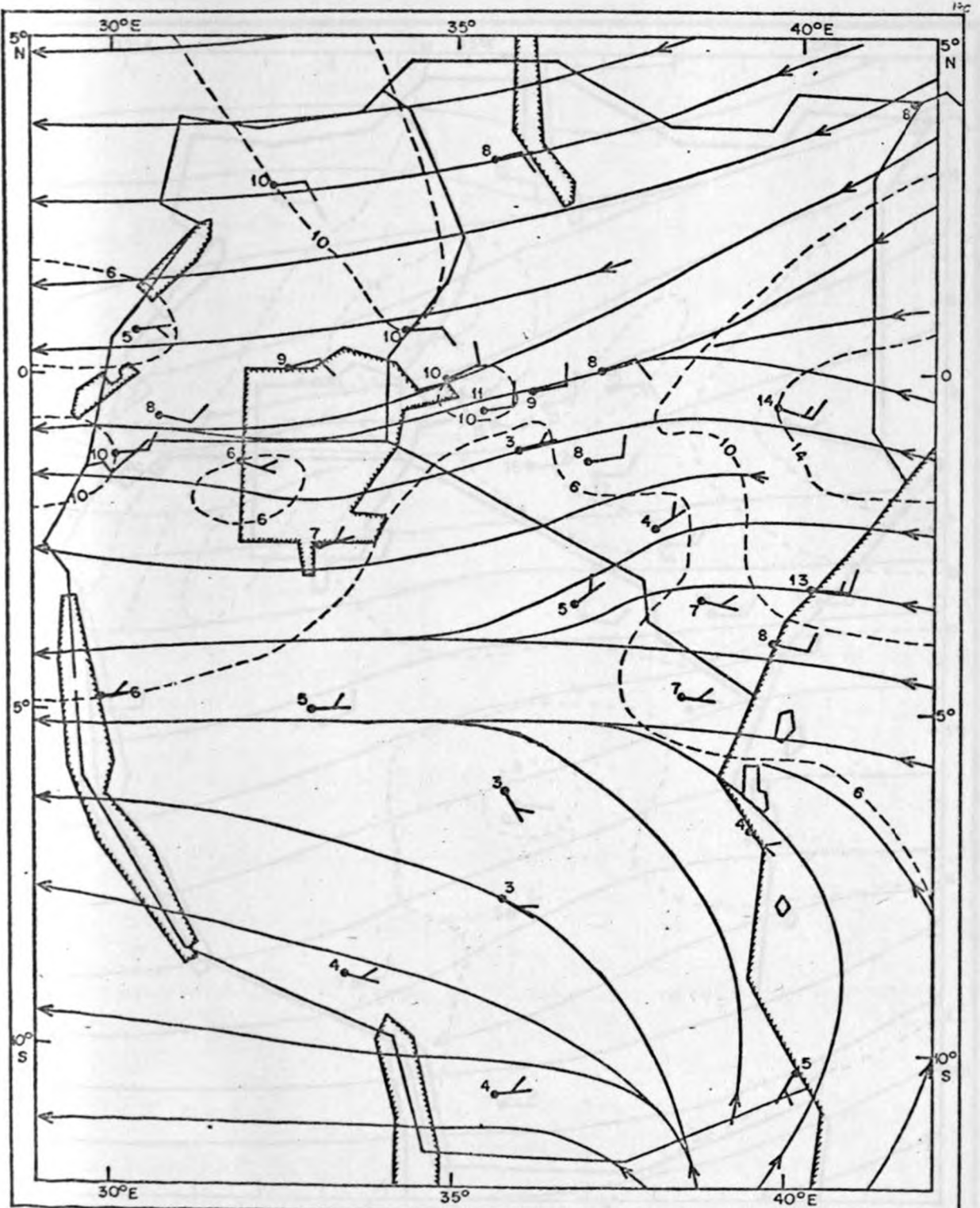


Fig. 17(c) : Mean wind field at 5490 m AMSL in May.

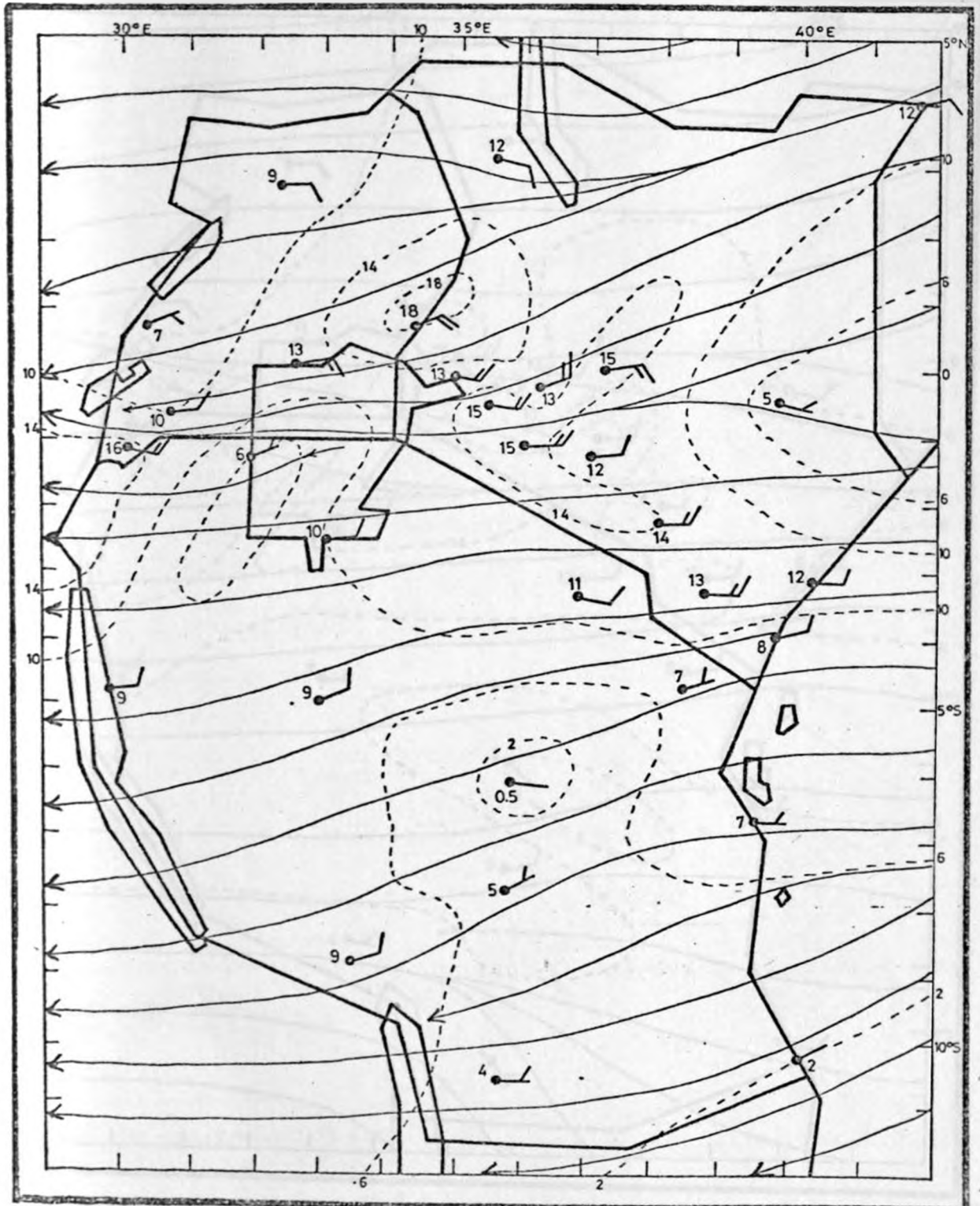


Fig. 18(a) : Mean wind field at 7320 m AMSL in March.

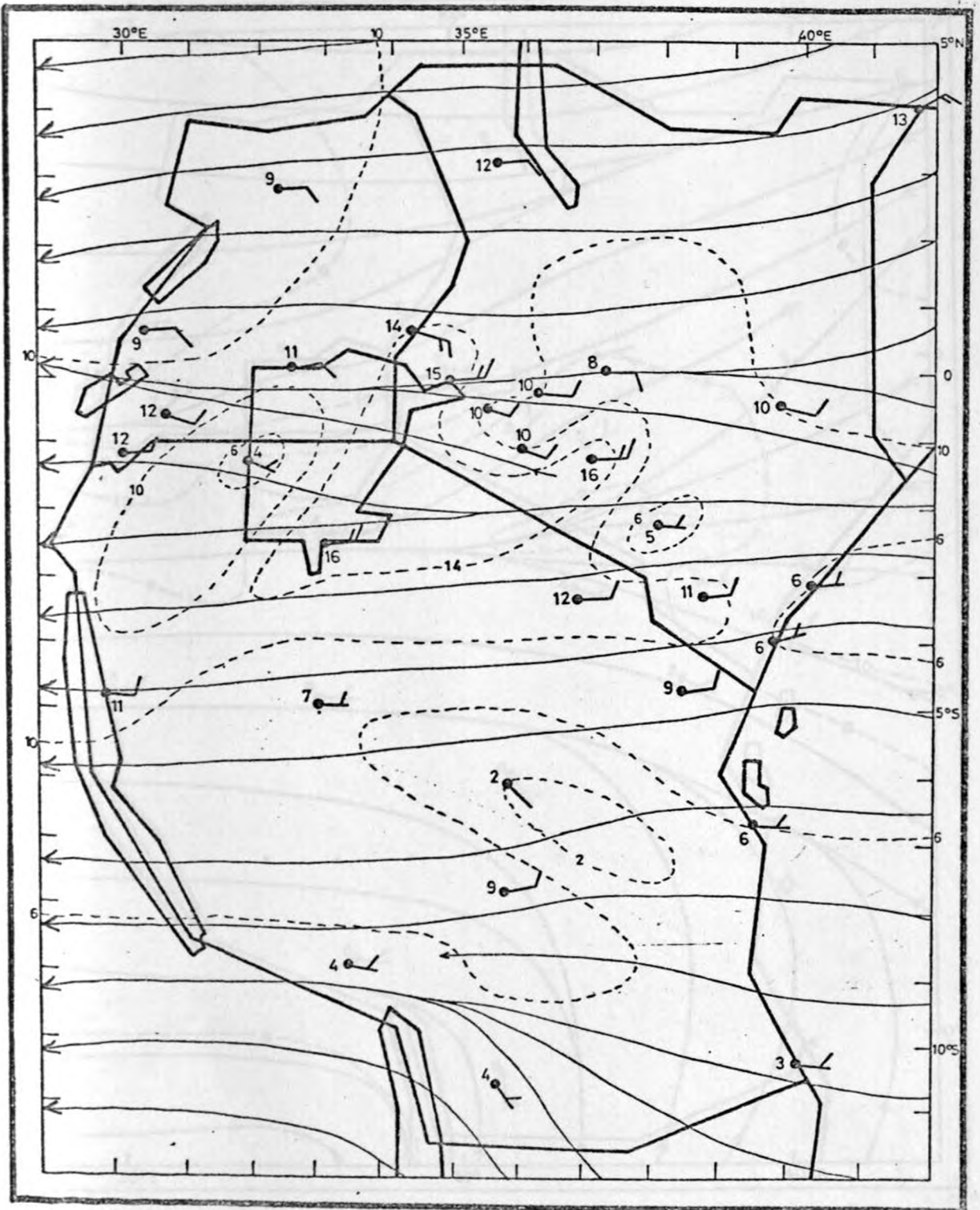


Fig. 18(b) : Mean wind field at 7320 m AMSL in April.

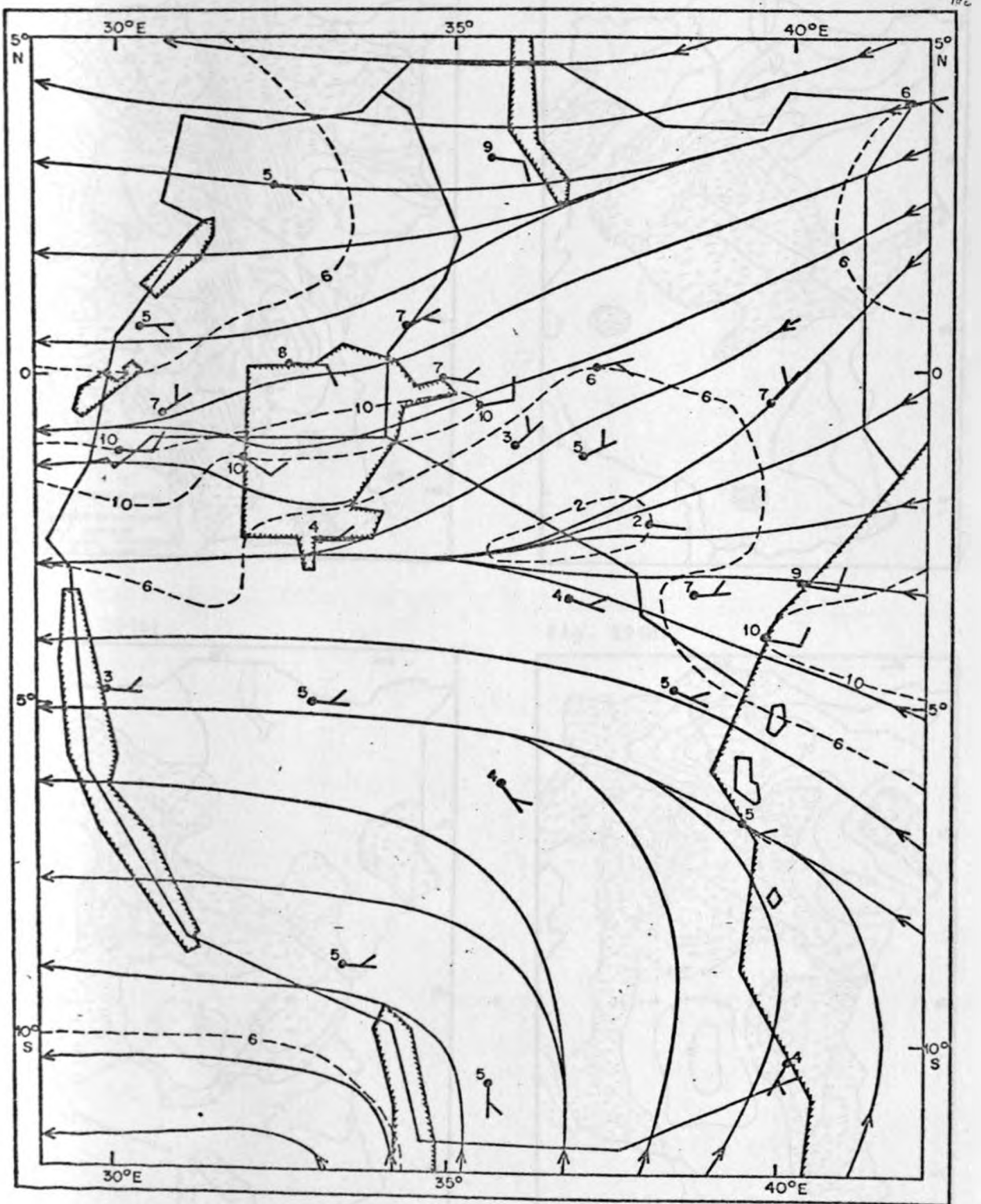


Fig. 18(c) : Mean wind field at 7320 m AMSL in May.

Fig. 19(a)

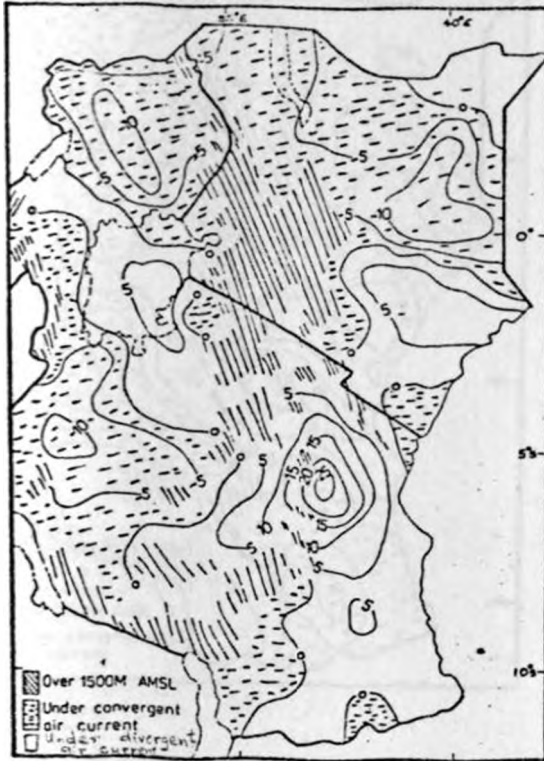


Fig. 19(b)

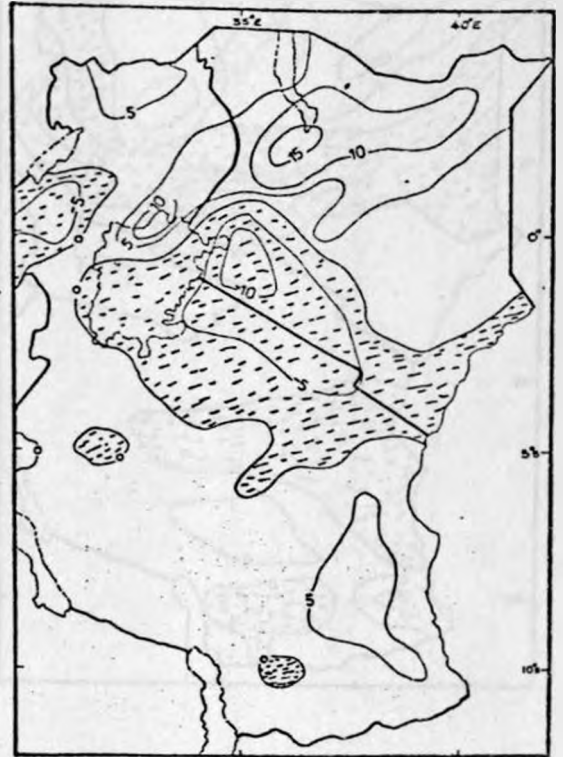


Fig. 19(c)

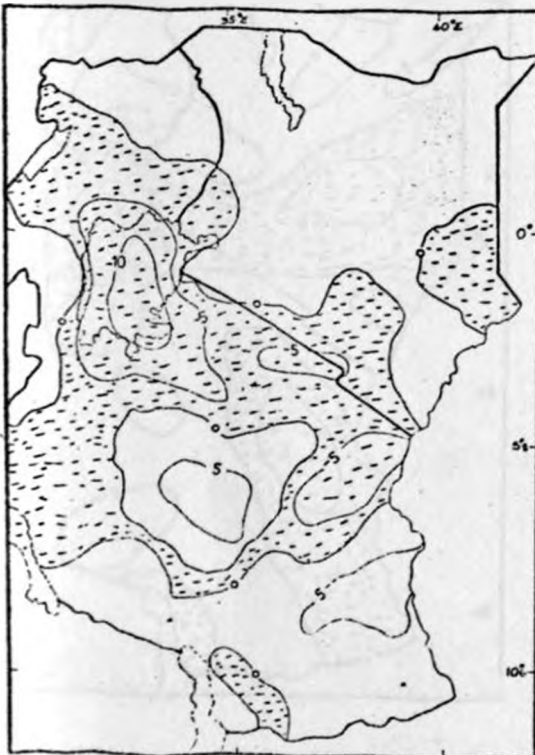


Fig. 19(d)

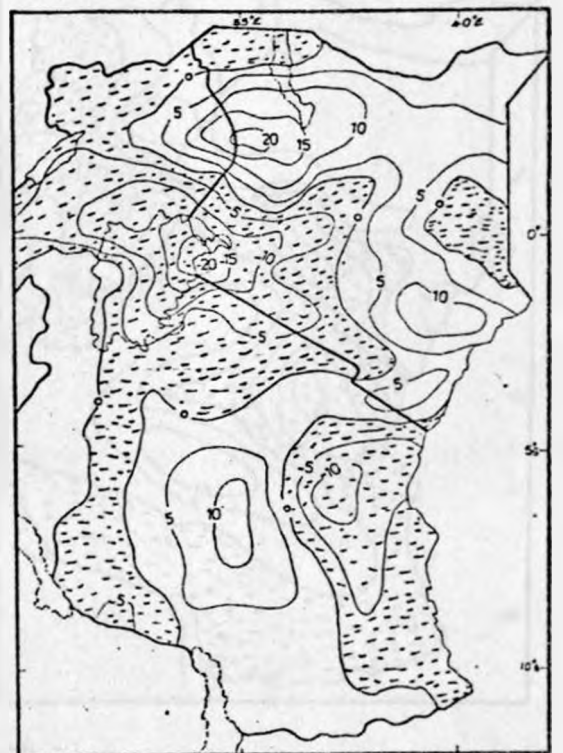


Fig. 19 : Mean divergence field ($\times 10^{-6} \text{ s}^{-1}$) in March :
 (a) 1525 m AMSL, (b) 3050 m AMSL, (c) 5490 m AMSL,
 (d) 7320 m AMSL.

Fig. 20(a)



Fig. 20(b)



Fig. 20(c)

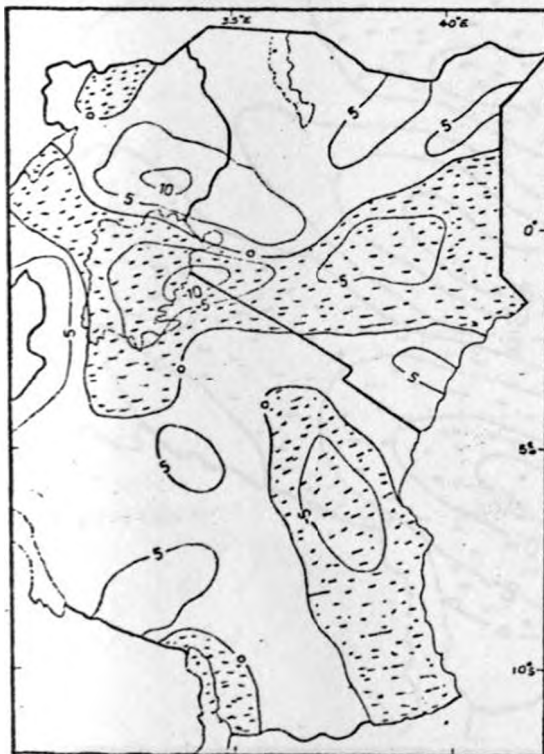


Fig. 20(d)

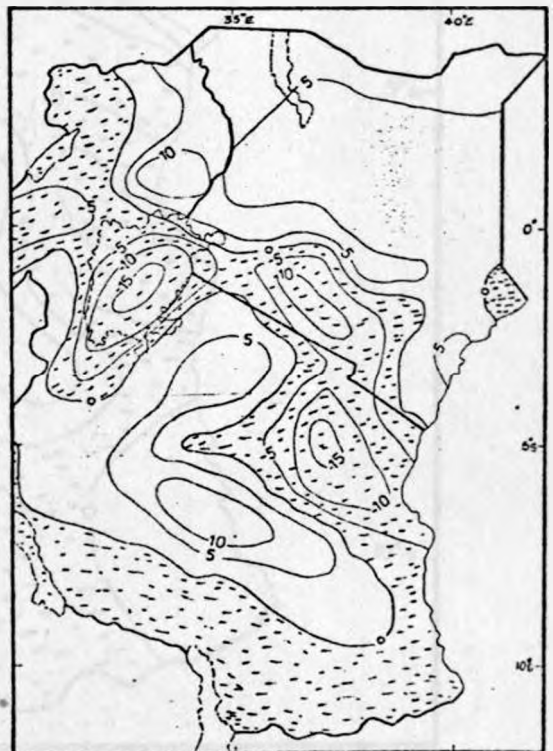


Fig. 20(a-d) : Mean divergence field ($\times 10^{-6} \text{ s}^{-1}$) in April.:
 (a) 1525 m AMSL, (b) 3050 m AMSL, (c) 4270 m AMSL,
 (d) 5490 m AMSL.

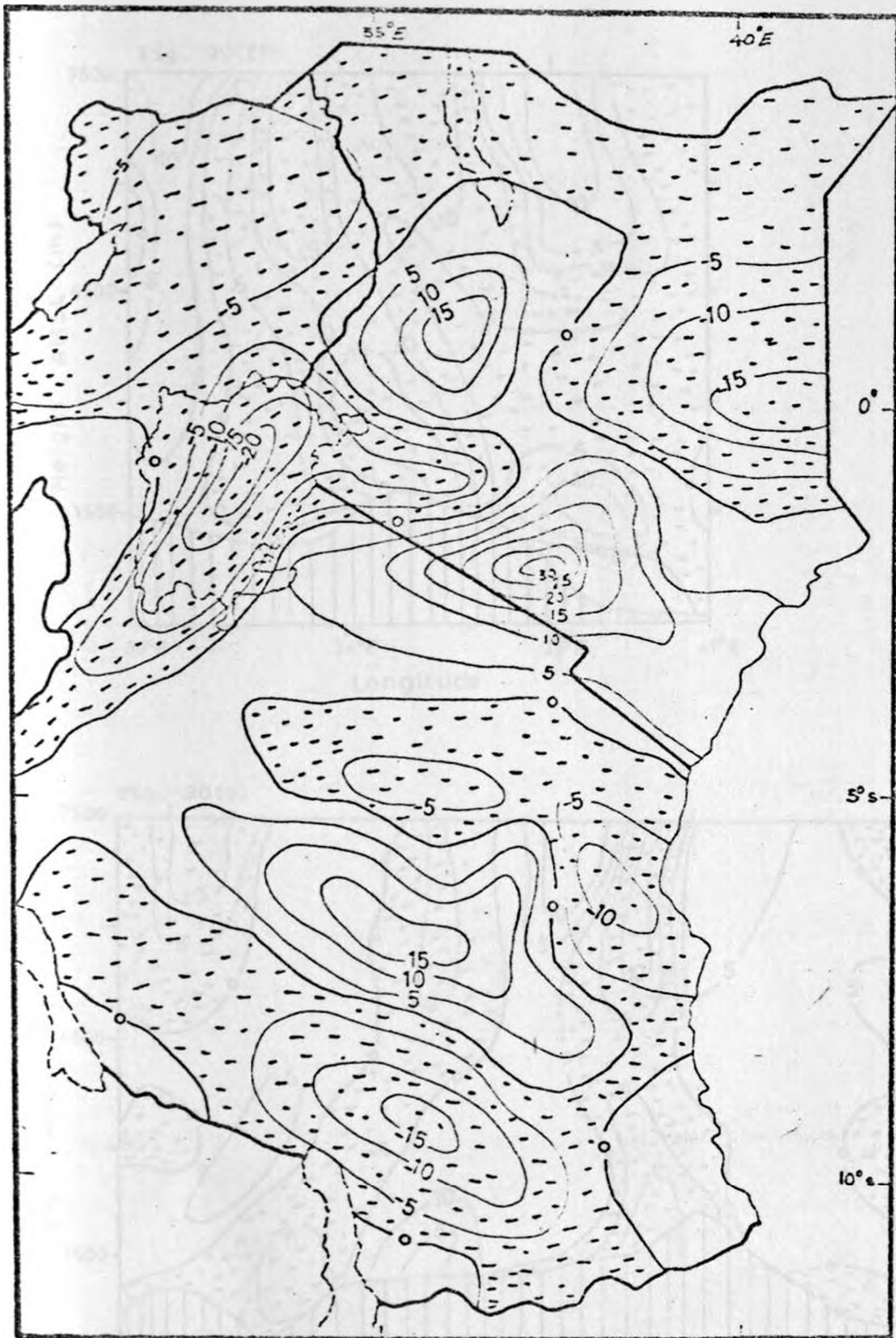


Fig. 20(e) : Mean divergence field ($\times 10^{-6} \text{ s}^{-1}$) at 7320 m AMSL in April.

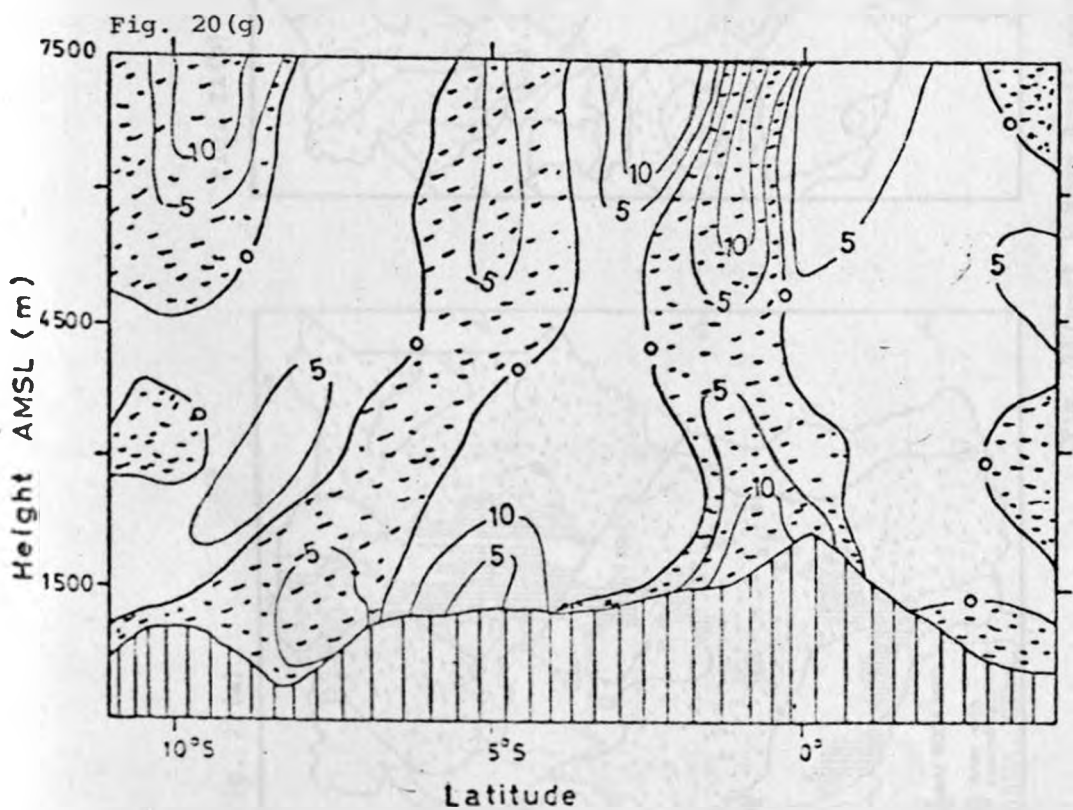
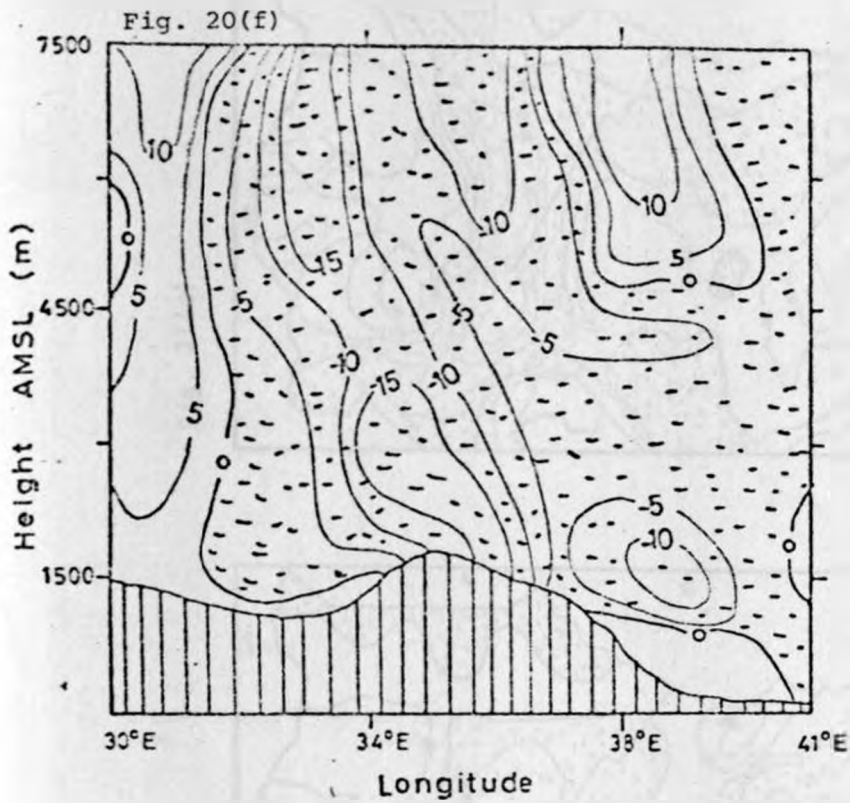


Fig. 20(f-g) : Vertical cross-section of April mean divergence ($\times 10^{-6} \text{ s}^{-1}$) : (f) along longitude 1°S , (b) along longitude 36°E .

Fig. 21(a)

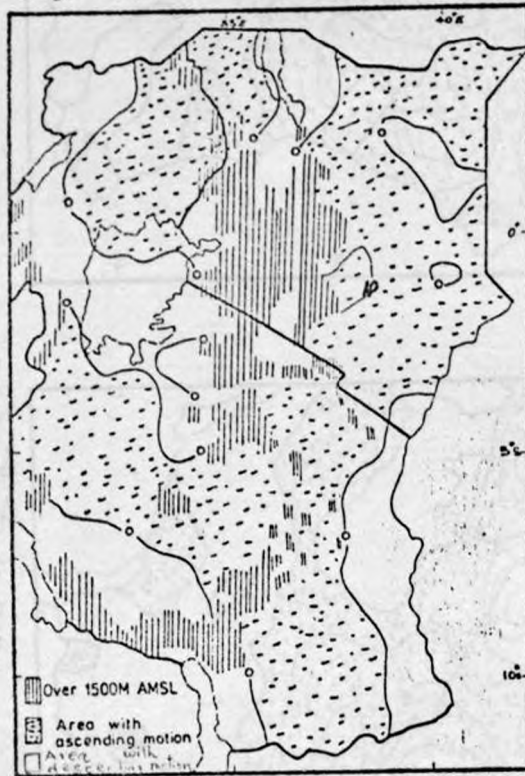


Fig. 21(b)



Fig. 21(c)

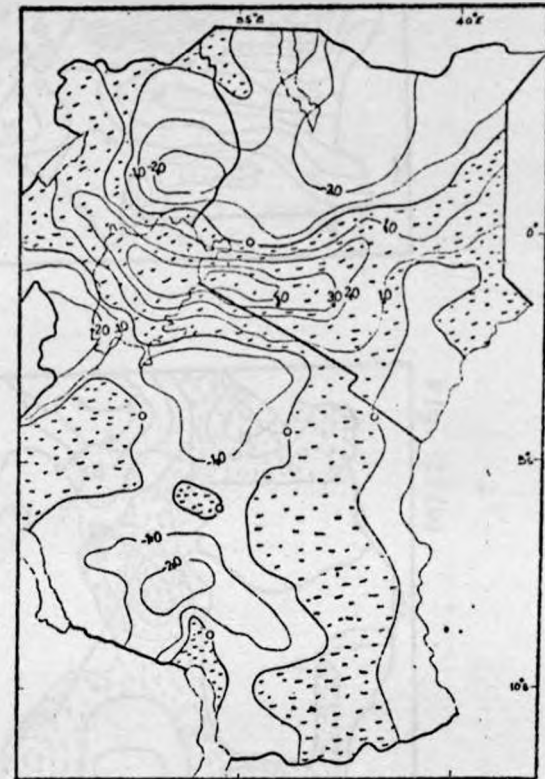


Fig. 21(a-c) : Mean April vertical motion field ($\times 10^{-2} \text{ ms}^{-1}$) :
(a) 1525 m AMSL, (b) 3050 m AMSL, (c) 5490 m AMSL.

Fig. 22(a)



Fig. 22(b)

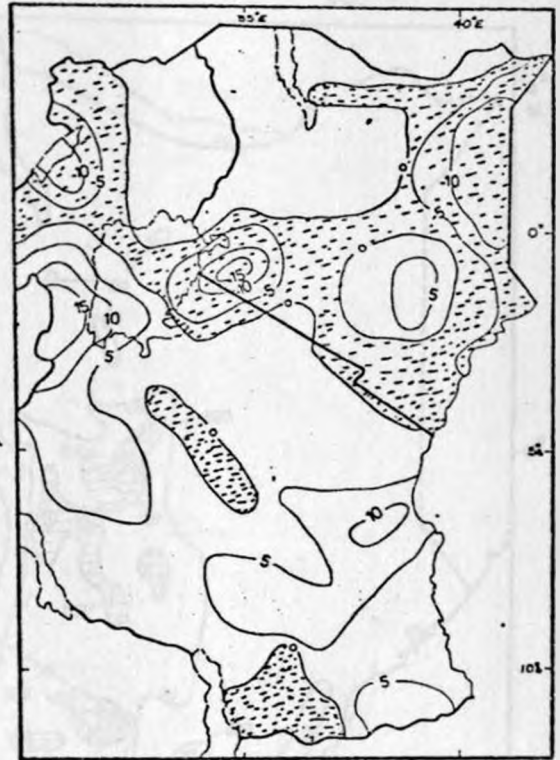


Fig. 22(c)



Fig. 22(d)



Fig. 22(a-d) : Mean divergence field ($\times 10^{-6} \text{ s}^{-1}$) in May :
 (a) 1525 m AMSL, (b) 3050 m AMSL,
 (c) 5490 m AMSL, (d) 7320 m AMSL.

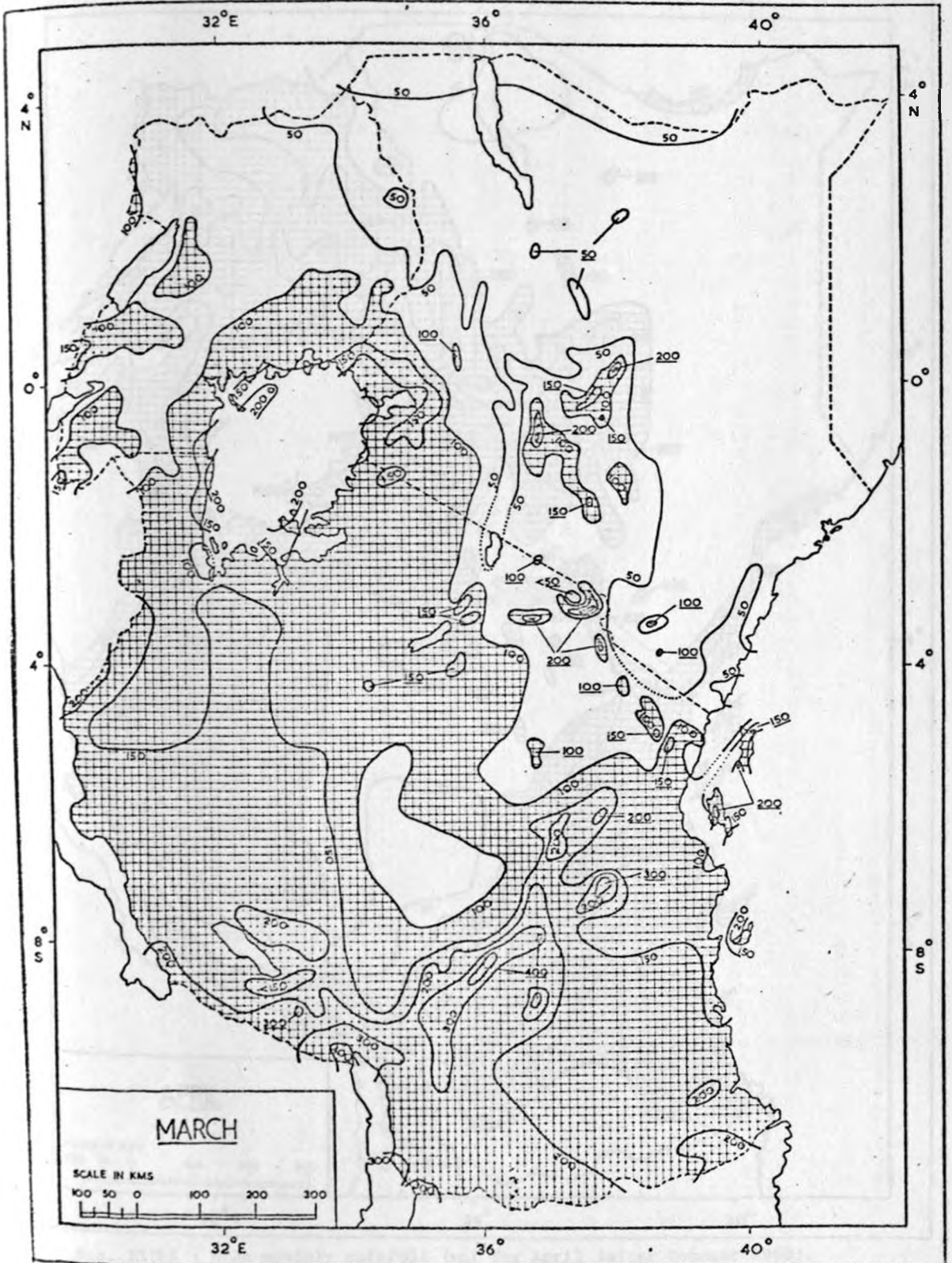


Fig. 23(a) : Mean monthly rainfall (mm) for March (after Tomsett 1969).
Shaded area receives over 100 mm.

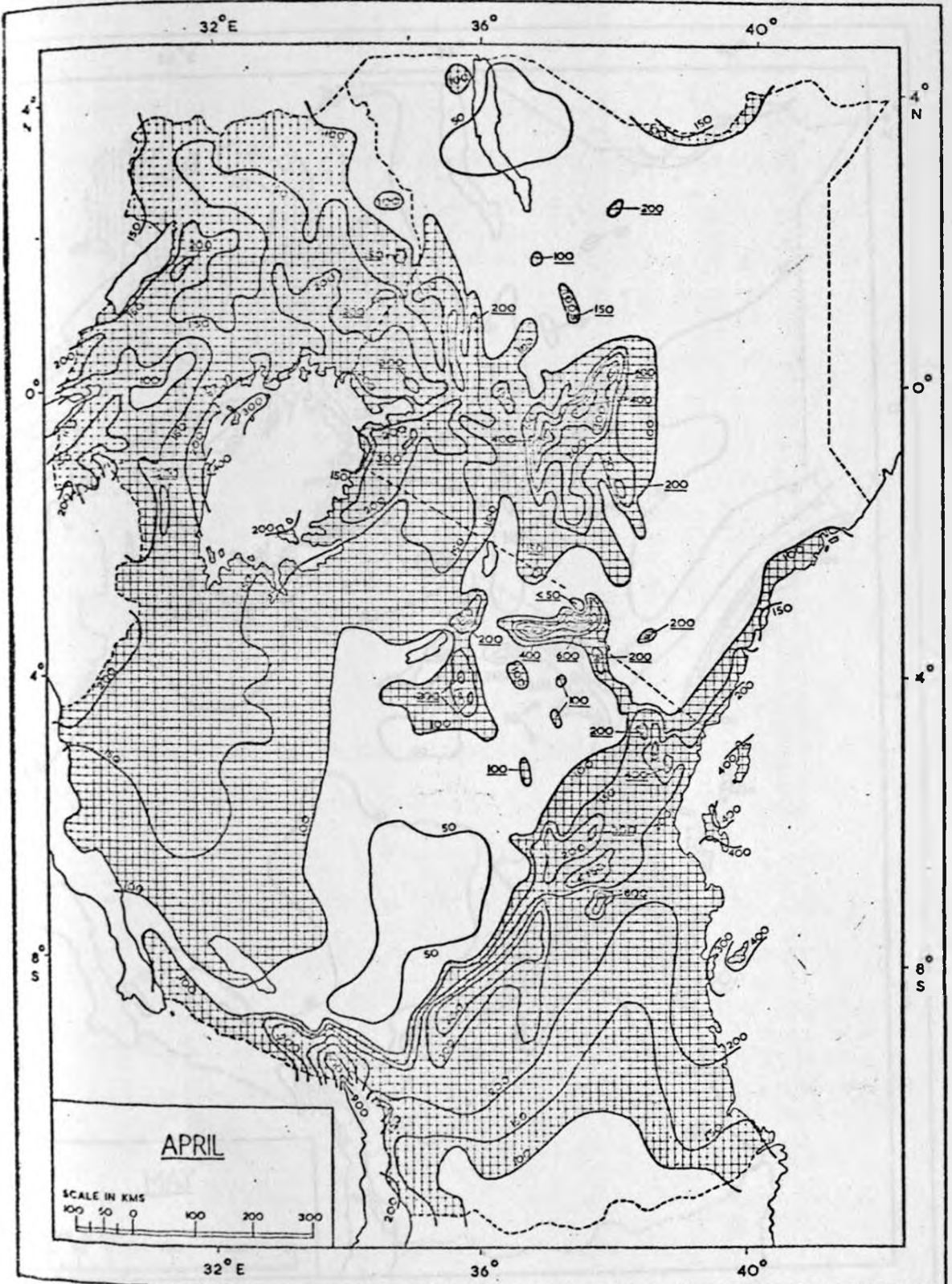


Fig. 23(b) : Mean monthly rainfall (mm) for April (after Tomsett 1969).
Shaded area receives over 100 mm.

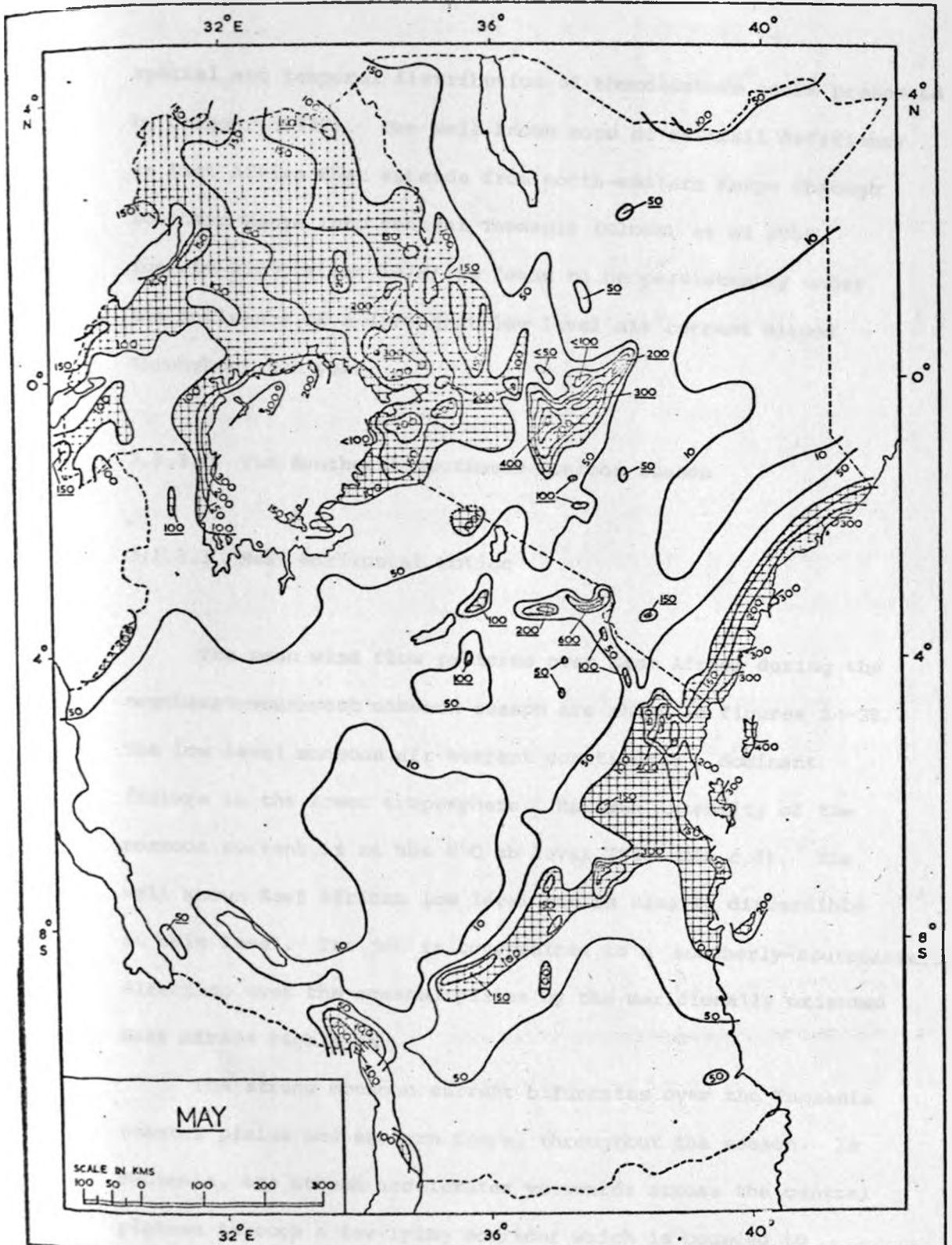


Fig. 23(c) : Mean monthly rainfall (mm) for May (after Tomsett 1969).
Shaded area receives over 100 mm.

spatial and temporal distribution of thunderstorm areas presented by Chaggar (1977). The well known zone of rainfall deficiency in East Africa that extends from north-eastern Kenya through southern Kenya into central Tanzania (Glover et al 1954, Tomsett 1969, Hills 1978) is found to be persistently under the influence of a divergent low level air current almost throughout the year.

3.1.3.0 The Southeast-Southwest Monsoon Season

3.1.3.1 Mean Horizontal Motion

The mean wind flow patterns over East Africa during the southeast-southwest monsoon season are shown in figures 24-28. The low level monsoon air current constitutes a dominant feature in the lower troposphere. Maximum intensity of the monsoon current is at the 850 mb level (Figs. 24a,c,d). The well known East African low level jet is clearly discernible at this level. The jet is constrained to a southerly-southeasterly direction over the coastal plains by the meridionally oriented East Africa highlands.

The strong monsoon current bifurcates over the Tanzania coastal plains and eastern Kenya, throughout the season. In Tanzania, one stream accelerates westwards across the central plateau through a low-lying corridor which is bounded to the north by the Hanang-Ngorongoro mountain systems. Another persistent feature in the monsoon system is the confluent

zone over western Kenya/eastern Uganda. This area has very light winds ($1-2 \text{ ms}^{-1}$). The isotach analyses (Figs. 24a,c,d) show a speed maximum of upto 13.5 ms^{-1} over coastal Kenya, a secondary maximum of upto 8.5 ms^{-1} over central Tanzania and a speed minimum in the lake region. The SE/SW monsoon current intensifies progressively from May to reach a maximum in July/August (Figs. 24c-d), then decays in September/October.

The southeasterly monsoon current is evident also at the 700 mb level (Figs. 25a-c). However, its intensity is weaker than at the 850 mb level. Maximum speed at this level is about 7.5 ms^{-1} . The strong easterly current that was present over central Tanzania at 850 mb is absent at this level. An interesting feature at the 700 mb level is the confluence and/or cyclonic circulation over western Kenya. The cyclonic circulation over the western Kenya highlands and the lake Victoria region is most intense as well as extensive at the 700 mb level. One recognises the circulation as being part of that around the lake Victoria trough (Asnani and Kinuthia 1979). During the period when the SE/SW monsoon current has peak intensity (July/August), this area of cyclonic circulation links up with the southern portion of the northern summer ITCZ, now over the Sudan at these longitudes (Thompson 1965). The presence of the trough in the lake Victoria region has important implications in the daily evolution of weather in the area. The coupling of the trough system with the normally existing lake Victoria meso-scale circulation systems leads to highly augmented weather activities that are characterised by violent thunderstorms/hailstorms and heavy rainfall (Chaggar 1977).

Henderson (1949) and Chaggar (1977) have observed that the causes of the July/August rainfall peak in this area are of complex nature. Different reasons regarding the causes of northern summer rains in western Kenya have been suggested. They range from convective processes in moist unstable air to effects of cold frontal zones (Henderson 1949). Other authors (Glover et al 1954, Tomsett 1969, Trewartha 1972) have alluded that the northern summer rainfalls in western parts of East Africa are caused by westerly incursions from the Congo. Nakamura (1968) noted that there seemed to be a relation between the rains in western Kenya and the occurrence of westerly winds between 700-500 mb at Nairobi in July/August. It now seems clear from the study that these rains are a result of local cyclonic circulations centred over western Kenya/eastern Uganda. We would like to suggest further that the occasional northern summer rainfalls experienced in Nairobi area, and which have been associated with moist westerly winds, may be due to intensification of the cyclonic circulation system, which then extends eastwards into the Kenya highlands. It is indeed, apparent from the streamlines that, by the time the southeast monsoon current reaches western Kenya, it has lost most of its moisture over the eastern highlands. However, we observe from figures 25b-c that moisture from the lake Victoria is advected into the area through the strong lake Victoria meso-scale circulation. This highlights the well known fact that lake Victoria plays a major role in the weather activities in western Kenya and eastern Uganda during the SE/SW monsoon

season. Most of the rains in this area occur in the afternoon hours (Thompson 1957b, Tomsett 1975), a manifestation of the intensification of the cyclonic circulation by the inflowing lake Victoria breeze.

The air flow at the 600 mb level (Figs. 26a-c) has some interesting features. It is characterised by the presence of closed circulations in all the three SE/SW monsoon months. These vortices are accompanied by asymptotes of confluence oriented in a southwest-to-northeast direction. This level is apparently the transition one between the strong low level SE/SW monsoon current and the easterly current aloft. The vortices separate northeasterly flow from the now weak southerly flow in the south.

Associated with the vortices at the 600 mb level are westerly winds extending from central Tanzania to the area around Nairobi (Figs. 26b-c). Westerly winds in equatorial regions are believed to be rain bringers (for reasons given in Section 1.2.1.3). However, it has been found (Johnson and Morth 1960, Nakamura 1968) that there are many occasions of rainless westerlies between 750-550 mb in the vicinity of Nairobi during June-October. Figures 26b-c show the westerlies in the neighbourhood of Nairobi to be associated with an extensive anticyclone which is a persistent feature in the region from June to September. Outflow from this anticyclone would tend to inhibit further development of clouds formed in the low level southeast monsoon current on the east-facing slopes of the Kenya highlands. In addition, during this season, an

inversion layer whose base is at about 700 mb level, usually lies over Nairobi area (Taljaard 1955). The combined effects of the 700 mb inversion and the prevailing anticyclonic circulation agree with the dryness prevalent in the region during this season, inspite of extreme cloudiness (Table 1).

At the 500 mb level (Figs. 27a-c), the flow in June (Fig. 27a) is southeasterly south of 4°S and northeasterly north of this latitude. The confluence between the two air currents lies in a west southwest-to-east northeast direction across Tanzania and southern Kenya. In July (Fig. 27b) and August (Fig. 27c), the anticyclone over Nairobi at the 600 mb level is still evident but less extensive. South of this anticyclone there is a zone of confluence between northeasterly and southeasterly air currents.

At the 400 mb level (Figs. 28a-c), the vortices observed at the medium levels are characteristically absent. The winds begin picking up strength. In general, the wind speeds are found to increase from the surface to about 850 mb and decrease thereafter to become very light between 600 mb and 500 mb. Above the 500 mb level the wind speeds do increase. The 400 mb level air flow over the region is more or less easterly north of the equator and turning to southeasterly south of the equator. The air current at this level is only weakly confluent.

3.1.3.2 Mean Divergence and Vertical Motion Fields

Figures 29-32 show the mean divergence patterns for June through August. The vertical motion field for the month of July is presented in figures 33a-c. On the 850 mb level charts (Figs. 29a-c) we observe a divergent zone along the East African coastal plains. This divergent zone coincides with the highly diffluent area in the southeast-southwest monsoon current. A small area of convergent monsoon current is evident just north of the equator. This results from slight deceleration of the air in the EALLJ after having attained maximum speed at Garissa. The zone of divergence extends, as was the SE/SW monsoon, upto 700 mb (Fig. 30a-c). Above the 700 mb level convergence alternates with divergence in the vertical (Figs. 31-32). The overall vertical motion over the coast is downward (Figs. 33a-c) with a maximum of about $5 \times 10^{-2} \text{ ms}^{-1}$ at the 700 mb level (Fig. 33b). While the main monsoon current along the coast is divergent, the monsoon air that branches into central Tanzania and northwestern Kenya appears convergent (Figs. 29a-c). The convergence over these areas is confined to the very low levels as the monsoon current itself.

In the vicinity of Nairobi, we find that, though we have low level divergence at 850 mb, the vertical motion at this level is upward (Fig. 33a), a manifestation of orographically induced vertical motions. At the 600 mb level (Fig. 30d) we have divergence in the anticyclone over the areas, resulting in downward

motion by the 500 mb level (Fig. 33c). Thus, although we have high amounts of low clouds (Atkinson and Sadler 1970) which form through orographic lifting of the moist southeast monsoon air, the prevailing downward motion in the medium levels inhibits their further growth resulting in the observed dry conditions (Fig. 34b) in the area.

We have observed earlier that northwestern Tanzania, southern Uganda and southwestern Uganda lie in a monsoon current that is convergent in the low levels and overlain by a divergent air current at 700 mb (Figs. 30a-c). This configuration results in the observed downward motion (Figs. 33b-c). The only area with a deep layer of convergent monsoon air is the wedge-shaped zone that runs from western Kenya to northwestern Uganda (Figs. 34b-c). The vertical motion field (Figs. 33a-c) in this zone is upward in the lower troposphere. The observed vertical motion in west Kenya agrees very well with the well known severe thunderstorm/hailstorm activities in the area (Chaggar 1977). We have already discussed this in detail in section 3.1.3.1.

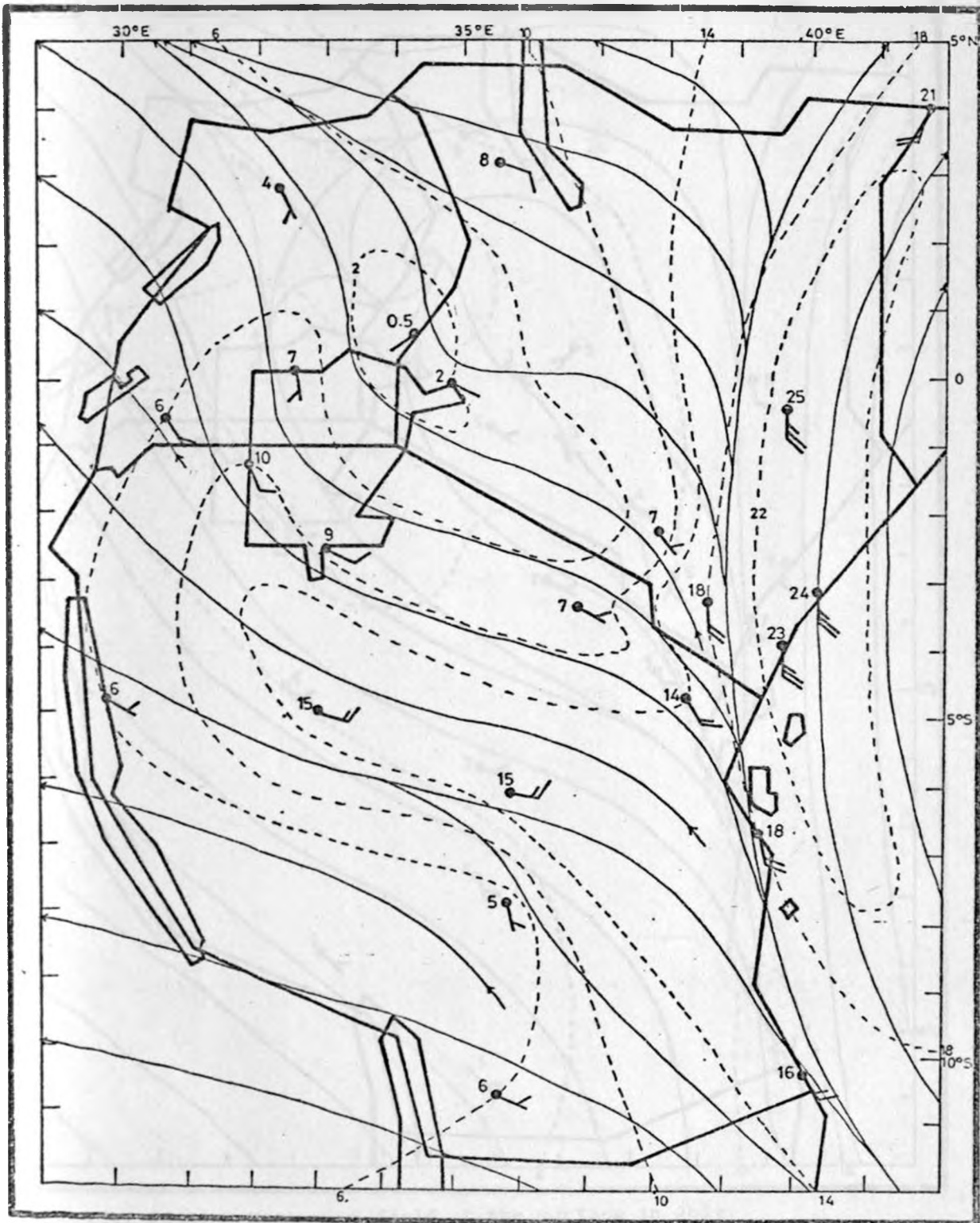


Fig. 24(a) : Mean wind field at 1525 m AMSL in June.

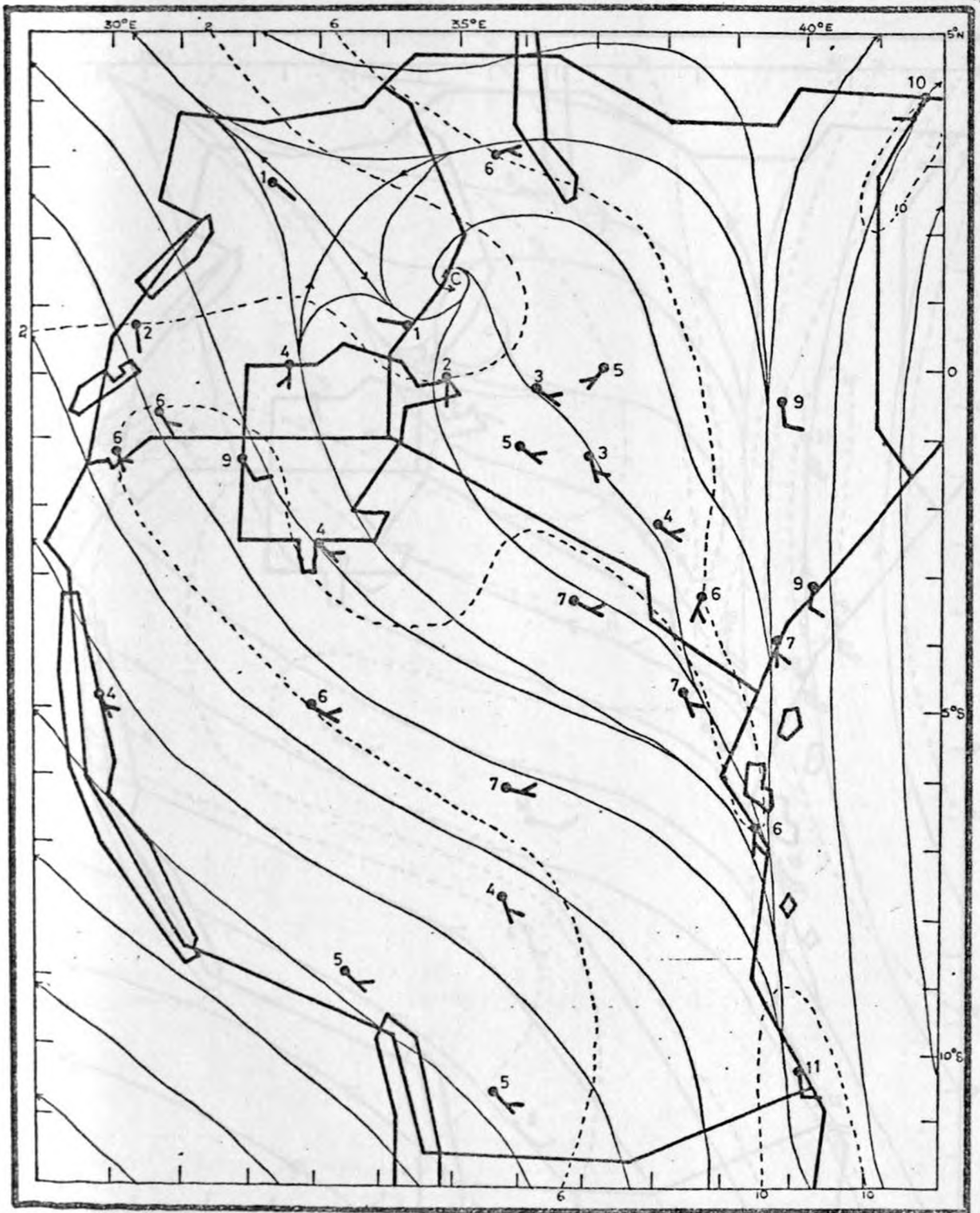


Fig. 24(b) : Mean wind field at the surface in July.

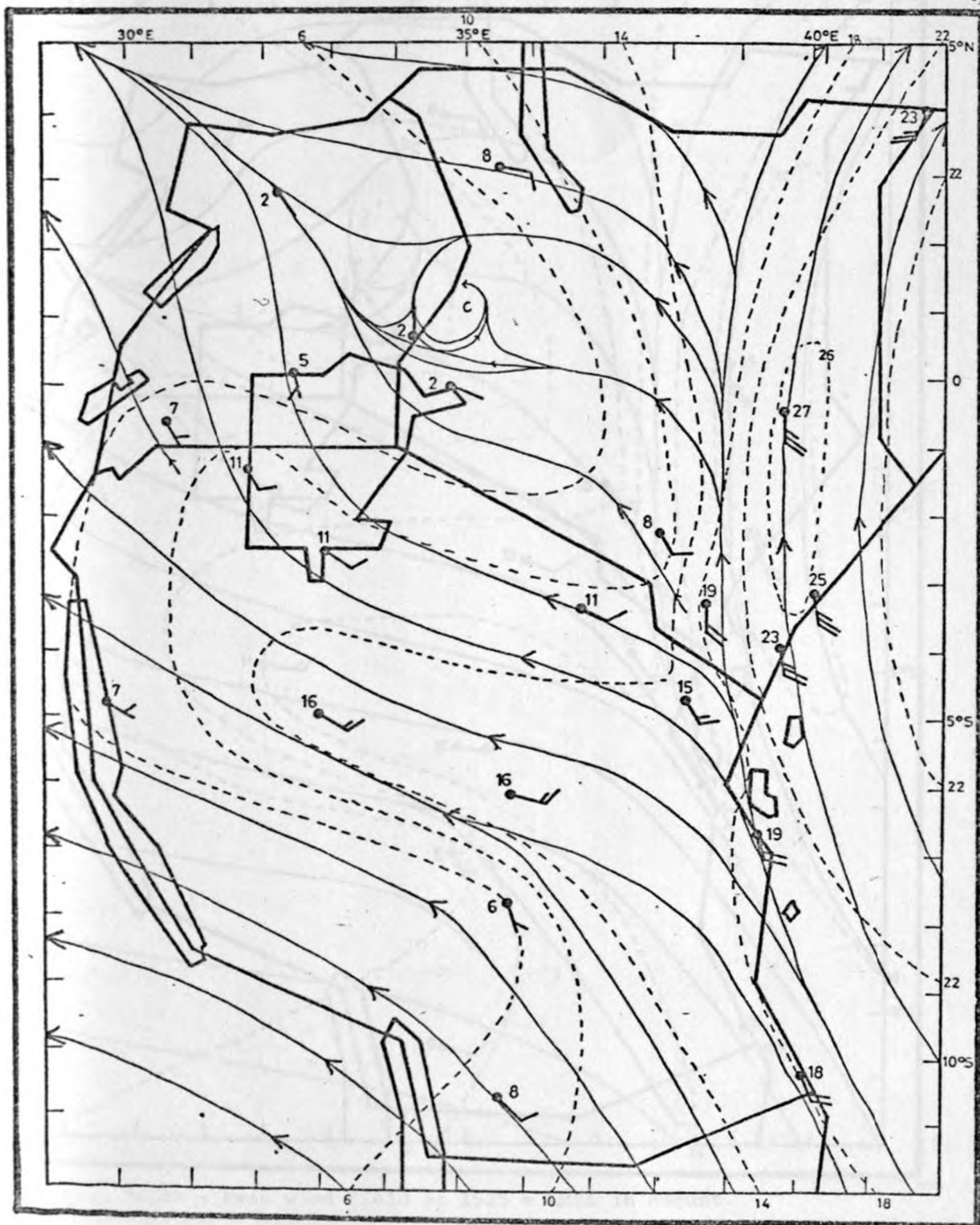


Fig. 24(c) : Mean wind field at 1525 m AMSL in July.

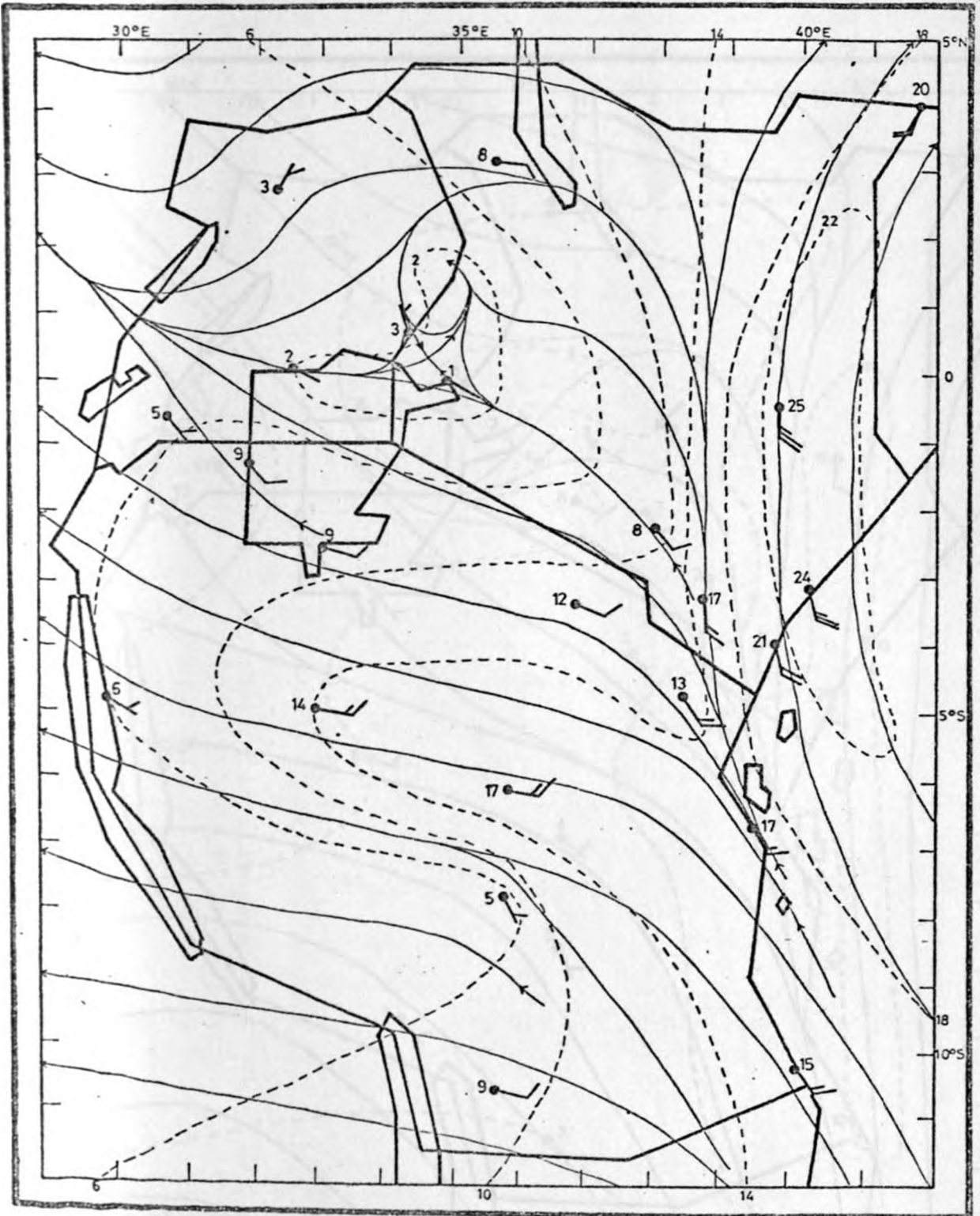


Fig. 24(d) : Mean wind field at 1525 m AMSL in August.

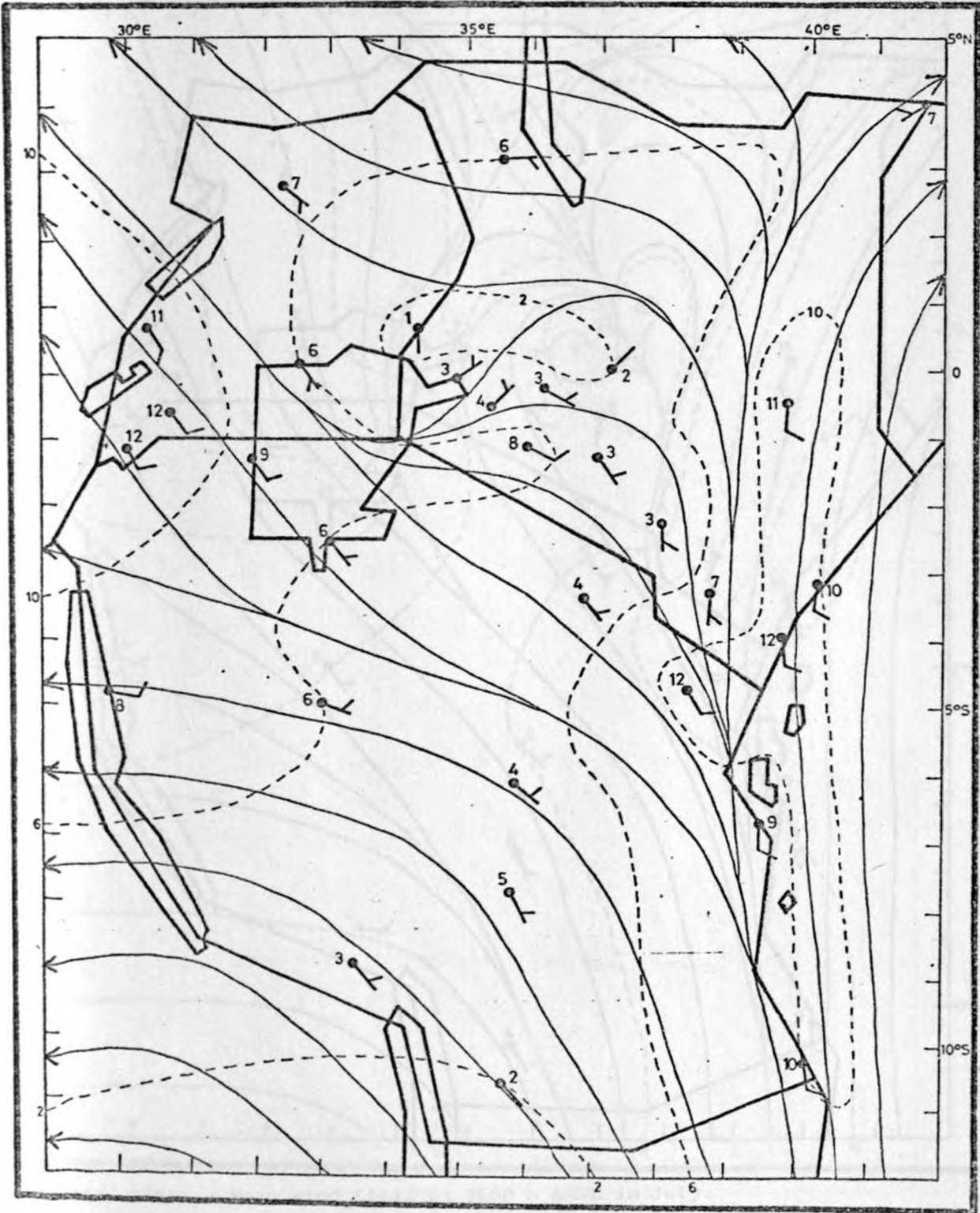


Fig. 25(a) : Mean wind field at 3050 m AMSL in June.

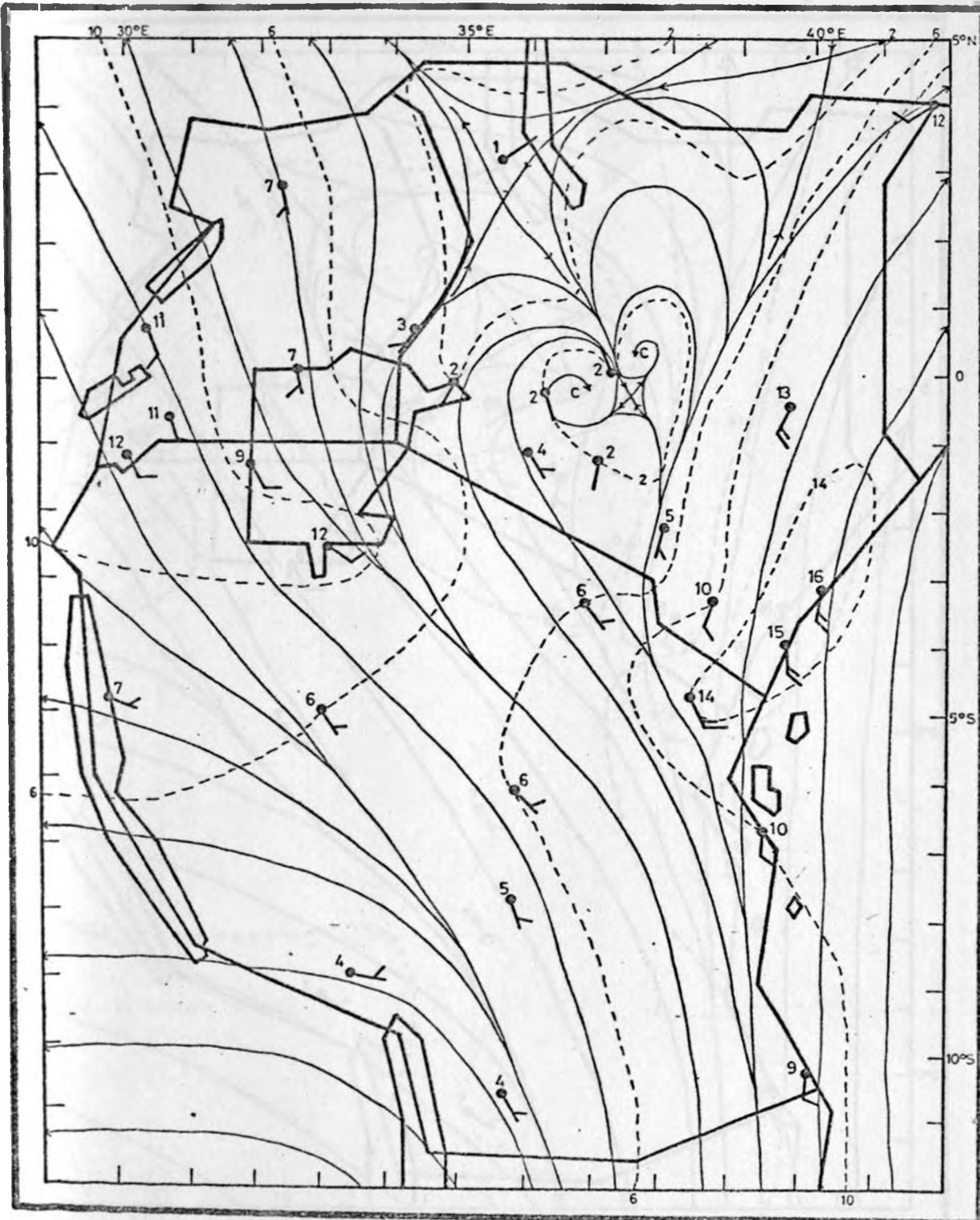


Fig. 25(b) : Mean wind field at 3050 m AMSL in July.

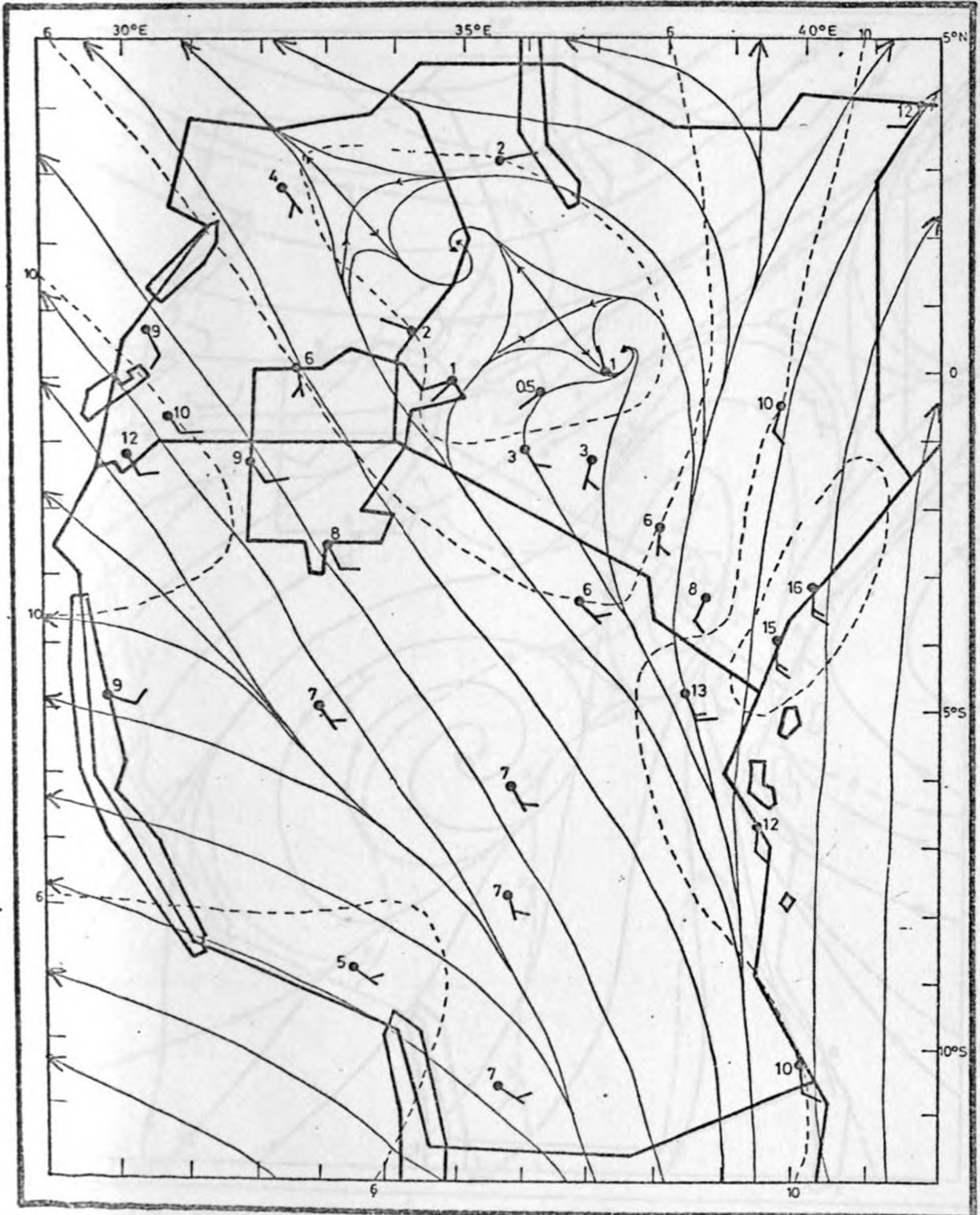


Fig. 25(c) : Mean wind field at 3050 m AMSL in August.

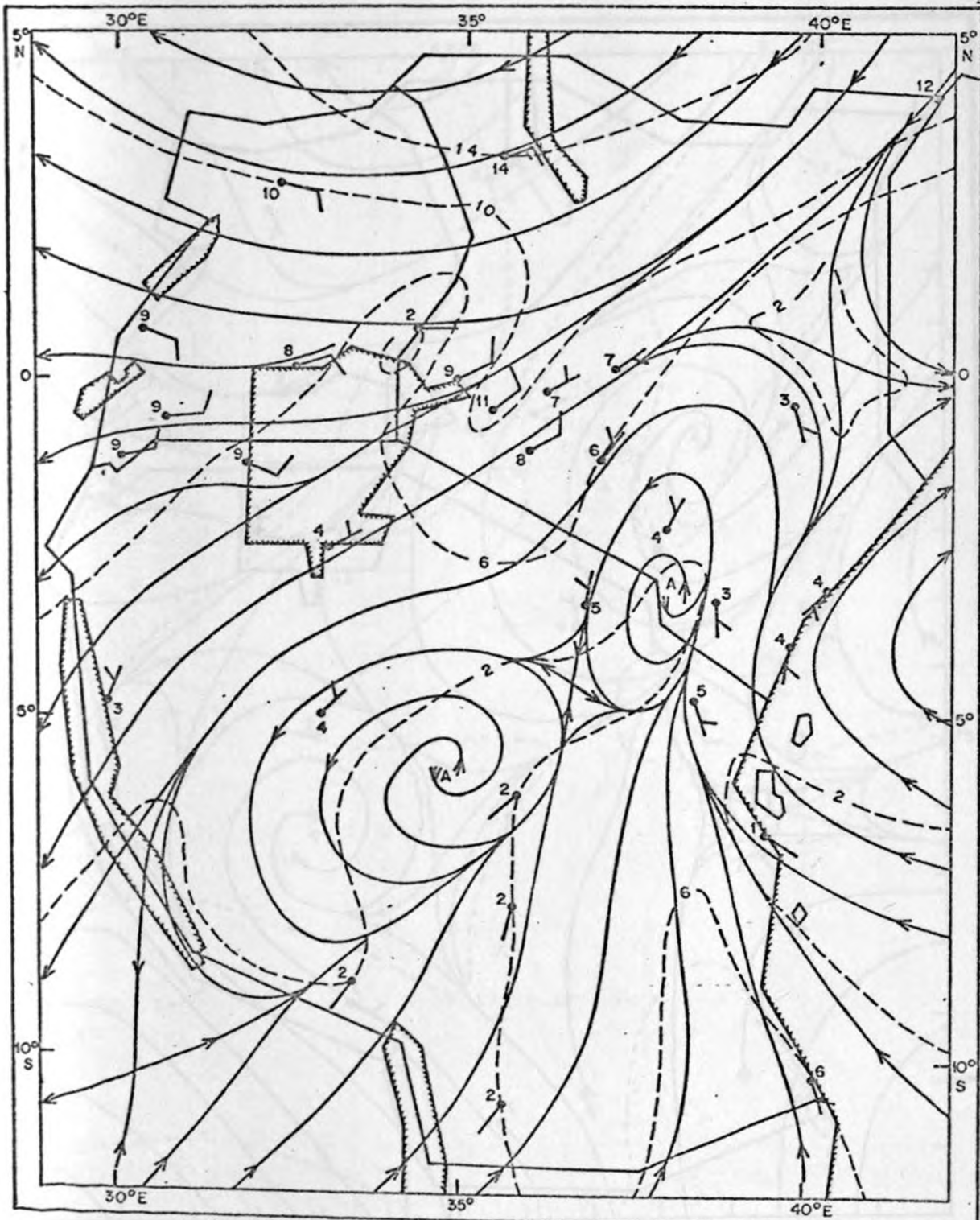


Fig. 26(a) : Mean wind field at 4270 m AMSL in June.

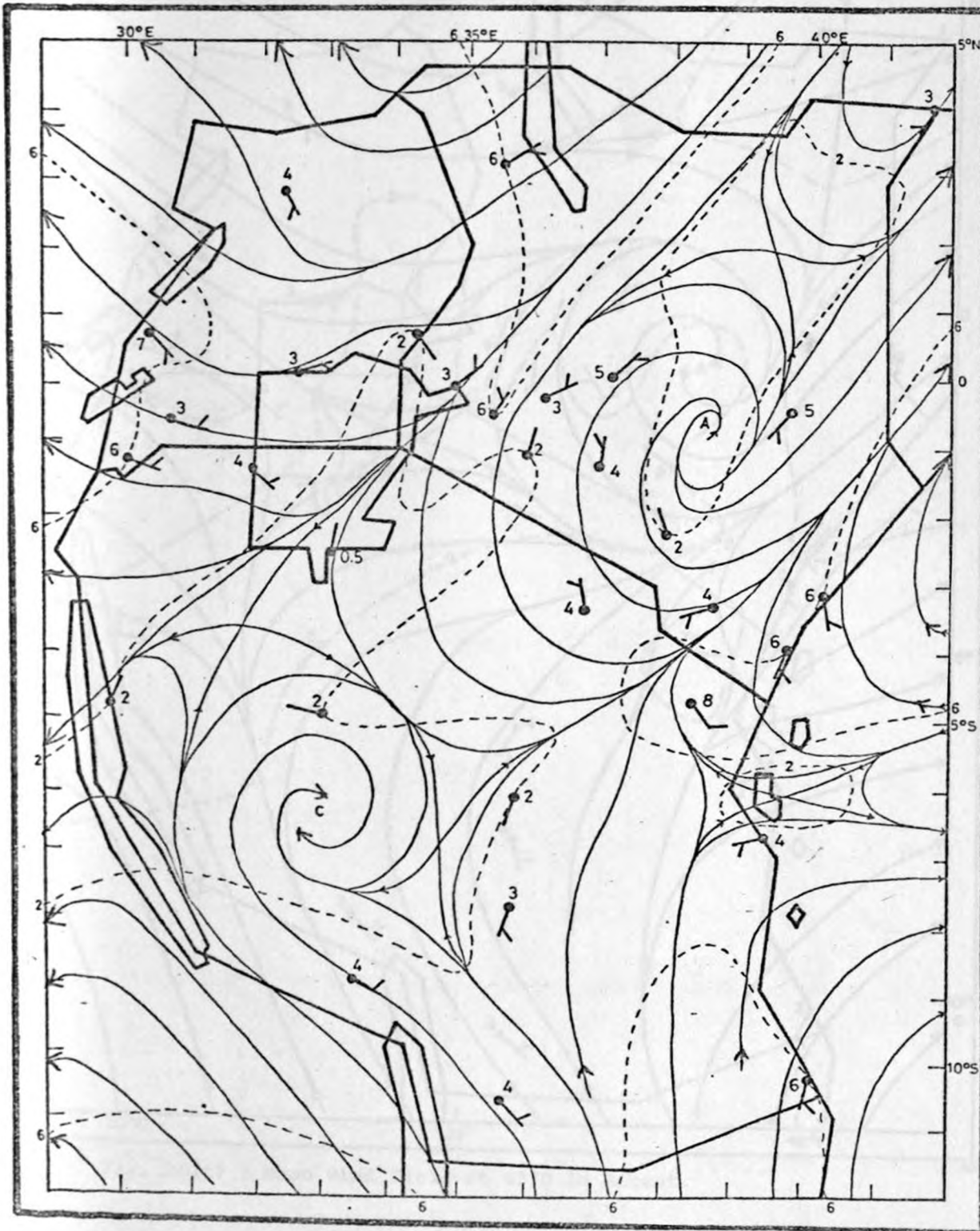


Fig. 26(b) : Mean wind field at 4270 m AMSL in July.

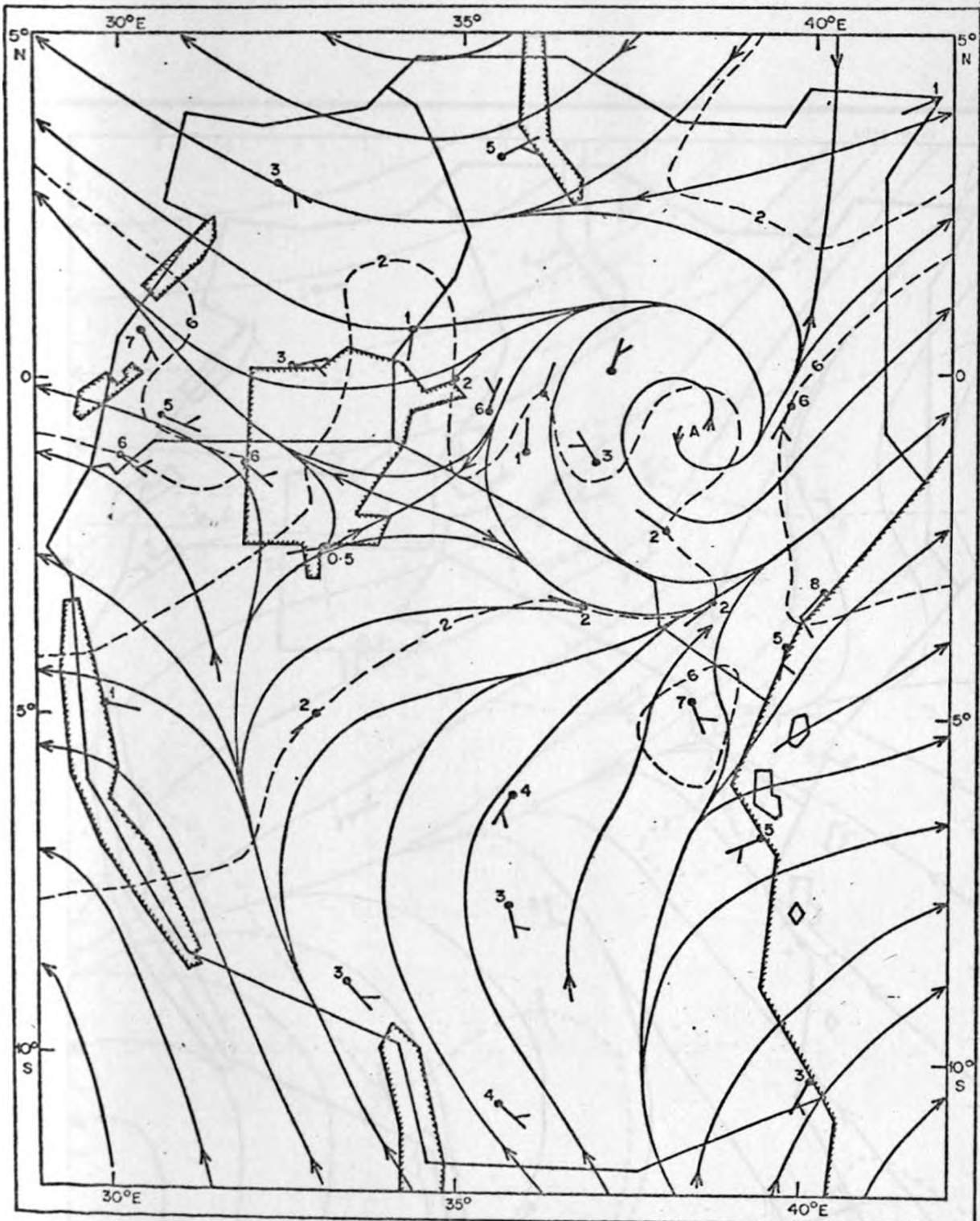


Fig. 26(c) : Mean wind field at 4270 in August.

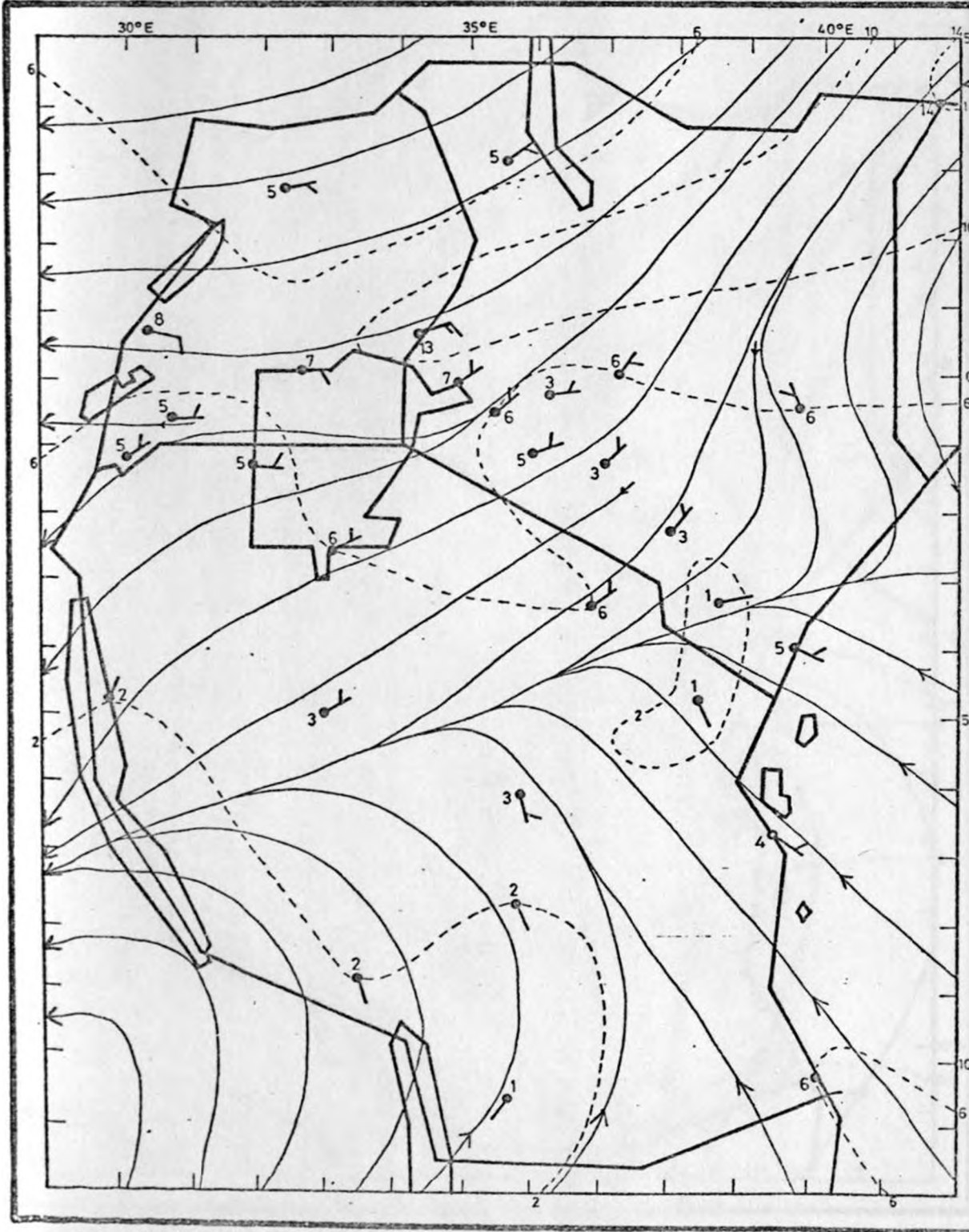


Fig. 27(a) : Mean wind field at 5490 m AMSL in June.

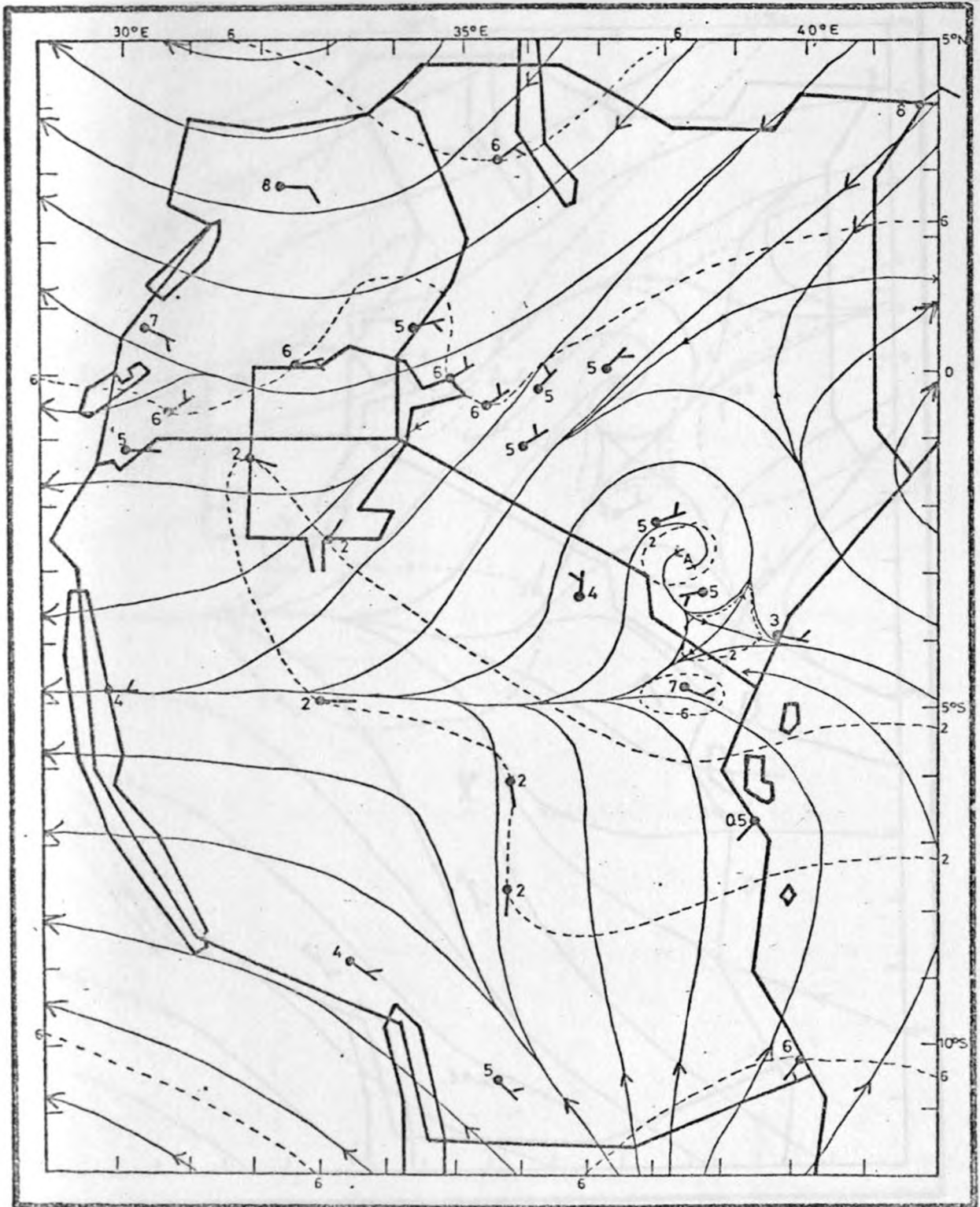


Fig. 27(b) : Mean wind field at 5490 m AMSL in July.

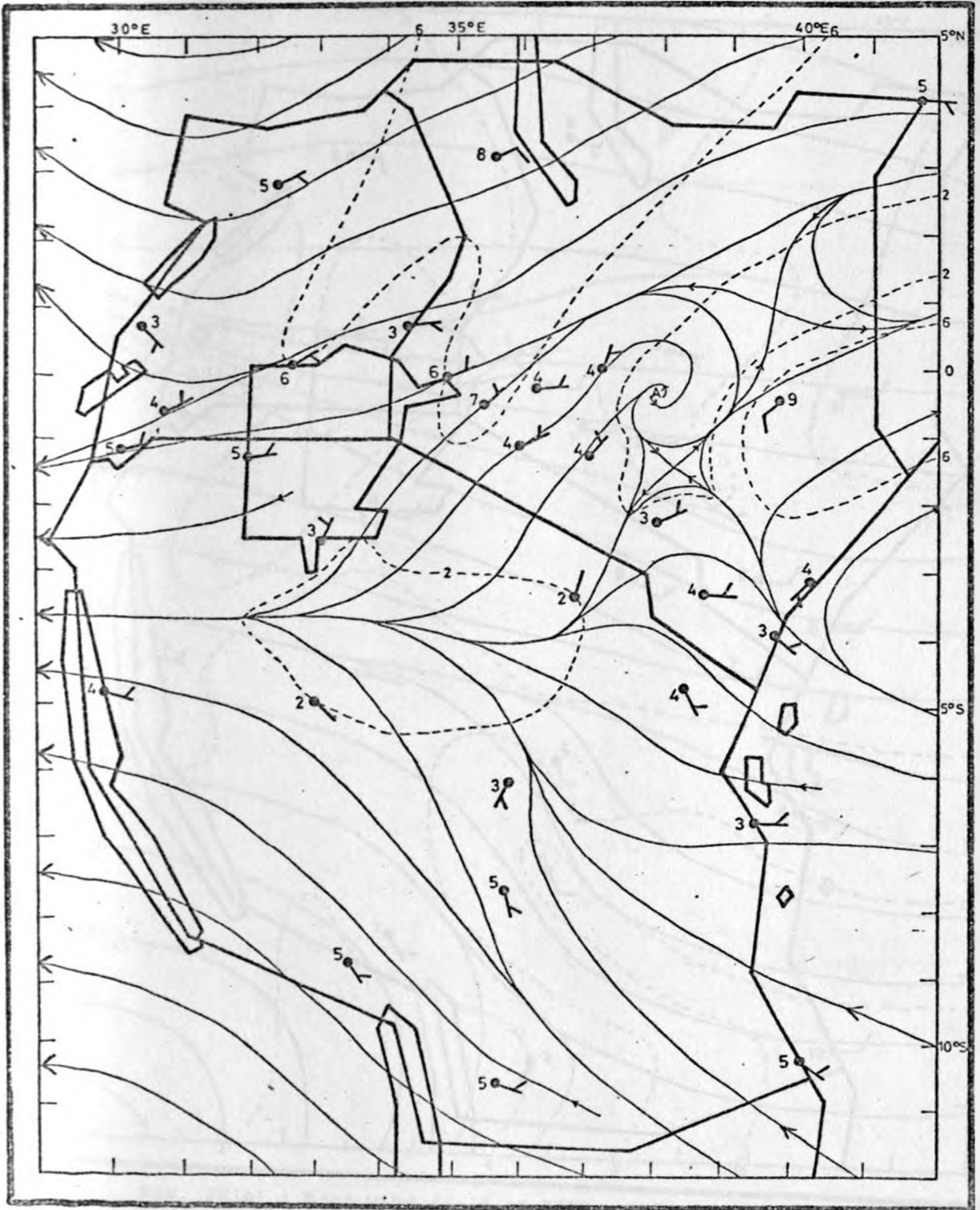


Fig. 27(c) : Mean wind field at 5490 m AMSL in August.

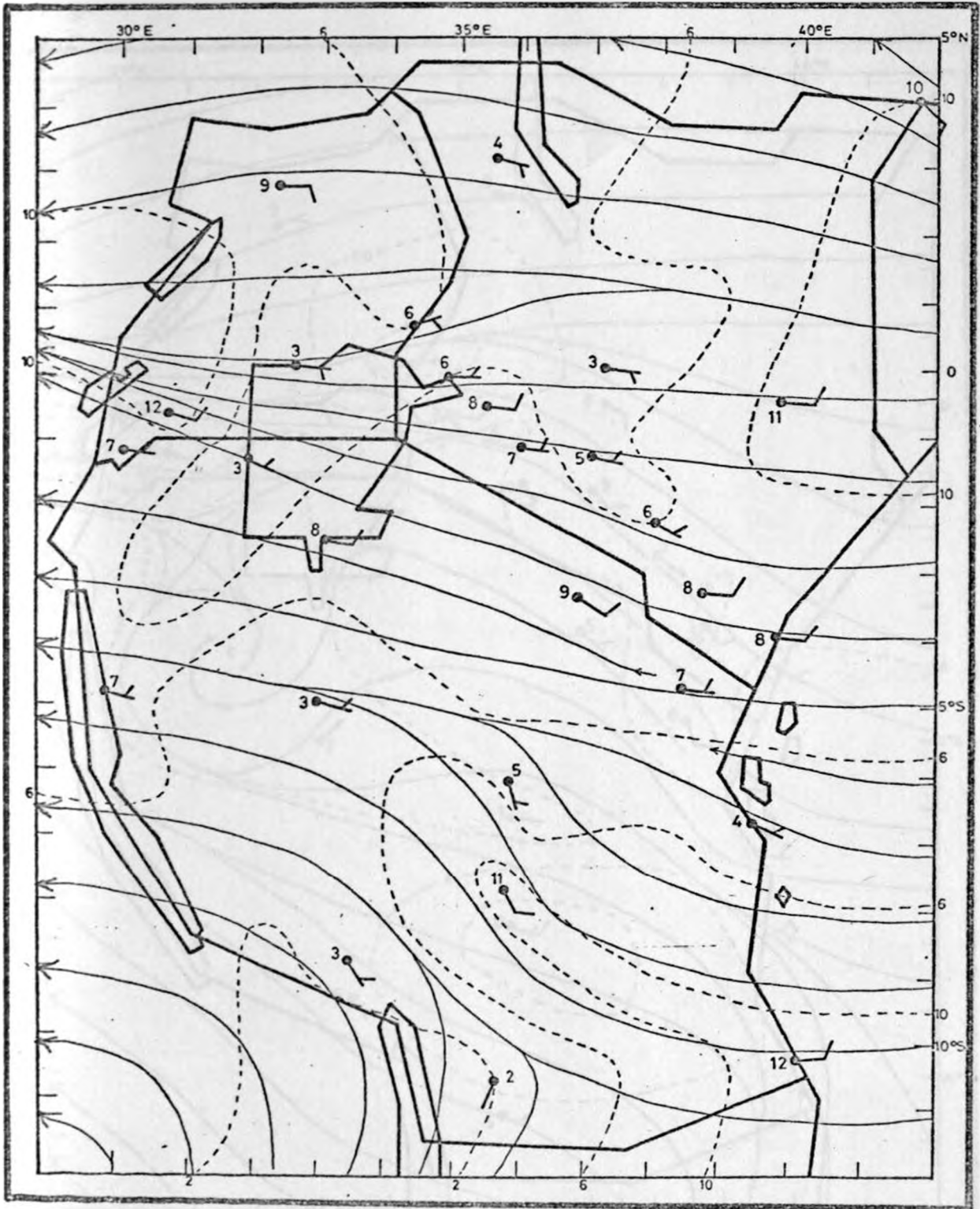


Fig. 28(a) : Mean wind field at 7320 m AMSL in June.

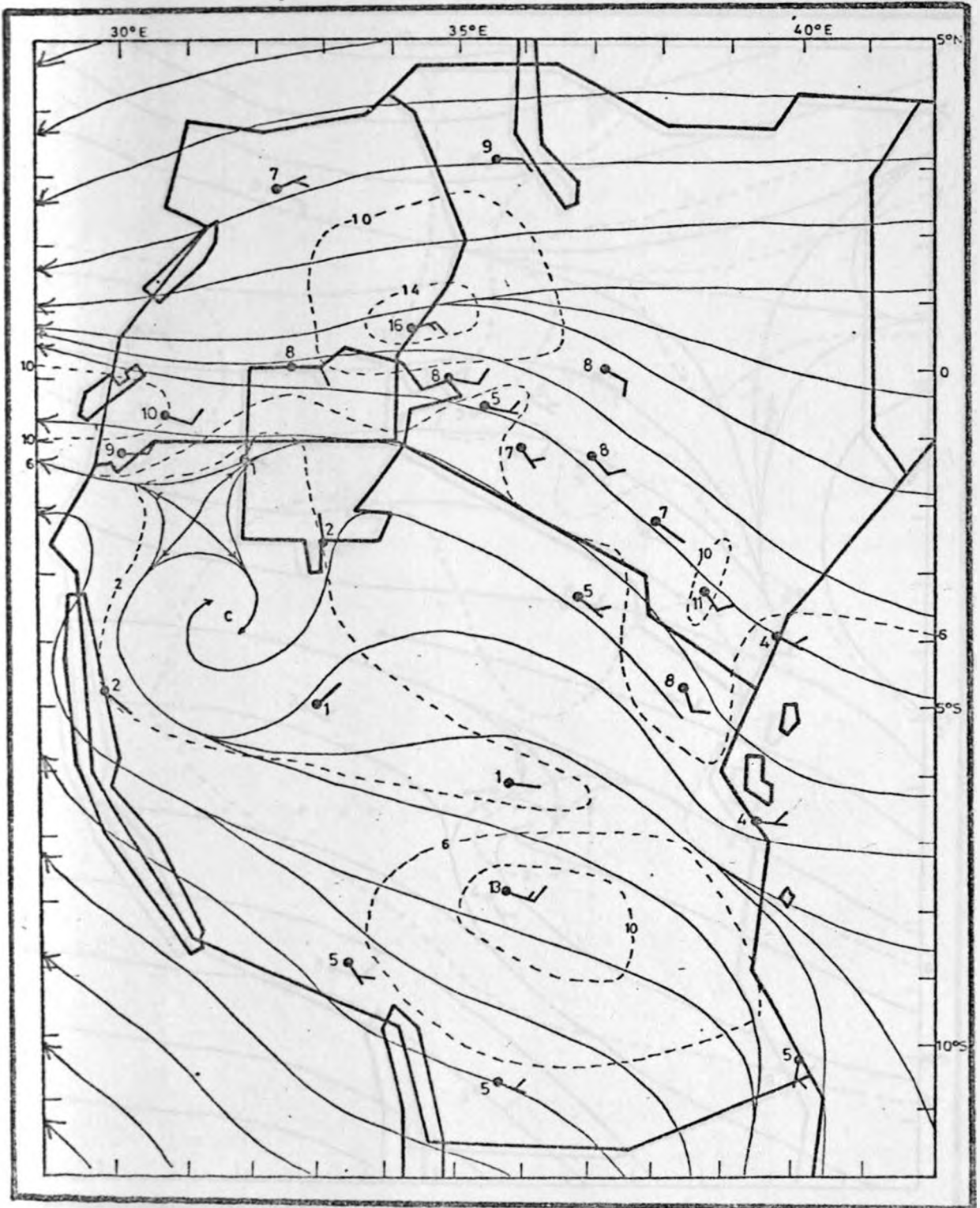


Fig. 28(b) : Mean wind field at 7320 m AMSL in July.

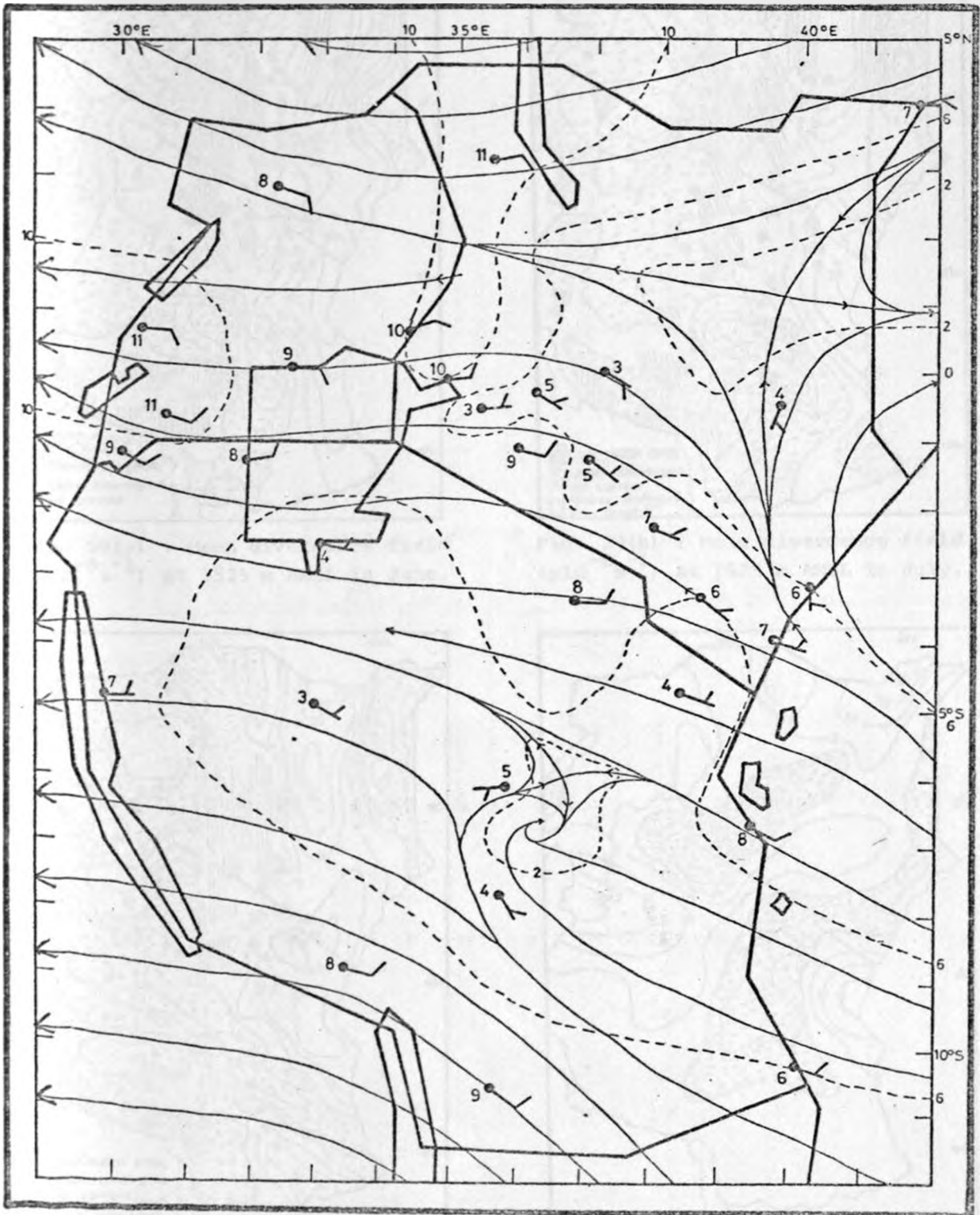


Fig. 28(c) : Mean wind field at 7320 m AMSL in August.

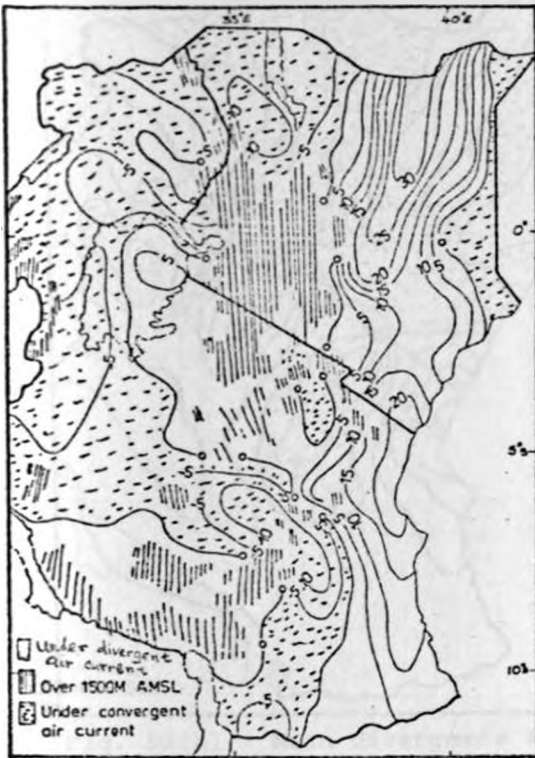


Fig. 29(a) : Mean divergence field ($\times 10^{-6} s^{-1}$) at 1525 m AMSL in June.



Fig. 29(b) : Mean divergence field ($\times 10^{-6} s^{-1}$) at 1525 m AMSL in July.



Fig. 29(c) : Mean divergence field ($\times 10^{-6} s^{-1}$) at 1525 m AMSL in August.

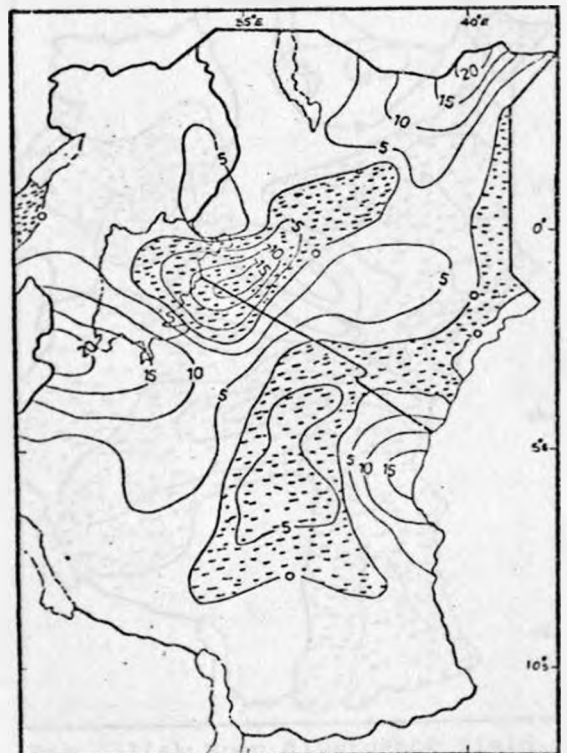


Fig. 30(a) : Mean divergence field ($\times 10^{-6} s^{-1}$) at 3050 m AMSL in June.



Fig. 30(b) : Mean divergence field
($\times 10^{-6} \text{ s}^{-1}$) at 3050 m AMSL in July.

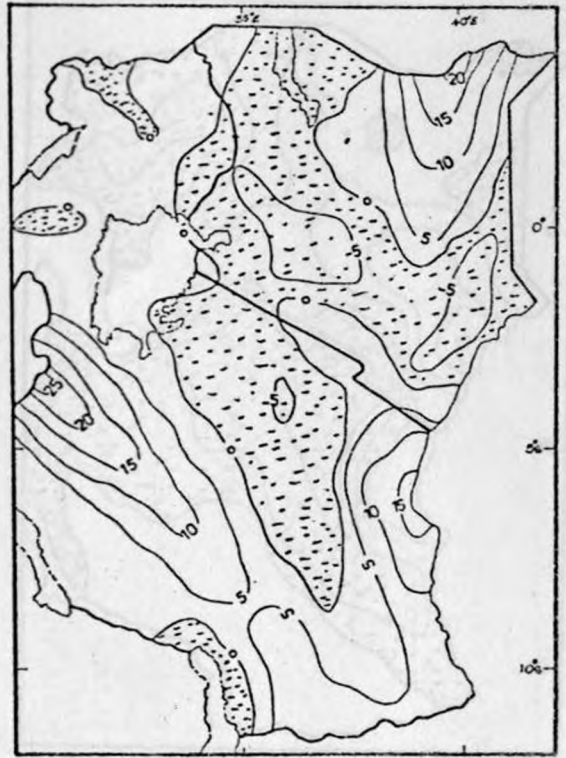


Fig. 30(c) : Mean divergence field
($\times 10^{-6} \text{ s}^{-1}$) at 3050 m AMSL in August.



Fig. 30(d) : Mean divergente field
($\times 10^{-6} \text{ s}^{-1}$) at 4270 m AMSL in July.

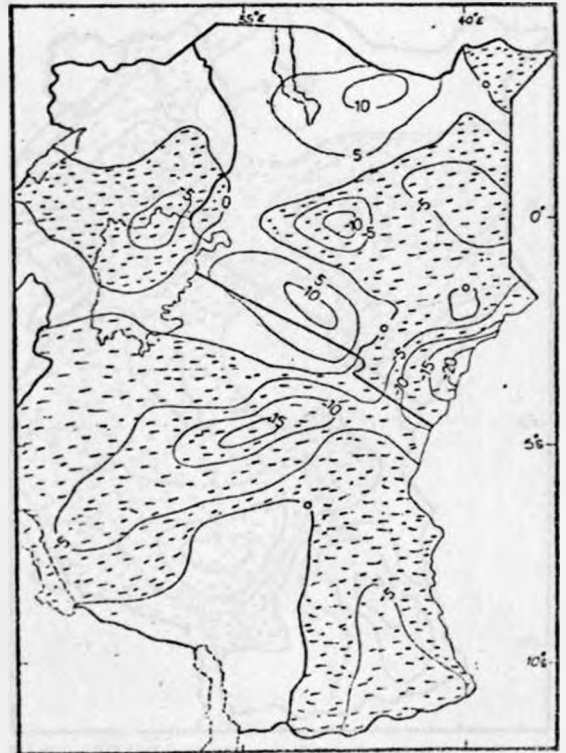


Fig. 31(a): Mean divergence field
($\times 10^{-6} \text{ s}^{-1}$) at 5490 m AMSL in June.

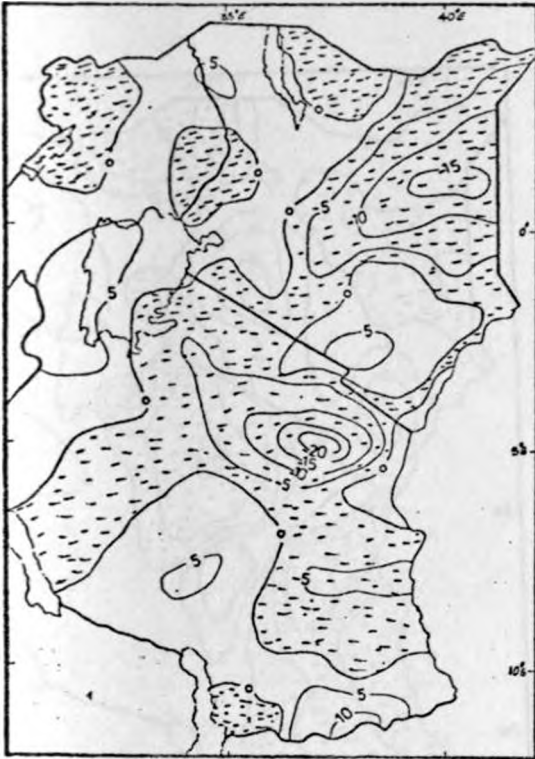


Fig. 31(b) : Mean divergence field ($\times 10^{-6} \text{ s}^{-1}$) at 5490 m AMSL in July.

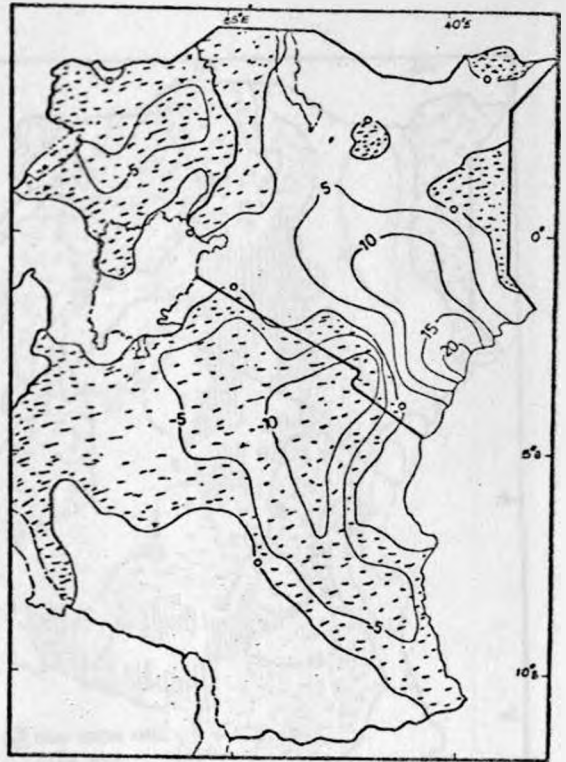


Fig. 31(c) : Mean divergence field ($\times 10^{-6} \text{ s}^{-1}$) at 5490 m AMSL in August.

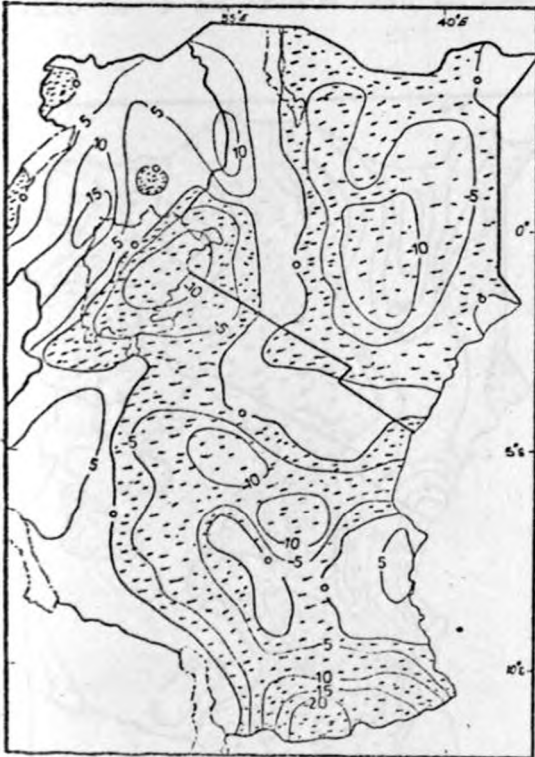


Fig. 32(a) : Mean divergence field ($\times 10^{-6} \text{ s}^{-1}$) at 7320 m AMSL in June.

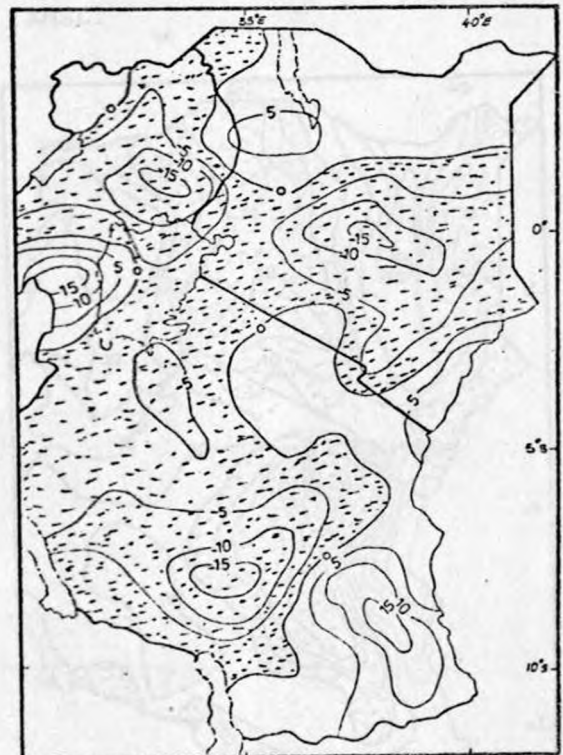


Fig. 32(b) : Mean divergence ($\times 10^{-6} \text{ s}^{-1}$) at 7320 m AMSL in July.

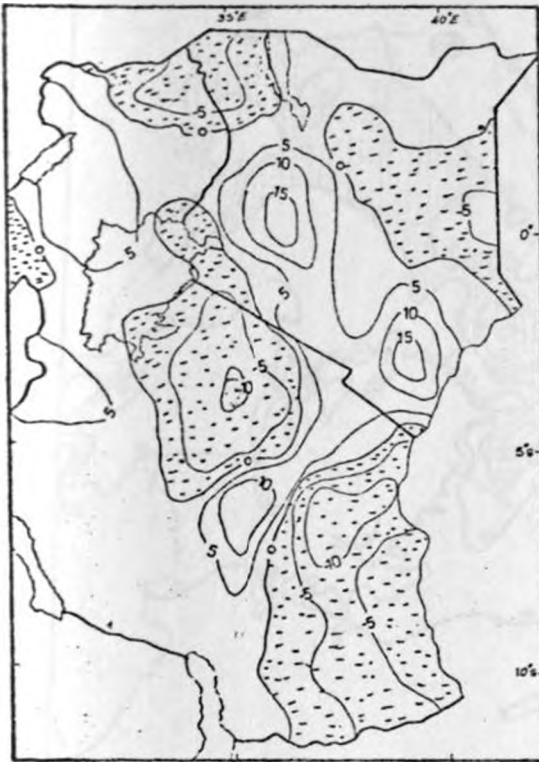


Fig. 32(c) : Mean divergence field ($\times 10^{-6} \text{ s}^{-1}$) at 7320 m AMSL in August.

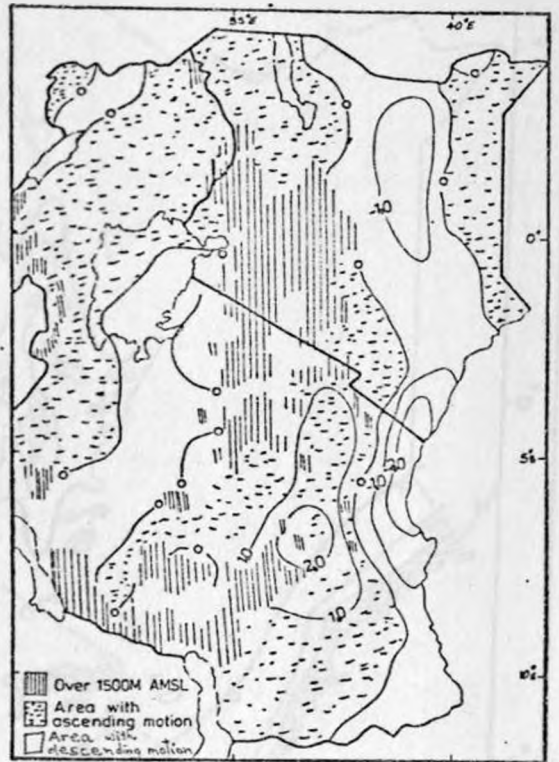


Fig. 33(a) : Mean July vertical motion field ($\times 10^{-2} \text{ ms}^{-1}$) at 1525 m AMSL.

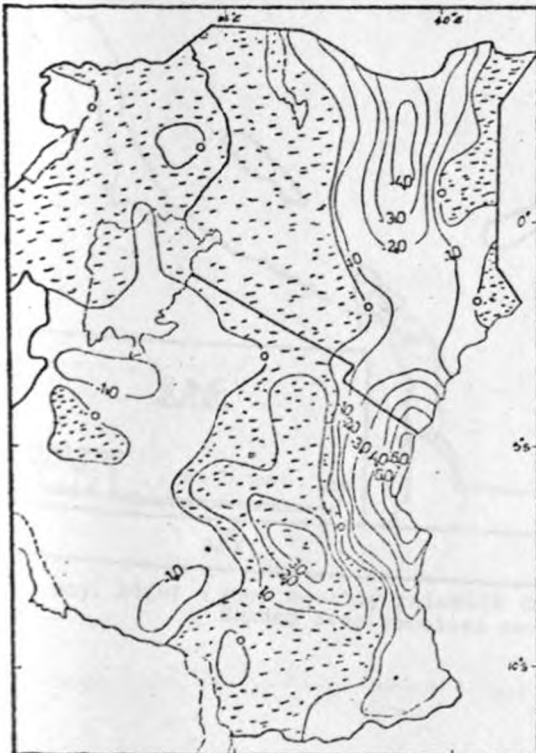


Fig. 33(b) : Mean July vertical motion field ($\times 10^{-2} \text{ ms}^{-1}$) at 3050 m AMSL.

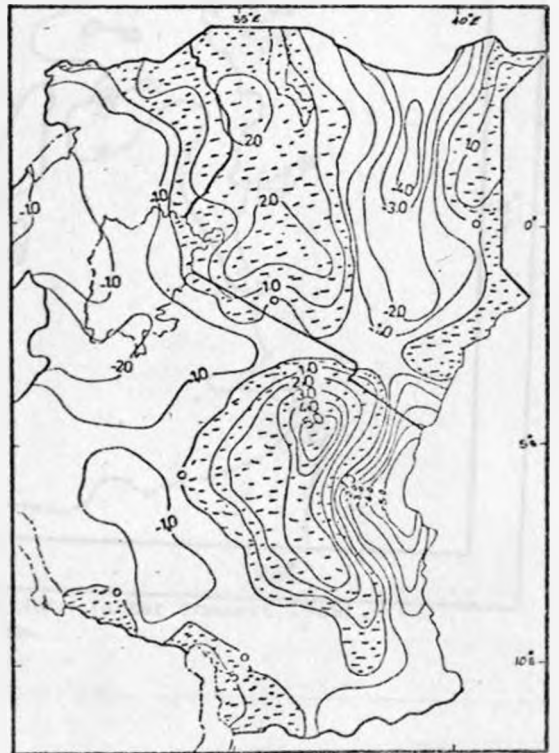


Fig. 33(c) : Mean July vertical motion field ($\times 10^{-2} \text{ ms}^{-1}$) at 5490 m AMSL.

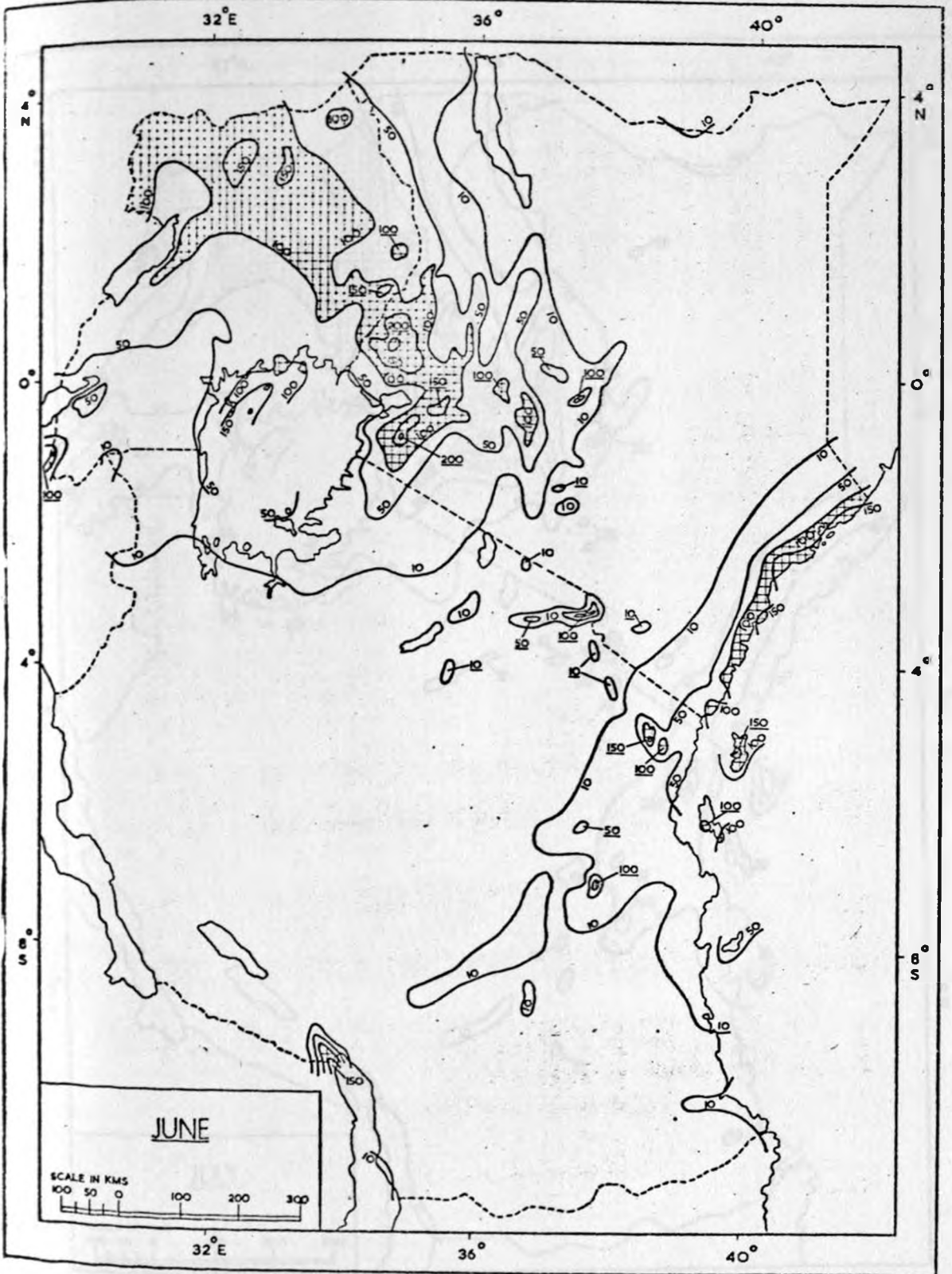


Fig. 34(a) : Mean monthly rainfall (mm) for June (after Tomsett 1969).
Shaded area receives over 100 mm.

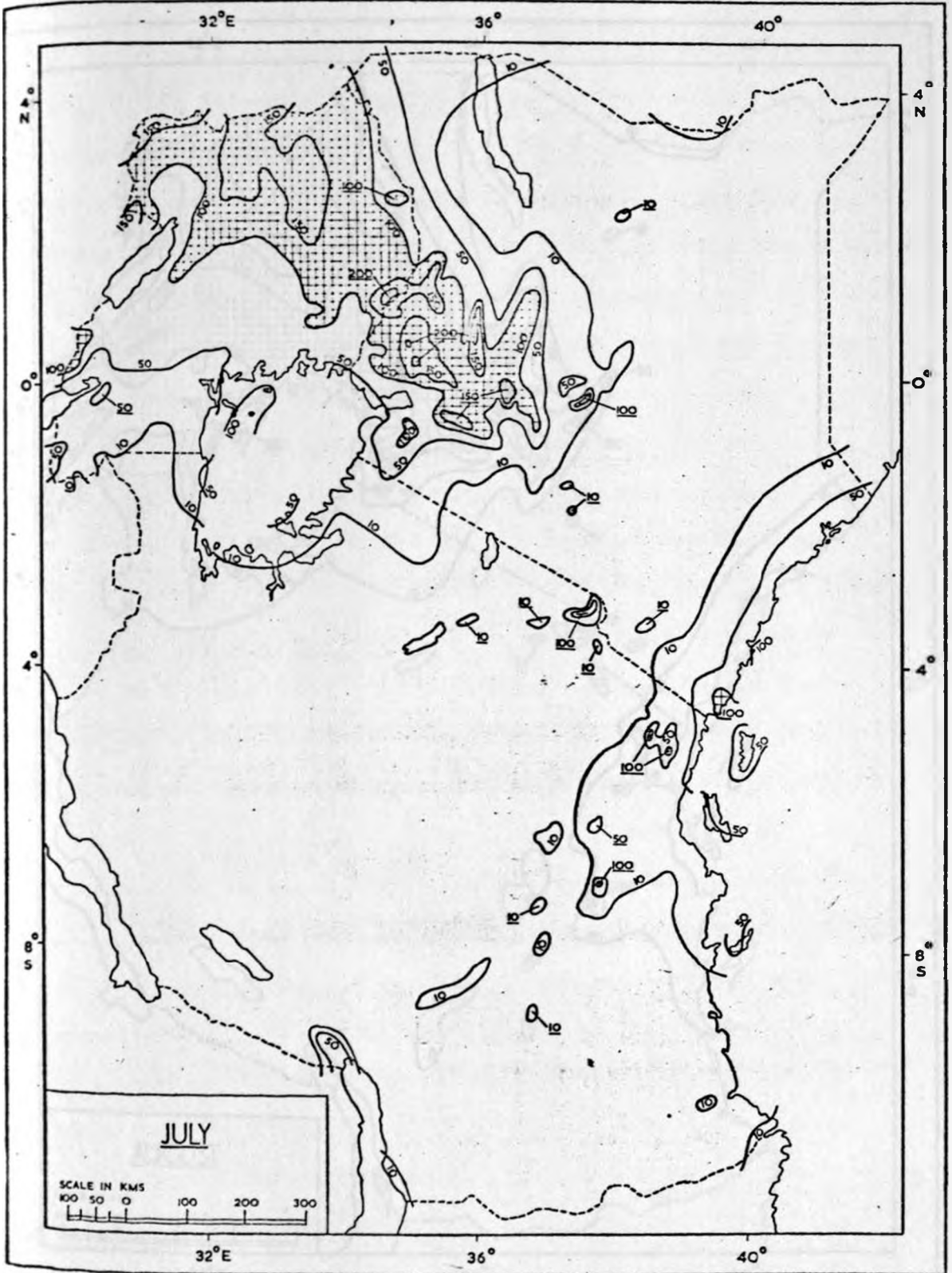


Fig. 34(b) : Mean monthly rainfall (mm) for July (after Tomsett 1969).
Shaded area receives over 100 mm.

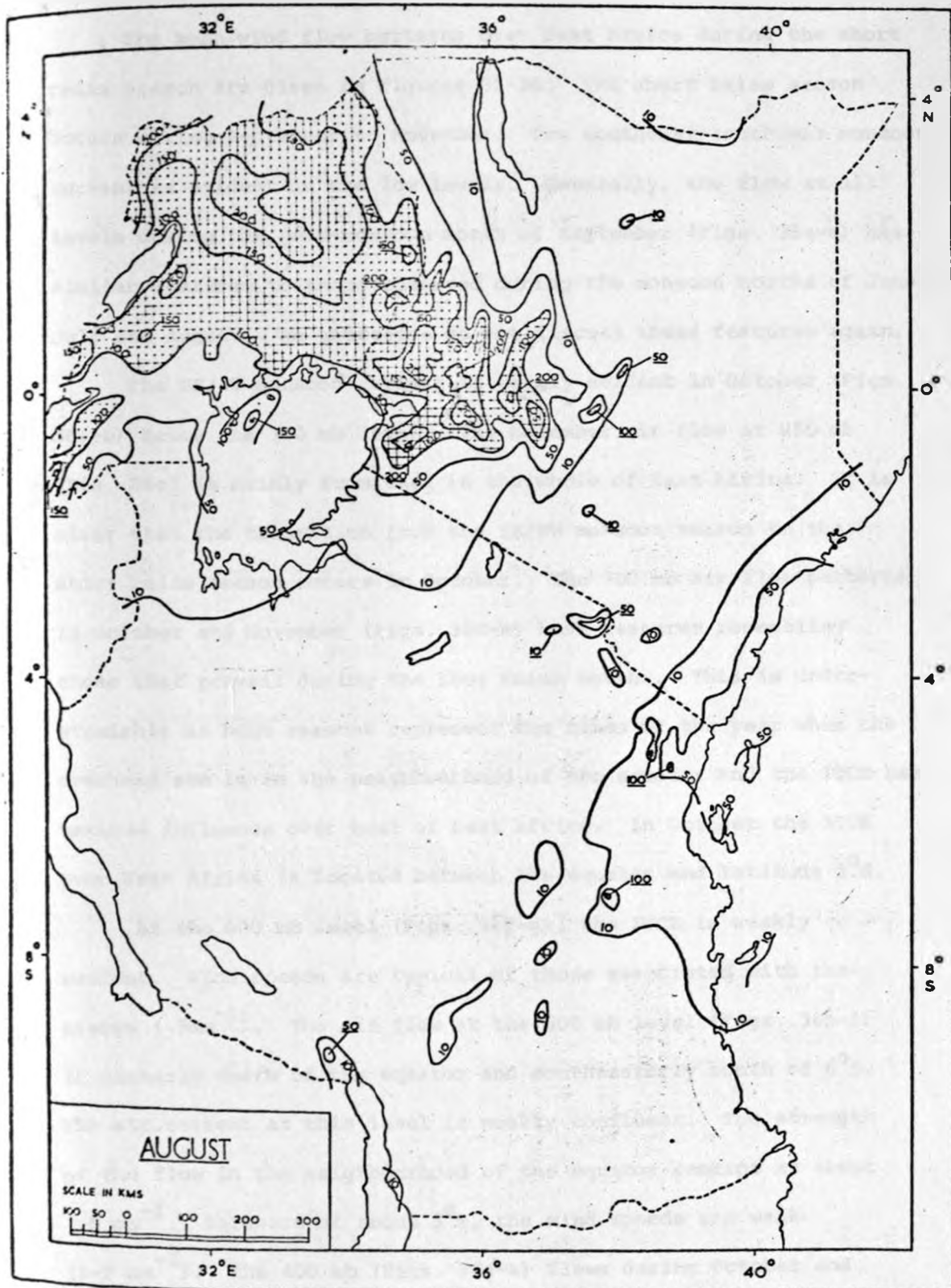


Fig. 34(c) : Mean monthly rainfall (mm) for August (after Tomsett 1969).
Shaded area receives over 100 mm.

3.1.4.0 The Short Rains Season

3.1.4.1 Mean Horizontal Motions

The mean wind flow patterns over East Africa during the short rains season are given in figures 35-36. The short rains season occurs during September to November. The southeast-southwest monsoon current is evident in the low levels. Generally, the flow at all levels during the post-monsoon month of September (Figs. 35a-e) has similar features to those observed during the monsoon months of June, July and August. We therefore do not discuss these features again.

The SE/SW monsoon current is weakly evident in October (Figs. 36a-b) below the 700 mb level. The November air flow at 850 mb (Fig. 36c) is mainly from east in the whole of East Africa. It is clear that the transition from the SE/SW monsoon season to the short rains season occurs in October. The 700 mb air flow patterns in October and November (Figs. 36d-e) have features resembling those that prevail during the long rains months. This is understandable as both seasons represent the times of the year when the overhead sun is in the neighbourhood of the equator and the ITCZ has maximum influence over most of East Africa. In October the ITCZ over East Africa is located between the equator and latitude 1°S .

At the 600 mb level (Figs. 36f-g), the ITCZ is weakly evident. Wind speeds are typical of those associated with the trades ($\sim 5\text{ms}^{-1}$). The air flow at the 500 mb level (Figs. 36h-i) is easterly north of the equator and southeasterly south of 6°S . The air current at this level is weakly confluent. The strength of the flow in the neighbourhood of the equator remains at about 7.5ms^{-1} . Poleward of about 5°S , the wind speeds are weak ($1-2\text{ms}^{-1}$). The 400 mb (Figs. 36j-k) flows during October and November resemble those at 500 mb.

3.1.4.2 Mean Divergence and Vertical Motion Fields

The divergence fields associated with the wind flow during September, October and November are presented in figures 37-38 and 40. We only present the vertical motion for October (Figs. 40a-c), the middle month of the short rains season. The divergence/convergence patterns in September (Figs. 37a-c) are very similar to those established during the SE/SW monsoon months of June, July and August. This is especially so at the 850 mb level (Fig. 37a) where the magnitude of divergence ($\sim 3 \times 10^{-5} \text{ s}^{-1}$) remains the same. We also observe from the figures that much of the western part of East Africa is under the influence of a convergent air current. However, the convergence that was observed over western Kenya/eastern Uganda during the northern summer months has weakened considerably. In fact, northwestern Kenya is divergent at most levels. Tomsett's rainfall atlas shows that the rainy zone (Fig. 41a) in September has shifted slightly southwestwards of its August location. This agrees with the spatial patterns of divergence field in September.

The 850 mb level divergence patterns in October (Fig. 38a) are similar to those observed during the SE/SW monsoon months. However, the magnitude of divergence in the now rapidly decaying monsoon current has decreased. The maximum value of divergence is about $2.5 \times 10^{-5} \text{ s}^{-1}$ at the 850 mb level in northeast Tanzania. At the 700 mb level (Fig. 38b) we observe an organised convergence zone running across the near-equatorial part of East Africa.

The convergence zone extends 2°N to 1°S over eastern Kenya and narrows over the Kenya highlands and lake region where maximum values of convergence ($\sim 1.5 \times 10^{-5} \text{ s}^{-1}$) are reached. Over the western part of East Africa, the convergence zone branches northwards into northwestern Uganda as observed during the long rains months. Another branch of this zone links up with the convergent area over western Tanzania. One difference between the divergence patterns in October and those observed in April is that the secondary convergent zone over southern Tanzania in April, is absent in October above the 850 mb level. This could partly explain the relatively raininess of southern and southwestern Tanzania in April as compared to October (Fig. 41b), in spite of the ITCZ being located in more or less the same position in both months.

We also notice that at the 600 mb level (Fig. 38c) the ITCZ in October, unlike that in April, is not recognisable as a continuous zone of convergence. Only eastern Kenya and northwestern Uganda are under the influence of a convergent air current at this level. The only area with a relatively deep layer of convergent (Figs. 38a-d) air current covers most of Uganda, the lake Victoria region and northwestern Tanzania. The vertical motion in this area is upward in the lower troposphere (Figs. 39a-c). From Tomsett's rainfall charts we observe that the wet zone during this month (Fig. 41b) roughly corresponds to the area where the air flow is convergent in a deep-layer. In eastern Kenya, there is convergence in the layer 700-600 mb (Figs. 38b-c). However, divergence in the low

levels results in downward motion (Figs. 39a-c), a possible cause for the observed dryness. The middle level of 500 mb is characterised by reversed patterns of divergence/convergence depending on what was prevailing in the lower layers.

In November (Figs. 40a-d), the eastern plains of East Africa are under the influence of divergent air current at the 850 mb level (Fig. 40a). The air flow in the western and northern parts of Kenya is convergent. The ITCZ is well-defined across East Africa at the 700 mb level (Fig. 40b). The general spatial patterns of divergence/convergence are similar to those observed in May at the same level. The air current in western Tanzania is convergent only in the lowest levels, being overlain by a deep divergent layer above 850 mb. The divergence field in eastern Tanzania starts reversing from low level divergence to upper level convergence in the medium levels (Figs. 40c-d). As is the case in October, the areas of deep convergence are located in western Uganda, lake region and the Kenya highlands.

On the whole, the short rains season is associated with the retreating of the SE/SW monsoon in September/October and the establishment of the ITCZ in October/November. However, even though the ITCZ is over the area, the observed low level divergence/convergence patterns remain almost similar to those established during the SE/SW monsoon season. Subsequently, the rainy areas are those that do not come directly under the influence of the retreating monsoon air current which is divergent at low levels.

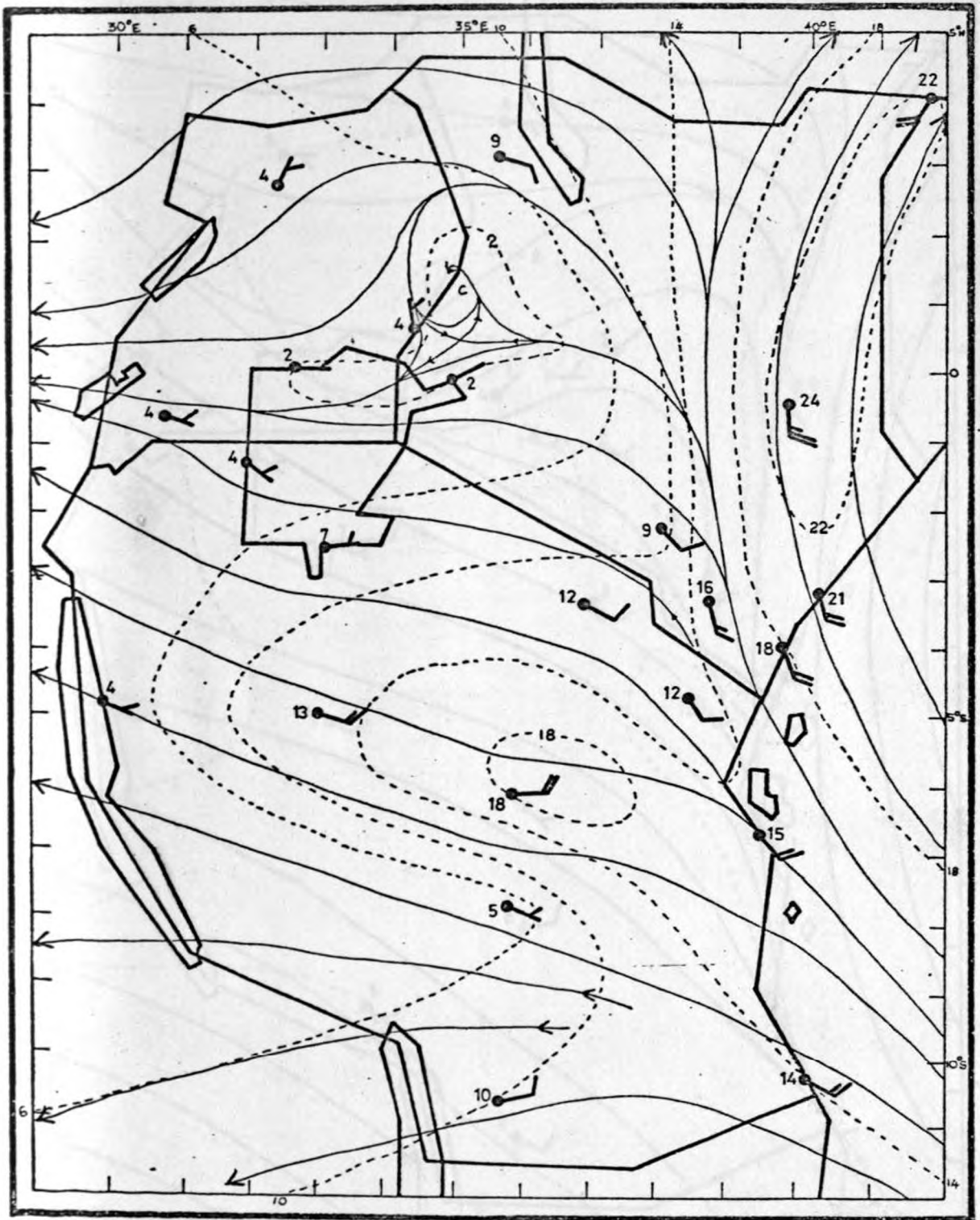


Fig. 35(a) : Mean wind field at 1525 m AMSL in September.

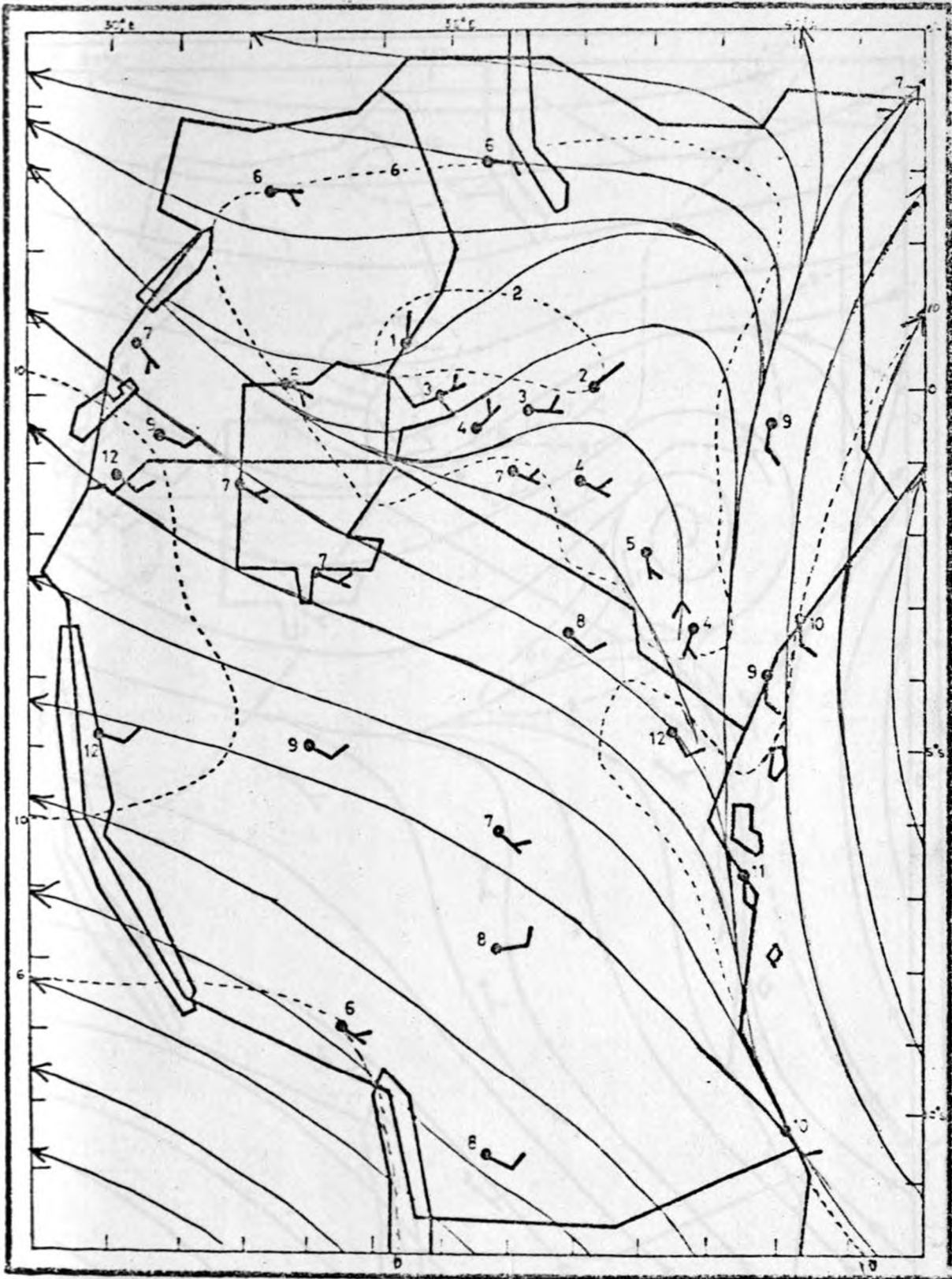


Fig. 35(b) : Mean wind field at 3050 m AMSL in September.

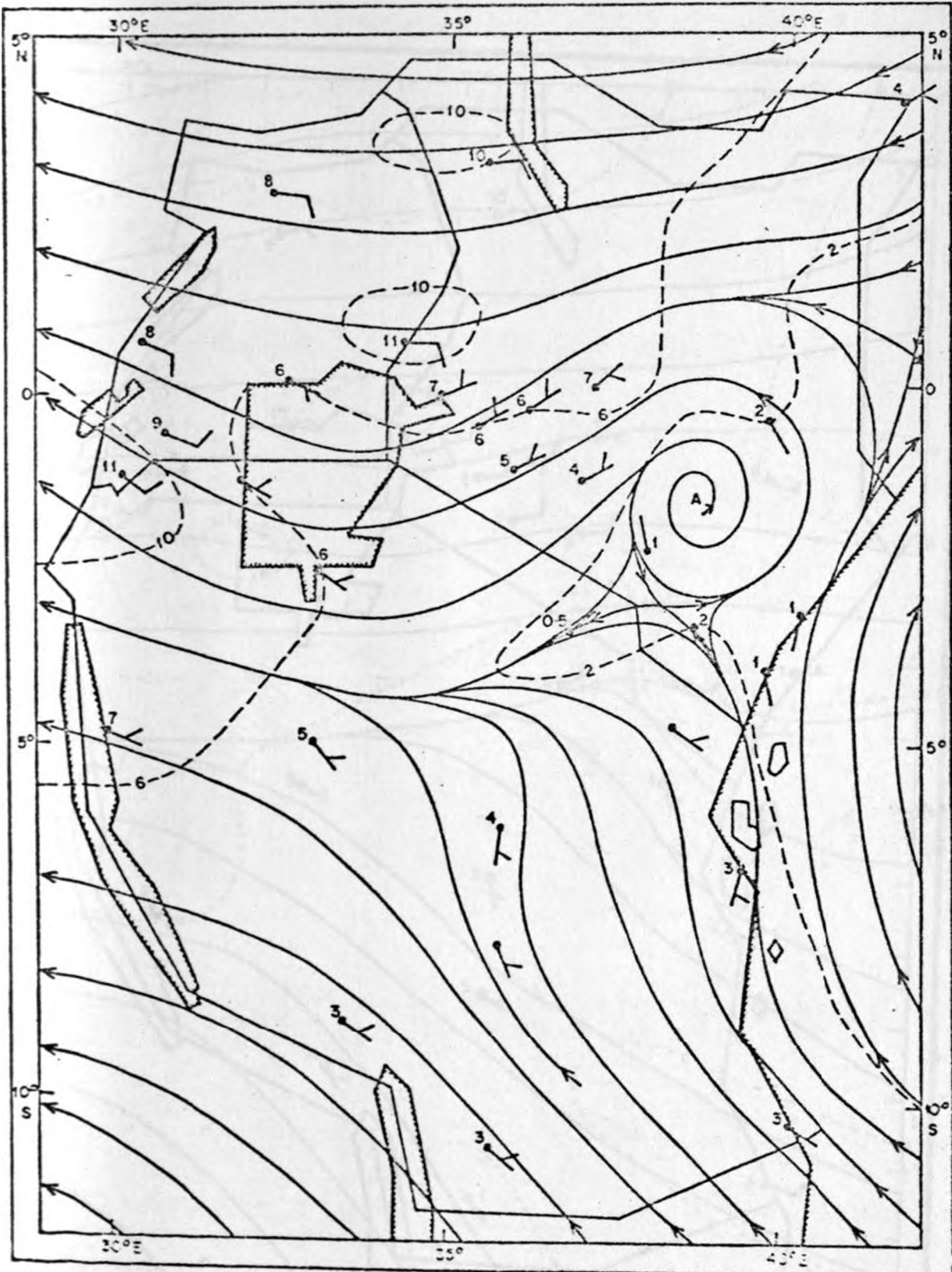


Fig. 35(c) : Mean wind field at 4270 m AMSL in September.

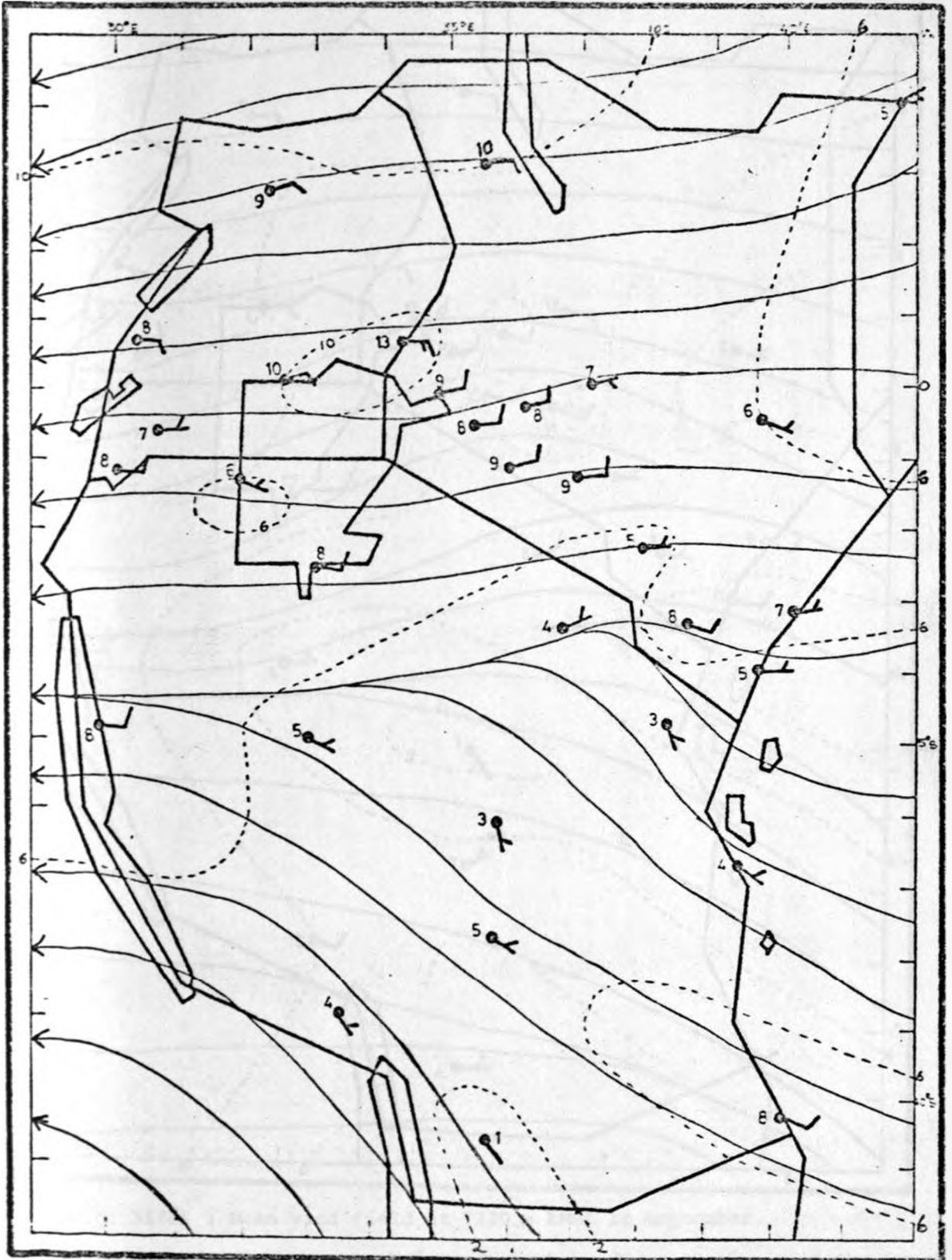


Fig. 35(d) : Mean wind field at 5490 m AMSL in September.

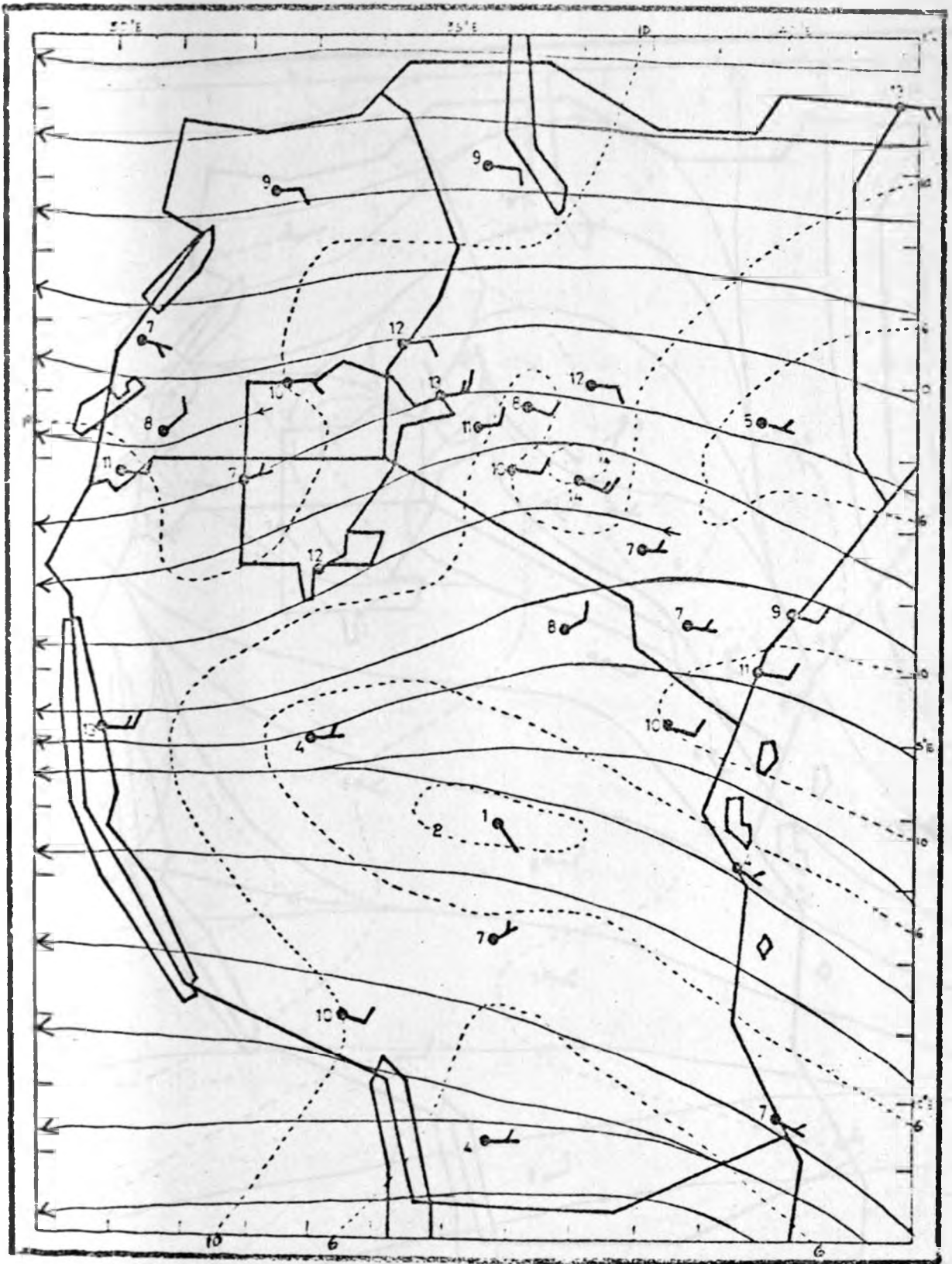


Fig. 35(e) : Mean wind field at 7320 m AMSL in September.

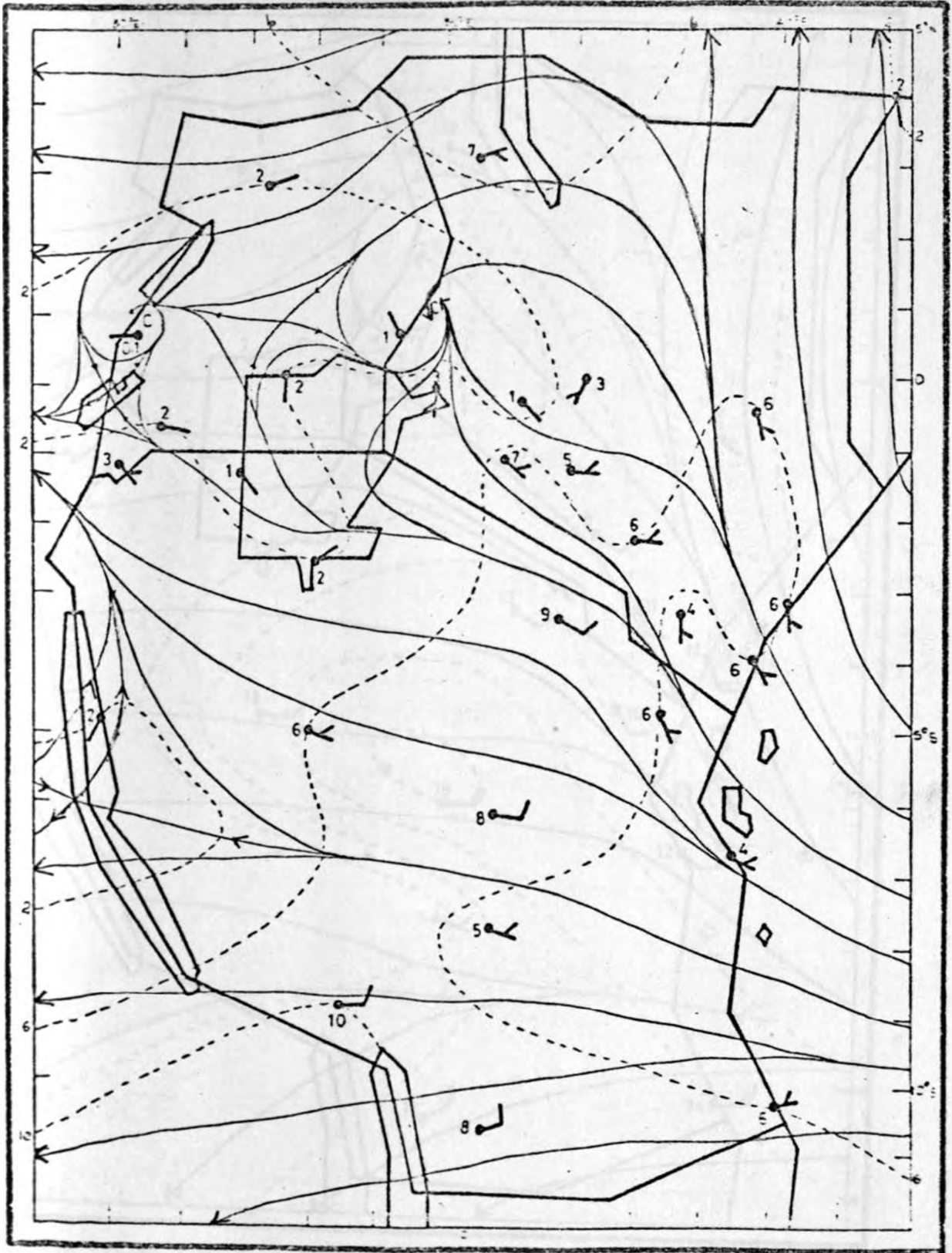


Fig. 36(a) : Mean wind field at the surface in October.

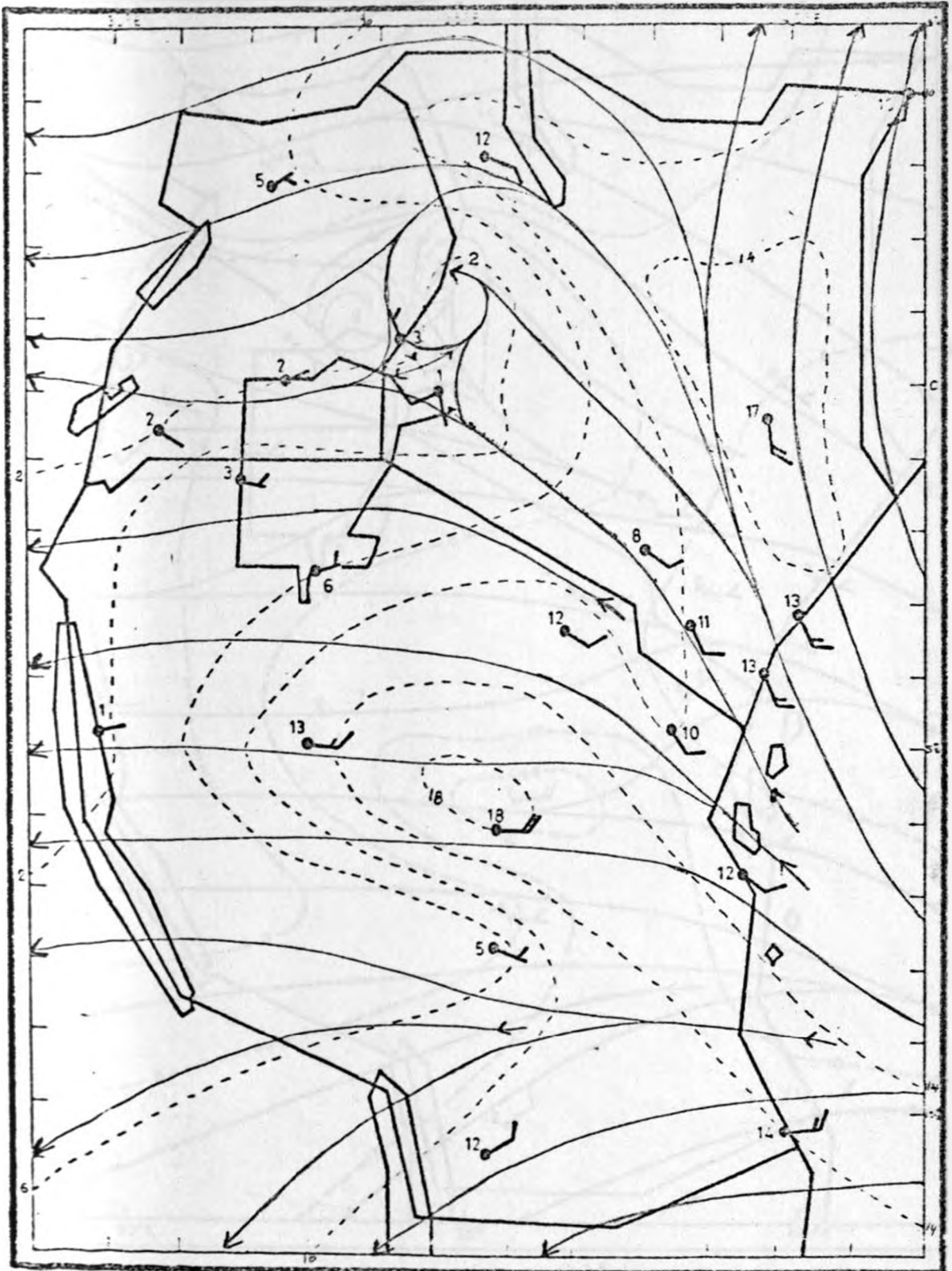


Fig. 35(b) : Mean wind field at the 1525 m AMSL in October.

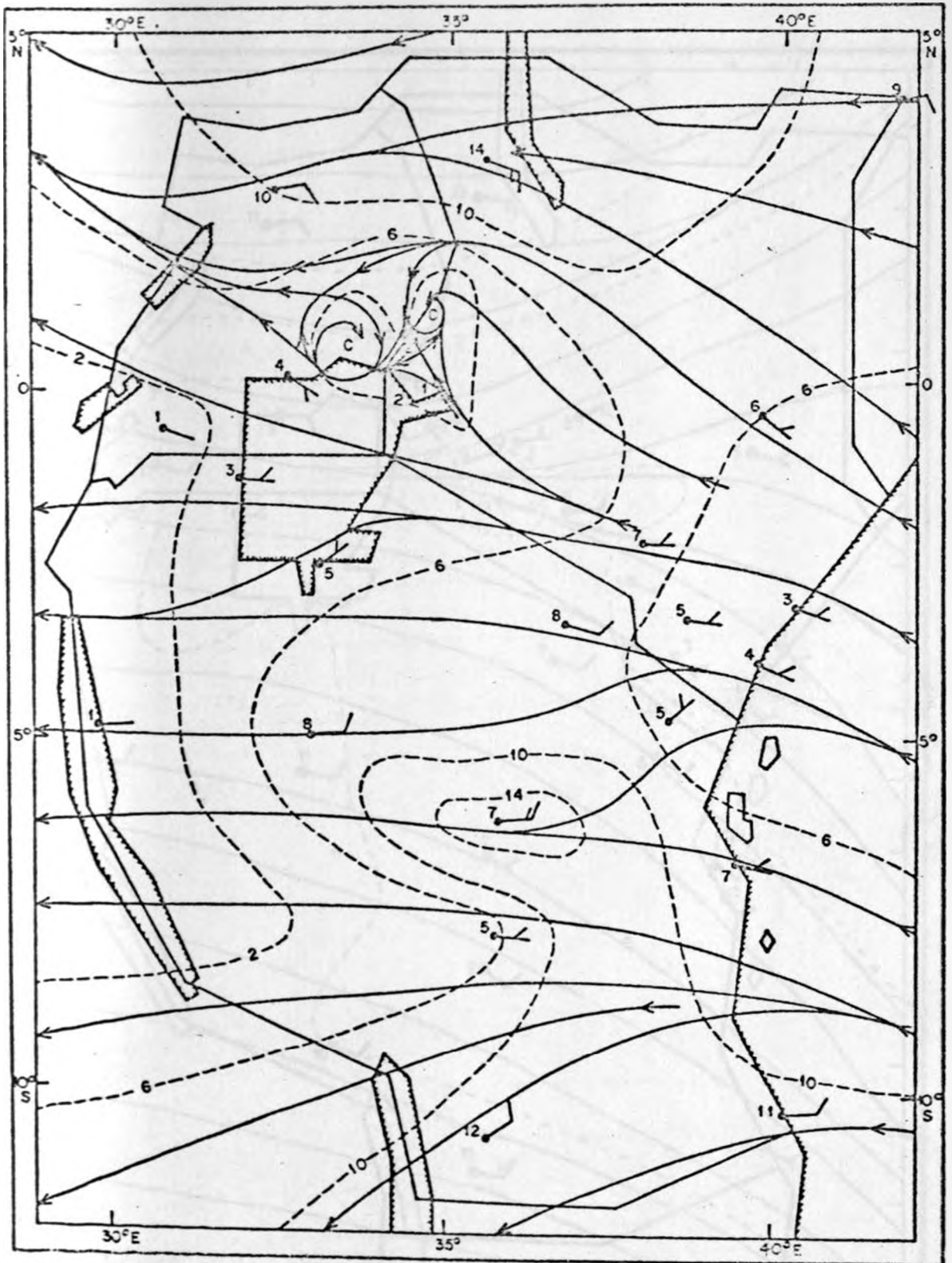


Fig. 36(c) : Mean wind field at 1525 m AMSL in November.

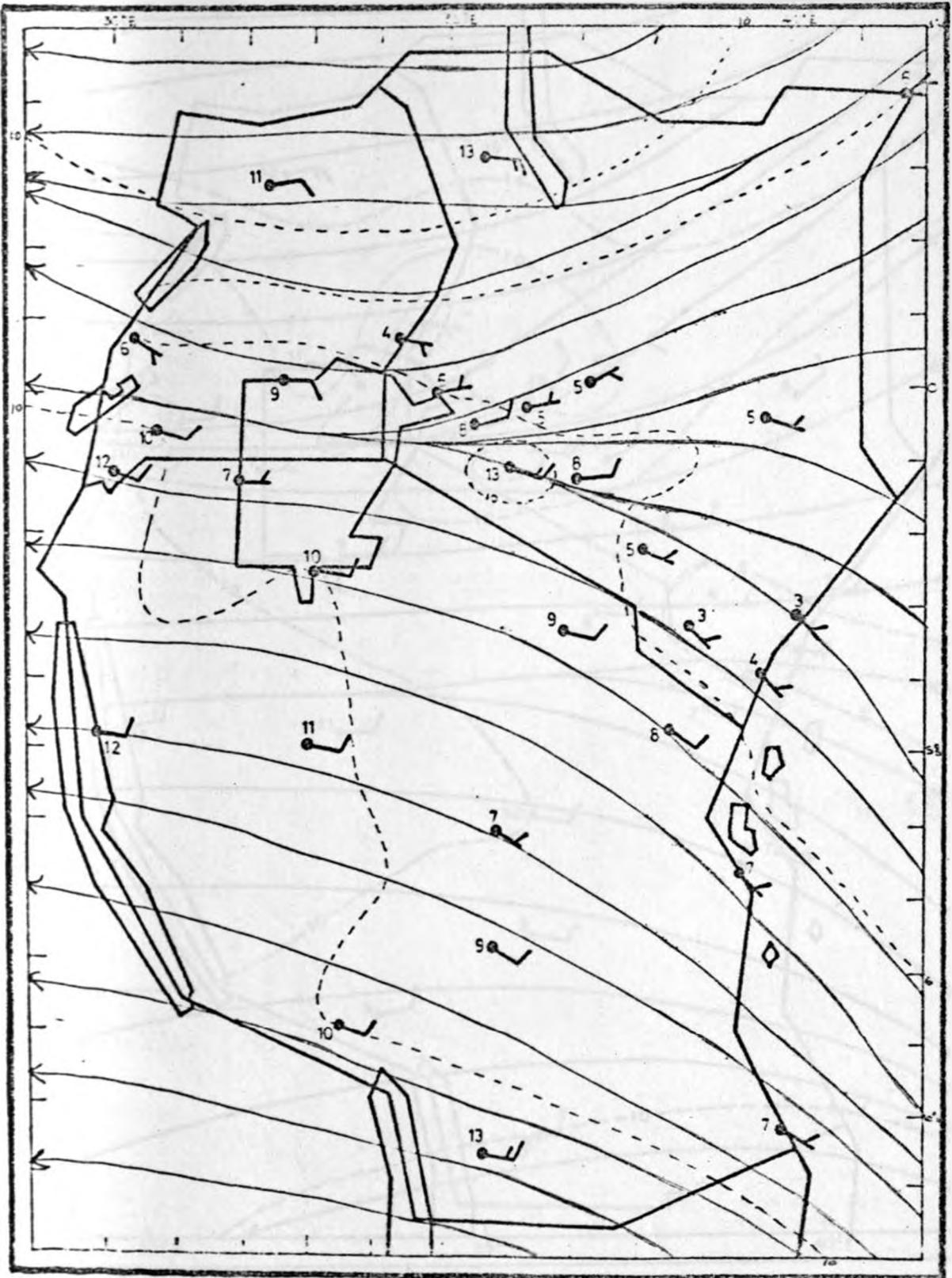


Fig. 36(d) : Mean wind field at 3050 m AMSL in October.

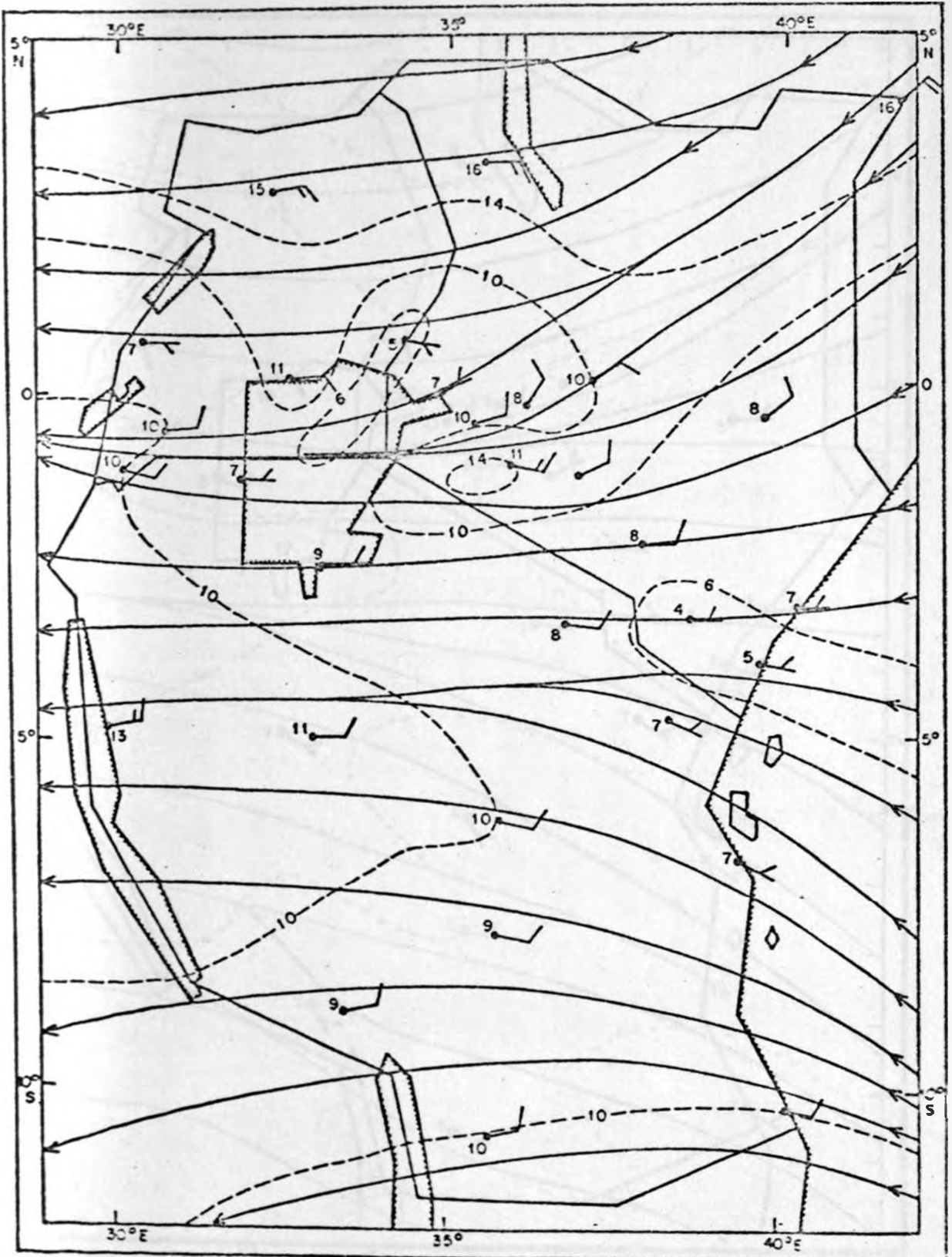


Fig. 36(e) : Mean wind field at 3050 m AMSL in November.

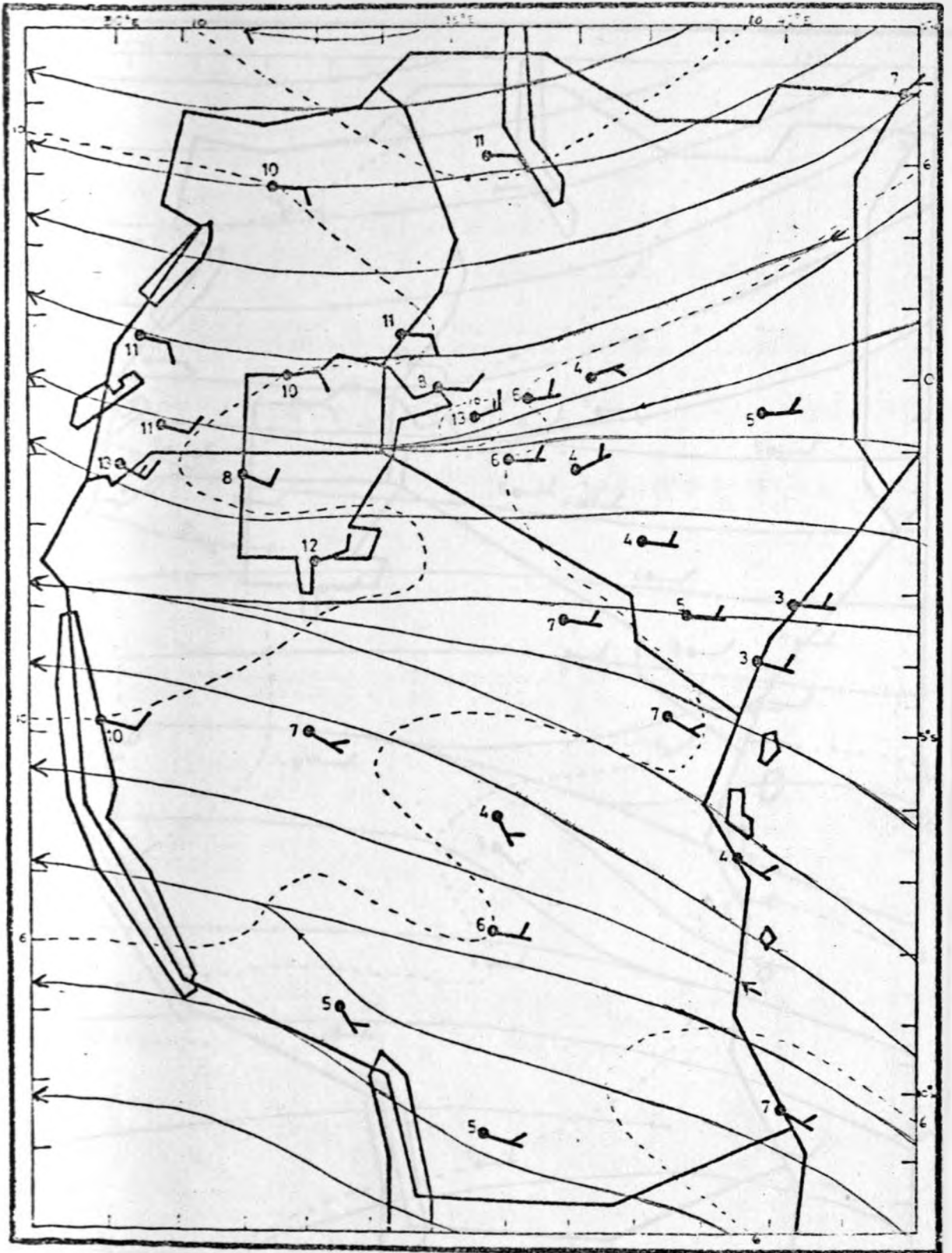


Fig. 36(f) : Mean wind field at 4270 m AMSL in October.

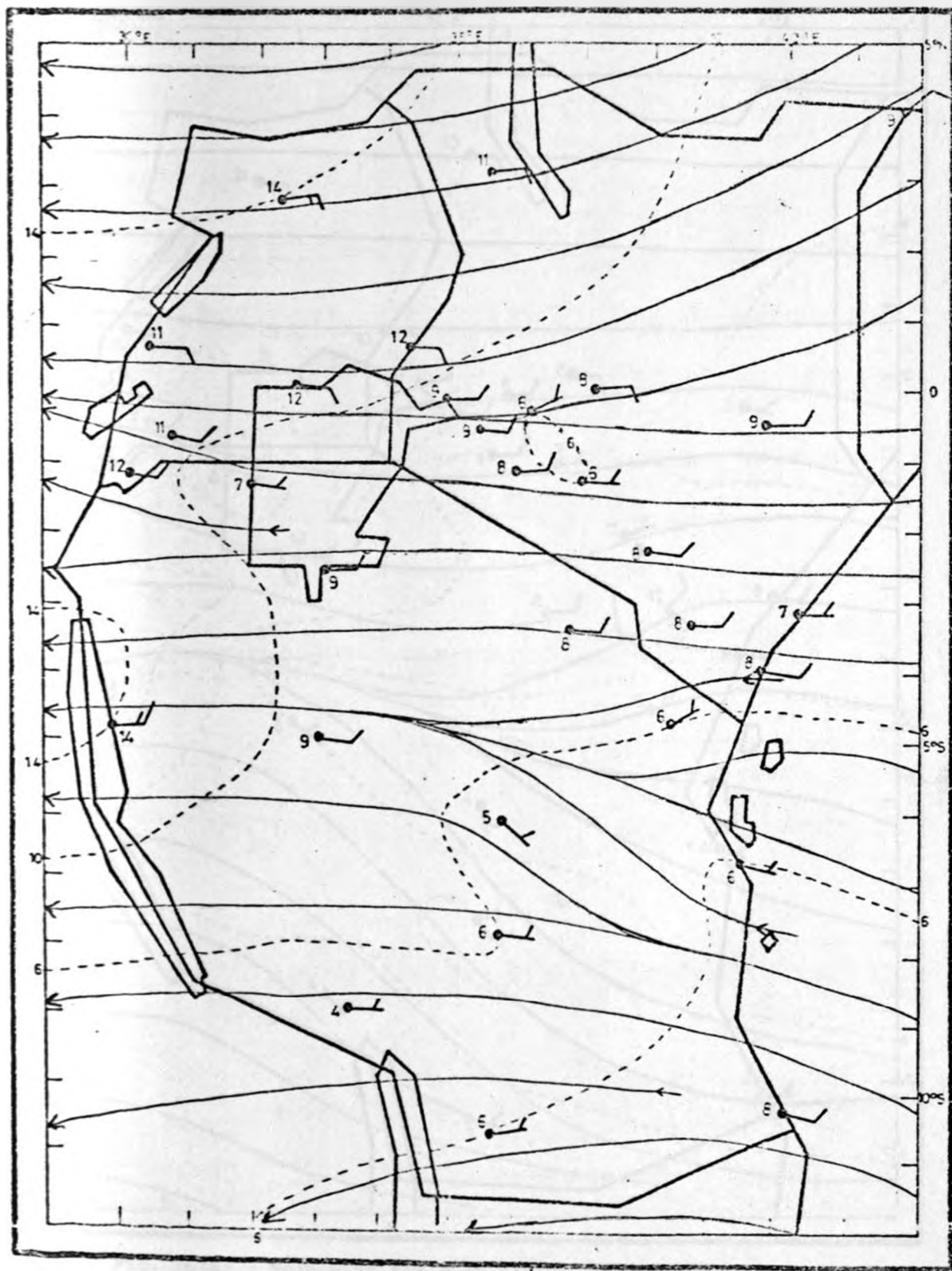


Fig. 36(g) : Mean wind field at 4270 m AMSL in November.

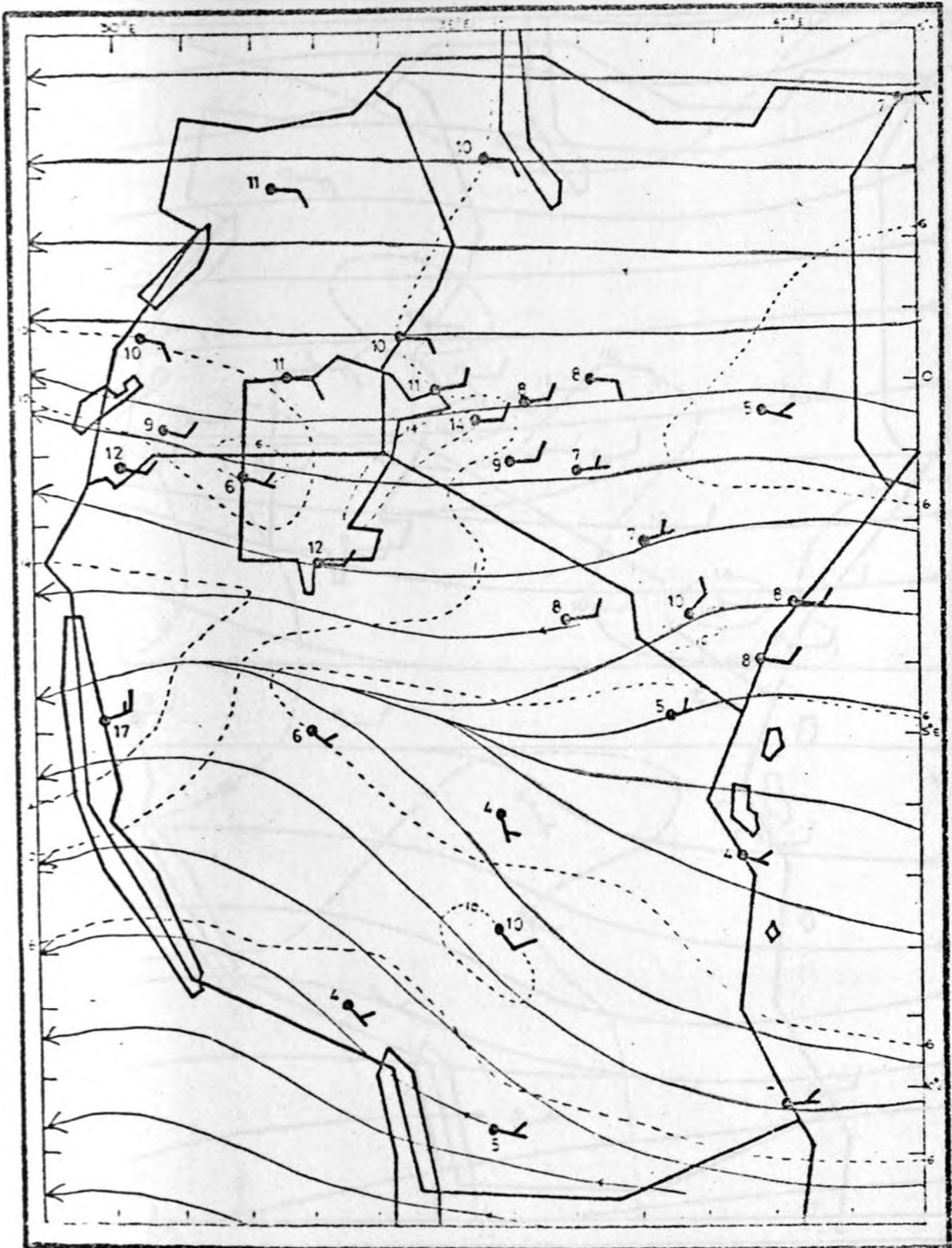


Fig. 36(h) : Mean wind field at 5490 m AMSL in October..

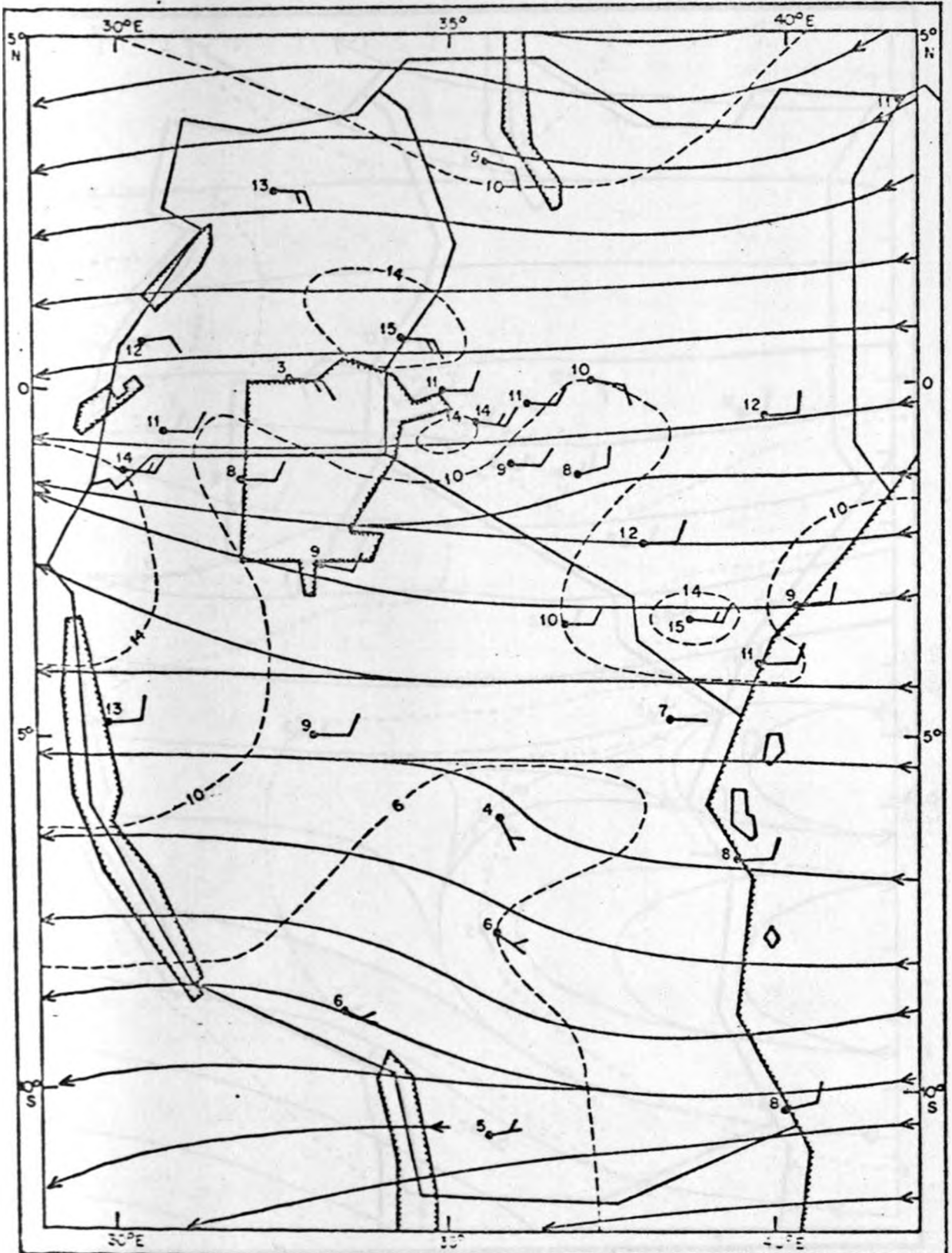


Fig. 36(i) : Mean wind field at 5490 m AMSL in November.

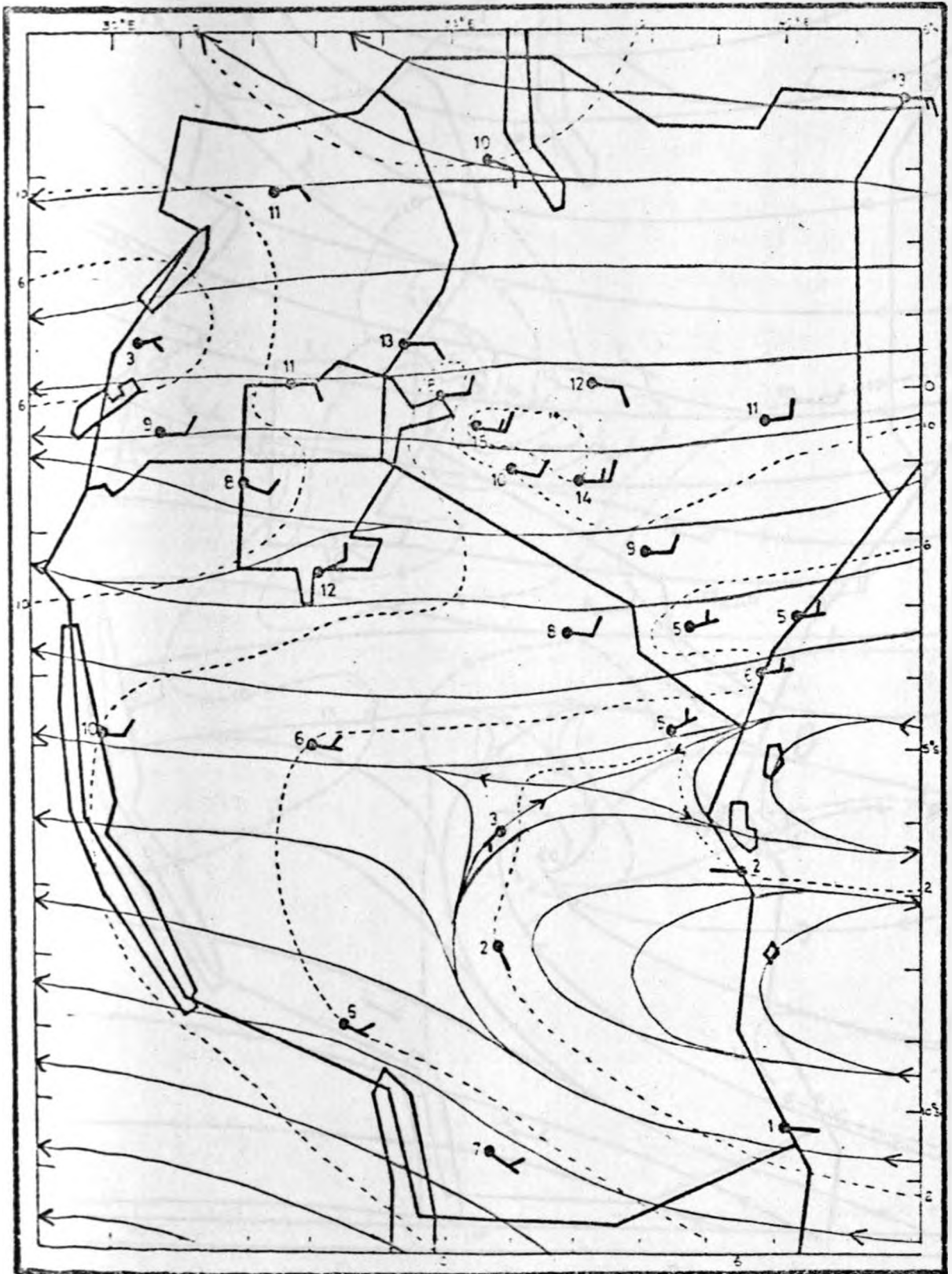


Fig. 36(j) : Mean wind field at 7320 m.AMSL in October.

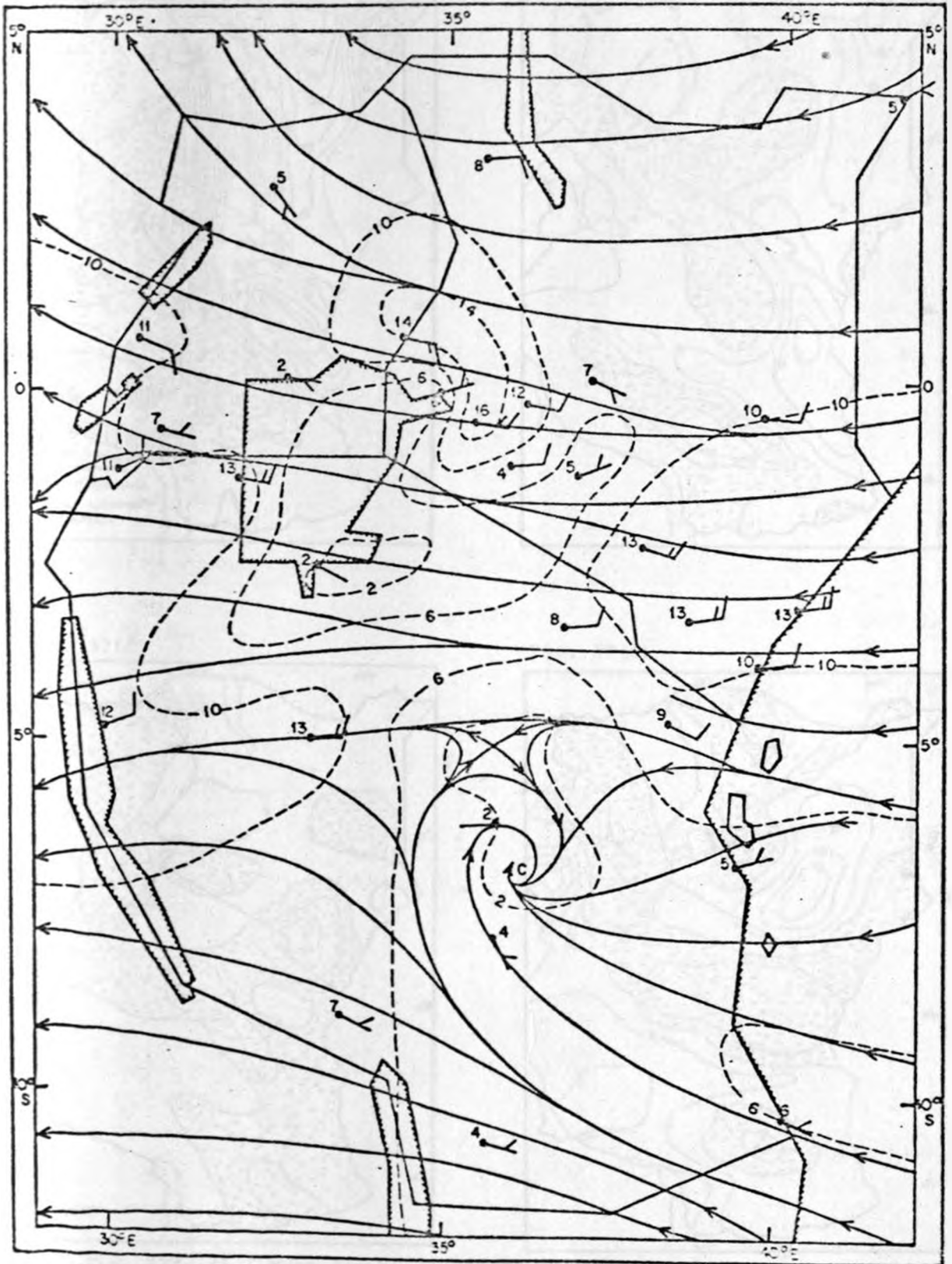


Fig. 36(k) : Mean wind field at 7320 m AMSL 'in November.

Fig. 37(a)



Fig. 37(b)

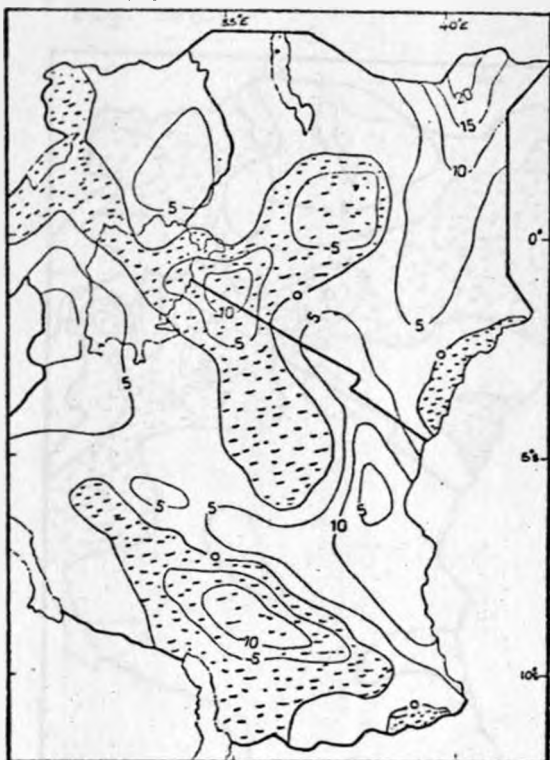


Fig. 37(c)



Fig. 37(d)



Fig. 37(a-d) : Mean divergence field ($\times 10^{-6} \text{s}^{-1}$) in September :
 (a) 1525 m AMSL, (b) 3050 m AMSL,
 (c) 5490 m AMSL, (d) 7320 m AMSL.

Fig. 38(a)

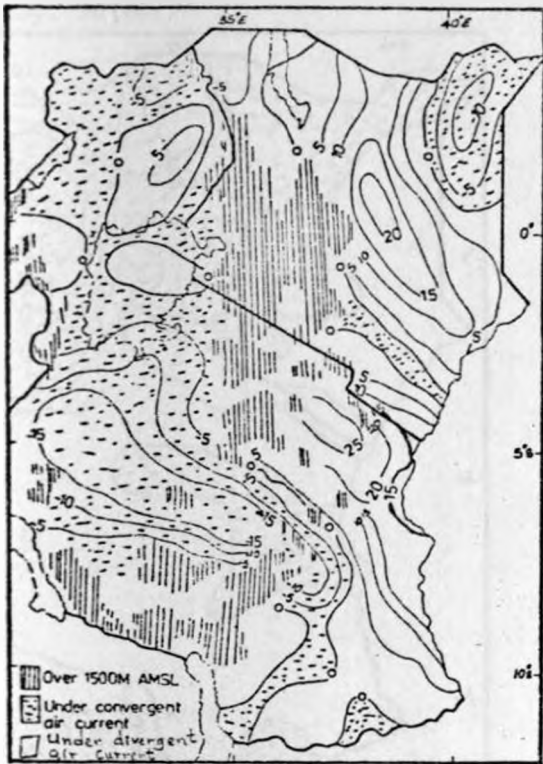


Fig. 38(b)

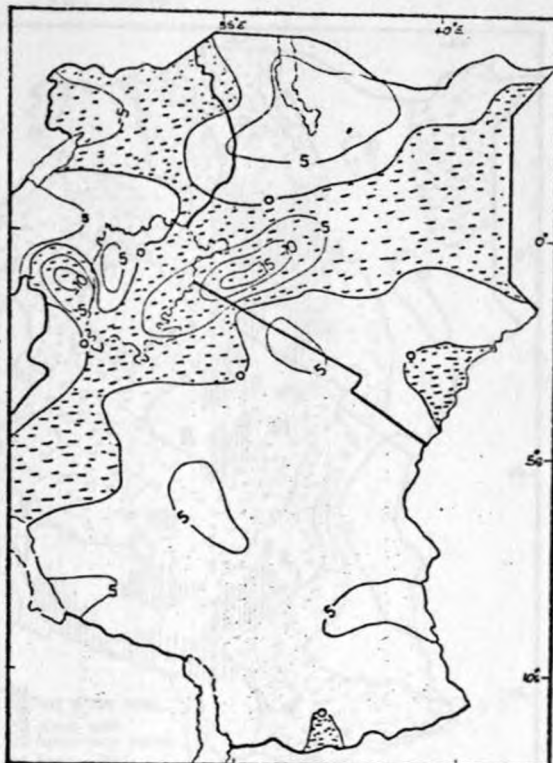


Fig. 38(c)

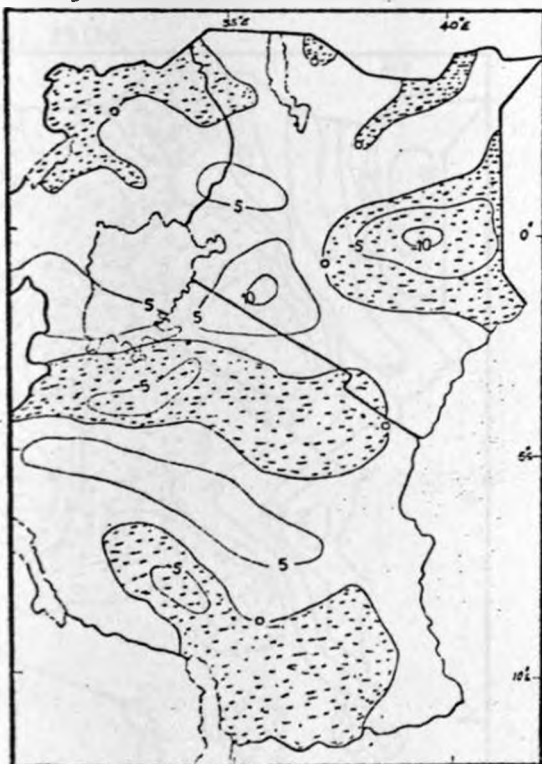


Fig. 38(d)



Fig. 38(a-d) : Mean divergence field ($\times 10^{-6} \text{ s}^{-1}$) in October :
 (a) 1525 m AMSL, (b) 3050 m AMSL,
 (c) 4270 m AMSL, (d) 5490 m AMSL.

Fig. 38(e)-

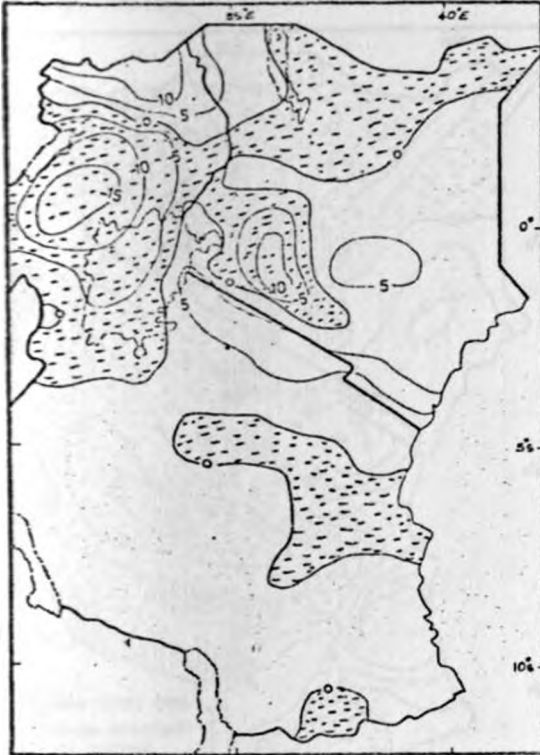


Fig. 38(e) : Mean divergence field ($\times 10^{-6} \text{ s}^{-1}$) at 7320 m AMSL in October.

Fig. 39(a)

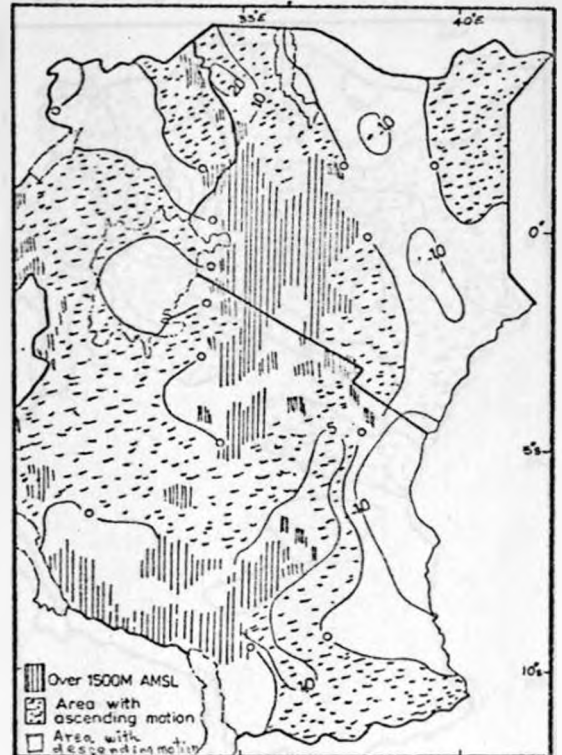


Fig. 39(c)

Fig. 39(b)

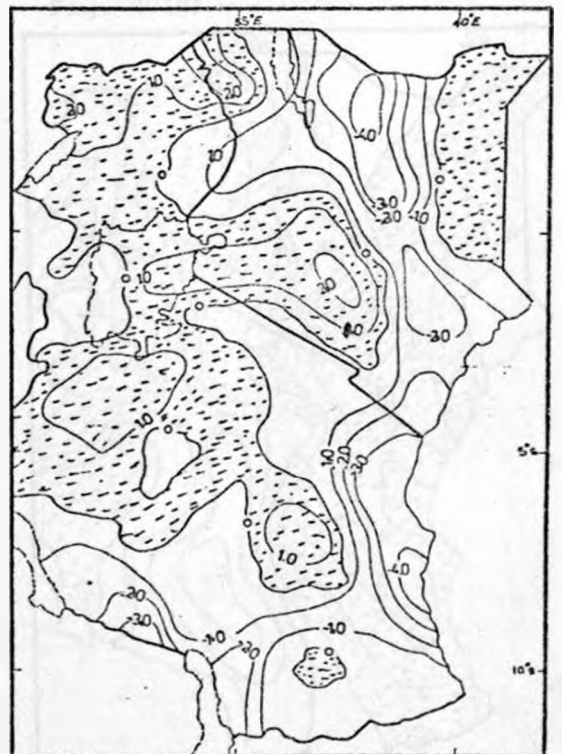
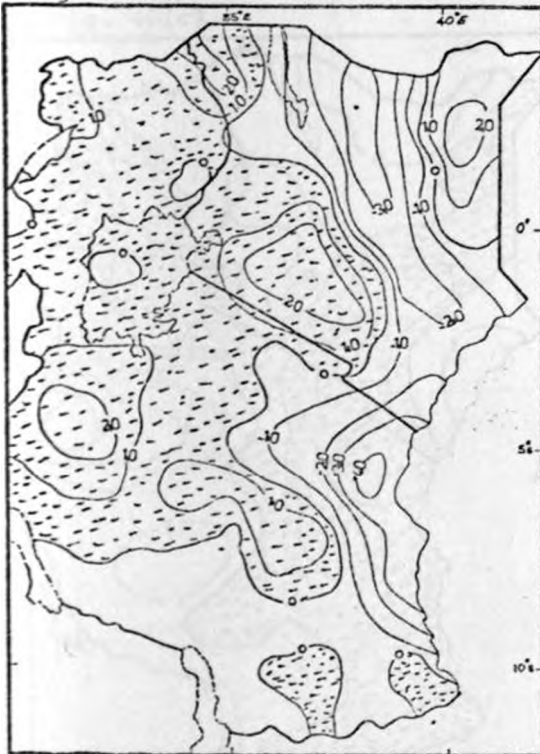


Fig. 39(a-c) : Mean October vertical motion field ($\times 10^{-2} \text{ ms}^{-1}$) :
 (a) 1525 m AMSL, (b) 3050 m AMSL, (c) 5490 m AMSL.

Fig. 40(a)



Fig. 40(b)

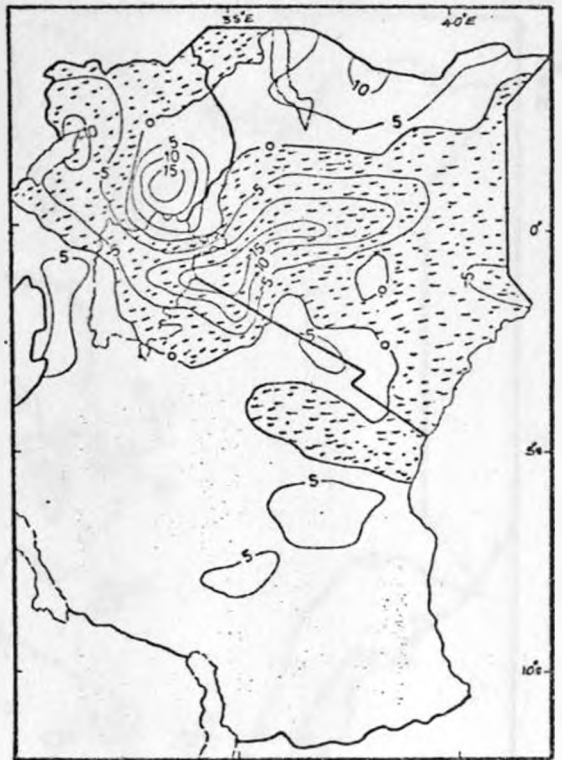


Fig. 40(c)

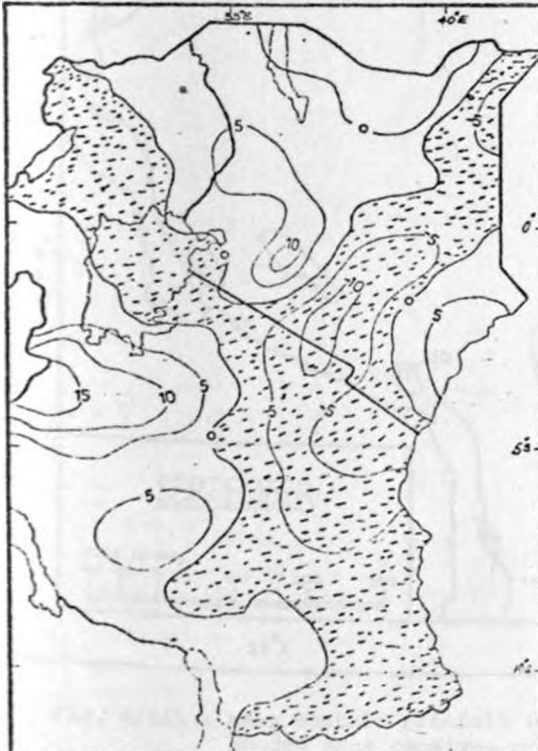


Fig. 40(d)

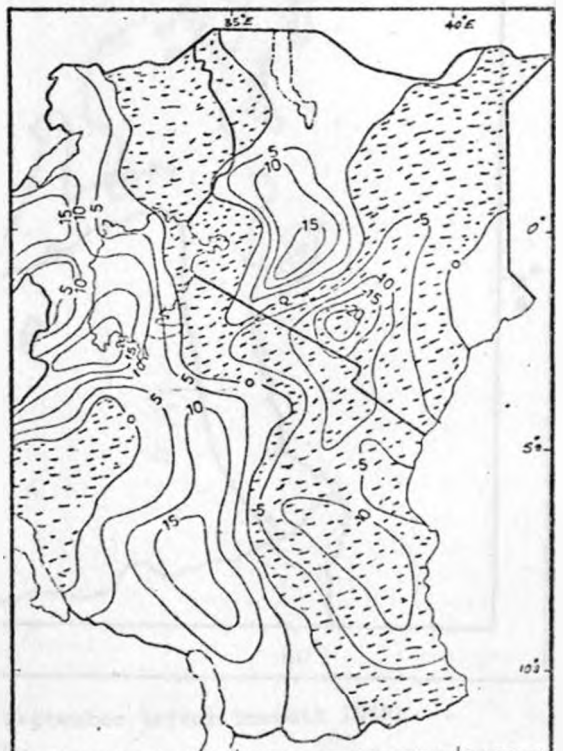


Fig. 40(a-d) : Mean divergence field ($\times 10^{-6} \text{ s}^{-1}$) in November :
 (a) 1525 m AMSL, (b) 3050 m AMSL,
 (c) 5490 m AMSL, (d) 7320 m AMSL.

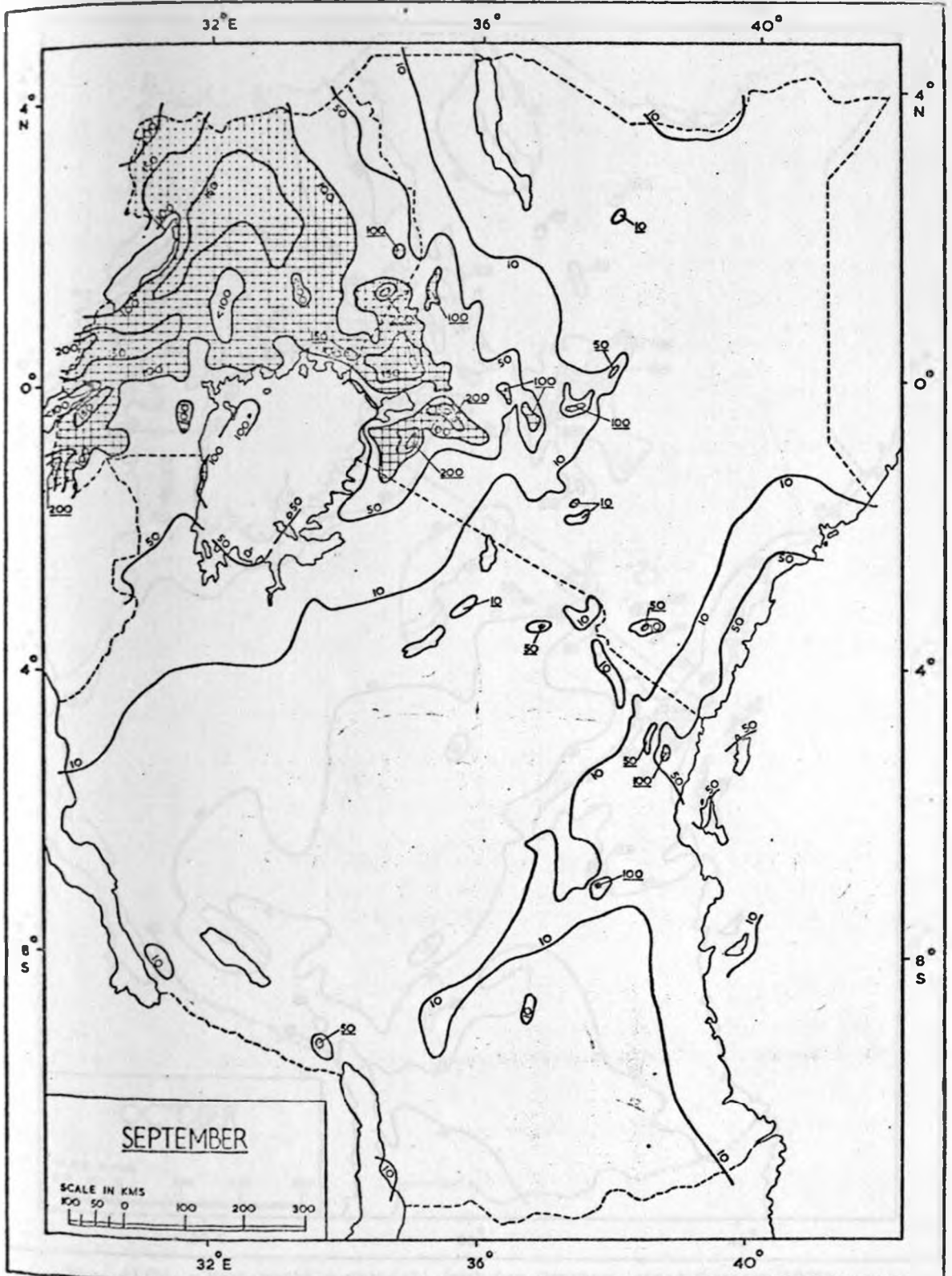


Fig. 41(a) : Mean monthly rainfall (mm) for September (after Tomsett 1969).
Shaded area receives over 100 mm.

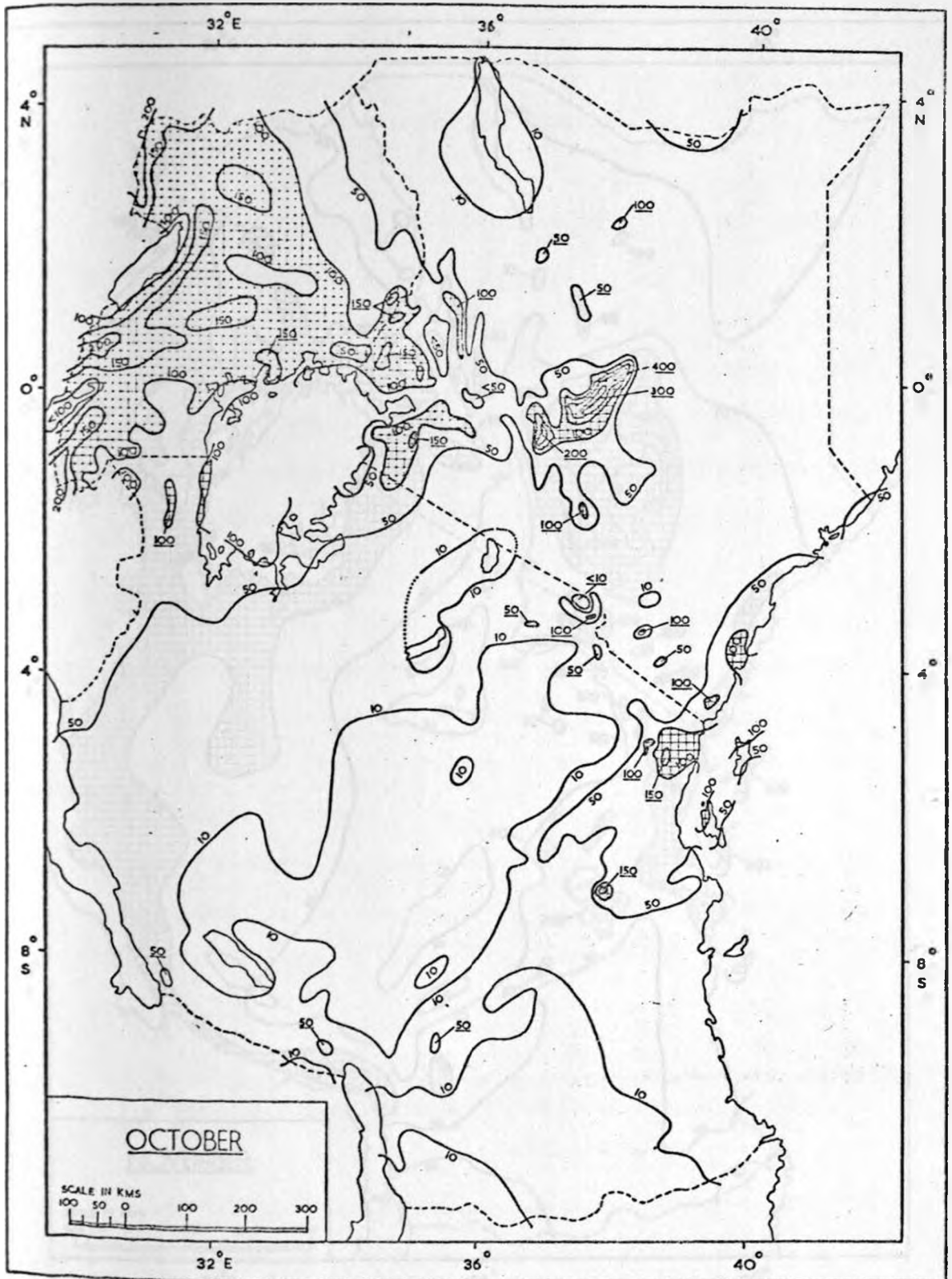


Fig. 41(b) : Mean monthly rainfall (mm) for October (after Tomsett 1969).
Shaded area receives over 100 mm.

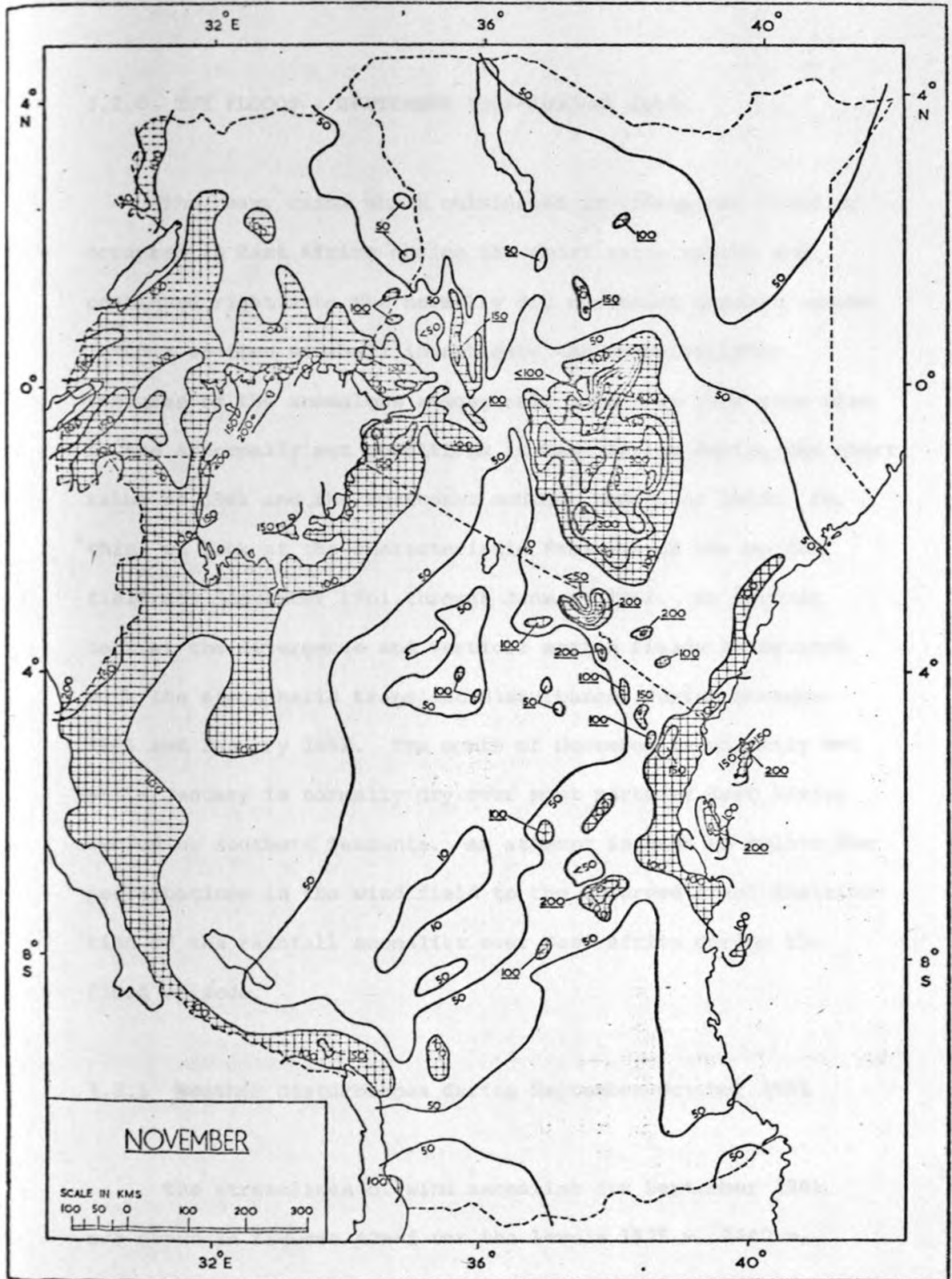


Fig. 41(c) : Mean monthly rainfall (mm) for November (after Tomsett 1969).
Shaded area receives over 100 mm.

3.2.0 THE FLOODS : SEPTEMBER 1961-JANUARY 1962

The heavy rains which culminated in widespread flooding occurred in East Africa during the short rains season and continued right into the normally dry northeast monsoon season. In this section we shall investigate the characteristic features of the anomalous atmospheric wind flow that gave rise to the abnormally wet conditions in East Africa during the short rains of 1961 and the northeast monsoon season of 1962. For this, we look at the characteristic features of the motion field for September 1961 through January 1962. We further look at the divergence and vertical motion fields associated with the atmospheric transient disturbances during November 1961 and January 1962. The month of November is normally wet while January is normally dry over most parts of East Africa excluding southern Tanzania. An attempt is made to relate the perturbations in the wind field to the observed areal distribution of the rainfall anomalies over East Africa during the flood episode.

3.2.1 Weather Disturbances during September-October 1961

The streamlines of wind anomalies for September 1961 are shown in figures 42a-f for the levels 1525 m, 2440 m, 3050 m, 4270 m, 5490 m and 7320 m AMSL. We note that at 850 mb (Fig. 42a), the whole of southern and western Tanzania

is under the influence of an anticyclonic (diffluent) flow. In northeastern Tanzania/SE Kenya and the lake region, there exist cyclonic vortices. Over all, the anomalous wind vectors vary from southwesterly to southeasterly and the ensuing confluences are located over the central parts of East Africa. At the 800 mb level (Fig. 42b) we observe similar streamline patterns to those at 850 mb level. The 700 mb level (Fig. 42c) streamlines reveal similar features to those observed in the lower levels. However, the anticyclonic vortices in southern Tanzania show a slight equatorward shift from their position at 800 mb. The central parts of Kenya and most of Uganda are still under the influence of the highly confluent flow. This pattern is maintained upto 500-400 mb (Figs. 42e-f).

On the whole, we note that the wind deviation fields for September 1961 are characterised by the presence of anticyclones that are located in southern Tanzania and off the northeastern part of Kenya; zones of marked confluence, and cyclonic vortices in Kenya, northern Tanzania and Uganda. These features tilt equatorward with height below the 600 mb level. From the rainfall anomalies (Fig. 42g), we find that the main areas which experienced above normal rainfall in September 1961 include Uganda, northern parts of Tanzania and most parts of Kenya. The spatial distribution of areas with above normal rainfalls agrees very well with the areas with cyclonic vortices and/or confluent streamlines in the wind deviation field. In this study we do not present the divergence and vertical motion fields associated with the transient

weather systems of September 1961. This will only be done for the months of November 1961 and January 1962.

One disturbing feature is the small area of very high rainfall anomalies along the Kenyan coast (Fig. 42g). The streamline analyses in this area do not agree with the high positive anomalies. But, on scanning through the daily rainfall totals at the coastal stations during the month of September, we found that these high anomalies were due to very heavy rains that were concentrated within only 2-3 days. At Lamu (2°S , 41°E) for example, the monthly total was 487.3 mm. Of this, 68.1 mm fell on 25 September, 219.2 mm on 26, 105.4 mm on 27 and 28.4 mm on 28 September. At Mombasa (4°S , 40°E) the monthly total was 300 mm of which 23.1 mm was recorded on 24 September, 149.9 mm on 25, 49.5 mm on 26, and 14.7 mm on 27 September. Thus 67% of the monthly total for Lamu fell between 26-27 September while the same percentage (67%) of Mombasa's September rainfall fell between 25-26 September.

We believe that the coastal rains of September 1961 could have been caused by an easterly wave which hit the coast around 24 September and dissipated within 4-5 days of its arrival. Similar wave disturbances are known to affect the Kenya coast (Fremming 1970). The easterly wave reported by Fremming hit the Kenyan coast between 5-7 September 1967. The non-appearance of the disturbance in the September 1961 streamlines is perhaps due to the fact that the wind deviations are monthly ones. It would be an interesting study to specifically look at the wind departure fields associated with the

weather systems that gave rise to the heavy rainfalls of 25-28 September 1961. Generally, September 1961 was dry until around 24-25 September.

In October 1961 (Figs. 43a-f), we observe very similar features to those in the streamline patterns of monthly wind departures of September 1961. This is so especially as regards the anticyclone in southern Tanzania and the confluence and cyclonic vortices in northern Tanzania, Kenya highlands and Uganda. Nonetheless, we find from the figures that in October, unlike September, much of northeastern Tanzania is confluent at most levels upto 500-400 mb (Figs. 43e-f). The weather systems seem to have extended southwards in October, when compared with the situation in September. In general, the zone under cyclonic circulation and/or confluence is oriented in a southeast-to-northwest direction.

We compare the distribution of rainfall anomalies (Fig. 43g) and the streamlines of wind departures. It is evident from the figures that the areas with highest values of above normal monthly totals coincide very nearly with the observed confluent zones in the fields of wind departures. Although the rainfall anomalies in figure 43g show that nearly the whole of East Africa had positive anomalies during October, we find that much of central and southern Tanzania had relatively low positive values. The reasons for this could be in the observed anticyclonic and/or diffluent flow in southern Tanzania throughout the lower troposphere (Figs. 43a-f).

3.2.2 Weather Disturbances during November 1961

The wettest month during the 1961/62 flood episode was November 1961. In this month (Fig. 44a), the whole of East Africa received above normal rainfall. The spatial distribution of these anomalies reveals that the area with more than +200 mm coincides with the normal location of the ITCZ in East Africa during the month of November (Fig. 40b). The flow patterns of the wind departures (Figs. 44b-g) show that the whole of East Africa is engulfed by a westerly-to-southwesterly air current during this month. The anomalous westerly flow (Fig. 44b) is found to be convergent in the eastern portion of East Africa. At the 800 mb level (Fig. 44c), there prevails a cyclonic centre over the western Kenya highlands. The cyclonic circulation off the East African coast has shifted equatorward of its 850 mb level position. From figures 44b-c we observe further that the westerly flow has a wave like configuration at the 850 mb level (Fig. 44b) and a closed vortex at the 800 mb level (Fig. 44c). One notes from figures 40a-b that the areas of confluence lie within the mean November position of the ITCZ.

At the 700 mb level (Fig. 44d), we observe the presence of an anticyclone over Tanzania, a zone of confluence over Uganda and northern Kenya and a cyclonic centre over the south-eastern lowlands of Kenya. The anticyclone over Tanzania is a persistent feature and its outflow converges into the cyclonic vortex in southern Kenya. The streamline patterns at the 600 mb and the 500 mb levels (Figs. 44e-f) show some cyclonic vortices

in western Tanzania. An asymptote of convergence runs in a NE to SW direction across Kenya into the vortices in western Tanzania. At the 400 mb level (Fig. 44g), the air flow is largely anticyclonic in the region. The observed configuration of low level inflows and upper level outflows is conducive to enhanced weather activities as was observed at the time.

The divergence and vertical motion fields for the wind anomaly fields of November 1961 are presented in figures 45a-i. We observe areas of deep convergence in the region. These areas with deep layers of convergent air current coincide with those parts of East Africa which experienced the highest above normal rainfall. The computed vertical motion field (Figs. 46a-e) is found to be upward in the layer 850-400 mb over the region with highest positive rainfall anomalies. The maximum value of vertical motion is about $5 \times 10^{-2} \text{ ms}^{-1}$.

In northeastern Kenya we observe that the spatial variation of rainfall anomalies is not easily explained by the spatial variation of the divergence/convergence field. Here, divergence is present at most levels (Figs. 45a-f). This contradicts with the observed large amounts of positive rainfall anomalies (Fig. 45a). The reasons for the discrepancy could be in the fact that the wind data used were particularly inadequate in the area. A number of pibal stations (Garissa, Malindi, Mandera) had no observations because of the prevailing out of normal wet conditions. The streamline and isotach analyses of the anomalous wind vectors over northeast Kenya should therefore be taken with considerable caution.

A vertical cross-section along the equator (Fig. 45h) shows that the zone of convergence over the Kenya highlands is deep and extends to the middle troposphere. The magnitude of convergence is about $1.5 \times 10^{-5} \text{ s}^{-1}$. Similar magnitudes were found in the mean wind field during the short rains season (Figs. 38b, 40b). The vertical motions for the disturbances are generally higher than those associated with the mean wind flow. The value of upto $5 \times 10^{-2} \text{ s}^{-1}$ (Fig. 46d) observed over the lake region and Kenya highlands is about twice as much as that observed in the neighbourhood of the ITCZ during the month of October. Figures 45g and 46e give a y-z cross-section of divergence and vertical motion respectively along longitude 36°E . We observe from these cross-sections that the zone of convergence has an equatorward tilt with height. The maximum convergence in this zone is located over the Kenya highlands.

3.2.3 Weather Disturbances during December 1961-January 1962

The streamlines of the flow associated with the disturbances that prevailed in December 1961 and January 1962 are shown in figures 47-48. The dominant feature in this flow is the westerly wind anomaly in the lower troposphere. During these two months, and especially in December, this westerly flow is very intense, having speeds of upto 11 ms^{-1} across central Tanzania (Figs. 47a-c). It is evident that the westerly flow is part of a cyclonic circulation around an extensive

cyclonic disturbance that is located over southeast Tanzania/northern Mozambique. The axis of the disturbance appears to tilt equatorward as well as northeastwards with height. We observe further that the cyclonic vortices observed over southeastern Tanzania at 800 mb, 700mb, 600 mb (Figs. 47b-d) in December, and at 700 mb (Fig. 48c) in January form part of the large cyclonic circulation over southern Africa. Also, these cyclonic disturbances are found to be capped at the 400 mb level by an anticyclonic outflow that is centred over southern Tanzania.

Climatologically (Thompson 1965, Ramage and Raman 1972), the cyclonic centres associated with the southern summer ITCZ are located between 15° - 20° S over these longitudes. It is apparent from this study that during the flood period of 1961/62 the ITCZ low centres were more extensive and were located equatorward of their normal positions.

We present (Figs. 49a-b) the observed wind flow at the 700 mb level during December 1961 and January 1962. We observe that the cyclonic disturbances over the southeastern part of the area have given rise to a westerly flow which has completely replaced the normally diffluent northeast monsoon current. Although our study area only covers East Africa, comparison between figures 49a-b and the mean flow patterns over southern Africa (Ramage and Raman 1972), reveals that the westerlies over Tanzania must have linked up with the Congo westerlies giving an extensive zone of westerlies covering Africa south of the equator. The presence of the westerly

flow over nearly the whole of East Africa on the mean charts of December 1961 and January 1962 manifest the persistence of the cyclonic disturbances over the area.

This is a very good example of westerly winds (incursions) over East Africa (Thompson 1957a, Nakamura 1968). In this case, the westerly flow is part of a cyclonic circulation around a large disturbance in southern Tanzania/northern Mozambique. The westerly current consists of two different air currents : one portion emanates from the Congo (Zaire)/SE Atlantic area and the other is recurved northeasterly current over northeast Tanzania/southern Kenya.

The divergence and vertical motion fields associated with the disturbances in January 1962 are given in figures 50a-f and 51a-c. Dominant in these figures is a zone running from northwestern Tanzania into southeastern Tanzania, with a deep layer of convergent air current (Figs. 50a-f). The ensuing vertical motion (Figs. 51a-c) is upward in the lower troposphere. The rainfall anomalies map (Fig. 52b) shows that values higher than +100 mm were recorded in this zone in January 1962. Some parts of southern Tanzania lie in a divergent air current and the resulting vertical motion is downward (Figs. 51a-c). The observed negative rainfall anomalies are in agreement with the observed divergence field. Over the Kenya highlands, the lake Victoria region and Uganda, we observe that the fields of divergence and vertical motion are now different from those observed during the month of

severe floods (November 1961). Generally, the weather conditions over Kenya and Uganda were near normal in January 1962.



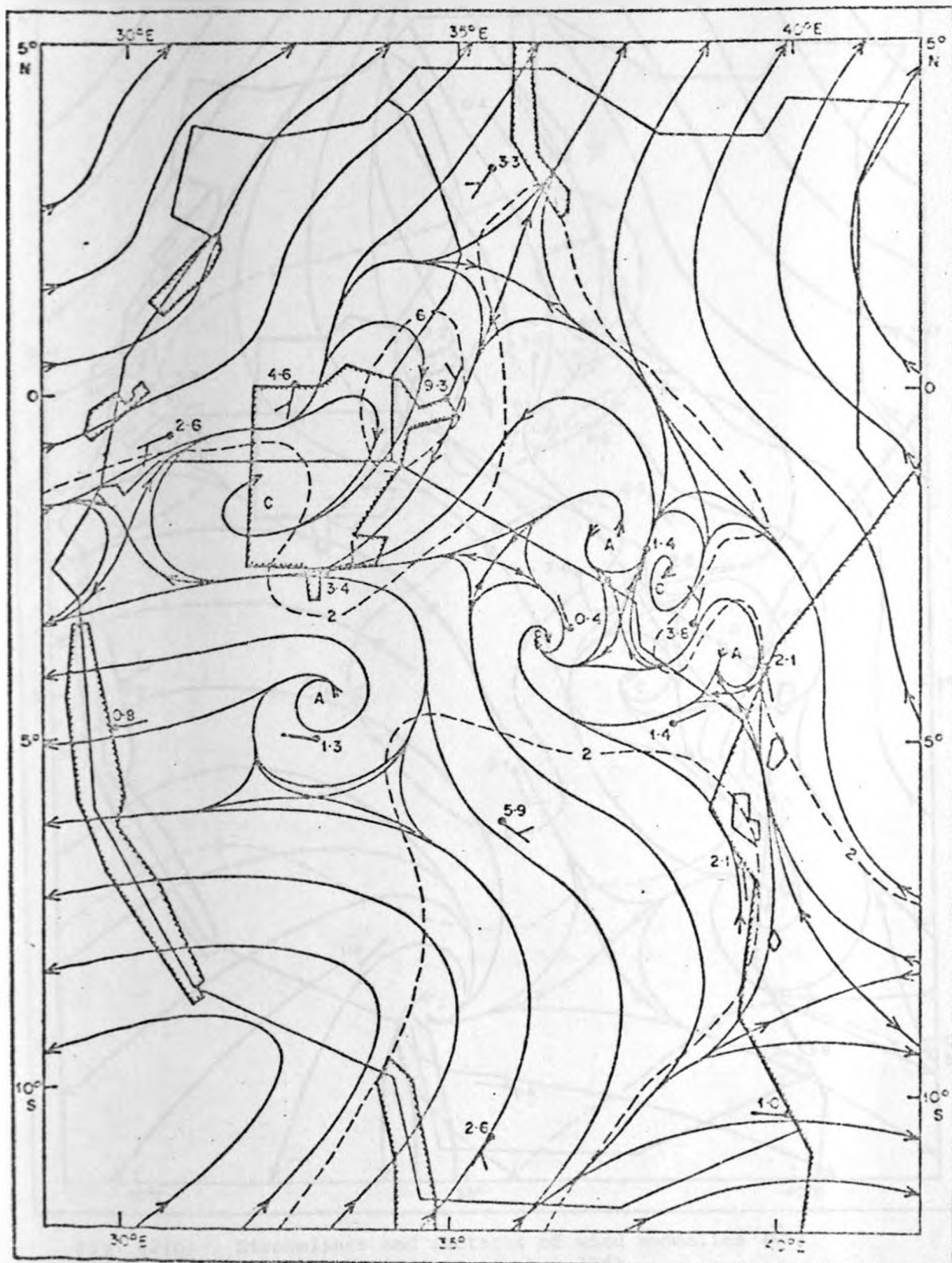


Fig. 42(a) : Streamlines and isotachs of wind anomalies (\bar{V}') at 1525 m AMSL in September 1961.

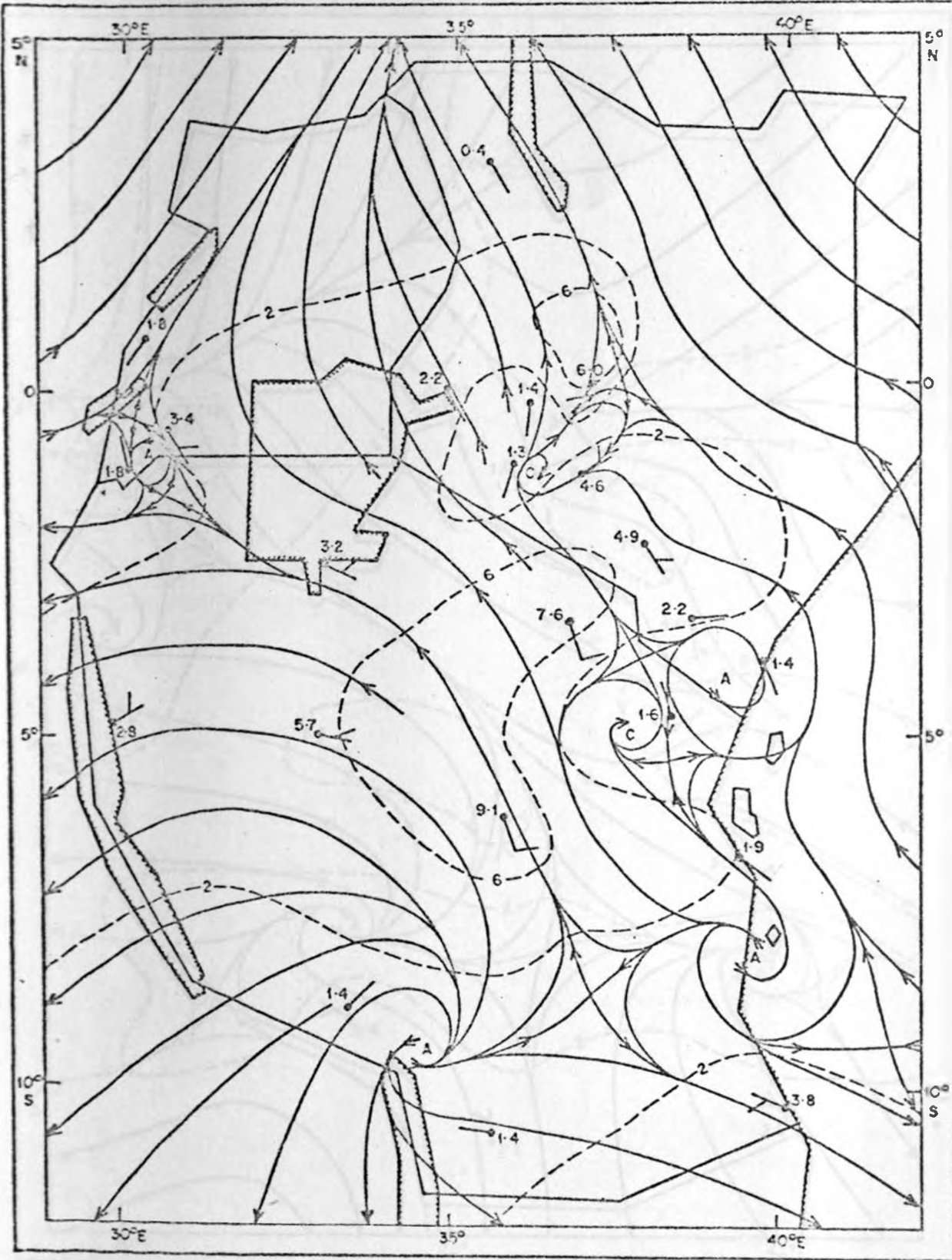


Fig. 42(b) : Streamlines and isotachs of wind anomalies (\vec{V}') at 2440 m AMSL in September 1961.

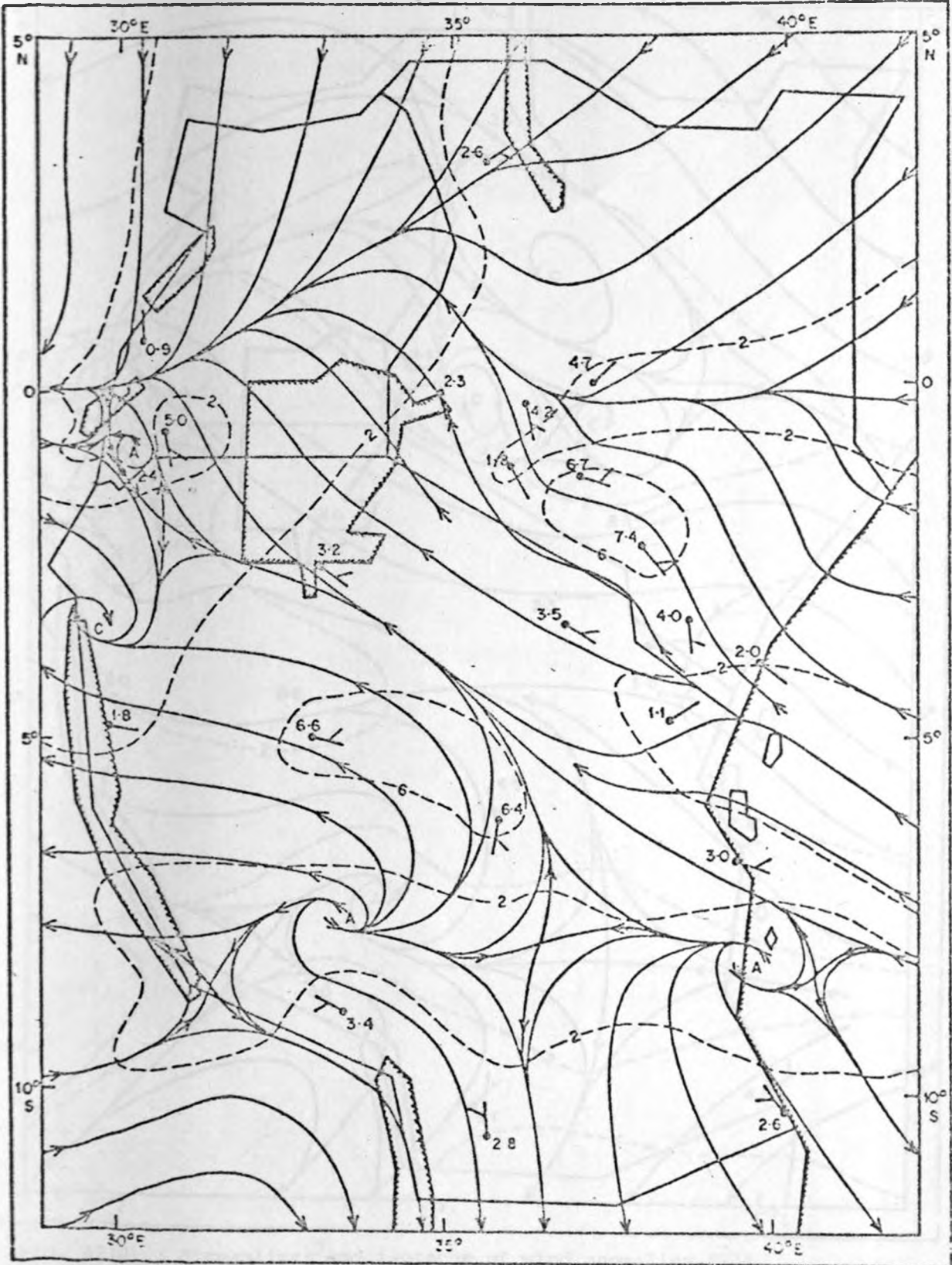


Fig. 42(c) : Streamlines and isotachs of wind anomalies (\vec{V}') at 3050 m AMSL in September 1961.

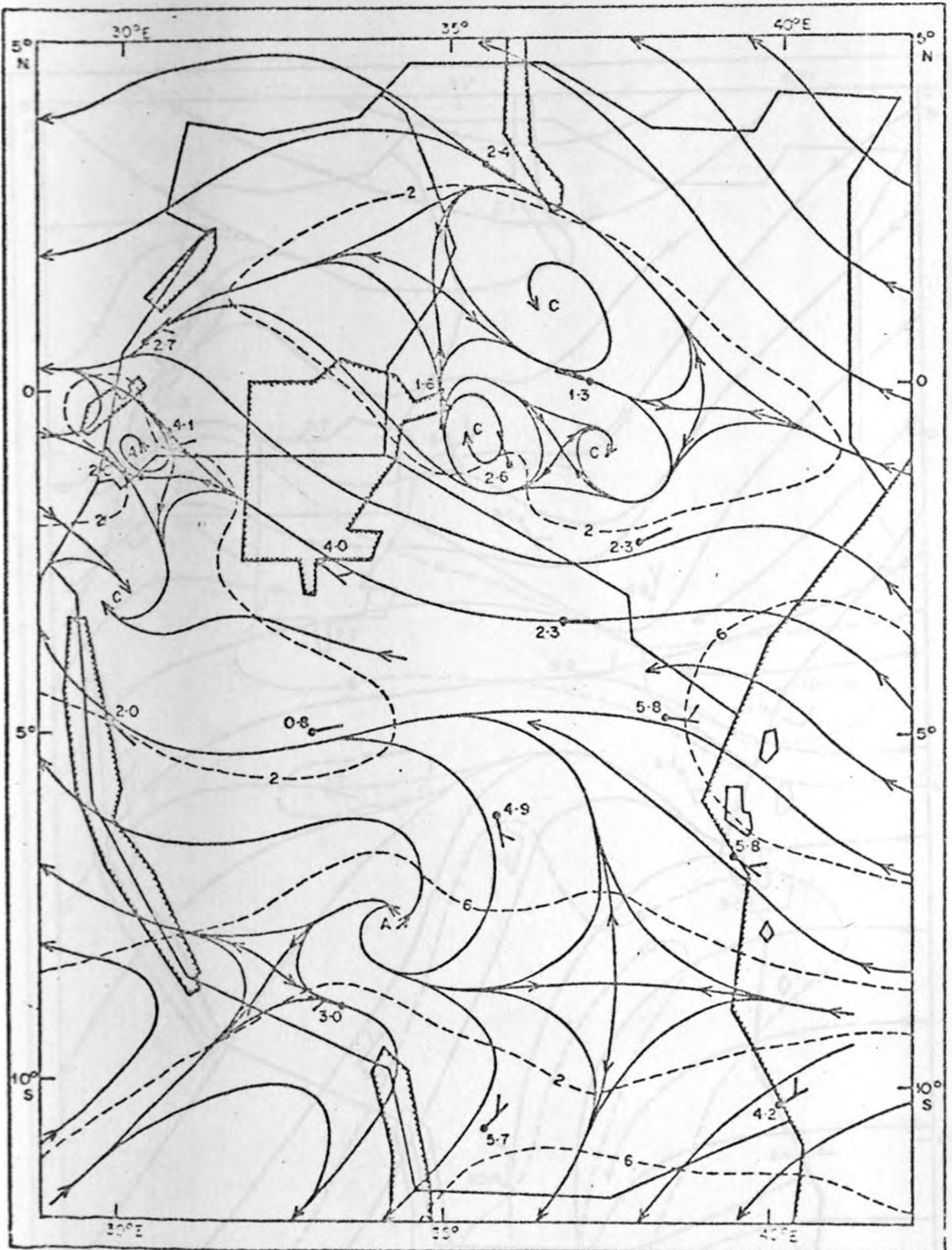


Fig. 42(d) : Streamlines and isotachs of wind anomalies (\bar{V}')
at 4270 m AMSL in September 1961.

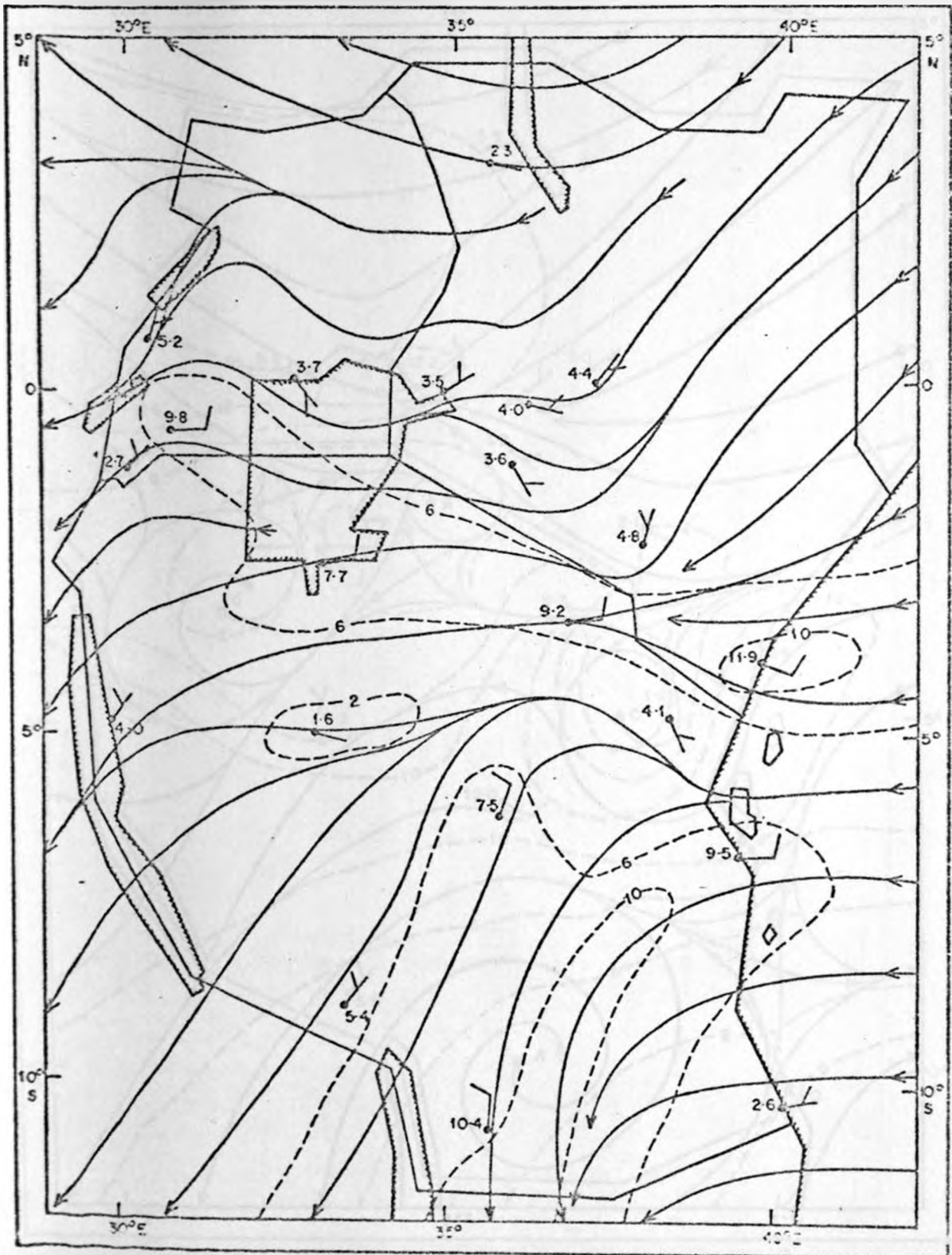


Fig. 42(e) : Streamlines and isotachs of wind anomalies (\vec{V}') at 5490 m AMSL in September 1961.

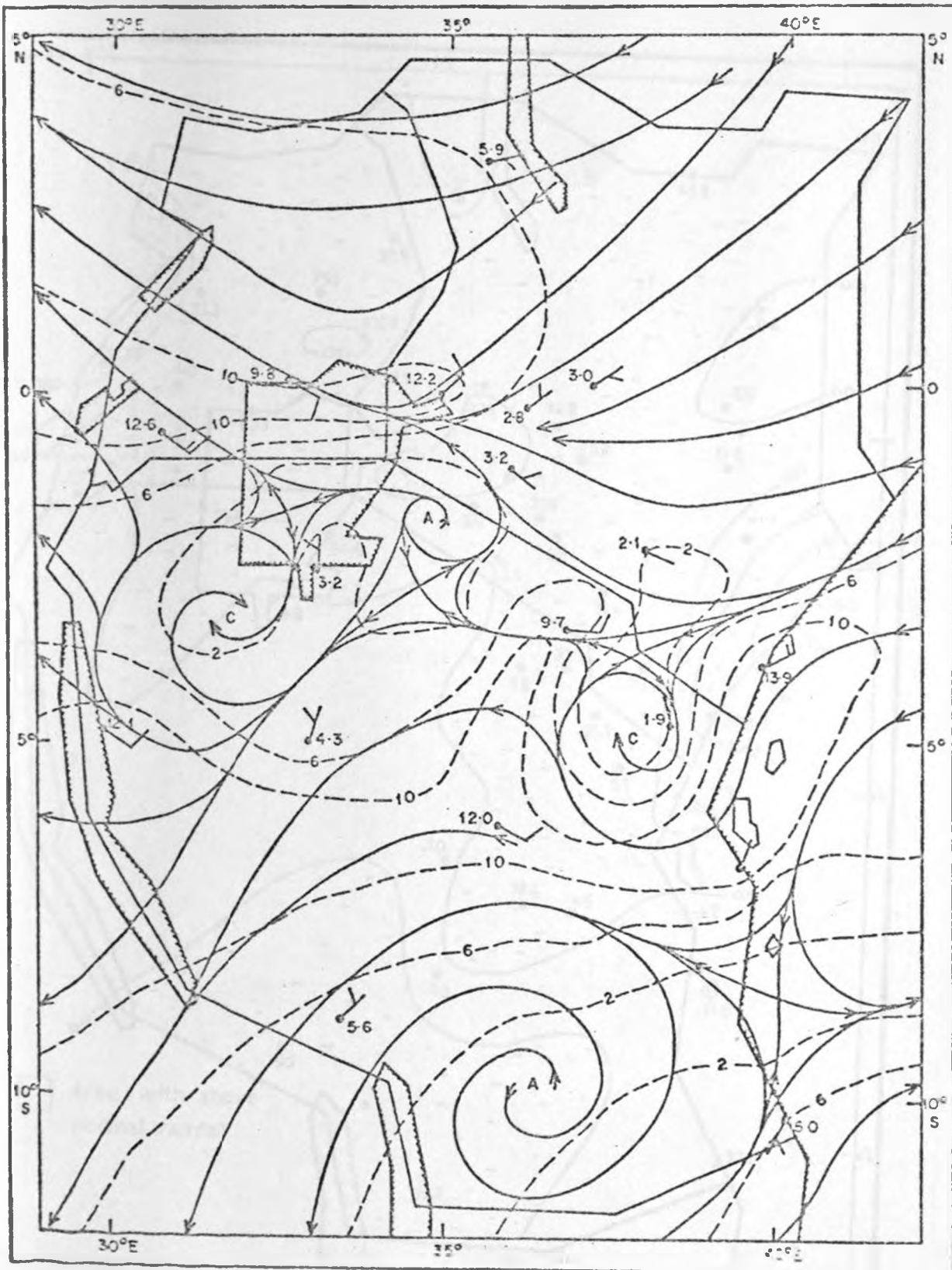


Fig. 42(f) : Streamlines and isotachs of wind anomalies (\vec{V}') at 7320 m AMSL in September 1961.

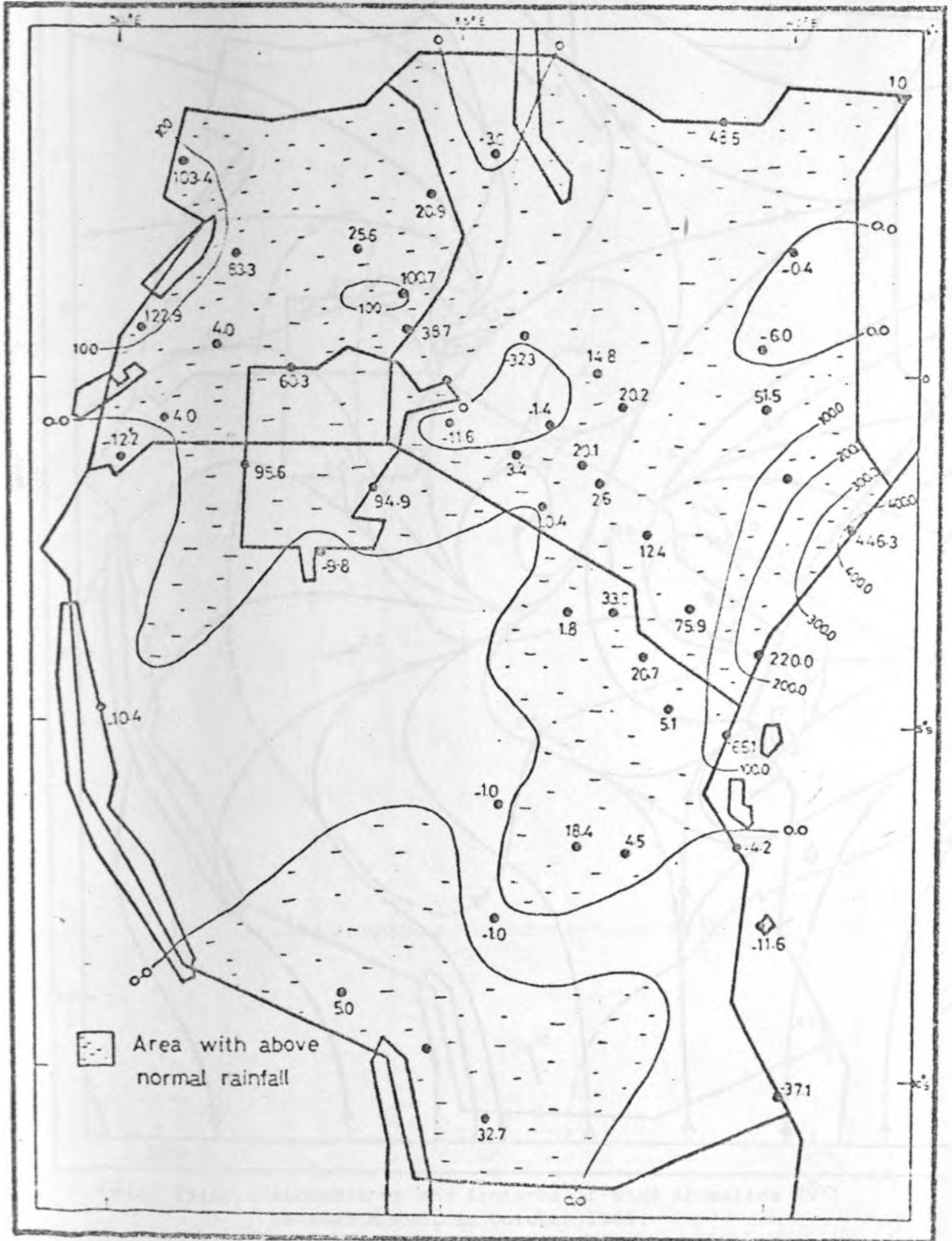


Fig. 42(g) : Rainfall anomalies (mm) for September 1961.

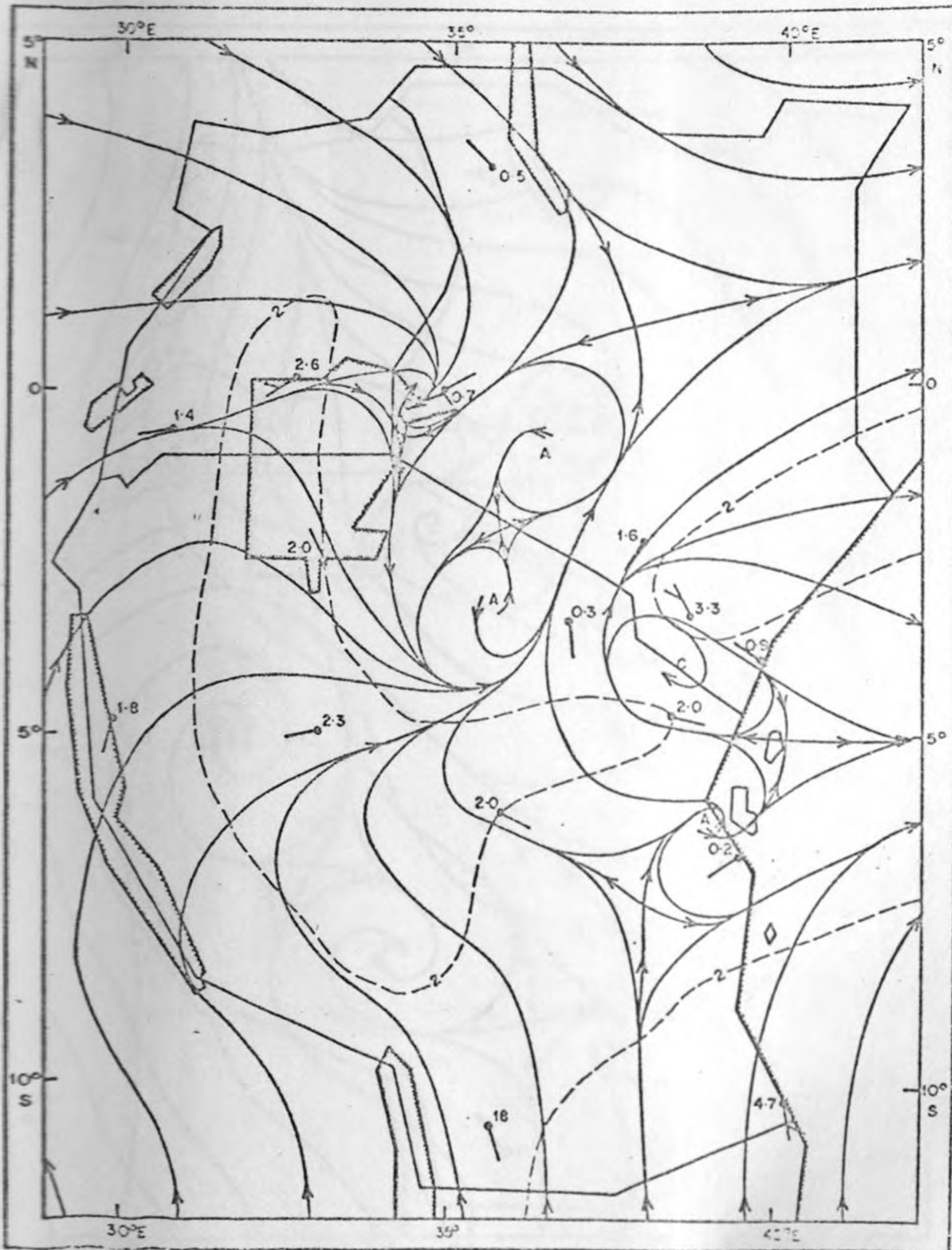


Fig. 43(a) : Streamlines and isotachs of wind anomalies (\vec{V}') at 1525 m AMSL in October 1961.

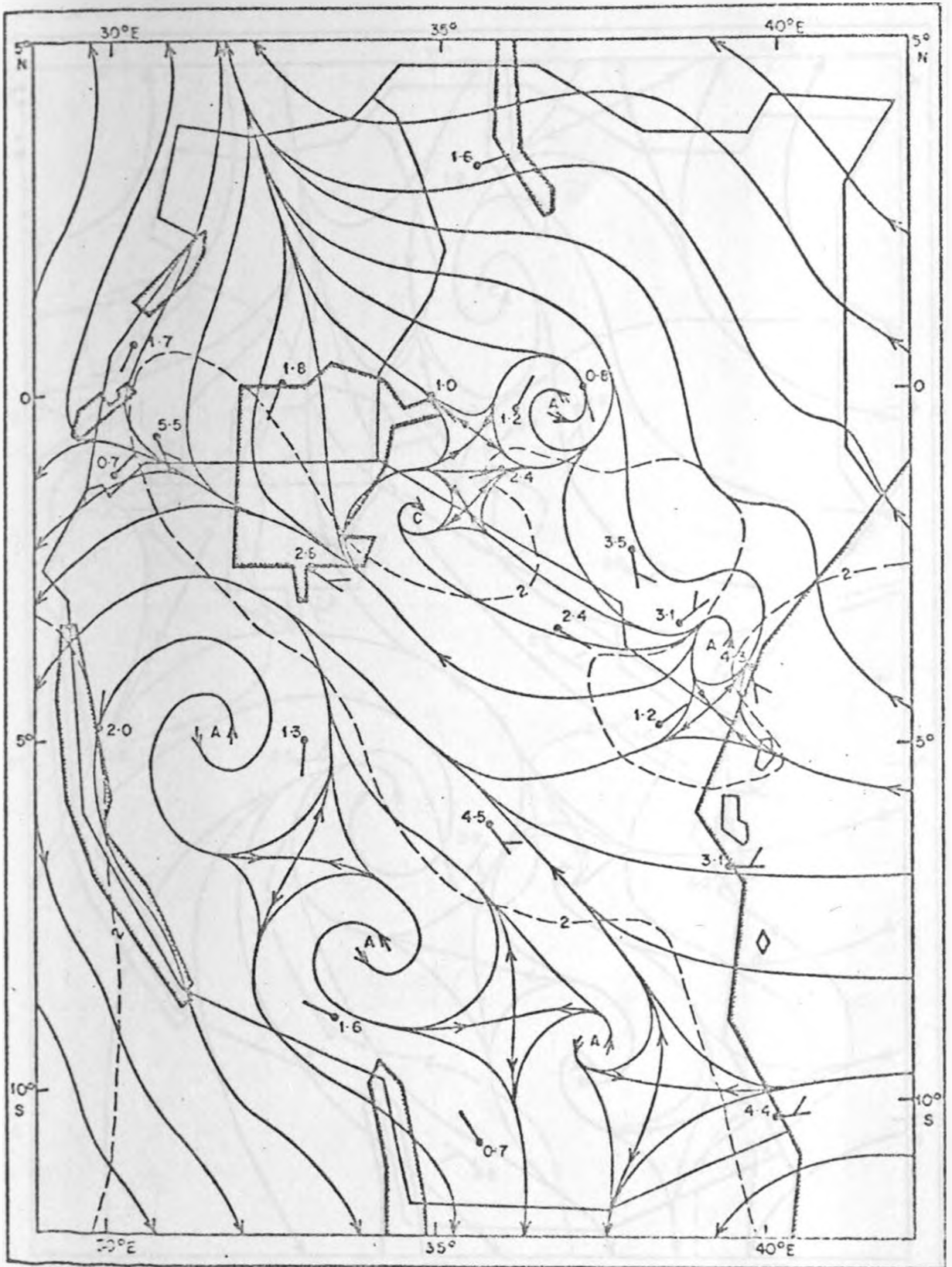


Fig. 43(b) : Streamlines and isotachs of wind anomalies (\vec{V}') at 2440 m AMSL in October 1961.



Fig. 43(c) : Streamlines and isotachs of wind anomalies (\vec{V}') at 3050 m AMSL in October 1961.

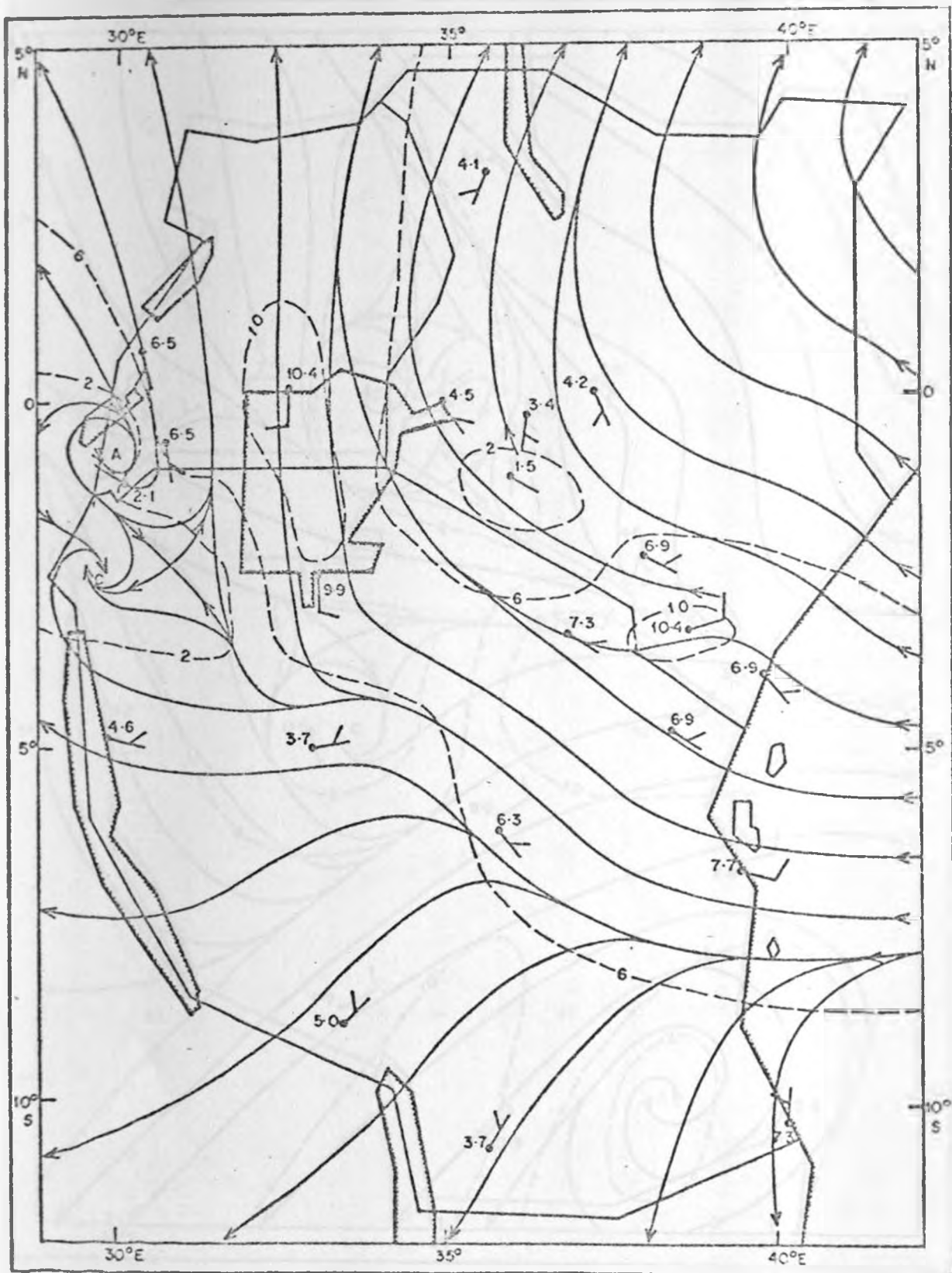


Fig. 43(d) : Streamlines and isotachs of wind anomalies (\vec{V}') at 4270 m AMSL in October 1961.

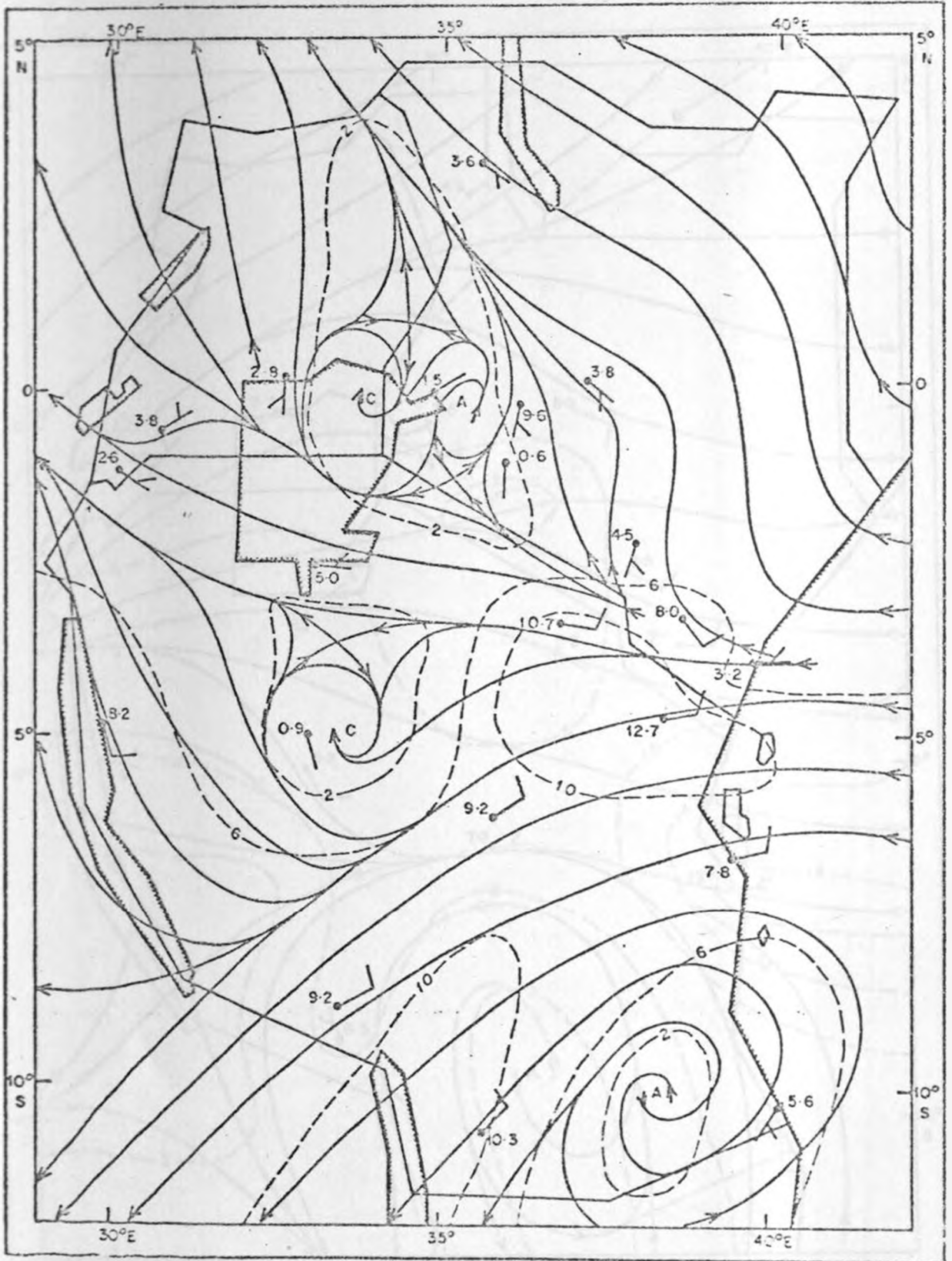


Fig. 43(e) : Streamlines and isotachs of wind anomalies (\vec{V}') at 5490 m AMSL in October 1961.

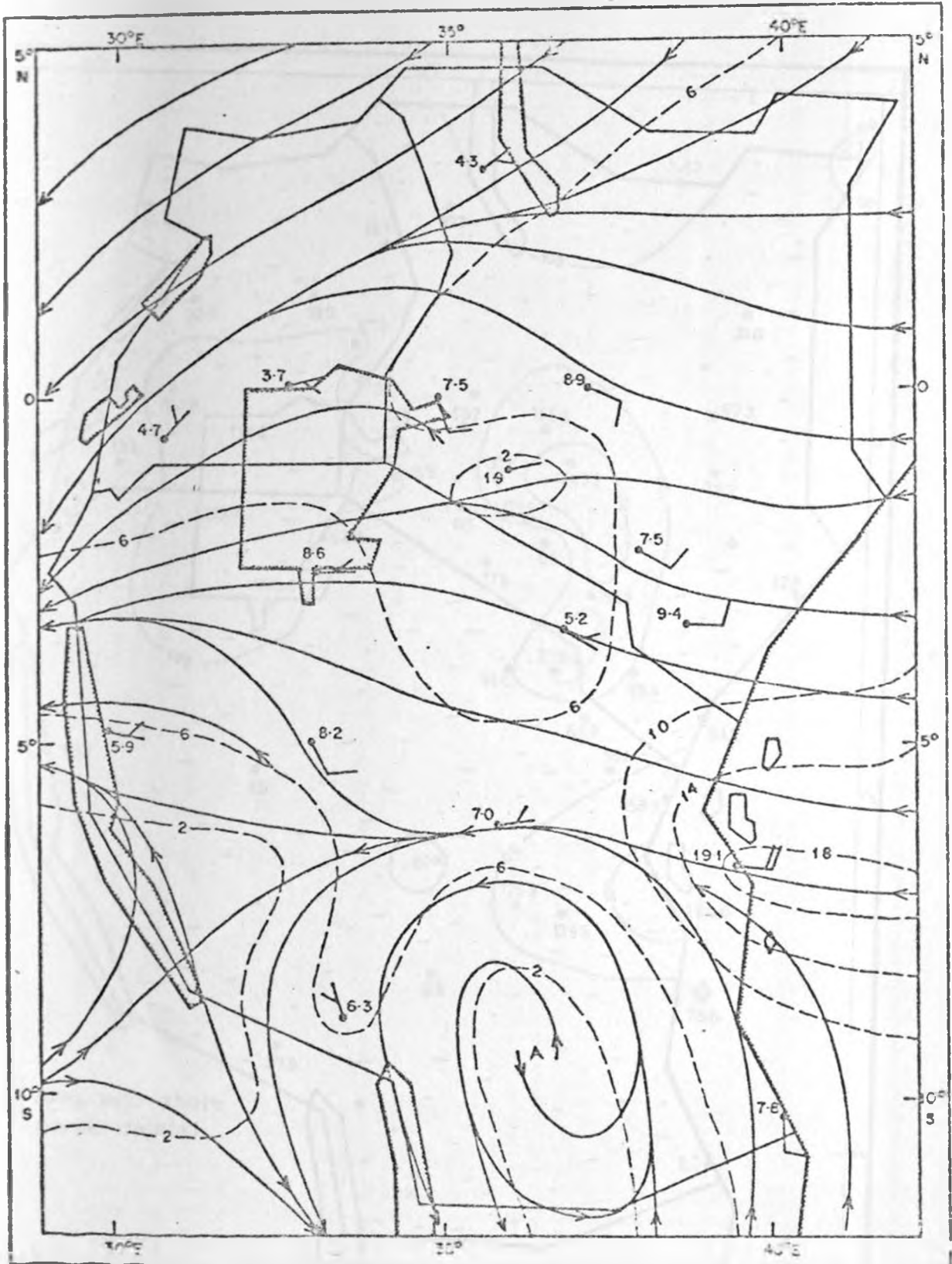


Fig. 43(f) : Streamlines and isotachs of wind anomalies (\bar{V}') at 7320 m AMSL in October 1961.

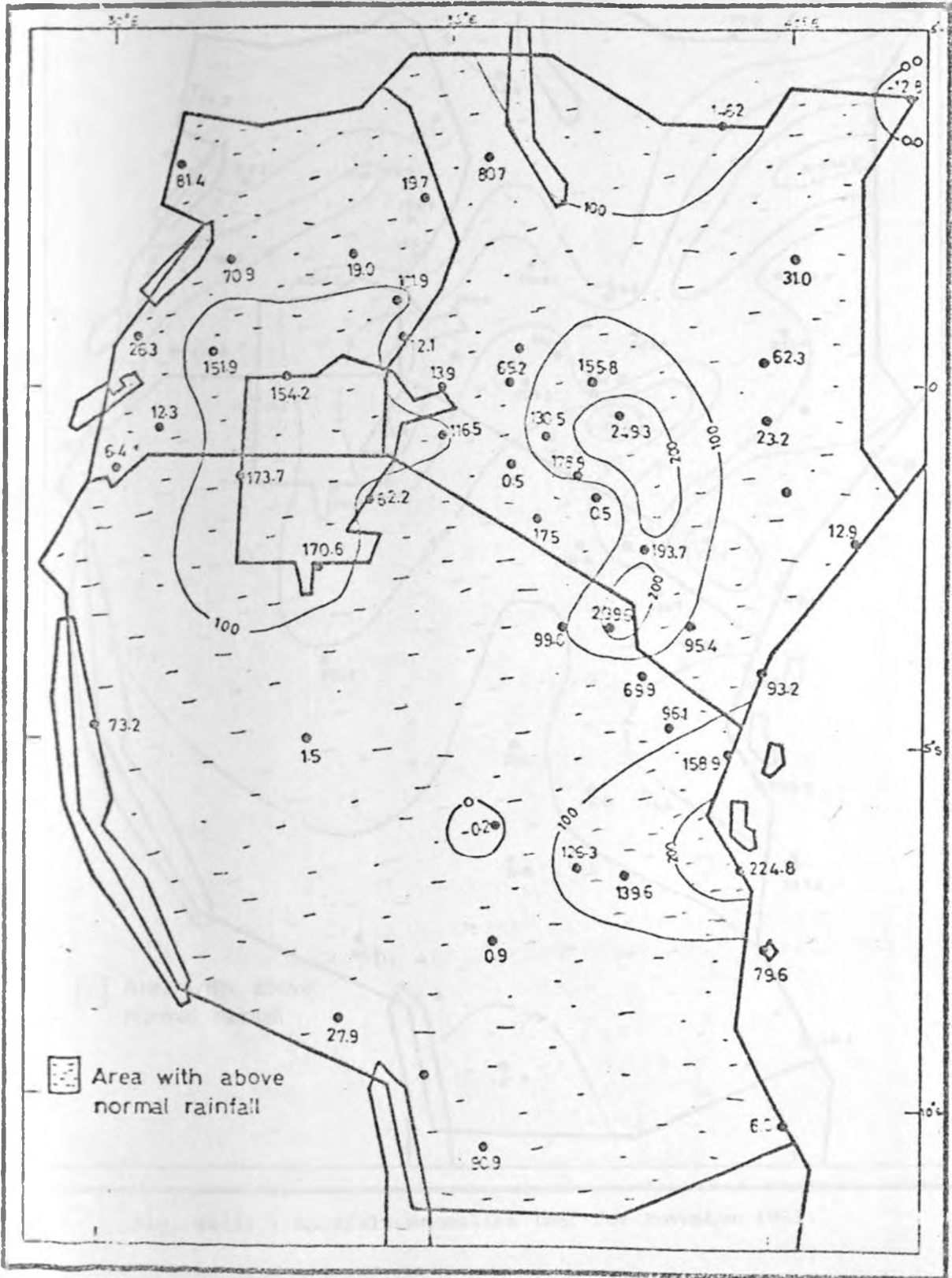


Fig.. 43(g) : Rainfall anomalies (mm) for October 1961.

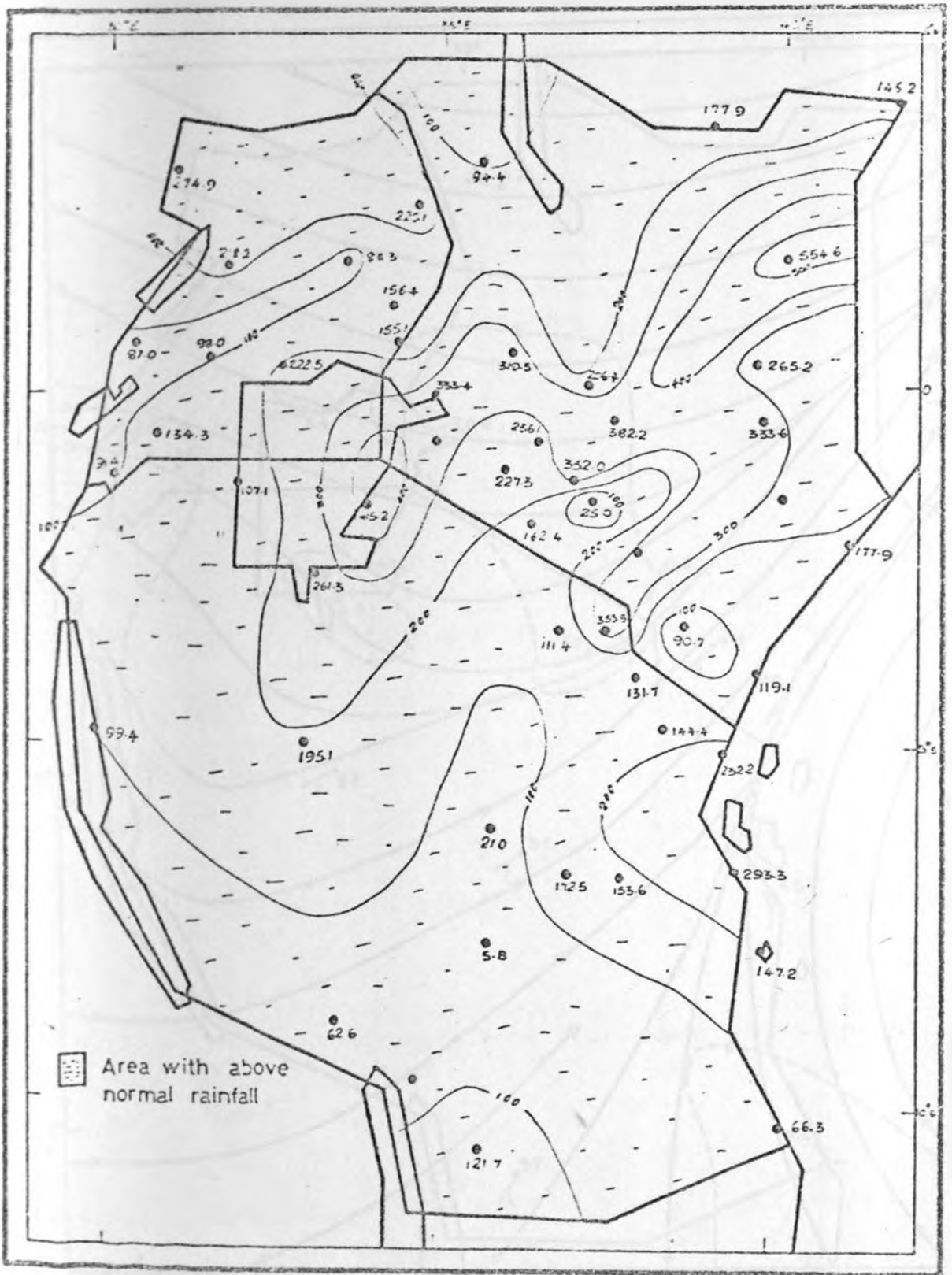


Fig. 44(a) : Rainfall anomalies (mm) for November 1961.

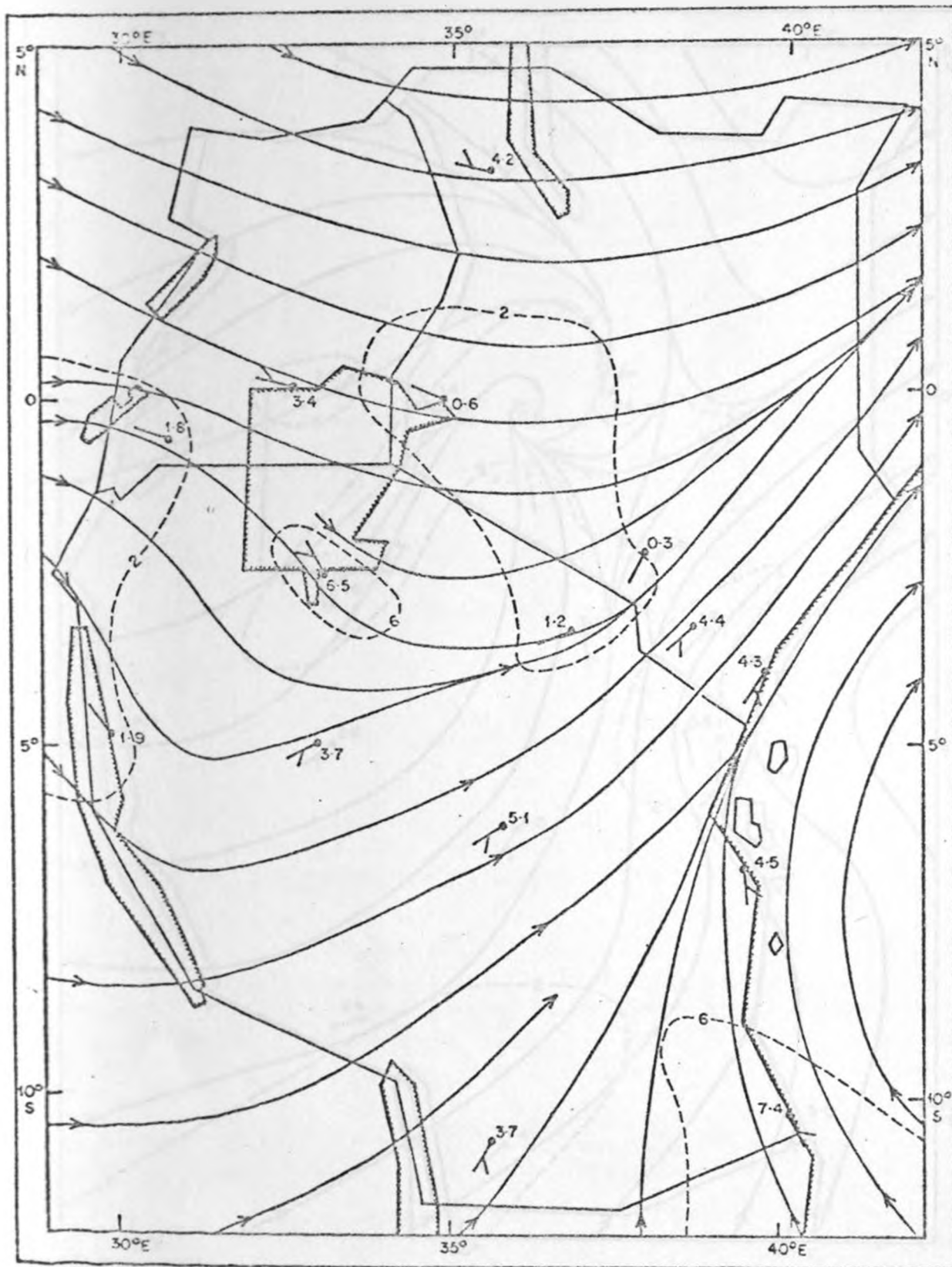


Fig. 44(b) : Streamlines and isotachs of wind anomalies (\vec{V}') at 1525 m AMSL in November 1961.

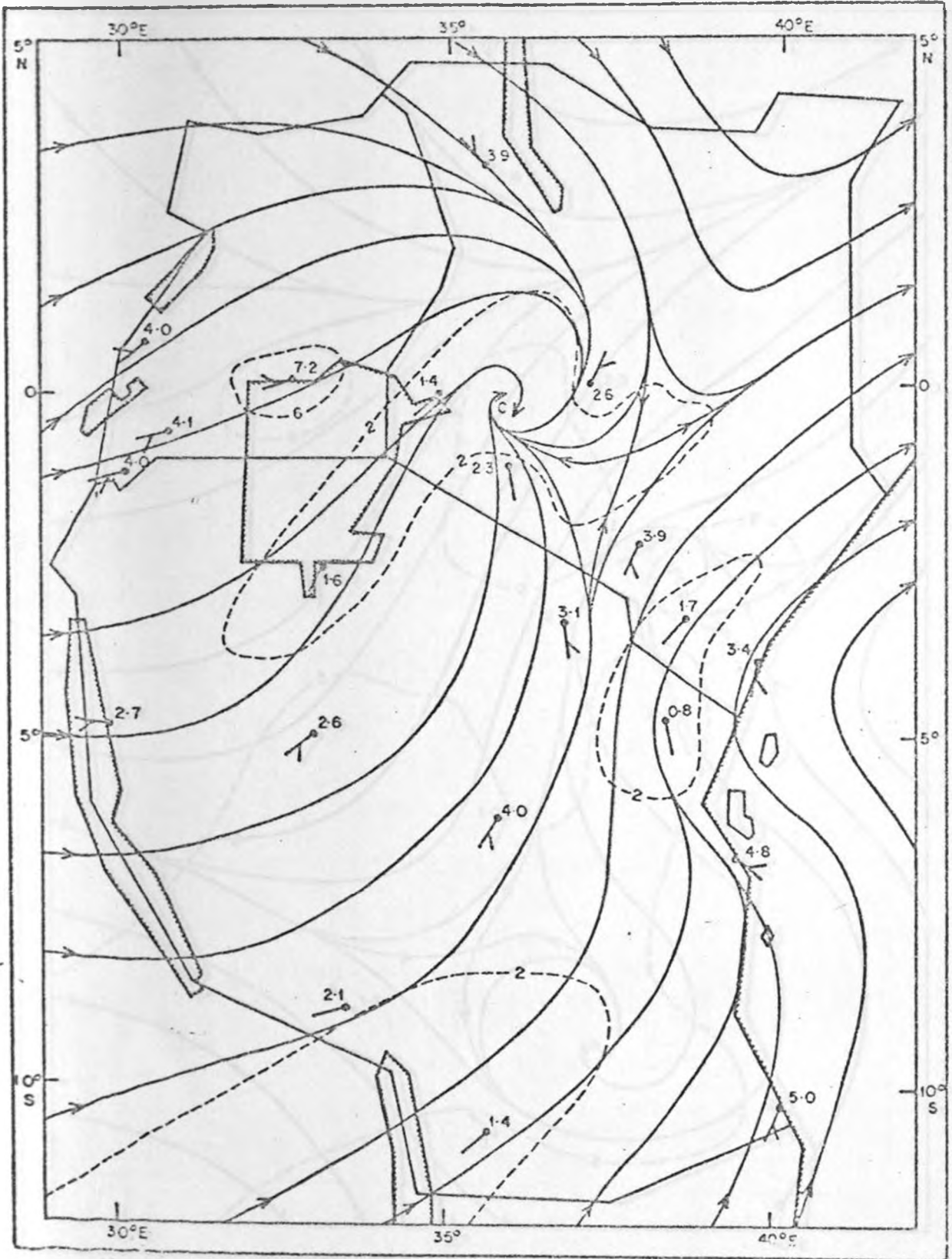


Fig. 44(c) : Streamlines and isotachs of wind anomalies (\vec{V}') at 2440 m AMSL in November 1961.

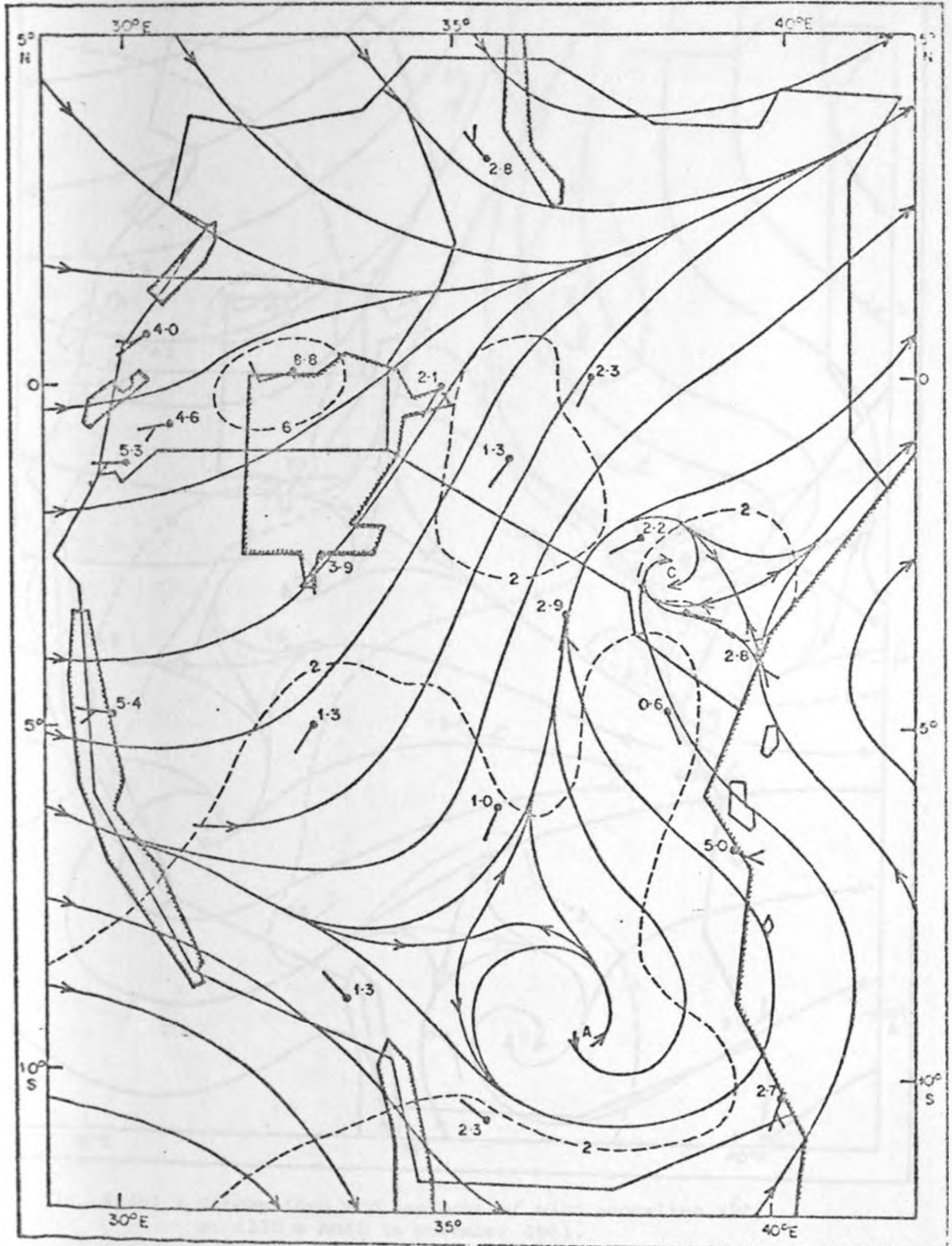


Fig. 44(d) : Streamlines and isotachs of wind anomalies (\bar{V}') at 3050 m AMSL in November 1961.

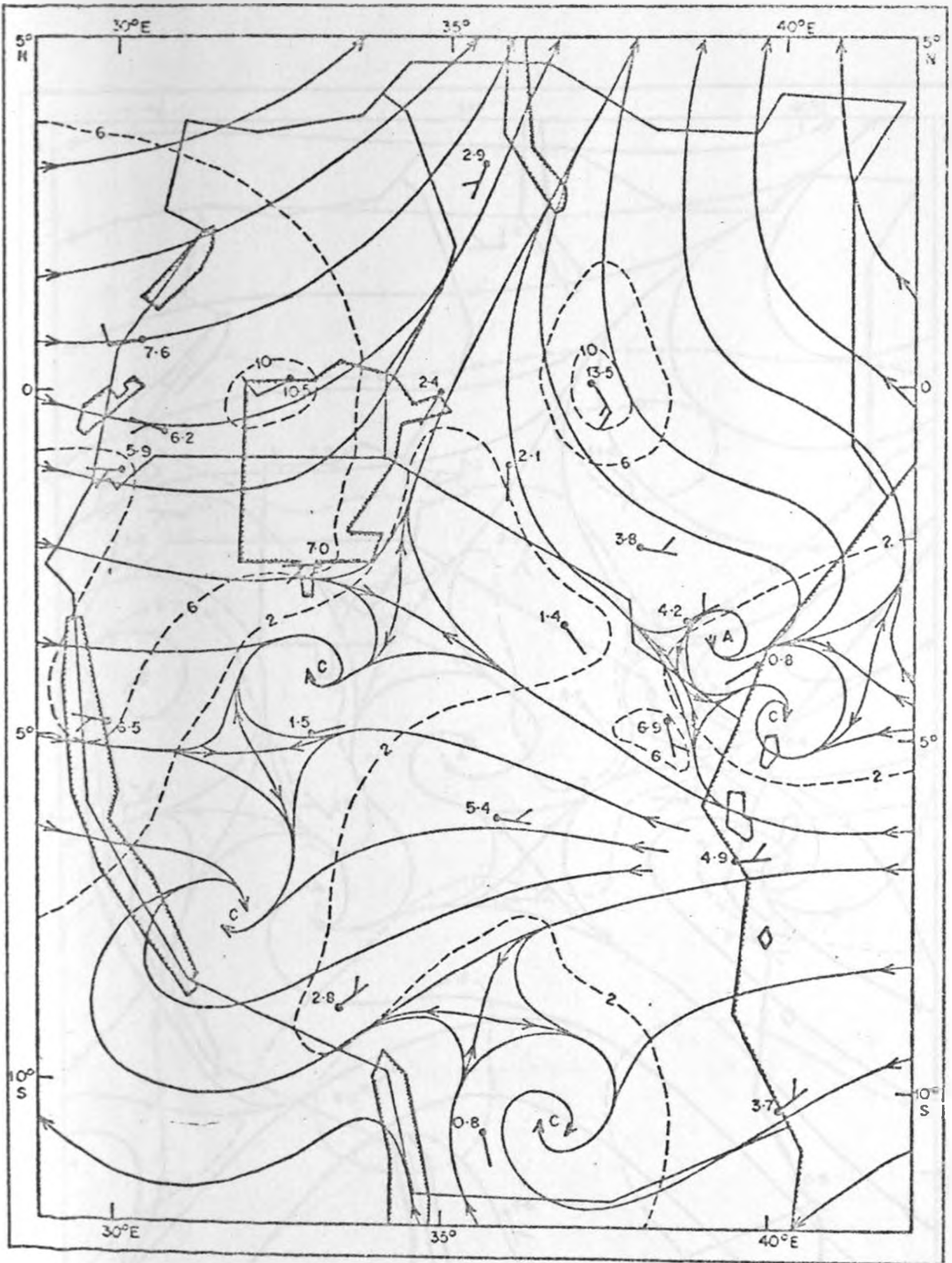


Fig. 44(e) : Streamlines and isotachs of wind anomalies (\vec{V}') at 4270 m AMSL in November 1961.

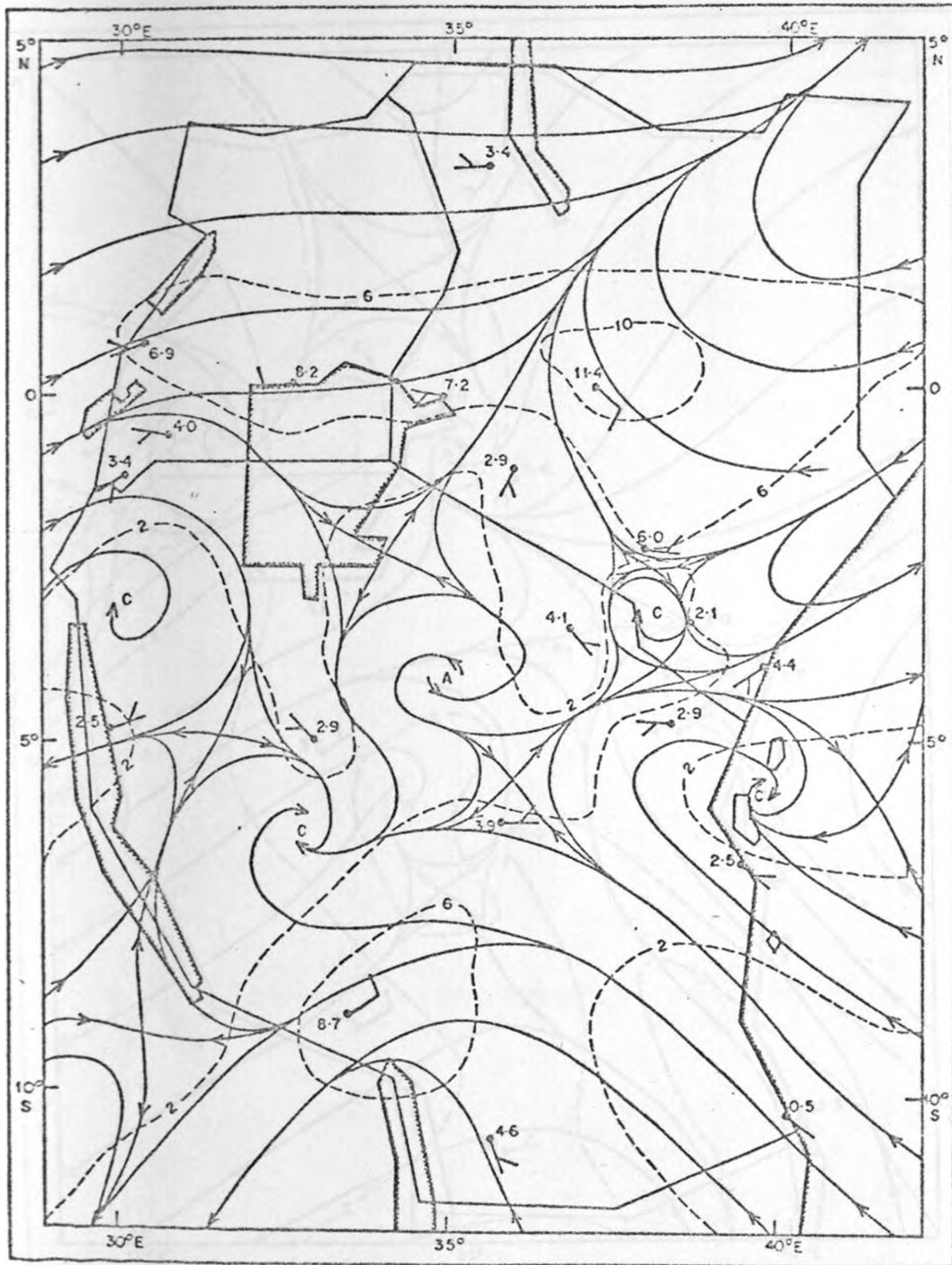


Fig. 44(f) : Streamlines and isotachs of wind anomalies (\vec{V}') at 5490 m AMSL in November 1961.

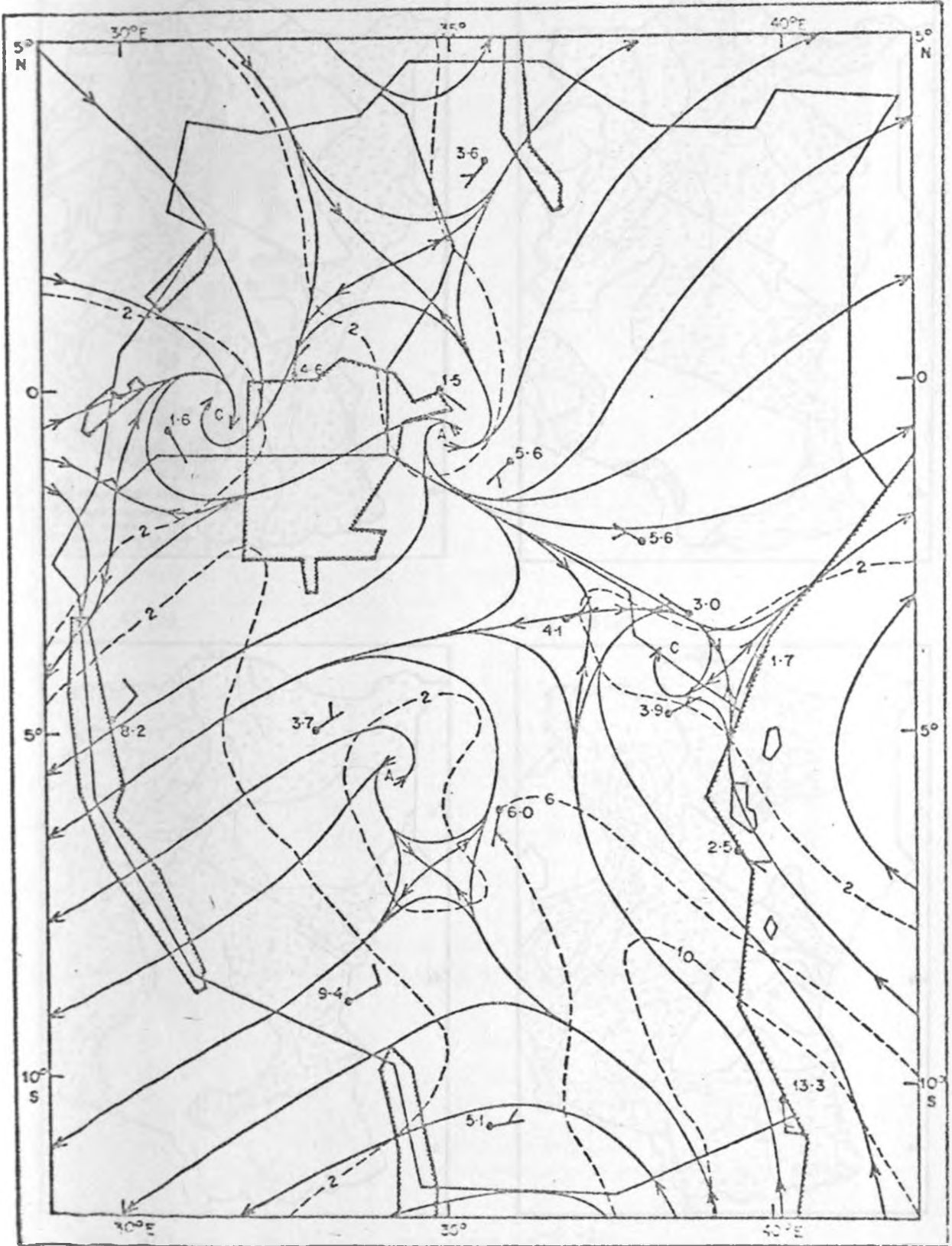


Fig. 44(g) : Streamlines and isotachs of wind anomalies (V') at 7320 m AMSL in November 1961.

Fig. 45(a)

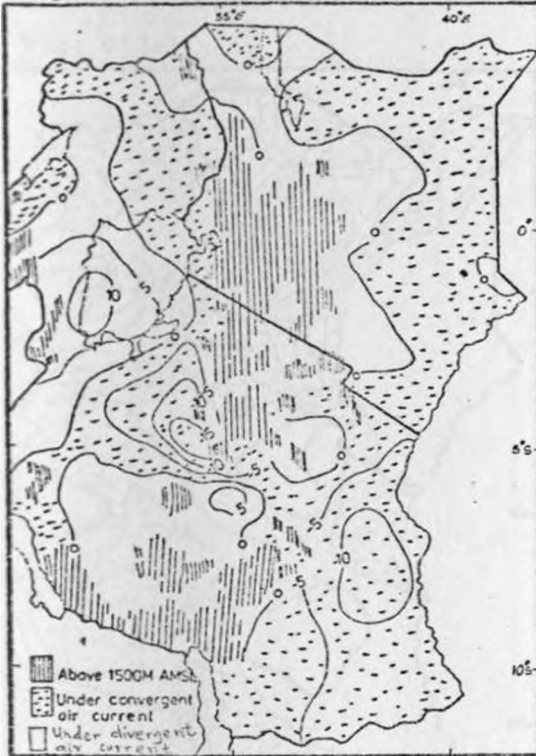


Fig. 45(b)

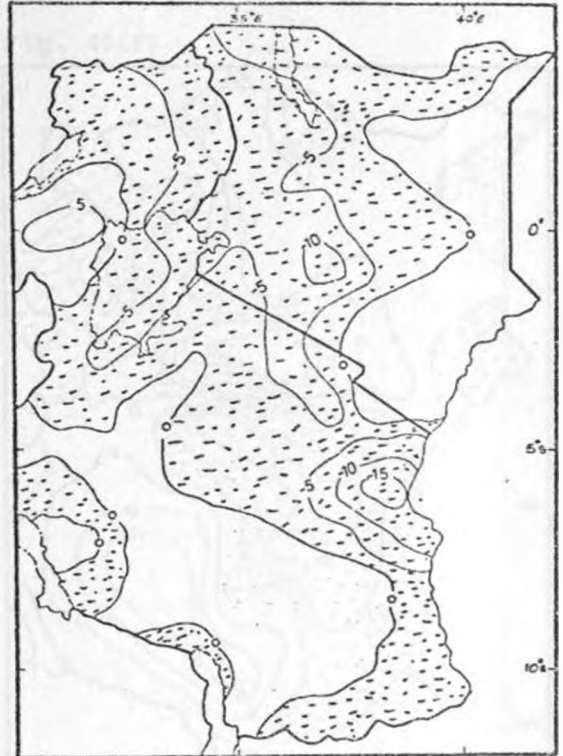


Fig. 45(c)

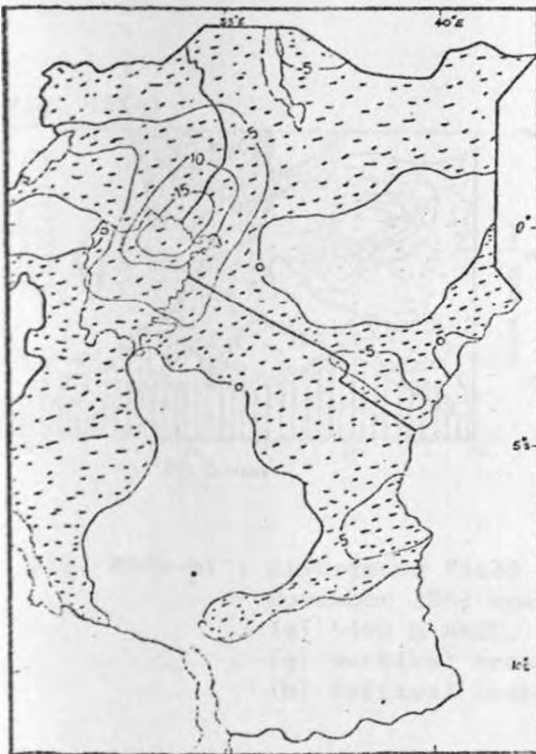


Fig. 45(d)

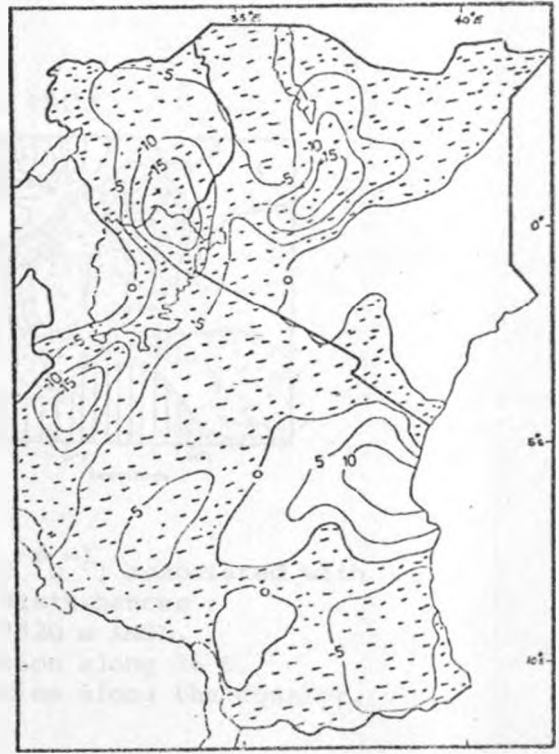


Fig. 45(a-d) : Divergence field ($D' \times 10^{-6} s^{-1}$) associated with November 1961 weather disturbances :
 (a) 1525 m AMSL, (b) 2440 m AMSL,
 (c) 3050 m AMSL, (d) 4270 m AMSL.

Fig. 45(e)

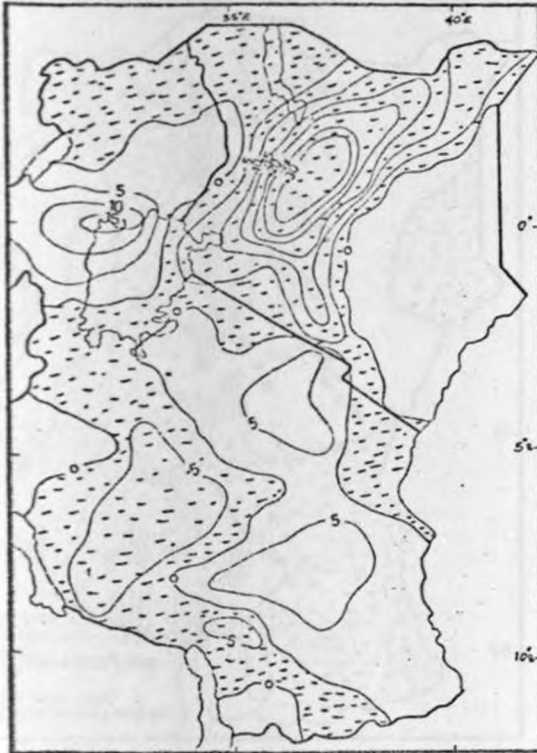


Fig. 45(f)

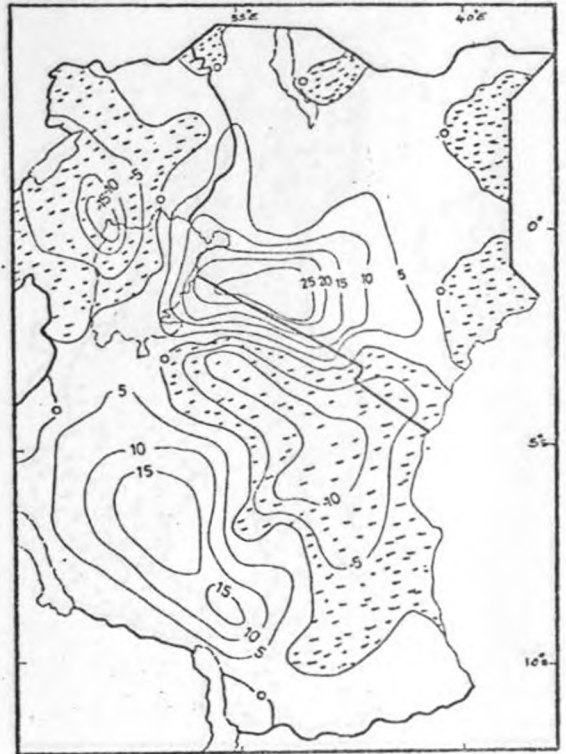


Fig. 45(g)

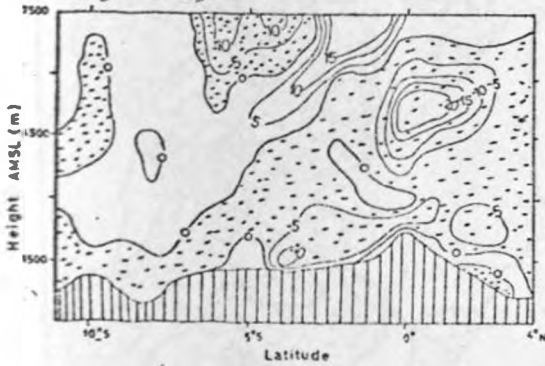


Fig. 45(h)

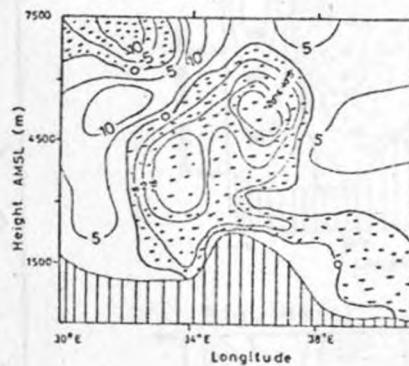


Fig. 45(e-h) : Divergence field ($D' \times 10^{-6} \text{ s}^{-1}$) associated with November 1961 weather disturbances :
 (e) 5490 m AMSL, (f) 7320 m AMSL,
 (g) vertical cross-section along 36°E ,
 (h) vertical cross-section along the equator.

Fig. 46(a)



Fig. 46(b)

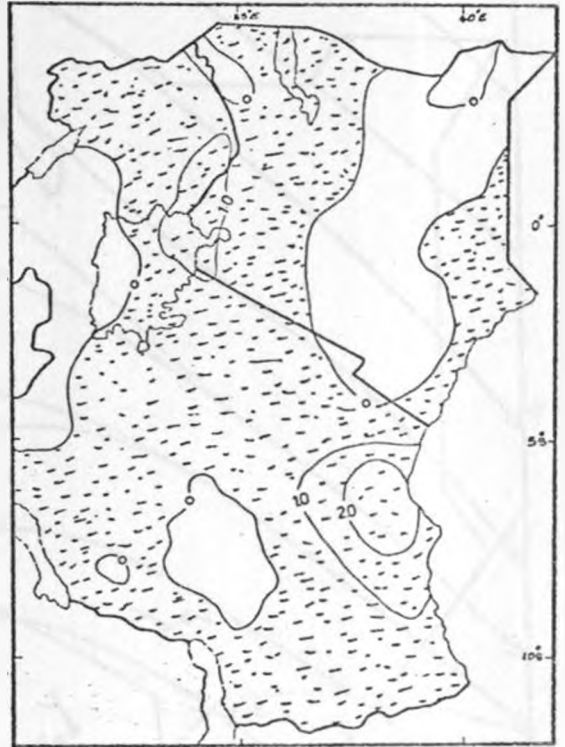


Fig. 46(c)

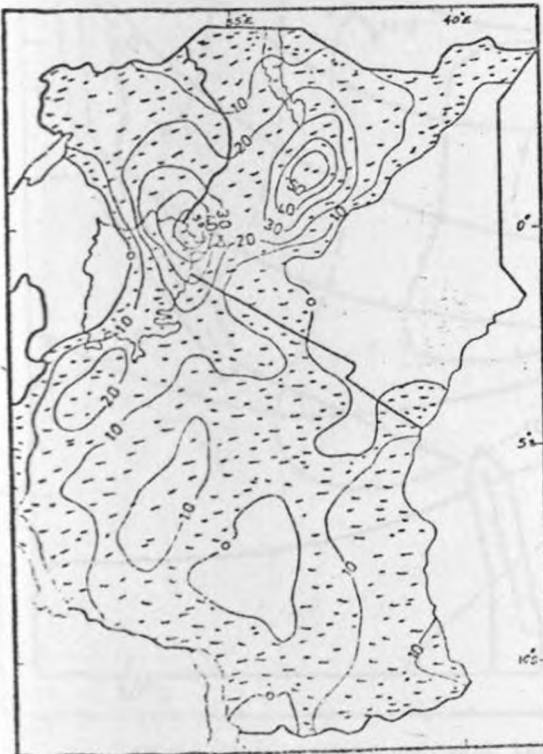


Fig. 46(d)

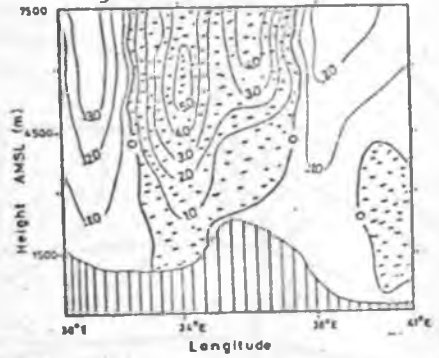


Fig. 46(e)

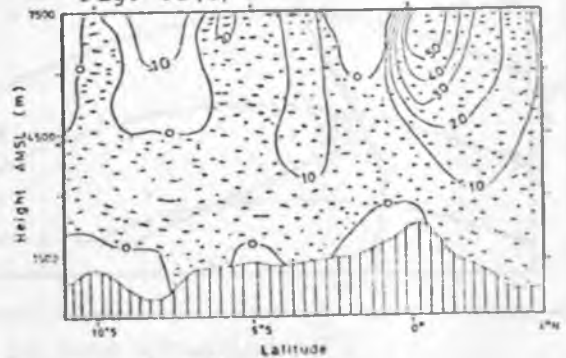


Fig. 46(a-e) : Vertical motion fields ($w \times 10^{-2} \text{ ms}^{-1}$) associated with weather disturbances in November 1961 :
 (a) 1525 m AMSL, (b) 3050 m AMSL, (c) 5490 m AMSL,
 (d) cross-section along the equator,
 (e) cross-section along 36°E .

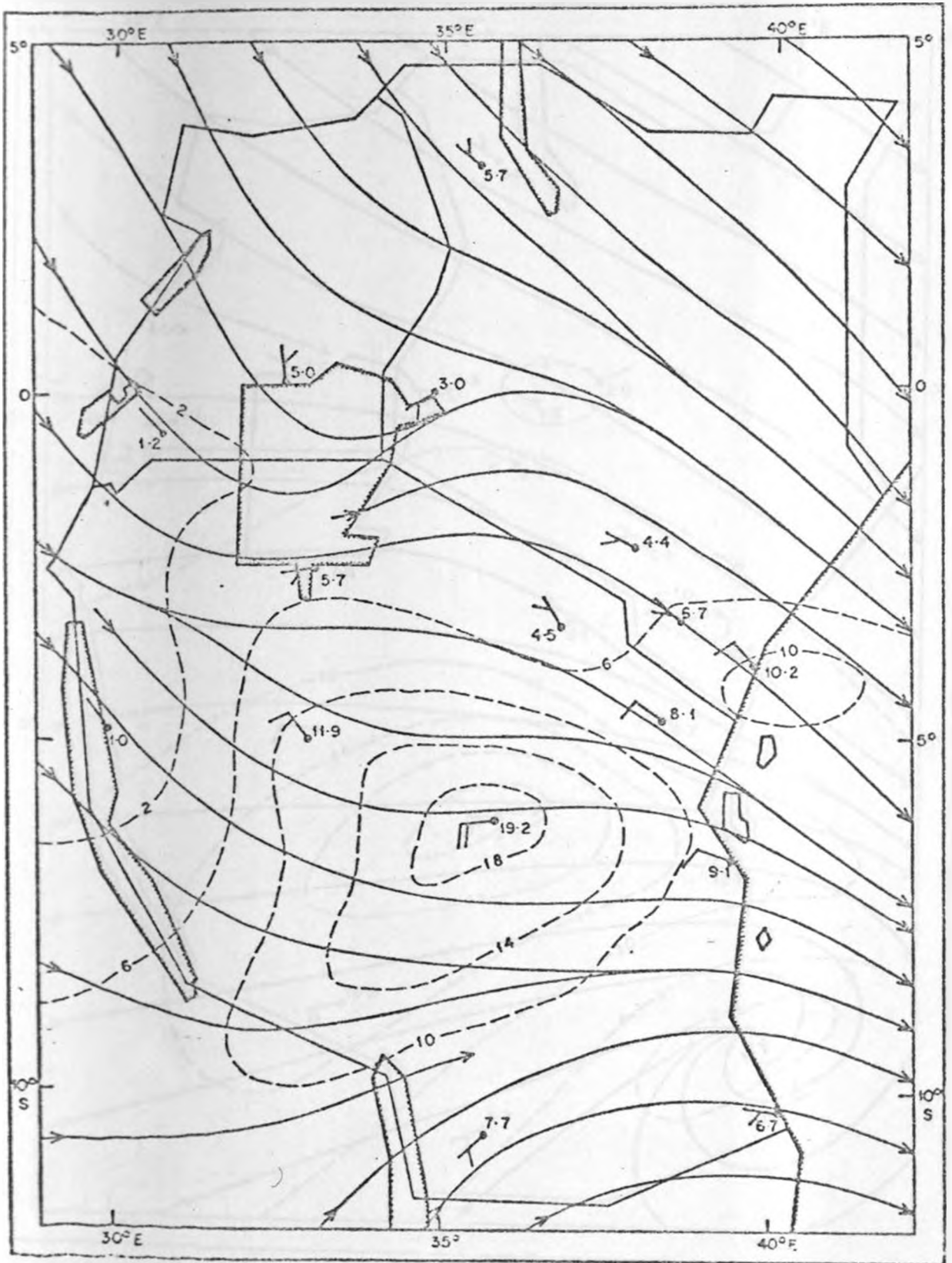


Fig. 47(a) : Streamlines and isotachs of wind anomalies (\vec{V}') at 1525 m AMSL in December 1961.

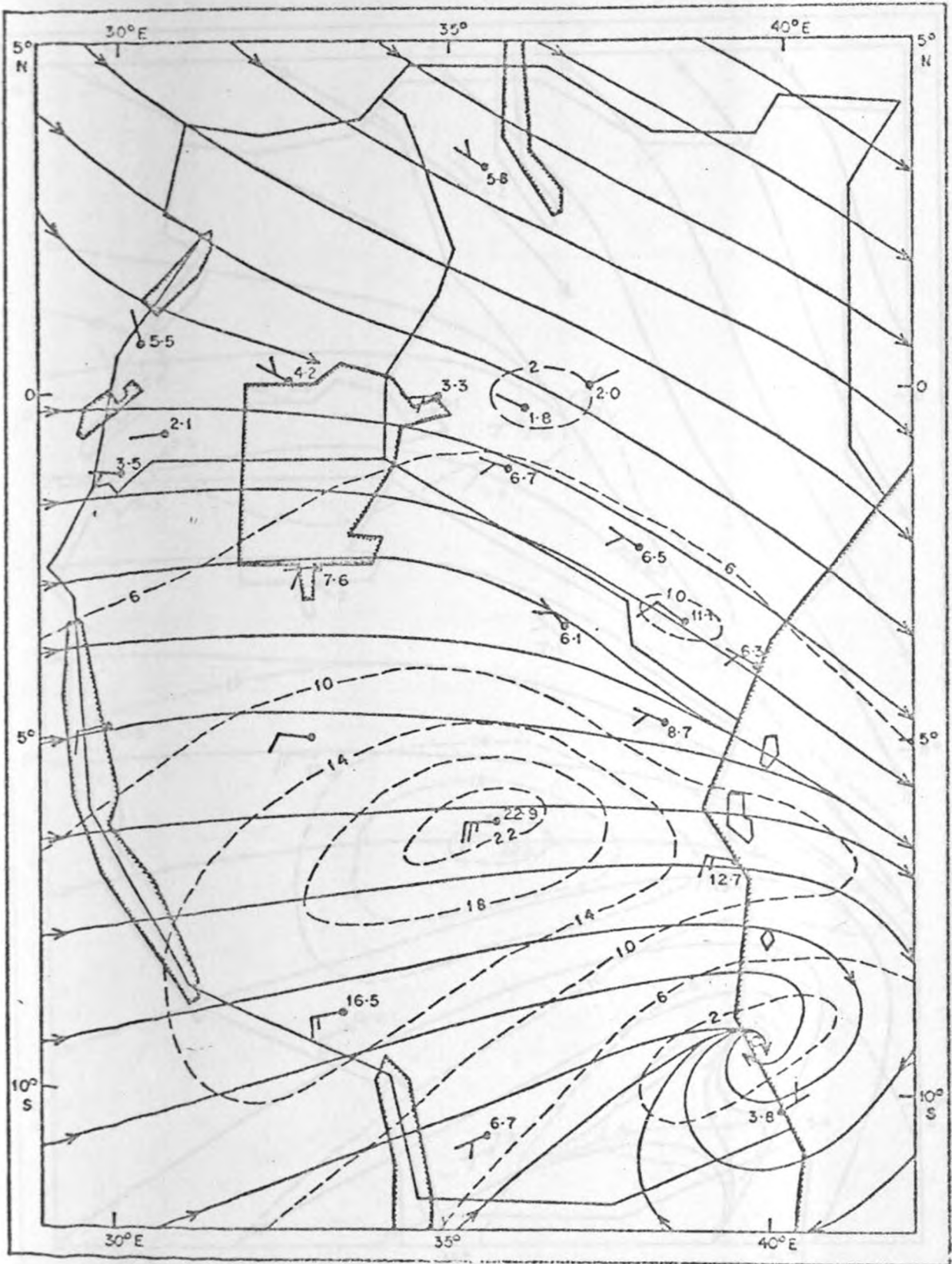


Fig. 47(b) : Streamlines and isotachs of wind anomalies (\vec{V}') at 2440 m AMSL in December 1961.

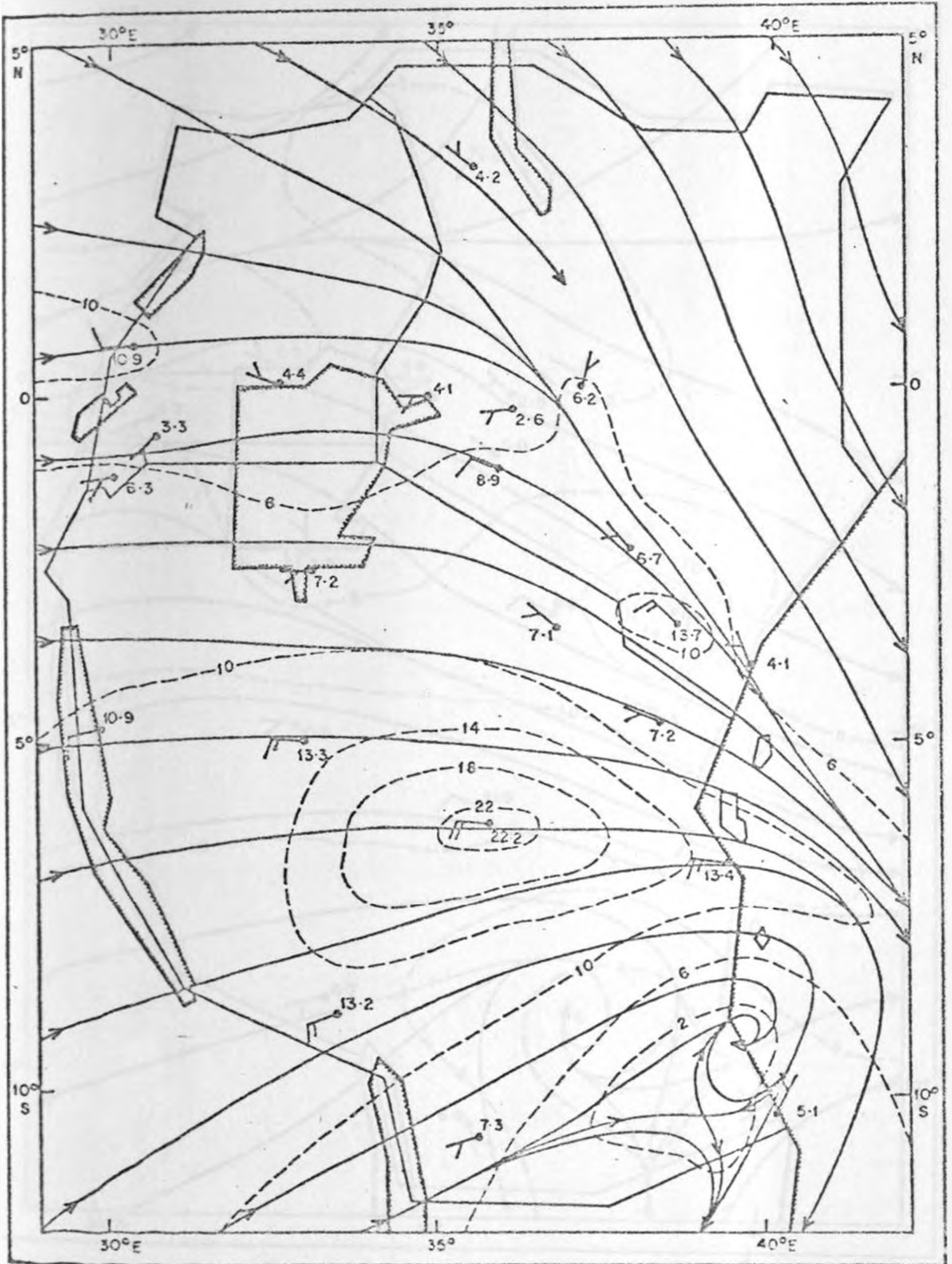


Fig. 47(c) : Streamlines and isotachs of wind anomalies (\vec{V}') at 3050 m AMSL in December 1961.

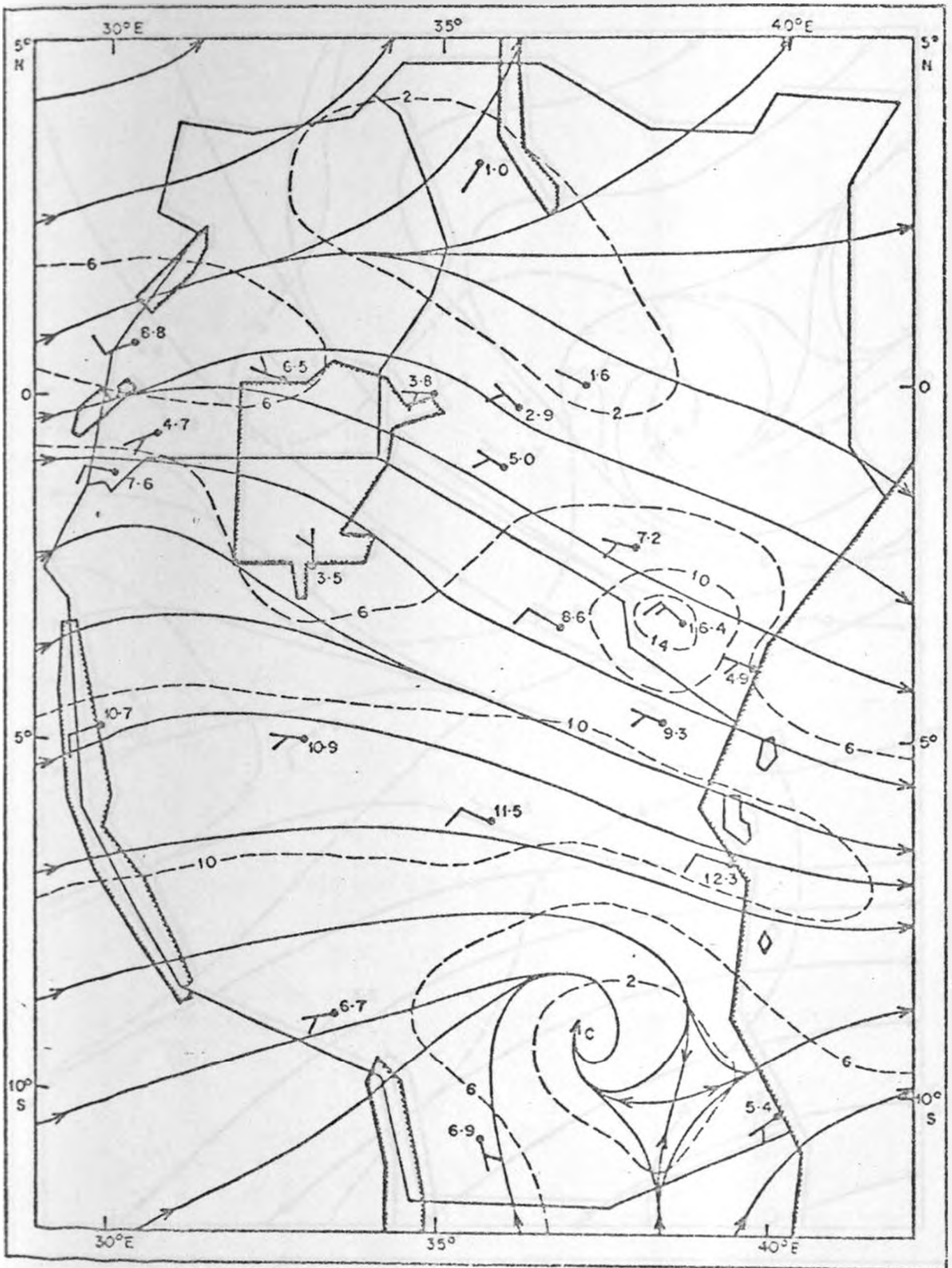


Fig. 47(d) : Streamlines and isotachs of wind anomalies (\vec{V}') at 4270 m AMSL in December 1961.

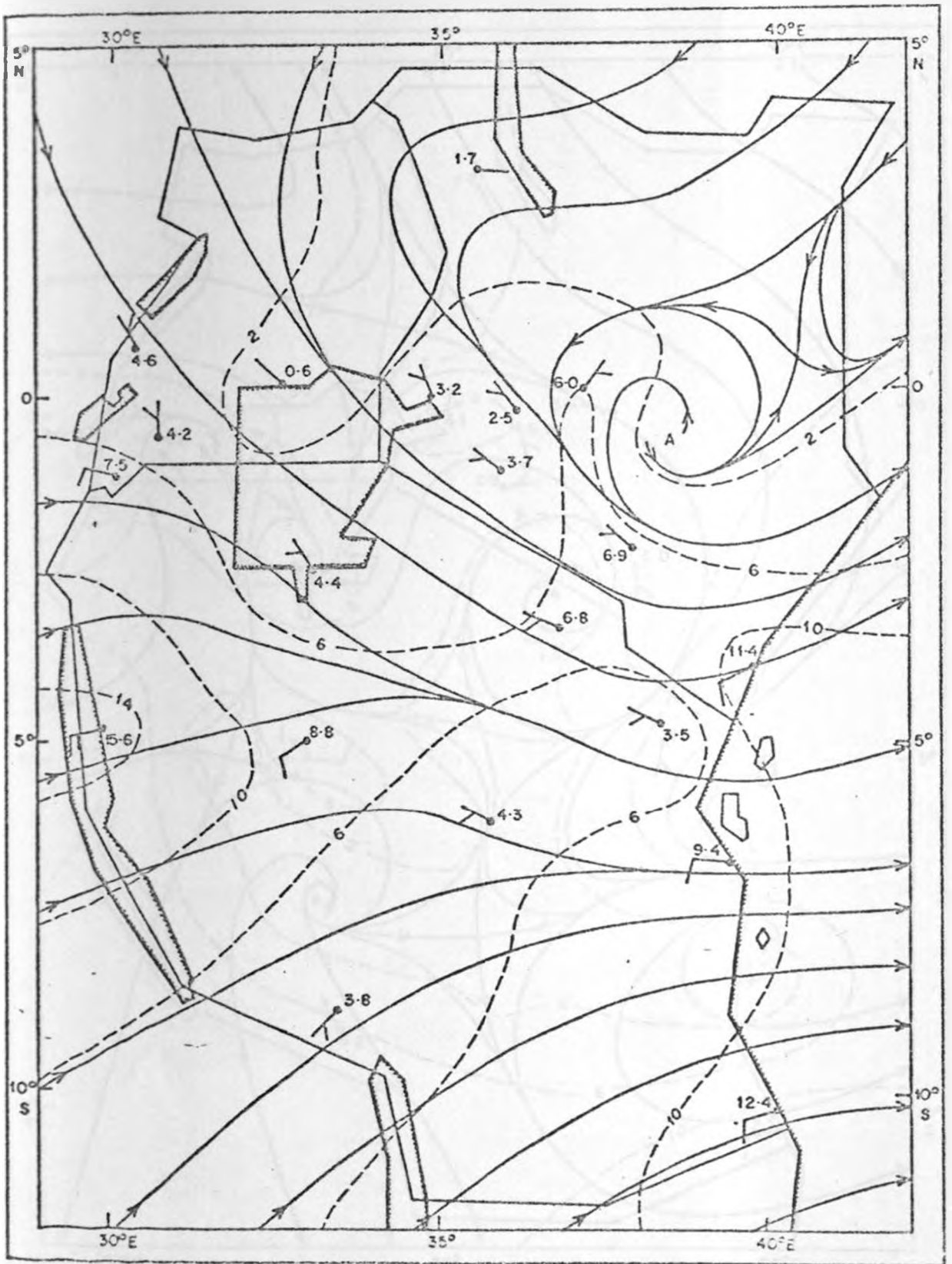


Fig. 47(e) : Streamlines and isotachs of wind anomalies (\vec{V}') at 5490 m AMSL in December 1961.

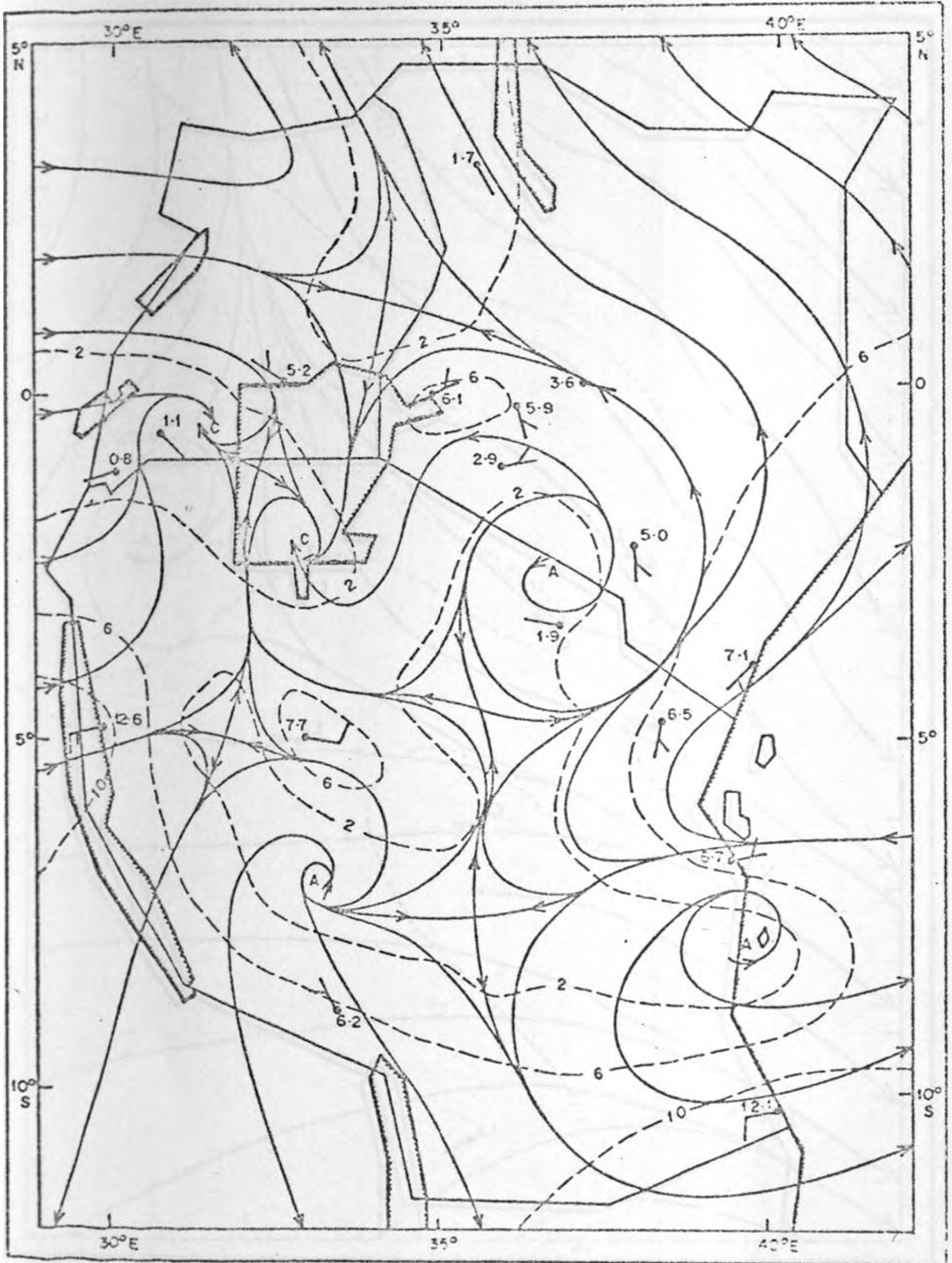


Fig. 47(f) : Streamlines and isotachs of wind anomalies (\vec{V}') at 7320 m AMSL in December 1961.

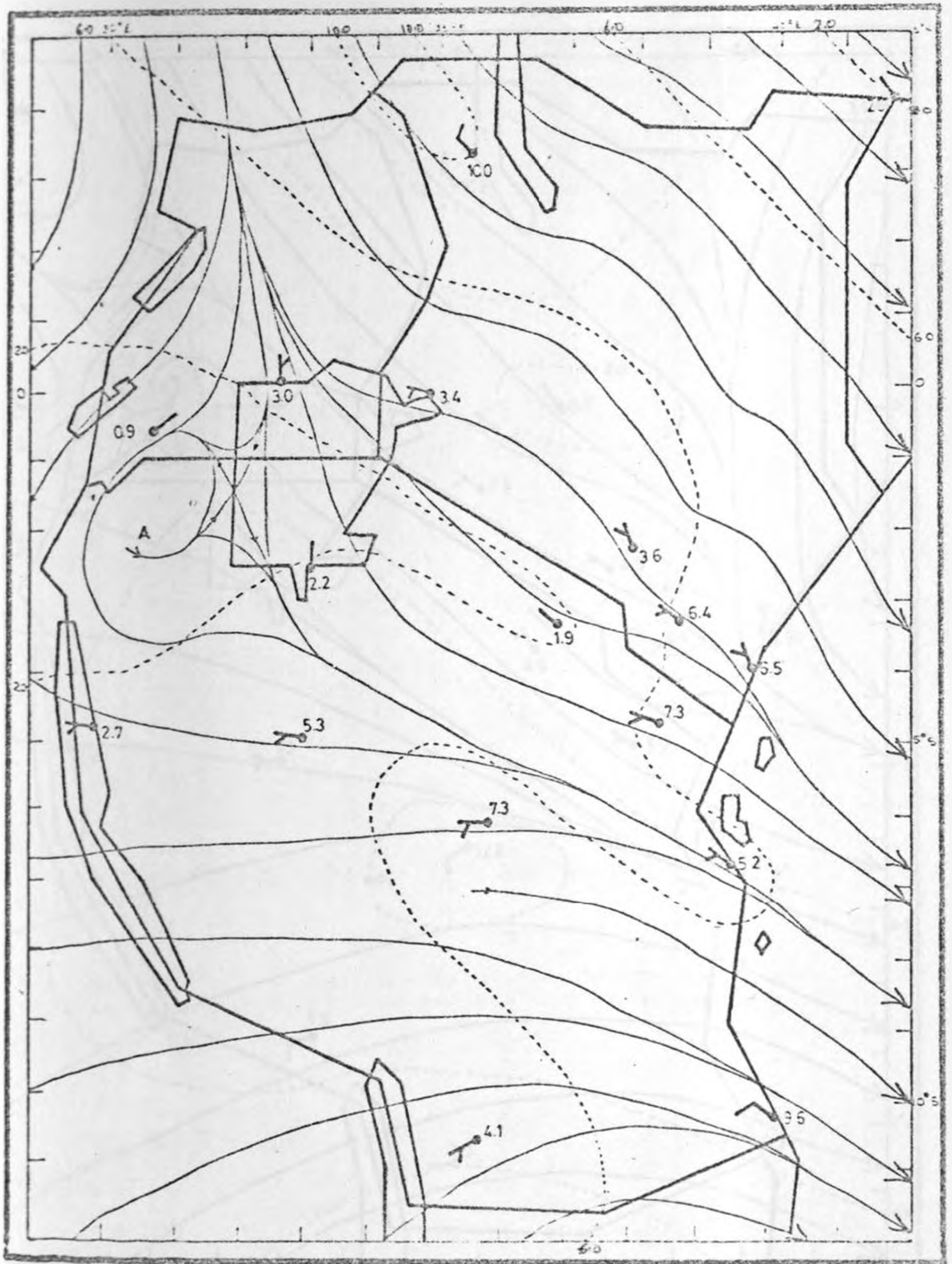


Fig. 48(a) : Streamlines and isotachs of wind anomalies (V') at 1525 m AMSL in January 1962.

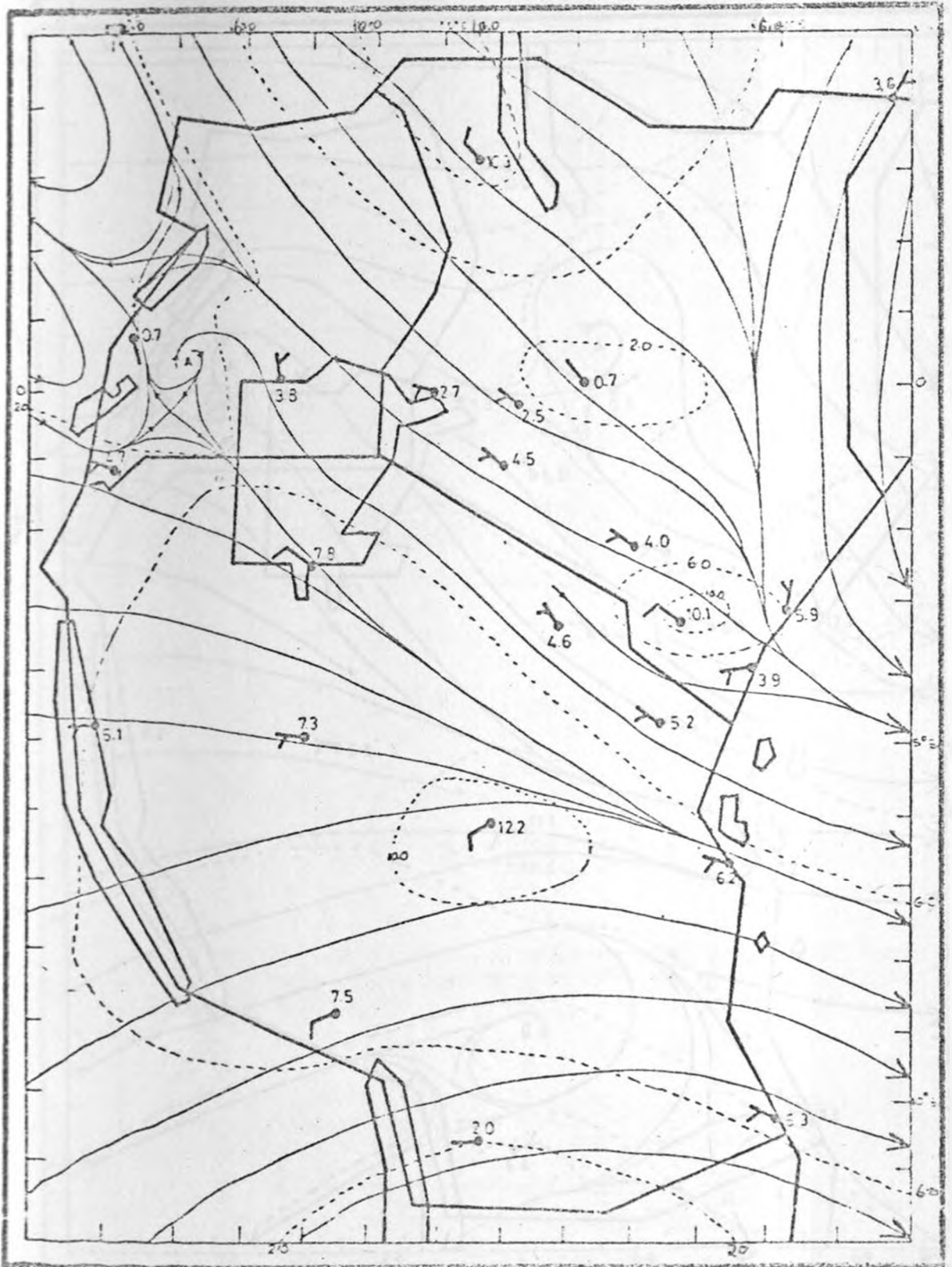


Fig. 48(b) : Streamlines and isotachs of wind anomalies (\bar{V}') at 2440 m AMSL in January 1962.

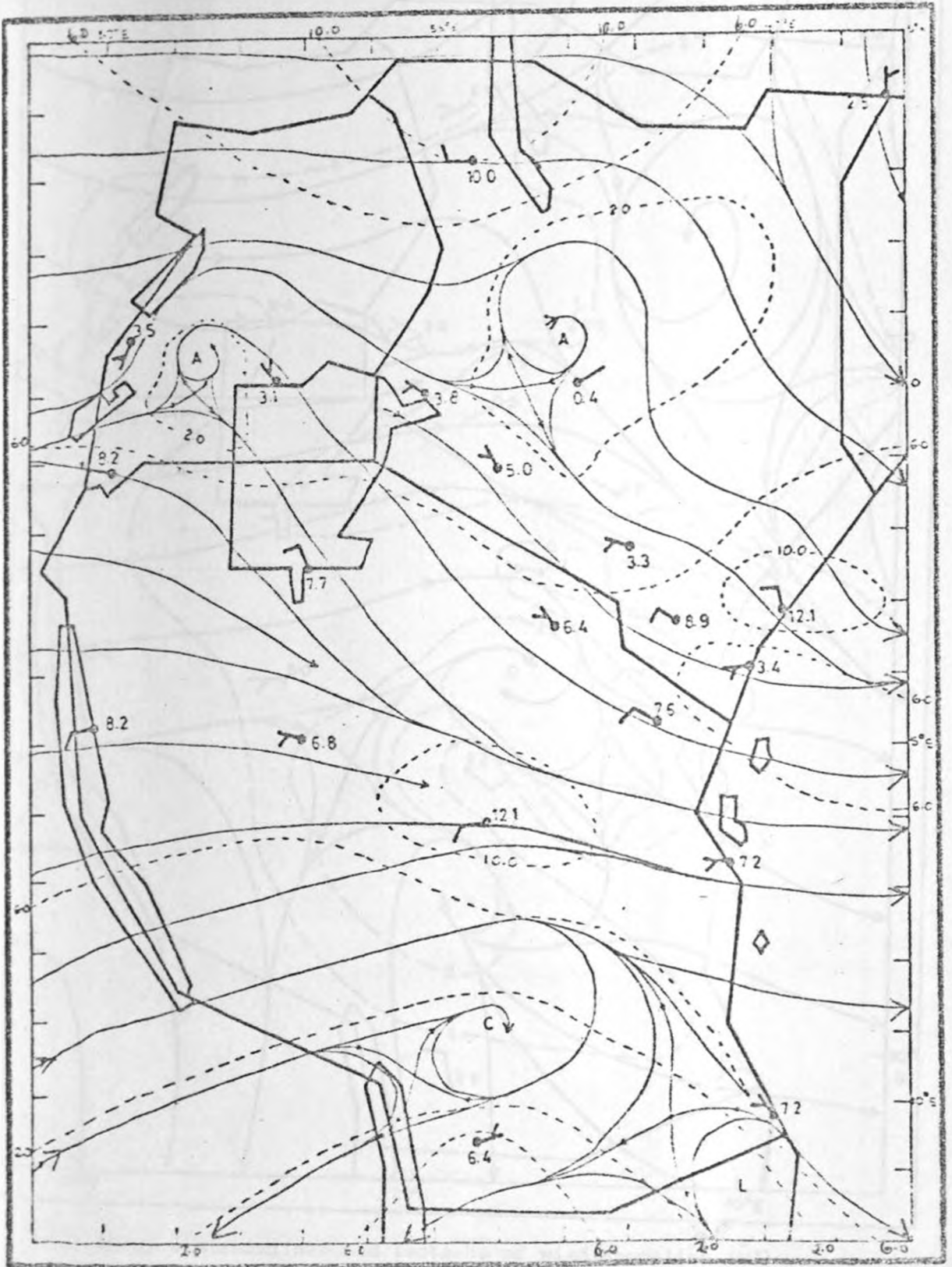


Fig. 48(c) : Streamlines and isotachs of wind anomalies (\bar{V}')
at 3050 m AMSL in January 1962.

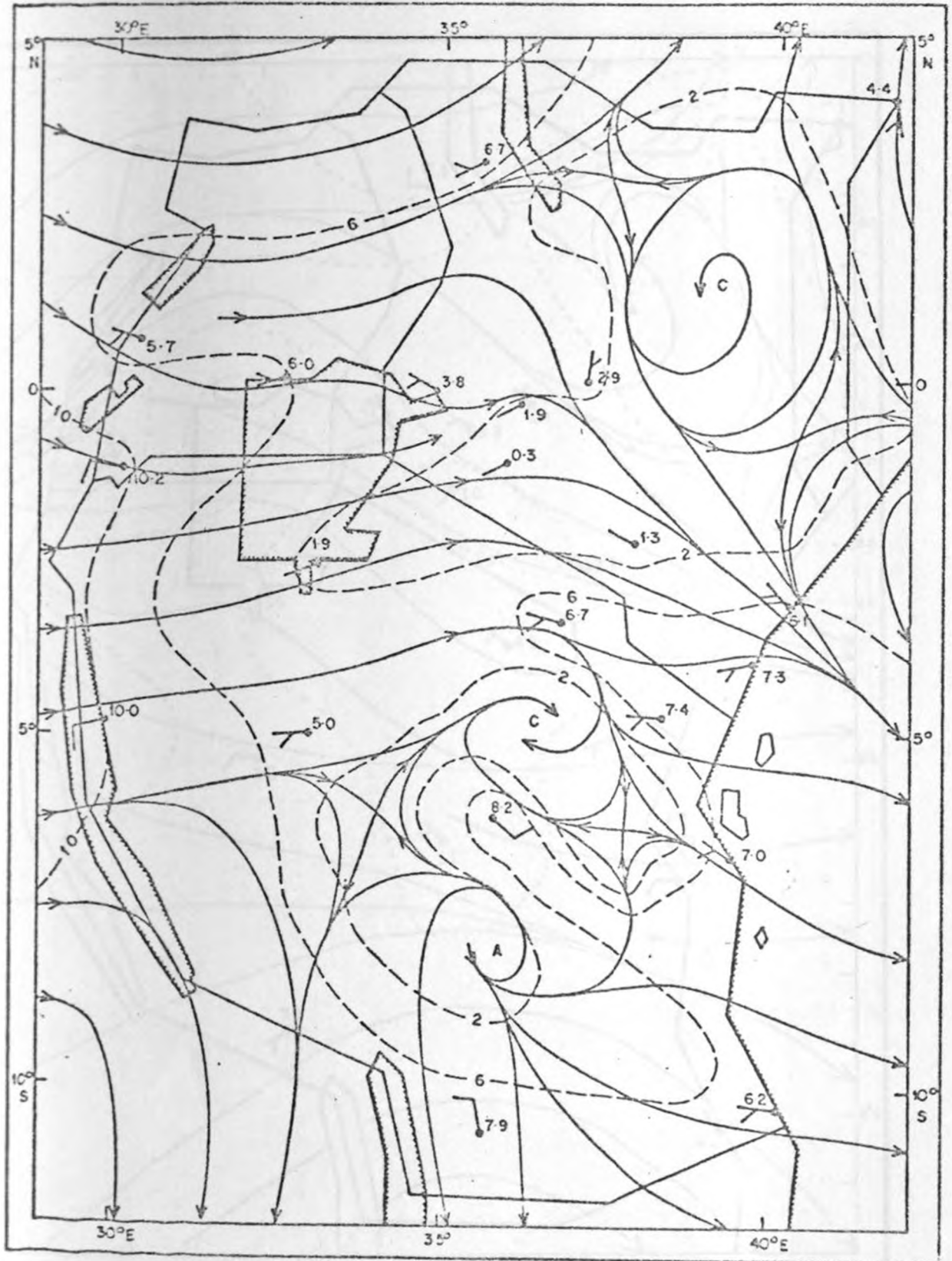


Fig. 48(d) : Streamlines and isotachs of wind anomalies (V') at 4270 m AMSL in January 1962.

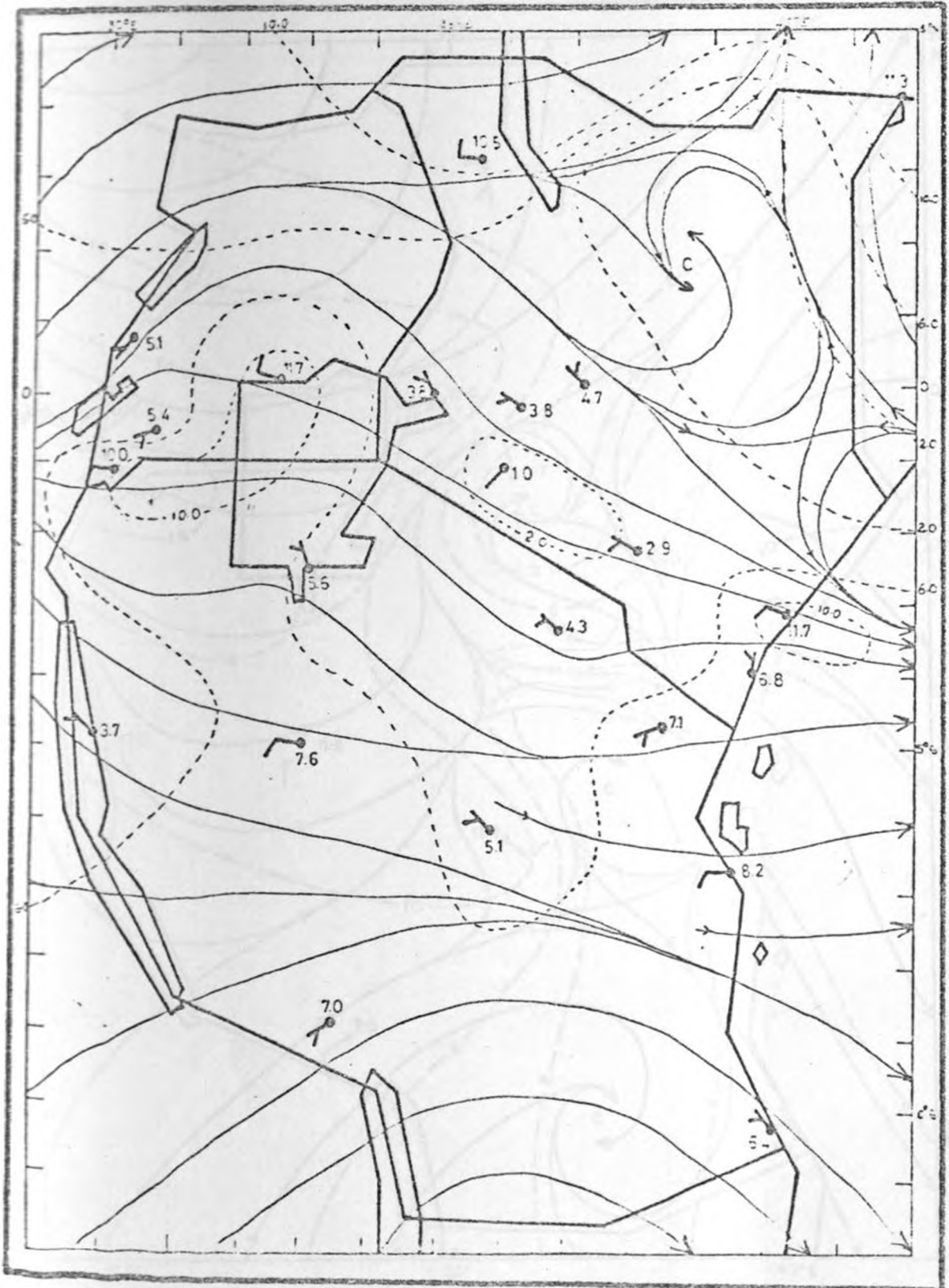


Fig. 48(e) : Streamlines and isotachs of wind anomalies (\vec{V}') at 5490 AMSL in January 1962.

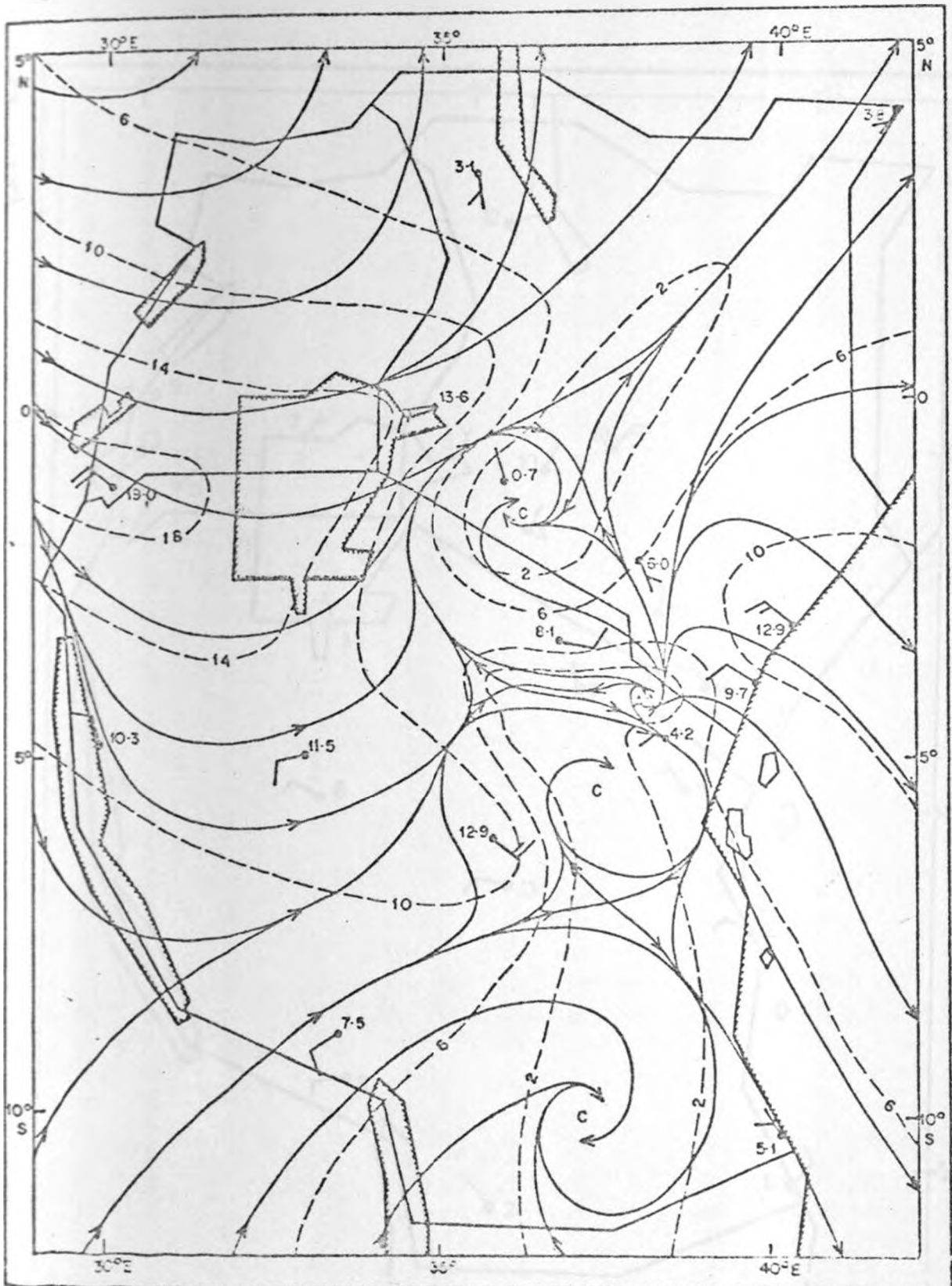


Fig. 48(f) : Streamlines and isotachs of wind anomalies (\vec{V}') at 7320 m AMSL in January 1962.

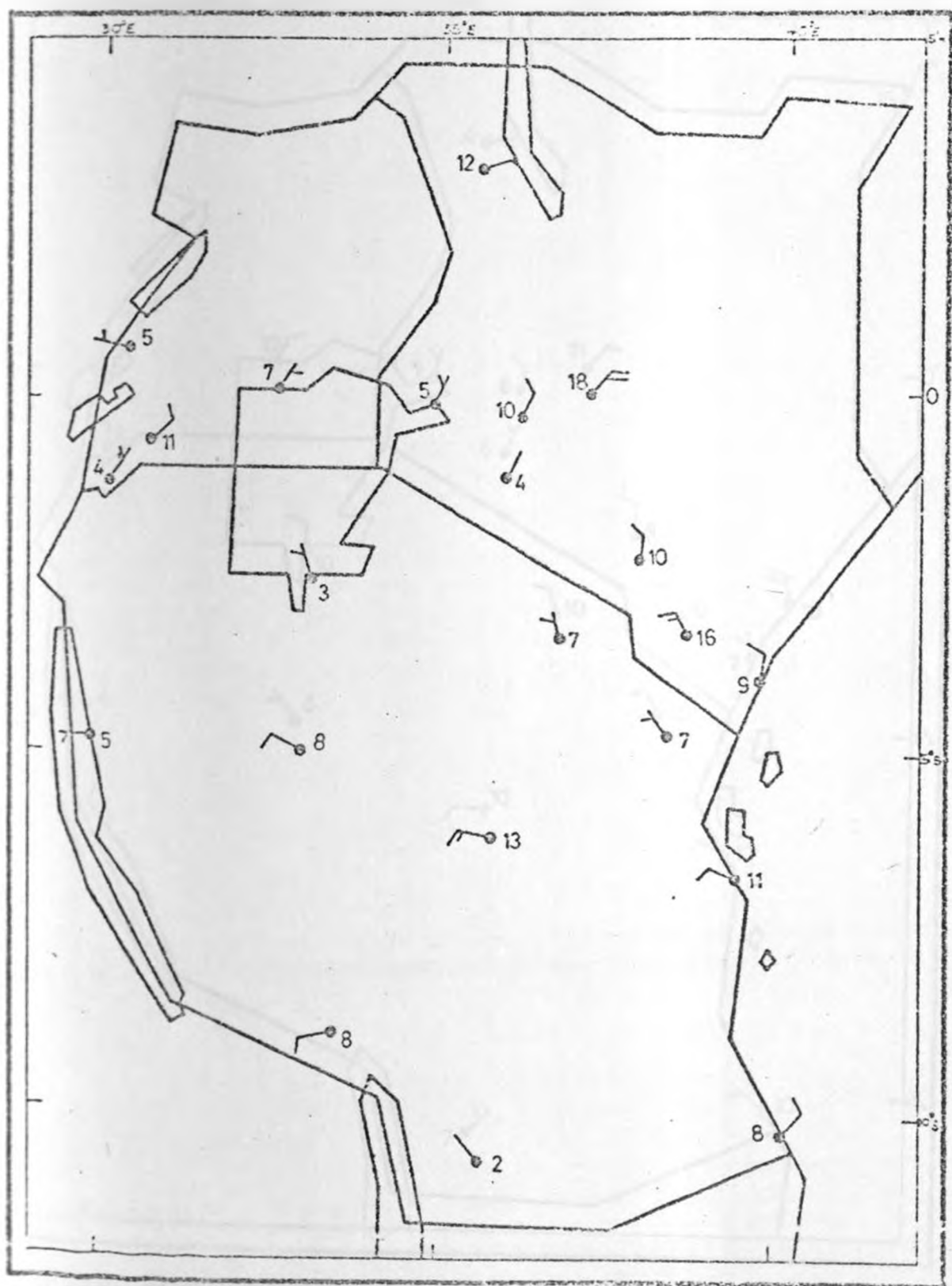


Fig. 49(a) : Observed mean wind vectors (speed in knots)
at 3050 m AMSL in December 1961.

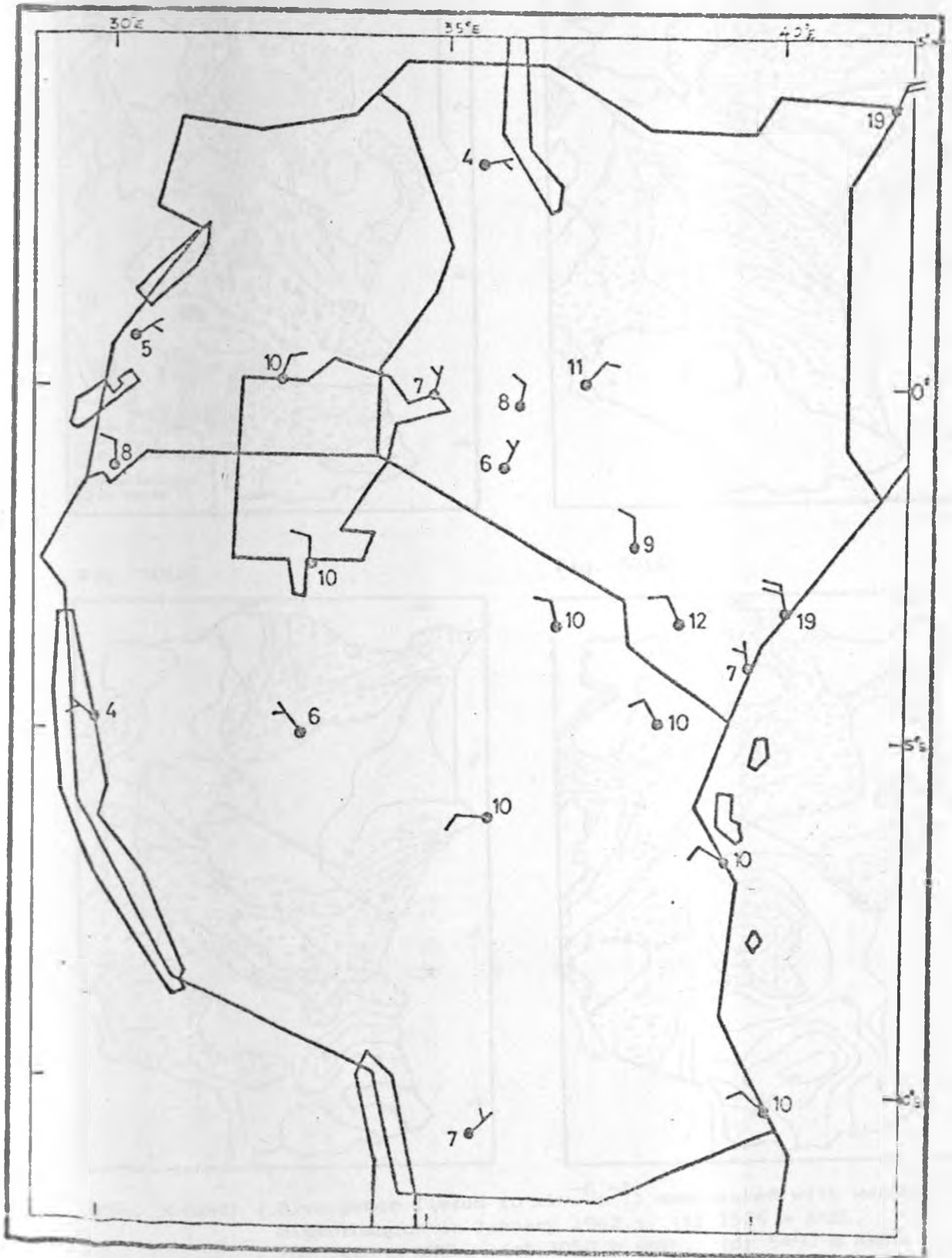


Fig. 49(b) : Observed mean wind vectors (speed in knots)
at 3050 m AMSL in January 1962.

Fig. 50(a)

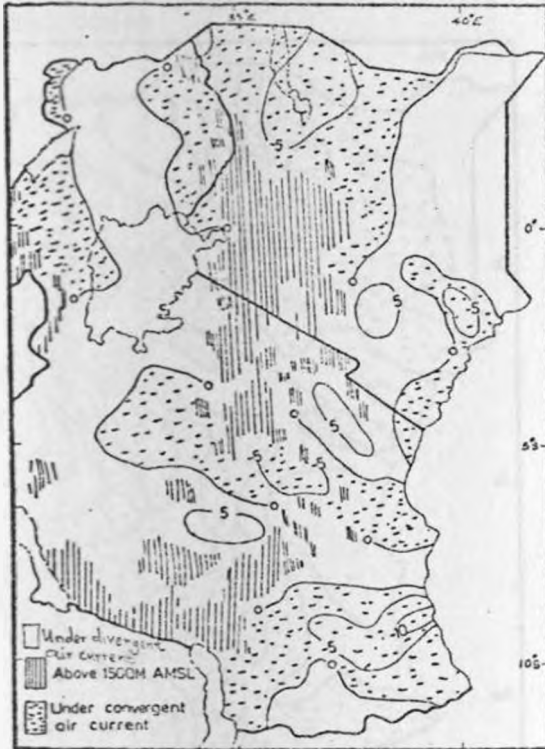


Fig. 50(b)

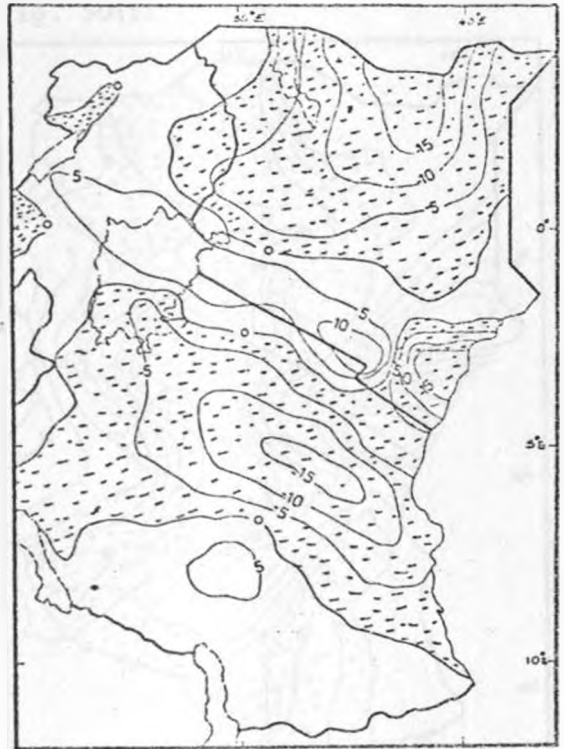


Fig. 50(c)

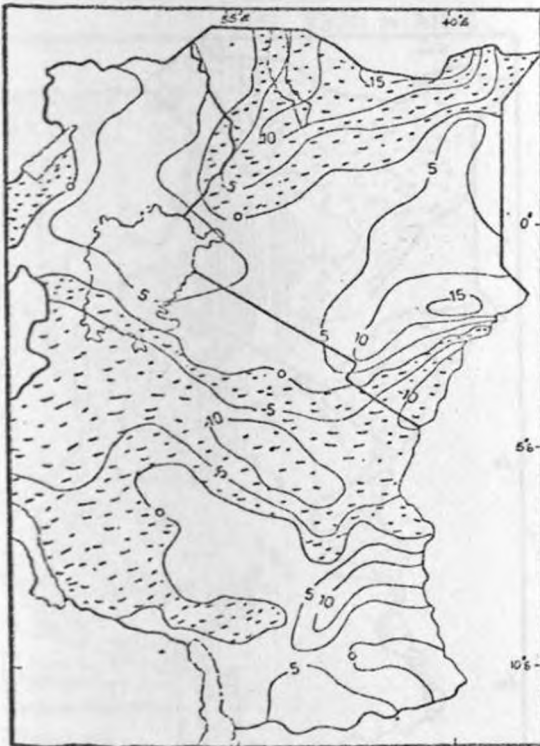


Fig. 50(d)

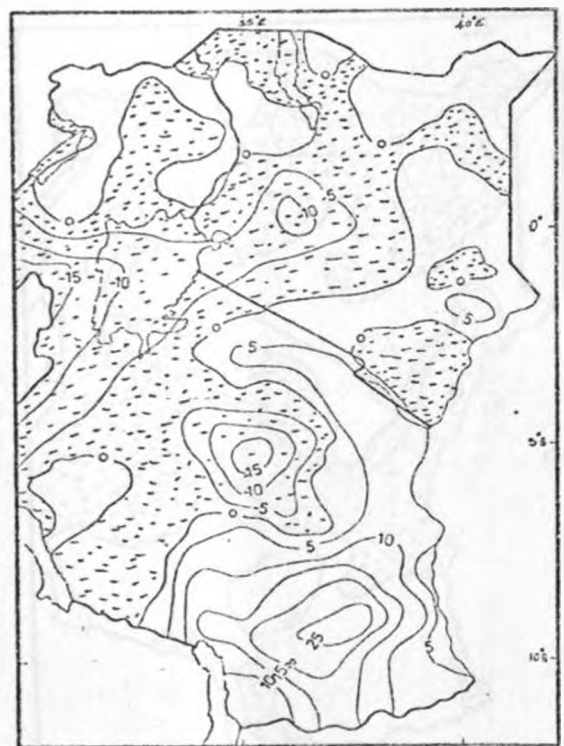


Fig. 50(a-d) : Divergence fields ($D \times 10^{-6} s^{-1}$) associated with weather disturbances in January 1962.: (a) 1525 m AMSL, (b) 2440 m AMSL, (c) 3050 m AMSL, (d) 5490 m AMSL.

Fig. 50(e)

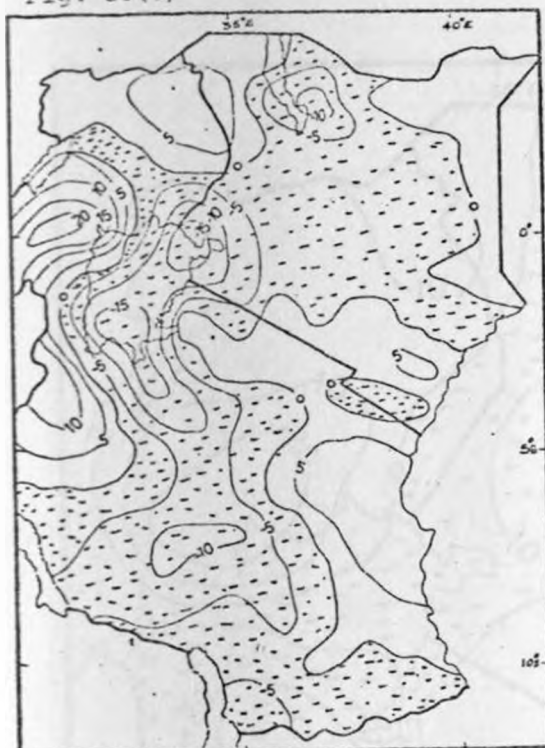


Fig. 50(f)

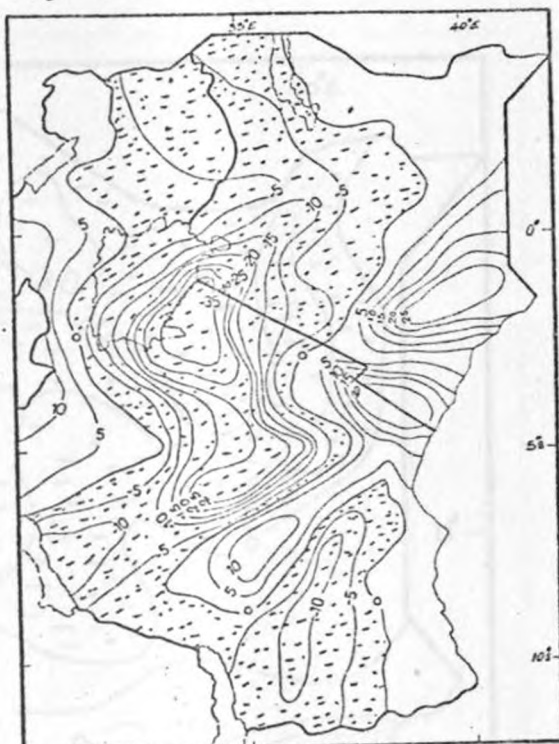


Fig. 50(e-f) : Divergence fields ($\text{D} \times 10^{-6} \text{s}^{-1}$) associated with weather disturbances in January 1962 : (e) 5490 m AMSL, (f) 7320 m AMSL.

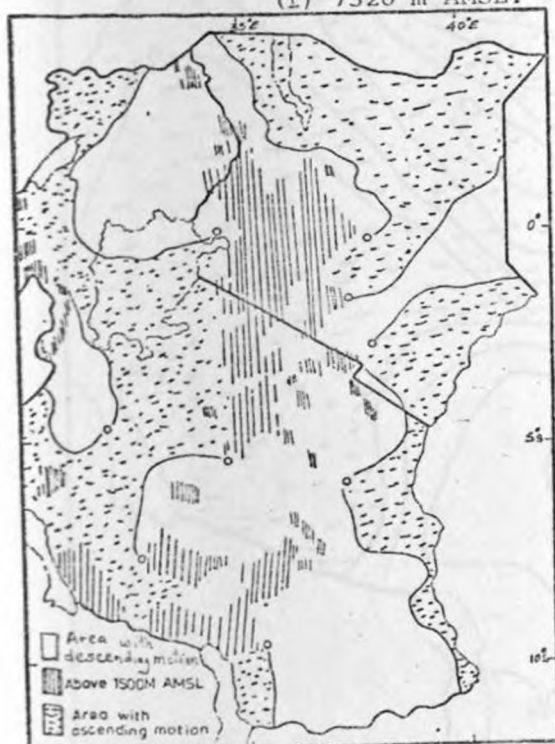


Fig. 51(a)



Fig. 51(b)

Fig. 51(a-b) : Vertical motion fields ($w \times 10^{-2} \text{ms}^{-1}$) associated with weather disturbances in January 1962 : (a) 1525 m AMSL, (b) 3050 m AMSL.

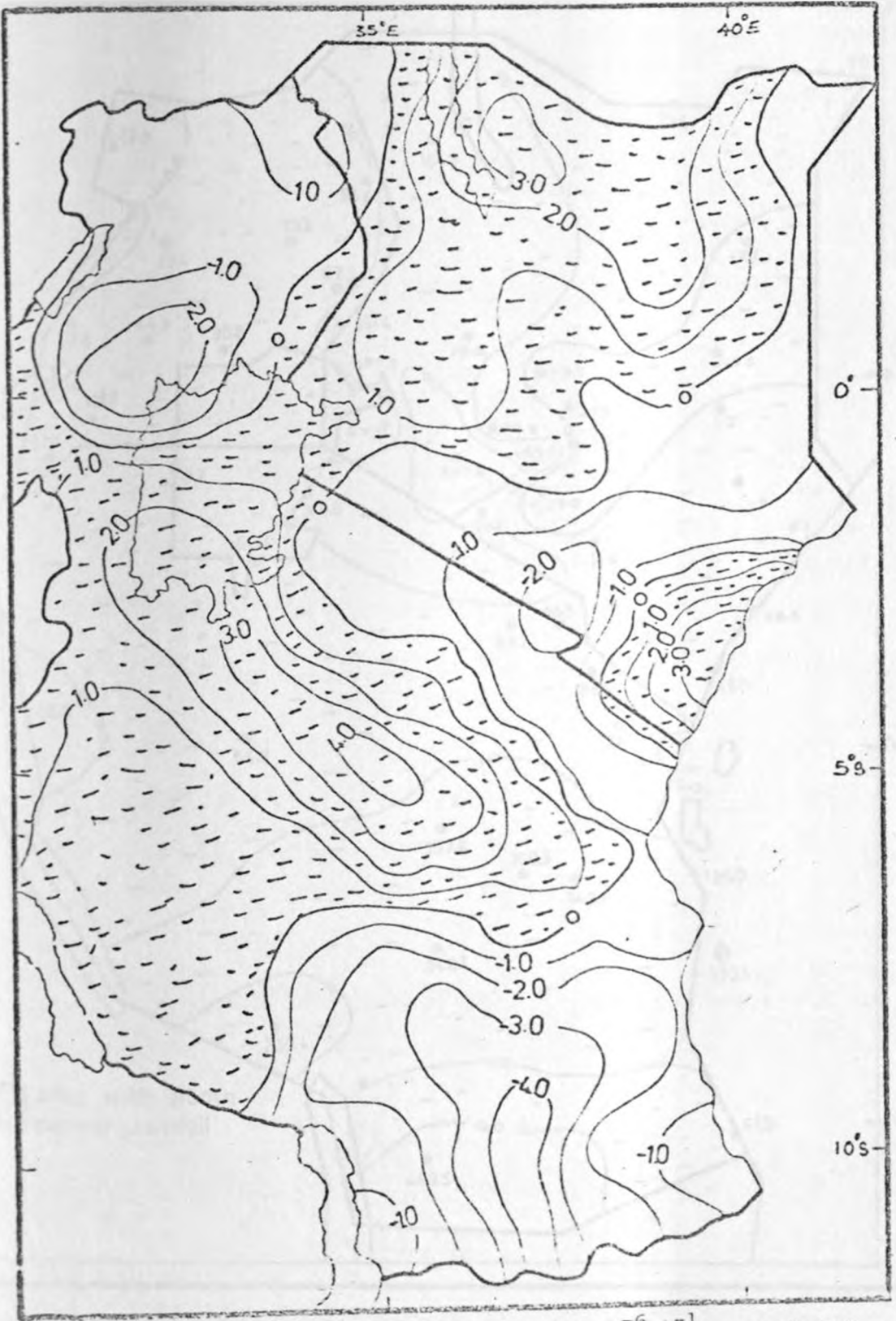


Fig. 51(c) : Vertical motion field ($w' \times 10^{-6} \text{ ms}^{-1}$) associated with weather disturbances in January : 5490 m AMSL.

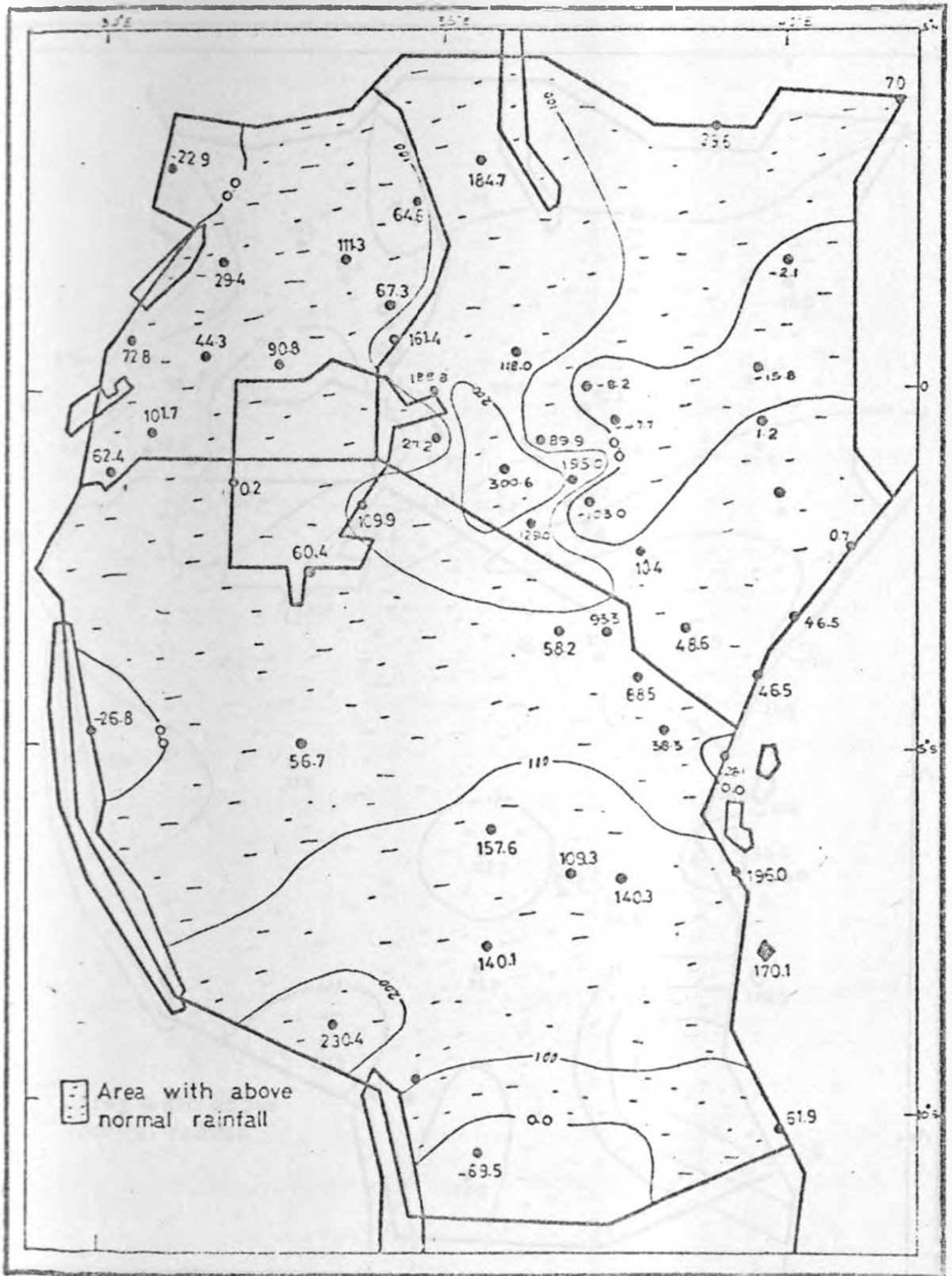


Fig. 52(a) : Rainfall anomalies (mm) in December 1961.

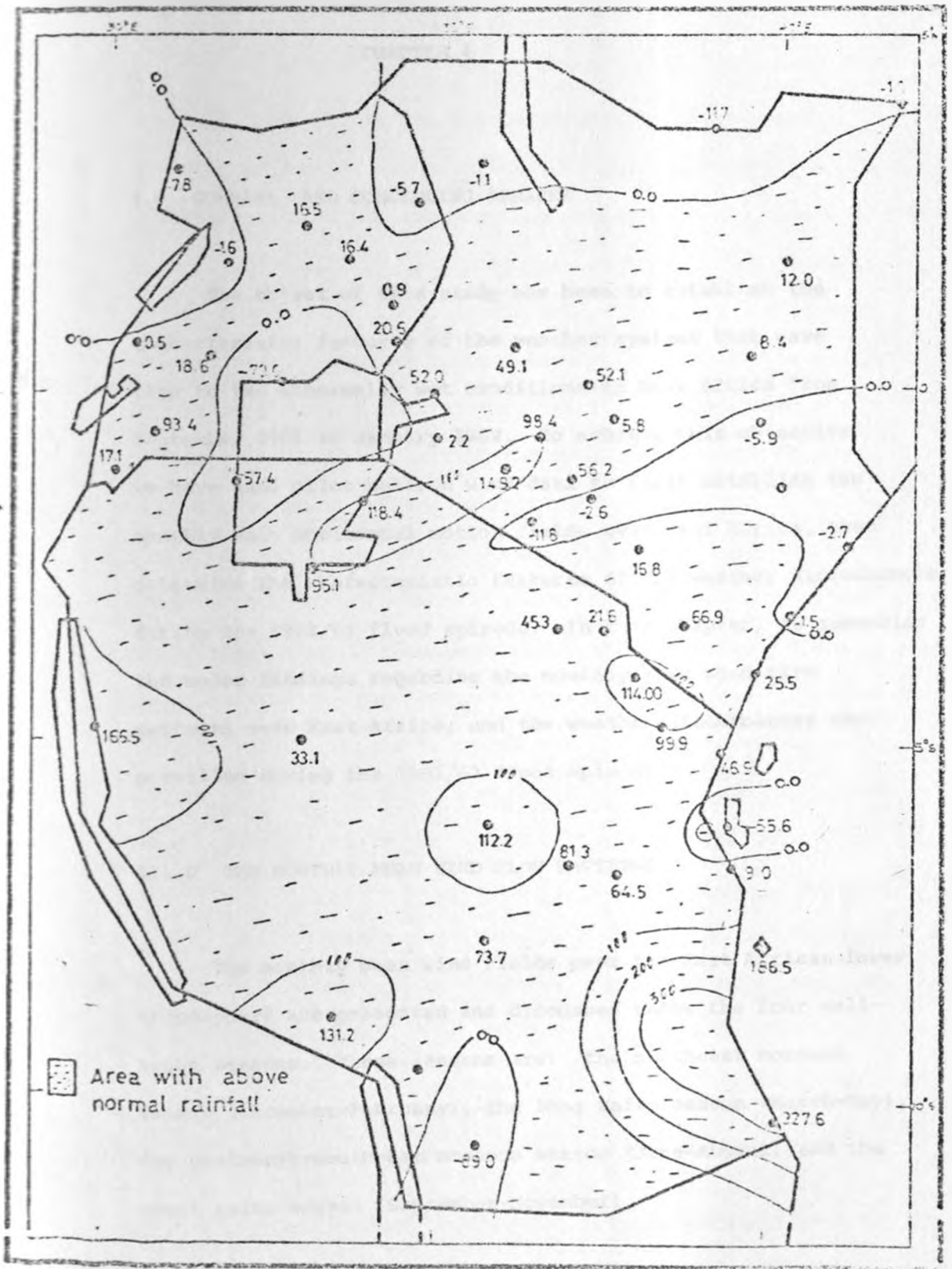


Fig. 52(b) : Rainfall anomalies (mm) in January 1962.

CHAPTER 4

4.0 SUMMARY AND CONCLUDING REMARKS

The object of this study has been to establish the characteristic features of the weather systems that gave rise to the abnormally wet conditions in East Africa from September 1961 to January 1962. To achieve this objective we have used pilot balloon wind data to first establish the monthly mean horizontal motion fields over East Africa, then determine the characteristic features of the weather disturbances during the 1961/62 flood episode. In this chapter, we summarise the major findings regarding the monthly mean wind flow patterns over East Africa, and the weather disturbances that prevailed during the 1961/62 flood episode.

4.1.0 THE MONTHLY MEAN WIND FLOW PATTERNS

The monthly mean wind fields over the East African lower troposphere are presented and discussed under the four well-known seasons. These seasons are: the northeast monsoon season (December-February), the long rains season (March-May), the southeast-southwest monsoon season (June-August) and the short rains season (September-November).

4.1.1 The Northeast Monsoon Season

In this season, the East African lower troposphere comes under the influence of the well known northeast monsoon air current which is generally hot and dry. During its early stages of development, the northeast monsoon air is confined to the lowest 3 km AMSL. As the season matures, the current intensifies and reaches maximum intensity in January-February when it also extends to the 4 km level. In March, the Northeast monsoon air current begins decaying first at the lowest levels and working upwards.

One important feature of the northeast current is its bifurcation over northeastern Kenya. Here, one branch flows westwards across northern Kenya into the interior of Africa. The other branch flows southwards, almost parallel to the East African coast. Findlater (1968) has made similar observations. The easterly air current in northern Kenya has mean speeds of about $7-10 \text{ ms}^{-1}$ while the northerly current along the Kenyan coast has mean speeds of about 5 ms^{-1} . The northeast monsoon current is confluent in the lake Victoria region and Uganda, but highly diffluent over Tanzania. Above the 4 km level the monsoon air is capped by an easterly air current. The intensity of the easterly current is maximum ($\sim 7.5 \text{ ms}^{-1}$) in the neighbourhood of the equator.

From this study, we have found that the northeast monsoon current is highly divergent over the eastern lowlands of Kenya and Tanzania. It is also observed that the maximum divergence value in the monsoon current is about $3 \times 10^{-5} \text{ s}^{-1}$

at the 850 mb level over northeastern Tanzania in February. In the lake region, northern Kenya and Uganda, the monsoon air is convergent and has maximum convergence values of about $1 \times 10^{-5} \text{ s}^{-1}$.

The computed vertical motion in the monsoon current is downward over eastern Kenya and northeastern Tanzania. Maximum downward motion is about $(3 \times 10^{-2} \text{ ms}^{-1})$ and is observed at the 700 mb level over northeastern Tanzania. The vertical motion in the lake Victoria region and Uganda is characteristically upward in agreement with the observed weather conditions in the area.

4.1.2 The Long Rains Season

The long rains season is characterised by the retreat of the northeast monsoon in the low levels and its gradual replacement by the southeast-southwest monsoon current. Initially, there is a dramatic change in the 850 mb level wind direction from northeasterly during the northeast monsoon months to mainly easterly in March and finally to southeasterly in April. The SE/SW monsoon current then establishes itself at the low levels in May, and the well-known East African low level jet becomes weakly evident at the 850 mb level. Generally, the mean air flow at 700 mb, 600 mb and 500 mb levels is characterised by the presence of a well-defined convergence zone (ITCZ) between northeasterly and southeasterly air currents. The location of the convergence zone is in

the neighbourhood of the equator. The air flow is found to be mainly easterly above the 5 km level.

From the divergence patterns for April and May, it is found that the ITCZ is well depicted as a zone of maximum convergence ($\sim 1.5 \times 10^{-5} \text{ s}^{-1}$) and ascending motion. Maximum upward motion ($\sim 4 \times 10^{-2} \text{ ms}^{-1}$) is found near the 500 mb level over the lake region and the Kenya highlands. The ITCZ in this season is found to slant equatorward with height below the 600 mb level. The slope of the ITCZ in the layer 850-600 mb is about 1:100. A secondary convergence zone is found within the SE/SW monsoon current over central Tanzania in April. The air current over northeastern Kenya and northeastern Tanzania remains divergent at the very low levels even during the long rains season. This divergence is overlain by convergence above the 700 mb level. The ensuing vertical motion in these areas is downward below the 500 mb level, with a maximum value of about 2 cms^{-1} at the 700 mb level.

The study further shows that the low level convergence patterns during the long rains season initially enter East Africa from western and southern Tanzania in February-March and then progress northwards with time. This will indicate that the southern summer ITCZ simultaneously enters the region from central and southern Africa.

4.1.3 The Southeast-Southwest Monsoon Season

The southeast-southwest monsoon air current is weakly evident in East Africa as early as April and May. The current intensifies progressively and acquires maximum intensity in July/August then decays thereafter. The mean peak speed in the monsoon current is about 13.5 ms^{-1} at the 850 mb level and occurs in the months of July and August.

The SE/SW monsoon current is found to be highly diffluent at the 850 mb level over the eastern lowlands of Kenya and Tanzania. The southerly monsoon current bifurcates into two branches over the Tanzanian coastal plains. One stream flows westwards across central Tanzania through a low lying corridor that is bounded to the north by the Hanang-Ngorongoro mountains and to the south by the Kapengere mountain chains. The maximum intensity in this westward branch is about 8 ms^{-1} at the 850 mb level. Similar bifurcation of the monsoon air is observed over northern Kenya. Here, one branch turns into a southeasterly-easterly current and flows into Uganda and southern Sudan. The other branch constitutes the monsoon current over northeastern Kenya and Somalia in this season. In the lake region, the air flow is very light ($1-2 \text{ ms}^{-1}$) but confluent in the low levels.

Over all, we have found in this study that the SE/SW monsoon air current influences the East African region for a longer period (April-October) than the northeast monsoon air (December-March). It is also much more intense than the

northeast monsoon current. However, the SE/SW monsoon air is shallower (surface - 3 km AMSL) than the northeast monsoon air which extends to the 4 km level during its period of maximum development.

The 600 mb level is found to contain some interesting weather systems in this season. The air flow is characterised by the presence of closed circulation cells that are oriented in a SW-to-NE direction across East Africa. These cells include an anticyclonic centre that is located over the eastern highlands of Kenya. Also, westerly winds are characteristically evident at this level. These westerlies span from central Tanzania into the area around Nairobi. Johnson and Morth (1960) and Nakamura (1968) observed in their studies the existence of rainless westerly winds at the 700-600 mb levels over Nairobi during June-October. The origin of these westerlies and reasons for their being rainless have, until now, remained obscure. It is evident from this study that these westerly winds are associated with the anticyclonic outflow from the 600 mb level anticyclone which is located in the vicinity of Nairobi. This medium level anticyclone is evident even at the 500 mb level during the peak monsoon months of July and August.

Outflow from this anticyclone would tend to inhibit further development of clouds that are formed in the low level moist monsoon air. The presence of medium level diffluence/divergence, together with the well-known 700 mb temperature inversion over Nairobi in this season results in the observed

rainlessness of the westerlies over Nairobi during June-October. The appearance of the medium level anticyclone over Nairobi on mean charts indicates that it is a dominant and frequent feature of the day-to-day air flow patterns over East Africa during the northern summer monsoon season.

Another weather phenomenon that is persistent during the SE/SW monsoon season is the cyclonic disturbance that is found over the lake Victoria region and western Kenya/eastern Uganda. The intensity of this disturbance is found to be maximum at the 700 mb level in July and August. The observed active weather conditions in western Kenya/eastern Uganda during July-August, a normally dry period in most parts of East Africa, could be attributed to an interplay between the lake-land breeze meso-scale systems and the observed larger scale cyclonic disturbance.

The divergence patterns reveal that the northern summer monsoon air current is, like the southern summer monsoon, highly divergent over the eastern lowlands of East Africa where maximum divergence is about $3 \times 10^{-5} \text{ s}^{-1}$ at the 850 mb level. In the interior, the monsoon current is found to be generally convergent in the low levels and divergent aloft. This is so especially over western Kenya, the lake Victoria region and eastern Uganda. The computed vertical motion in this season is typically downward along the main monsoon current and has a maximum value of $5 \times 10^{-2} \text{ ms}^{-1}$ at the 700 mb level. Maximum upward motions ($\sim 2 \times 10^{-2} \text{ ms}^{-1}$) are found in the middle troposphere over the lake Victoria region.

4.1.4 The Short Rains Season

The short rains season is characterised by the retreat of the SE/SW monsoon current in the period September-October and a gradual establishment of a convergence zone between the retreating SE/SW monsoon and the incoming northeast monsoon current. The main characteristics of the northern summer monsoon air current at the 850 mb level do persist through the post-monsoon months of September and October. In November, we find that the northern summer monsoon is totally absent and the low level air flow is wholly from the east. The ITCZ during this period is, like during the long rains, positioned near the equator. Its vertical extent appears to be somewhat shallower than is the case of the long rains season. However, the intensity of the ITCZ, as measured by the level of convergence, appears to be the same as is the case during the long rains season. The resulting vertical motion is slightly less intense in this season.

Over all, the results show that there is an area between 36°E and 39°E over eastern Kenya and northeastern Tanzania which is under the influence of a divergent low level air current almost throughout the year. The low level divergence is particularly marked during the monsoon seasons. This area roughly corresponds to the well known zone of rainfall deficiency in East Africa.

4.2 THE FLOODS OF 1961-1962

The results show that the onset of the flood episode was marked by a dramatic 2-3 day heavy downpour which affected the Kenyan coast between 25-28 September 1961. These intense rainfalls appear to have been caused by a westward moving disturbance which did not penetrate further into the interior. We believe this was an easterly wave although, as expected, our streamlines of monthly wind departures do not depict a wave.

The main weather disturbances that prevailed during September and October 1961 included an extensive anticyclonic disturbance over southern Tanzania, and cyclonic vortices and zones of marked confluence over Kenya, Uganda and northern Tanzania. These cyclonic disturbances were deep and covered most of the lower and middle troposphere. Strong low level inflows were evident in most parts of East Africa. The areas of marked low level inflows were characteristically capped aloft by marked outflow centred over the central parts of East Africa. The observed massive low level inflow and upper level outflow were typical of areas that exhibited very high above normal rainfall amounts.

The wettest month during the flood period was November 1961. The results reveal that during this month, East Africa came under the influence of a westerly-to-southwesterly perturbation which was superimposed on the mean wind flow. The perturbation manifested itself as a wavy pattern at the 850 mb level and developed into cyclonic vortices over the

Kenyan highlands and off the Kenyan coast at the 800 mb level. The position of these vortices coincided with the mean November position of the ITCZ. This will indicate that there was an unusual intensification of the rain bringing weather systems that are normally embedded in the ITCZ during the short rains.

The computed divergence fields associated with the disturbances which prevailed in November 1961 show that almost the whole of East Africa was engulfed by an extensively convergent air current. Highest convergence values ($\sim 1.5 \times 10^{-5} \text{ s}^{-1}$) and upward motion ($\sim 5 \times 10^{-2} \text{ ms}^{-1}$) were found over the Kenya highlands, the lake Victoria region and most parts of Uganda.

The westerly disturbance that was evident in November 1961 persisted all through December 1961 and January 1962. The streamlines of the westerly disturbance exhibited wavy patterns even in December 1961 and January 1962, at the 850 mb level. The disturbance manifested itself as closed cyclonic cells in the layer 800 mb to 600 mb. In December 1961 and January 1962, the vortices were centred over south-eastern Tanzania/northern Mozambique. This reveals that the disturbances were migrating southwards following the southward march of the ITCZ. It is apparent from this study that the cyclonic vortices over southeast Tanzania were part of an extensive cyclonic disturbance which existed over southern Africa.

In normal years, southern Tanzania is under the influence of northeast monsoon air currents during December to February. In December 1961 and January 1962, however, the westerly flow associated with the cyclonic disturbance in southern Tanzania completely replaced the normally diffluent northeast monsoon current over Tanzania. This constitutes one of the occasions when there is an incursion of westerly winds in East Africa (Thompson 1957a, Johnson and Morth 1960, Nakamura 1968).. These westerly winds originated from two source areas, one source consisted of a westerly flow from the Congo region and southeast Atlantic ocean and the other source from a recurved northeasterly current emanating from the southwest Indian ocean.

The appearance of the westerly disturbances in the mean wind departures for the months of November and December 1961, and, January 1962 implies that these disturbances were not only dominant but also persistent weather features during the 1961/62 flood episode.

ACKNOWLEDGEMENTS

I would like to extend my gratitude to my supervisor Dr. P.M.R. Kiangi for his guidance and encouragement throughout this study. I also wish to thank Mr. Masika of the Kenya Meteorological Department for his help during the initial stages of extraction of pilot balloon data.

I would also like to thank the Director of the Institute of Computer Science for allowing me to continue using the computer long after my research grant had been exhausted. Thanks to those staff members of the Institute of Computer Science who offered great help during the data extraction and analysis phases of this study.

Special words of appreciation go to my mother Lunyagi, and my daughter Ijusa for their patience throughout the course of this study.

Finally I would like to thank Mrs. Maria Nyawade for typing the manuscript and both Mr. Mwangi and Mr. Munyi for drafting the diagrams.

REFERENCES

- ADEFOLALU, D.O., 1974: On the scale interactions and the lower tropospheric summer easterly perturbation in tropical West Africa. Ph.D. dissertation, Florida State University, Tallahassee.
- ALUSA, A.L. and M.T. MUSHI, 1974: A study of the onset, duration and cessation of the rains in East Africa. Pre-print Vol. 1, International Tropical Meteorology meeting, Nairobi, Kenya - AMS, pp. 133-140.
- _____, 1976: The occurrence and nature of hailstorms in Kericho, Kenya. Proc. 2nd Sci. Conf. on Weather Mod., Boulder, Colorado - IAMAP/WMO, pp. 249-256.
- ANDERSON, D.L.T., 1976: The low level jet as a western boundary current. Mon. Wea. Rev. 104, 907-921.
- ARDANUY, P., 1979: On the observed diurnal oscillation of the Somali jet. Mon. Wea. Rev. 107, 1694-1700.
- ASPLIDEN, C.I., 1974: The low level wind field and associated perturbations over tropical Africa during northern summer. Pre-print Vol. 1, International Tropical Meteorology meeting, Nairobi, Kenya - AMS, pp. 218-223.
- ASNANI, G.C. and J.H. KINUTHIA, 1979: Diurnal variation of precipitation in East Africa. Kenya Met. Dept., Research report No. 8/79, 58 pp.

- ATKINSON, G.D., 1971: Forecasters' Guide to tropical Meteorology. USAF Tech. Report No. 240.
- _____ and J.C. SADLER, 1970: Mean cloudiness and Gradient-level-wind charts over the tropics. Vol. II, USAF Tech. Report No. 215.
- BANNON, P.R., 1979a: On the dynamics of the East African jet. I: Simulations of mean conditions for July. *J. Atmos. Sci.*, 36, 2140-2152.
- _____, 1979b: On the dynamics of the East African jet. II: Jet transients. *J. Atmos. Sci.*, 36, 2153-2168.
- BURPEE, R.W., 1972: The origin and structure of easterly waves in the lower troposphere of North Africa. *J. Atmos. Sci.*, 29, 77-90.
- CADET, D. and P. OLORY-TOGBE, 1977: The propagation of tropical disturbances over the Indian ocean during the summer monsoon. *Mon. Wea. Rev.*, 105, 700-708.
- _____ and G. REVERDIN, 1981: The monsoon over the Indian ocean during summer 1975. Part I : Mean Fields. *Mon. Wea. Rev.*, 109, 148-158.
- CARLSON, T.N., 1969: Synoptic histories of three African disturbances that developed into Atlantic Hurricanes. *Mon. Wea. Rev.*, 97, 256-276.
- CHAGGAR, T.C., 1977: Geographical distribution of monthly and annual mean frequency of thunderstorm days over eastern Africa. EAMD, Tech. Note, No. 26, 22 pp.

- DEAN, G.A. and N.E. LaSEUR, 1974: The mean structure and its synoptic-scale variation of the African Troposphere Pre-print Vol. 1, International Tropical Meteorology meeting, Nairobi, Kenya - AMS, pp. 224-228.
- DESAI, B.N., N. RANGACHARI and S.K. SUBRAMANIAN, 1976: Structure of the low level jet stream over the Arabian sea and pensinsular as revealed by observations in June and July during the Indo-Soviet Monsoon Experiment (ISMEX) 1973 and its probable origin. Indian J. Met. Geophys., 27, 263-274.
- FINDLATER, J., 1968: The month to month variation of winds at low level over eastern Africa. EAMD Tech. Memo. No. 12, 27 pp.
- _____, 1969a: A major low level air current near the Indian ocean during the northern summer. Quart. J. Roy. Met. Soc., 95, 362-380.
- _____, 1969b: Interhemispheric transport of air in the lower troposphere over the western Indian ocean. Quart. J. Roy. Met. Soc., 95, 400-403.
- _____, 1971: Mean monthly air flow at low levels over the western Indian ocean. Geophys. Mem., No. 115, HMSO London, U.K.
- _____, 1972: Aerial explorations of the low level cross-equatorial current over eastern Africa. Quart. J. Roy. Met. Soc., 98, 274-289.

- FINDLATER, J., 1974: The low-level cross-equatorial air current of the western Indian ocean during northern summer. *Weather*, 29, 411-416.
- _____, 1977: Observational aspects of the low-level cross-equatorial jet stream of the western Indian ocean. *Pure and Appl. Geophys.*, 115, 1251-1262.
- FLOHN, H., 1960: Equatorial westerlies over Africa, their extension and significance. *Proc. of Symp. on Trop. Met. in Africa*. Munitalp Foundation, Nairobi, Kenya, pp. 253-267.
- FORSDYKE, A.G., 1949: Weather forecasting in tropical regions. *Geophys. Mem. No. 82*, HMSO, London, U.K.
- _____, 1960: Synoptic models of the tropics. *Proc. of Symp. on Trop. Met. in Africa*. Munitalp Foundation, Nairobi, Kenya, pp. 14-23.
- FRAEDRICH, K., 1972: A simple climatological model of the dynamics and energetics of the nocturnal circulation at Lake Victoria. *Quart. J. Roy. Met. Soc.*, 98, 322-335.
- FREMMING, D., 1970: Notes on an easterly disturbance affecting East Africa 5-7 September 1967. *EAMD Tech. Memo.*, No. 13.
- GICHUIYA, S.N., 1970: Easterly disturbances in the southeast monsoon. *Proc. Symp. on Trop. Met. Honolulu, Hawaii*.
- GLOVER, J., P. ROBINSON and J.P. HENDERSON, 1954: Provisional maps of the reliability of annual rainfall in East Africa. *Quart. J. Roy. Met. Soc.*, 80, 602-607.

- GRAY, W.M., 1968: Global view of the origin of tropical disturbances and storms. *Mon. Wea. Rev.*, 96, 669-700.
- GRIFFITHS, J.P., 1959: The variability of the annual rainfall in East Africa. *Bull. Am. Met. Soc.*, 40, 361-362.
- GRUNDY, F., 1963: Rainfall and river discharge in Kenya during the floods of 1961-1962: A report. Kenya Government.
- HAMILTON, R.A. and J.W. ARCHBOLD, 1945: Meteorology of Nigeria and adjacent territory. *Quart. J. Roy. Met. Soc.*, 71, 231-265.
- HART, J.E., 1977: On the theory of the East African low level jet stream. *Pure and Appl. Geophys.*, 115, 1263-1282.
- HENDERSON, J.P., 1949: Some aspects of climate in Uganda. EAMD Mem., Vol. II, No. 5.
- HILLS, R.C., 1978: The organisation of rainfall in East Africa. *J. of Trop. Geog.*, 2, 47-49.
- JOHNSON, D.H. and H.T. MORTH, 1960: Forecasting research in East Africa. *Proc. of Symp. on Trop. Met. in Africa*. Munitalp Foundation, Nairobi, Kenya, pp. 56-137.
- _____, 1962: Rain in East Africa. *Quart. J. Roy. Met. Soc.*, 88, 1-19.
- _____, 1963: African Synoptic Meteorology. *Proc. of the WMO/FAO Seminar on Met. and the Desert Locust*. Tehran - 25 Nov.-11 Dec. 1963, pp. 48-90.
- KIANGI, P.M.R., M.M. KAVISHE and J.K. PATNAIK, 1981: Some aspects of the mean tropospheric motion field in East Africa during the long rains season. *Kenya J. of Sci. and Tech. (A)*, 2, pp. 91-103.

- KRISHNAMURTI, T.N. and H.N. BHALME, 1976: Oscillations of a monsoon system. Part I : Observational aspects. J. Atmos. Sci., 33, 1937-1954.
- _____, J. MOLINARI and H.L. PAN, 1976: Numerical simulation of the Somali jet. J. Atmos. Sci., 33, 2350-2362.
- LAMB, H.H., 1966: Climate in the 1960's : changes in the world's wind circulation reflected in prevailing temperature, rainfall patterns and the level of African lakes. The Geographical Journal, 132, 183-212.
- LUMB, F.E., 1966: Synoptic disturbances causing rainy periods along the East African coast. Met. Mag., 95, 150-159.
- _____, 1970: Topographic influences in thunderstorm activity near lake Victoria. Weather, 25, 404-410.
- MORTH, H.T., 1967: Investigation into the Meteorological aspects of the variations in the level of lake Victoria. EAMD Mem., Vol. IV, No. 2.
- NAKAMURA, K., 1968: Equatorial westerlies over East Africa and their climatological significance. Geographical Reports of Tokyo Metropolitan University, No. 3, pp. 43-61.
- NEAVE, C.F., 1967: Tropical storm "Lily" 19th April - 3rd May 1966 : An account of its history and behaviour. EAMD Mem., Vol. IV, No. 4.
- NEWELL, R.E., J.W. KIDSON, D.G. VINCENT and G.J. BOER, 1974: The general circulation of the tropical atmosphere and interactions with extratropical latitudes, Vol. 2, The M.I.T. Press, 371 pp.

- NGARA, T., 1977: Some aspects of the East African low level jet. M.Sc. thesis, Dept. of Met., University of Nairobi.
- _____, and G.C. ASNANI, 1978: Five-day oscillation in East African low-level jet. *Nature*, 272, 708-709.
- NIEUWOLT, S., 1978: Breezes along Tanzanian east coast. *Arch. Meteor. Geoph. Biokl, Ser. B*, 21, 189-206.
- _____, 1974: Interdiurnal rainfall variability in Tanzania. Pre-print Vol. 1, International Tropical Meteorology meeting, Nairobi, Kenya - AMS, pp. 252-257.
- NJAU, L.N., 1982: Tropospheric wave disturbances in East Africa. M.Sc. thesis, Dept. of Met., University of Nairobi.
- NYONI, E., 1981: Notes on archived meteorological data in the Kenya Meteorological Department. Kenya Met. Dept.
- OBASI, G.O.P., 1972: On the mathematical description of the lower tropospheric drift flow over the Indian ocean during the SE/SW monsoon. *J. of the Marine Biological Society of India*, Vol. 14, No. 1, pp. 84-101.
- OKEYO, A.E., 1982: A two-dimensional numerical model of the lake-land and sea-land breezes over Kenya. M.Sc. thesis, Dept. of Met., University of Nairobi.
- OKOOLA, R.E.A., 1982: Monsoon system over southwest Indian ocean during northern summer of 1979. M.Sc. thesis, Dept. of Met., University of Nairobi.
- OKULAJA, F.O., 1970: Synoptic flow perturbations over West Africa. *Tellus*, 22, 663-680.

- PALMER, C.E., 1951: Tropical Meteorology. Compedium of Meteorology. AMS, pp. 859-880.
- _____, 1952: Tropical Meteorology. Quart. J. Roy. Met. Soc., 78, 126-163.
- POTTS, A.S., 1971: Application of harmonic analysis to the study of East African rainfall data. J. of Trop. Geog., 33, 31-41.
- RAMAGE, C.S., and RAMAN, C.R.V., 1972: Meteorological atlas of the International Indian ocean Expedition, Vol. 2: Upper air.
- RAO, G.V. and H.M.E. Van de BOOGAARD, 1981: Structure of the Somali jet deduced from aerial observations taken during June-July, 1977. Monsoon Dynamics, Cambridge University Press, 322-331.
- RIEHL, H., 1954: Tropical Meteorology. McGraw-Hill Book Co., Inc., New York, 392 pp.
- SANSOM, H.W., 1953: The Lindi cyclone 15th April 1952: A survey of its meteorological history and behaviour. EAMD Mem., Vol. III, No. 1.
- _____, 1963: The structure and behaviour of the inter-tropical convergence zone. Proc. of the WMO/FAO seminar on Met. and the Desert locust. Tehran - 25 Nov.-11 Dec. 1963, pp. 91-101.
- _____, and S.N. GICHUIYA, 1971: Hailstorms in Kericho area. EAMD Tech. Memo. No. 22, 6 pp.